

1991

A Geophysical and Geological Study of the Farmville Triassic Basin

Charles G. James Jr.
Old Dominion University

Follow this and additional works at: https://digitalcommons.odu.edu/oeas_etds



Part of the [Geology Commons](#), and the [Geophysics and Seismology Commons](#)

Recommended Citation

James, Charles G.. "A Geophysical and Geological Study of the Farmville Triassic Basin" (1991). Master of Science (MS), Thesis, Ocean & Earth Sciences, Old Dominion University, DOI: 10.25777/sc6s-m109 https://digitalcommons.odu.edu/oeas_etds/351

This Thesis is brought to you for free and open access by the Ocean & Earth Sciences at ODU Digital Commons. It has been accepted for inclusion in OES Theses and Dissertations by an authorized administrator of ODU Digital Commons. For more information, please contact digitalcommons@odu.edu.

A GEOPHYSICAL AND GEOLOGICAL
STUDY OF
THE FARMVILLE TRIASSIC BASIN

by

Charles G. James Jr.
B.S. August 1984, Old Dominion University

A Thesis Submitted to the Faculty of Old Dominion University
in Partial Fulfillment of The Requirement For The
Degree of

MASTER OF SCIENCE

GEOLOGY

OLD DOMINION UNIVERSITY

1991

Approved by:

Ali A. Nowroozi (Advisor)

Ramesh Venkatakrisnan

Stanley S. Johnson

ABSTRACT

The Farmville basin is one of many Triassic basins which are found along the eastern coast of North America, and is the largest of the central string of basins in Virginia. Metavolcanic and metasedimentary rocks of the Chopawamsic Formation, as well as felsic intrusives are the primary lithologies surrounding the basin. A detailed gravity survey was conducted along six roads that trend approximately NW-SE, across the basin. Geologic, gravity, magnetic, and radiometric data were used to develop a kinematic model. Gravity anomalies were isolated using two-dimensional harmonic analysis methods to isolate the local, and regional anomalies. This analysis indicates that all the gravity anomalies are a result of structures that lie within the upper 8 kilometers of crust. Results of gravity modelling indicate that the basin is a fault controlled half-graben with an east dipping border fault, and that the basin is relatively shallow. Maximum depth of the basin, occurs along State Road 636, and is less than 1 kilometer. Modelling further suggests that the deepest portion of the basin is opposite the border fault, and is a result of the master (primary) fault laying underneath the basin rocks. In addition to the kinematic model, this study provides evidence of unique geologic features, such as a diabase/granophyre dike that has a maximum width of 688 meters.

Acknowledgements

I would like to extend special thanks to my thesis committee. Dr. Ali Nowroozi, Old Dominion University, provided me with a solid background in geophysics by pushing me beyond what I expected from myself. It was his commitment to me and his profession that enabled me to develop and analyze the geophysical data presented in this study. Dr. Ramesh Venkatakrishnan, Golder Associates/Old Dominion University, is responsible for my understanding of structural geology and geotectonics, and is the reason I became a geologist. His knowledge of every field of geology, gave me the insight to bring all the little pieces together and reconstruct the past events. Stanley S. Johnson, Virginia Division Of Mineral Resources, gave me insight on how to combine geophysics and geology to reconstruct a geologic event. He also provided me with geophysical equipment that allowed me to finish my field work. I am eternally grateful to Mark Corbin, Brett Waller, Bill Decker, Andy Watkins, Tammy Hill Warden, Tom Fekete, Charles James Sr., and Kim James for their help in the field during the 100 degree days of summer and the freezing conditions of winter. An extended thanks should be given to Mark Corbin and Brett Waller for their insight and help during the course of this study. No words can express my thanks to Bill Decker, for all the programs he

developed that aided me in the analysis of my geologic data. I also want to thank the Department of Geology, at Old Dominion University for its support during my graduate career.

I want to thank my family for their support. Without the support of my family I would have never gone back to graduate school. To my mom, dad, and brother, Dixie, Charles, and Bruce James, thank you for giving me the love, courage, and support to finish my thesis. To Joyce and Jake James, my Aunt and Uncle, who gave me a place to live, and treated me like a son, I will always love you for your selfless act, and support. To my grandma and grandpa, Margaret and Bruce Thomson, thank you for your love, and moral/monetary support. To my wife, Kim James, thank you for your patience, love and support during the course of my graduate school.

Finally, I am dedicating this thesis to my two grandfathers, Bruce Thomson and Hatcher James, who passed away before the completion of my thesis.

TABLE OF CONTENTS

	Page
ABSTRACT	i
ACKNOWLEDGEMENTS	ii
LIST OF TABLES	vii
LIST OF FIGURES	viii
LIST OF PLATES	x
CHAPTER	
1. INTRODUCTION	1
OBJECTIVES	2
2. METHODS OF INVESTIGATION	4
DATA COLLECTION	4
Geophysical	6
Geological	9
DATA ANALYSIS	11
Reduction Programs	11
Analysis Programs	12
3. GEOLOGY AND GEOPHYSICS	17
PREVIOUS WORK	17
STRATIGRAPHY	20
Chopawamsic Formation	20
"Granitic" Gneiss Undifferiated	23
Arvonnia Formation	24

Newark Supergroup	25
Dikes	27
GEOLOGICAL DATA	28
Folds	28
Foliation	28
Bedding	30
Joints	30
Rectified Stream Patterns	32
GEOPHYSICAL DATA	34
Gravity	34
Magnetic	34
Radiometric	36
PRECURSORY GEOLOGIC INTERPRETATION ...	36
Regional	36
Local	42
SUMMARY	48
4. GRAVITY MODELLING	49
U.S. HIGHWAY 460E	52
STATE ROAD 637	54
STATE ROAD 636	56
STATE ROAD 634	58
U.S. HIGHWAY 60	60
STATE ROAD 622	60
SUMMARY	62
5. INTERPRETATION	65
PREEXISTING THEORIES	65

STRUCTURAL GRAIN	66
FAULT REACTIVATION	67
STRUCTURAL MODEL	68
6. KINEMATIC MODEL	78
ALLEGHENIAN OROGENY	78
BASIN FORMATION	79
JURASSIC	81
POST-JURASSIC	82
COMPARISON AND CONTRAST	83
7. CONCLUSIONS	86
REFERENCES	88
APPENDICES	
I-A. Discussion Of GRAVAS FORTRAN	94
I-B. Discussion Of STATION FORTRAN	109
I-C. Comparison Of UPDW/UDD Algorithms	111
I-D. Analysis Of GRAVMOD FORTRAN	149
I-E. Analysis Of QUAD BAS	157
I-F. Discussion Of Remaining Programs	165
II. Listing of Gravity Data	173
III. Listing Of Geologic Data	183

LISTING OF TABLES

Table		Page
1.	Calculated Elevation Errors Of Surveyed Roads ...	8
2.	Stratigraphic Column Of Study Area	19
3.	Geophysical Characteristics Of Lithologies In The Study Area	21
4.	Lithologies And Densities Used in Modelling	50

LISTING OF FIGURES

Figure	Page
1. State Map Of Virginia	3
2. Reference Map Of The Study Area	5
3. Stereo Plot Of Poles To Foliation	29
4. Stereo Plot Of Poles To Bedding	31
5. Stereo Plot Of Poles To Joints	33
6. Stream Trend Analysis	35
7. Bouguer Gravity Field At +0.64 Kilometers	37
8. Bouguer Gravity Field At 2.89 Kilometers	39
9. Bouguer Gravity Field At 8.00 Kilometers	41
10. Lithologic Map Based On Gravity Field At +0.64 .	43
11. Second Vertical Derivative Gravity Map	46
12. Gravity Model Of Profile U.S. Highway 460E	53
13. Gravity Model Of Profile State Road 637	55
14. Gravity Model Of Profile State Road 636	57
15. Gravity Model Of Profile State Road 634	59
16. Gravity Model Of Profile U.S. Highway 60	61
17. Gravity Model Of Profile State Road 622	63
18. Structural Model Of The Farmville Basin	69
19. Idealized Model Of Basin With Single Fault	73
20. Idealized Model Of Basin With Multiple Faults-1.	75
21. Idealized Model Of Basin With Multiple Faults-2.	77
22. Kinematic Model Of The Farmville Basin	80

23.	Contour Plot Of Gravity Values Over A Sphere ...	112
24.	Second Derivative Plot Of Spherical Data-UDD ...	114
25.	Second Derivative Plot Of Spherical Data-UPDW ..	116
26.	Contour Plot Of Tasubi (1959) Data	118
27.	+15.9 KM Continuation Of Tasubi (1959) Data	120

LISTING OF PLATES

	Plate
Gravity Map	1
Aeromagnetic Map	2
Aeroradiometric Map	3
Geologic Map	4
Linament Map	5

CHAPTER 1

INTRODUCTION

Early Mesozoic sediments were deposited in a series of fault bounded troughs, during the breakup of Pangea. The sediments deposited in the Mesozoic age troughs on the east coast of North America are considered part of the Newark Supergroup (Cornet, 1977). Current and past geological and geophysical surveys and studies have been made of the Mesozoic age troughs. Several theories explaining the origin of Mesozoic age troughs or basins have been proposed by many authors (Russell, 1892; Lindholm, 1978; Ratcliffe and Burton, 1985; Swanson, 1986). The data used to develop and support the formation of smaller basins and/or troughs is based on the mechanisms from larger basins, such as the Newark-Gettysburg (Ratcliffe and Burton, 1985). That is why geologic and geophysical evidence from smaller Mesozoic basins is a necessity if existing "unifying" theories are to be substantiated. "Unifying" theories, such as Lindholm (1978) or Ratcliffe and Burton (1985) imply that a particular sequence of geologic events or mechanisms controlled the formation of all eastern North American Mesozoic basins.

The Farmville Basin is exposed in Buckingham, Prince Edward, and Cumberland Counties, Virginia (Figure 1). The Farmville basin exceeds 43 kilometers in length, and has a

maximum width of 16 kilometers (Figure 2). This basin was chosen for a geological and geophysical study because of its size, and the limited number of detailed geologic and geophysical investigations in the area. Geologic mapping was conducted to obtain a general understanding of the lithologies and structures in the study area. The geophysical surveys provided data that was used to interpret the subsurface lithologic and structural relationships. In addition, the geophysical data was a tool for identifying surface lithologies. This was possible because lithologies in the area have unique gravity-magnetic-radiometric signatures.

This thesis has three primary objectives. The first objective is to define distinct geologic and geophysical features within the study area. To accomplish this objective detailed field mapping and gravity readings were performed along the roads (profiles) shown in Figure 2. The profiles were chosen to reveal the greatest structural information given the constraints of this study. The second objective of this study was to develop a kinematic model to explain the formation of the Farmville Basin. The kinematic model presented is based on field data gathered and analyzed during this study, as well as information from previous studies (Johnson and others, 1985; Marr, 1980a, 1981; Brown, 1969; Wilkes and Lasch, 1979). The final objective was to compare and contrast the kinematic model from this study with existing models.

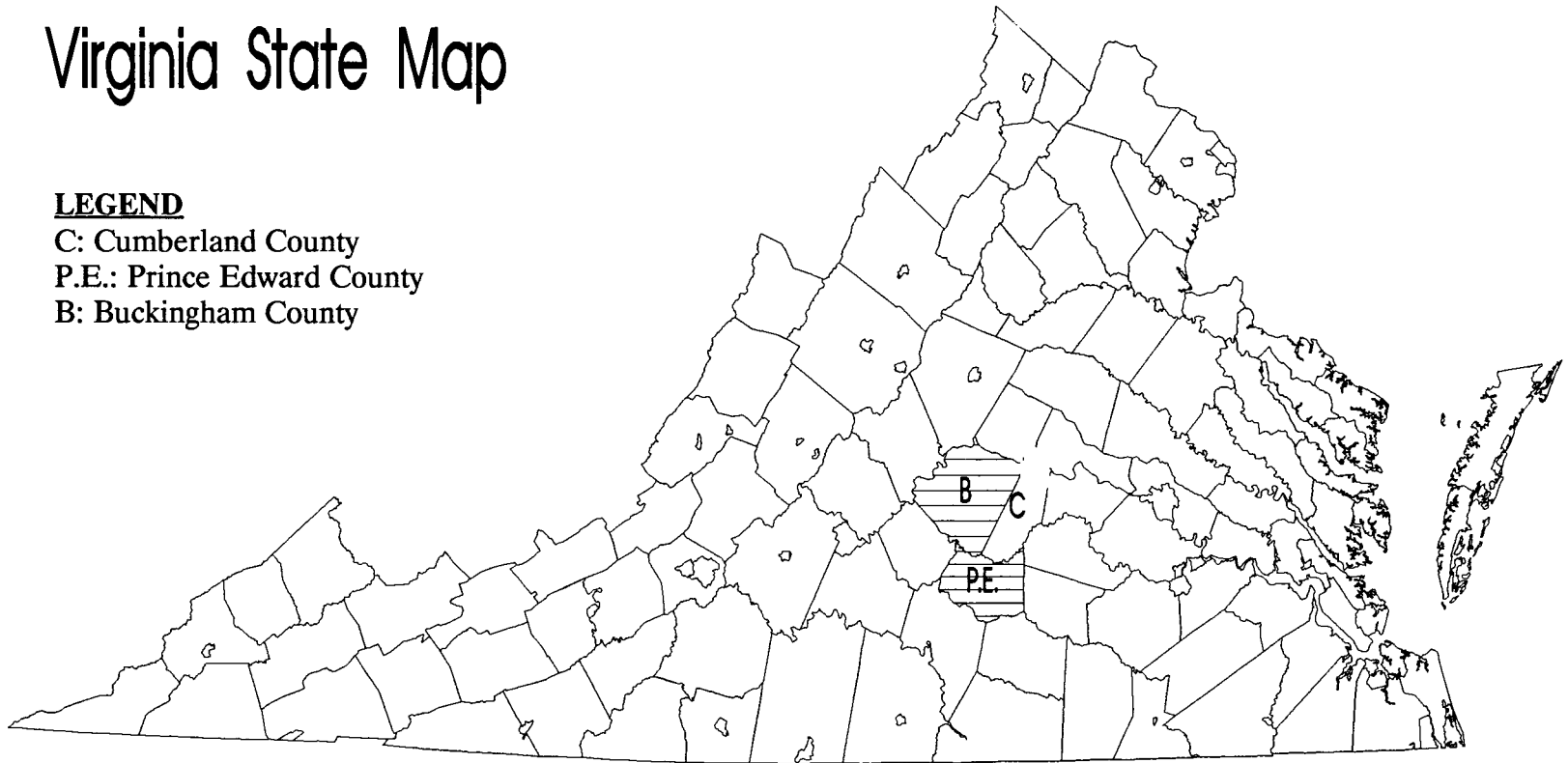
Figure 1: This figure is the state map of Virginia.

The study area is located in the counties highlighted by letters. Counties found in the study area are: Prince Edward, Cumberland, and Buckingham. A more detailed view of the study area is given in Figure 2.

Virginia State Map

LEGEND

- C: Cumberland County
- P.E.: Prince Edward County
- B: Buckingham County



CHAPTER 2

METHODS OF INVESTIGATION

Conclusions of a study are directly affected by the methods used to collect and analyze pertinent data. Gravimetric and geologic field data was gathered during this investigation. After collecting all geophysical and geologic field data, information from a variety of sources was compiled (Marr 1980a, 1981; Brown, 1969; Virginia Division of Mineral Resources Farmville Aeromagnetic Map, 1970a; Virginia Division Of Mineral Resources Dillwyn Aeromagnetic Map, 1970; Virginia Division Of Mineral Resources Farmville Aeroradiometric Map, 1978; Virginia Division Of Mineral Resources Dillwyn Aeroradiometric Map, 1978). All information was analyzed using computer and manual techniques. A hypothesis was developed from these analyzes to explain the mechanisms behind the formation of the Farmville Basin. This chapter is divided into data collection and data analysis.

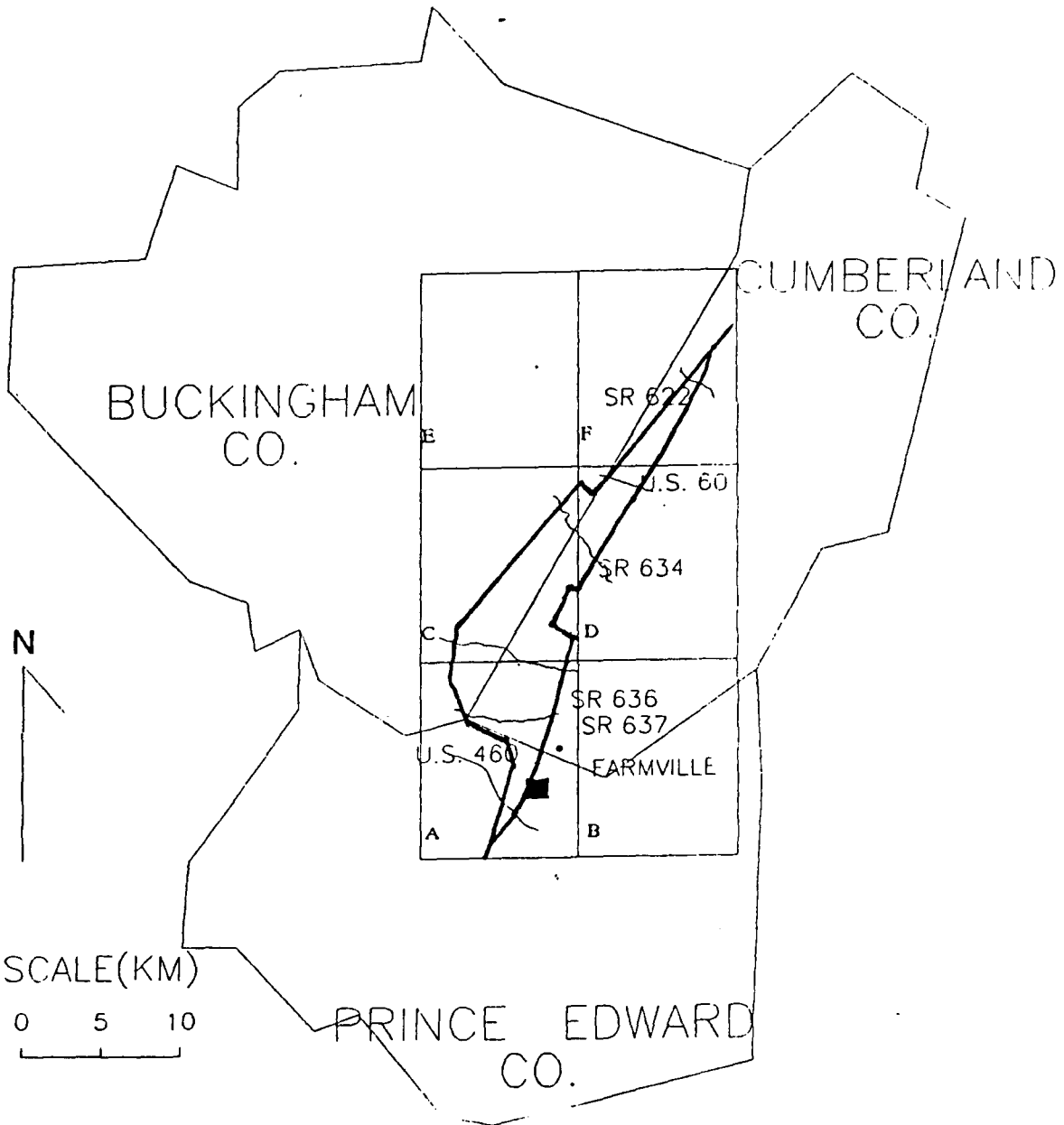
DATA COLLECTION

Established field techniques were used to collect geophysical and geological data. Because field techniques used to collect geophysical and geological data differ they are examined separately.

Figure 2: Shown is a detailed view of the counties in which study area is located. Gravity readings were taken on all roads shown on this map. The letters define the respective 7 1/2 minute quadrangles comprising the study area. The quadrangles comprising the study area are as follows: A: Farmville, B: Rice, C: Willis Mountain, D: Hillcrest, E: Dillwyn, and F: Gold Hill. The bold square within the Farmville quadrangle is the town of Farmville.

Note: State Road 637 does not cross the entire basin, as a result, surveying was conducted off road to connect State Road 637 with Highway 15.

EXPLODED VIEW OF STUDY AREA



Gravity Data

The field techniques used to collect gravimetric data followed the techniques established by Nettleton (1954). Gravimetric data was gathered along roads trending NW-SE across the basin (Figure 2). The NW-SE trend of the roads is perpendicular to regional geophysical and geologic trends minimizing the affects of regional trends on the local models. A total of 695 gravimetric readings were taken along roads crossing the Farmville Basin. The gravity readings were taken along U.S. Highways 460E and 60, and State Roads 637, 637, 634, and 622 (Figure 2). Each road was surveyed to establish the location and elevation of each gravimetric station. Station elevation was determined using a Geotec-Al 21 automatic level and English Transit Rod. Stations were spaced 61 meters apart. To minimize surveying errors, foresight and backsight readings were taken for each station. Three readings corresponding to the top-middle-bottom cross-hairs of the level were taken for each sighting to determine station spacing. Sighting information was used in conjunction with contour maps to determine station locations. The terminus and beginning of each surveyed road had a benchmark with the exception of State Road 637. In addition, most of the roads had intermediate bench marks allowing errors to be determined for every station. The only exception is State Road 637 (Table 1).

Several benchmarks were available along State Road 637;

however, a benchmark was not available at the road terminus. The nearest benchmark in which to tie to this profile was 7 kilometers from the terminus of State Road 637. A spot elevation was used to end the line. As a result, the last 25 stations on State Road 637 could have a maximum error of +/- 0.3 meters.

Latitude and longitude of gravimetric stations located on the topographic maps were determined using a Numonics 2400 series digitizer. The digitizer cursor was placed over each station and the latitude and longitude, in degrees, were written to an ASCII computer file. Gravity readings were taken at each station in the field, after the above steps.

A LaCoste-Romberg Model-G (#289) gravimeter was used to obtain the gravity measurements. The G-model gravimeter has a range of over 7000 milligals (mgal), a drift rate of less than 1 mgal/month, and a reading accuracy of +/- 0.01 (LaCoste-Romberg, 1978). A gravity reading was taken at the Farmville gravity base station, at the beginning and end of each day. This station was established by Johnson and Ziegler (1972). Using the closed loop technique, a reading was taken periodically at the first station of each loop. Gravimetric readings were reduced to Free Air and Bouguer anomalies using the program GRAVAS FORTRAN (Appendix I-A). The gravity readings from this study, in addition to the published data of Johnson and others (1985), were hand contoured (Plate 1). The

Table 1: Calculated elevation errors for the six roads surveyed.

ELEVATION ERRORS OF SURVEYED ROADS

ROAD SURVEYED	ELEVATION ERROR
U.S. HIGHWAY 460E	-0.14619 cm/station
STATE ROAD 637	+0.30400 m for line
STATE ROAD 636	+0.03056 cm/station
STATE ROAD 634	+0.01111 cm/station
U.S. HIGHWAY 60	+0.00 cm/station
STATE ROAD 622	-0.02586 cm/station

Note: Elevation for State Road 637 could not be calculated for each station because a benchmark was not available at the end of the road.

contour gravity map was digitized using the program DIGIT BAS (Decker, 1987) and contoured at an interval of 1 milligal (mgal) using the program CONTOUR SAS (Appendix II-A). Comparison of the hand drawn and computer generated contour maps showed no discernable differences. This ensured that the computer generated data is a close approximation of the actual gravity field, allowing the data to be used in computer analysis.

Magnetic And Radiometric Data

Magnetic and radiometric data presented in this study was taken from Virginia Division Of Mineral Resources Aeromagnetic 15-minute Maps (Dillwyn, 1970; Farmville, 1970), and Aeroradiometric 15 minute Maps (Dillwyn, 1978; Farmville, 1978). Airborne maps were used instead of ground data because of the extremely erratic readings being obtained from the ground equipment. Both airborne surveys were flown at an altitude of 152 meters above ground level, and used a flight spacing of 0.8 kilometers. The flight lines were flown in an E-W direction. The aeromagnetic and areoradiometric maps are at 1:62,500 scale and are illustrated in Plates 2 and 3, respectively.

Geologic Data

Geologic maps and rectified stream data aided in the development of a kinematic model of the Farmville Basin.

Geologic data was collected during an eight week period in December, January, and February of 1987. The field mapping was done to distinguish different lithologies, to define the basin's margin, and to identify geologic trends (Plate 4). This data was used in determining correlations between geological and geophysical signatures. Field mapping was primarily conducted in streams that parallel the roads shown in Figure 2. The structural features measured included the strike and dip of foliation, bedding, and joints. In addition, lithologic information was recorded for each outcrop.

A rectified drainage map was constructed for the study area (Plate 5). Construction of this map was done to identify significant drainage trends, and to determine if they were geologically controlled. Procedures used in the stream analysis are as follows:

- 1) Digitizing of permanent streams (blue line) in the Farmville, Willis Mountain, Hillcrest, Rice and Gold Hill 7.5 minute quadrangles.
- 2) Analysis of data using programs developed to isolate significant azimuthal drainage trends.

Digitization of the stream maps was done using the Numonics 2400 digitizer and the program DIGIT BAS (Decker, 1987). Streams were digitized in a upstream-downstream direction with each stream assigned an identification number. Using the program RECTIFY BAS (Decker, 1988), the digitized streams were divided into straight line segments if the next

stream point varied 5 degrees or more from the previous point.

DATA ANALYSIS

Geophysical and geological data was interpreted using a series of existing programs, and programs specifically developed during the course of this research. The interpreted information was correlated and a kinematic model was developed based on the data. Because the computer programs are crucial to interpretations presented in this study, their purpose and algorithms are explained in the following section.

Reduction Programs

Reduction programs, as defined in this study, are computer programs that perform repetitive corrections to raw data. STATION FORTRAN and GRAVAS FORTRAN are the two reductions programs used to correct the elevation and gravity data, respectively. STATION FORTRAN (I-B) converts station foresight and backsight level readings to elevations. In addition, the program calculates station spacing, total elevation change, and total elevation error for each station. Output from STATION FORTRAN was verified by comparing the program output with hand calculated values for State Road 622. The comparison indicated that STATION FORTRAN generated the correct values and thus was used in determining the same information for the remaining lines.

GRAVAS FORTRAN (I-A) converts dial readings of the

LaCoste Romberg gravity meter (Model G, #289) to Free Air and Bouguer anomalies. The program first converts gravimetric dial readings to observed gravity values. Observed gravity values are corrected for elevation and mass differences between stations. Observed gravity values are then corrected for solar and lunar fluctuations (tides), and instrumental drift. Finally, GRAVAS FORTRAN applies Free Air and Bouguer corrections to the observed data, resulting in the Free Air and Bouguer anomalies for each station. A comparison of the Bouguer anomalies from this study and data from Johnson and Ziegler (1972) was conducted to ensure the gravimeter was properly calibrated. A difference of + 0.02 milligals was determined between the Bouguer values of this study and the Bouguer value of Johnson and Ziegler (1972). The + 0.02 milligal difference remained constant for all the compared readings. This comparison indicates the gravimeter was properly calibrated. The + 0.02 milligal difference between the Bouguer values is attributed to the settling of the base station.

Analysis Programs

Analysis programs, as defined in this study, simplify and group data so that interpretation of the information is possible. UPDW FORTRAN and GRAVMOD FORTRAN are the two analysis programs that were used to interpret the geophysical data. In addition, the programs QUAD BAS, and SNET (Decker,

1988) were used to aid in the analysis of the stream and structural data, respectively.

Two programs were reviewed to isolate regional and local gravimetric anomalies. An evaluation was conducted of each program to determine the best program, because of differences in the methods used to analyze the data. UPDW FORTRAN and UDD FORTRAN (Appendix I-C) use algorithms based on two dimensional harmonic analysis (Bhattacharayya, 1965), and coefficient averaging (Henderson, 1960), respectively. Both programs are able to calculate upward/downward continuation, and 2nd derivative values from potential field data. Each method has advantages and disadvantages; however, after thorough evaluation it was determined the two-dimensional harmonic analysis method was best suited for this study. A complete discussion of the evaluation is given in Appendix I-C. A upward/downward continuation and second derivative map of the gravimetric data was produced using UPDW FORTRAN. The contour maps of the gravity data was produced to obtain evenly spaced gravity nodes. CONTOUR SAS (Appendix I-F) gridded the raw data, then produced a contour map from the data. After examining the contour maps for errors, the gridded data was analyzed using UPDW FORTRAN.

Slight differences exist between modules used to perform upward/downward continuation, and the nTH vertical derivative in UPDW FORTRAN. The theory and methodology of this method is given in Appendix I-C. Two tests were developed to verify

that output from UPDW FORTRAN was correct. Each test used the potential field data of Tasubi (1959).

First, the potential field data of Tasubi (1959) was continued upward +15.9 kilometers, using UPDW FORTRAN. The output generated by UPDW FORTRAN was contoured and compared to the hand calculated values of Tasubi (1959), Appendix I-C. The comparison showed that differences between the two maps is negligible. To test the n^{TH} vertical derivative algorithm of UPDW FORTRAN, the 1st vertical derivative of Tasubi's data was calculated. The data was contoured and compared to the same map in Agarwal's dissertation (1968). The comparison showed little difference between the two maps. Both tests indicated the algorithms used in UPDW FORTRAN produced valid and usable output.

The GRAVMOD FORTRAN program (Appendix I-D) allows the user to create a two-dimensional model of the subsurface geology. The input data is based on surface lithologies and their associated densities. The underlying principle and theory of this program is based on methods developed by Talwani (1964, 1965). Talwani's method allow a geophysist to approximate subsurface geology by polygons of an assigned density. Further explanation of the theory and method are given in Appendix I-D. This program was checked by producing a simple polygonal model. The results of the test proved the program produced accurate results.

In order to analyze the rectified stream data, QUAD BAS

(Appendix I-E) was developed to isolate, and identify significant drainage trends within the area. The program's algorithm is based on a paper by Abdel-Rahman Hay (1978) that deals with sampling and statistical analysis of multimodal orientation data. In this paper, azimuthal trends are identified using randomly spaced circular sampling units called quadrats. Significant trends are then determined using Poisson's distribution. The algorithm was modified in order that the analysis of the data could be done with randomly spaced square quadrats. In addition, equally spaced circular or square quadrat analysis could be chosen with azimuthal trends and significant trends identified for each quadrat. Discussion of the theory involved in this type of analysis is continued in the Appendix I-E.

To help in the analysis of the structural data the program SNET (Decker, 1988) was used. This program projects structural data onto a stereo graphic net, either Wulff or Schmidt. Once projected onto the net the data is contoured, and T statistics can be performed. The program also includes a file and record maintenance option.

Graphing programs were developed to present the analyzed data in an understandable form. The majority of these programs are written in SAS, with the remainder of the graphical programs written in BASIC. These programs include MODEL SAS, TWOLINE SAS, and CONTOUR SAS. Listings of these programs are found in Appendix I-F along with a brief

discussion of the function of each program.

CHAPTER 3

GEOLOGY AND GEOPHYSICS

Current ideas for the formation of the Newark Supergroup rift basins all involve reactivation of Paleozoic age structures. The basin geometry is invariably controlled by the basement fabric (structural grain); however, little research has been done to understand the internal geometry and true three-dimensional shape of the basins'. This study attempts to develop new data that might be used in the evaluation of mechanisms responsible for the formation of the Newark Supergroup.

PREVIOUS WORK

The Farmville Basin is one of many Mesozoic age basins found in the eastern United States. It is the largest of five basins composing the central system of Mesozoic basins in Virginia (Johnson, 1981). The study area is located in the Gold Hill, Willis Mountain, Hillcrest, and Farmville quadrangles (Figure 2). Several geophysical studies and surveys were conducted within the area of study, including aeromagnetic (Virginia Division of Mineral Resources (VDMR), 1970; 15-minute Farmville and Dillwyn maps), aeroradiometric (VDMR, 1978; 15-minute Farmville and Dillwyn maps), and gravity (Johnson et al., 1985) surveys. The airborne

surveys had flight line spacings of 0.8 kilometer at 152 meters above ground level. A regional gravity map (Johnson and others, 1985) covered approximately 5, 15 minute quadrangles and contains 1202 gravity stations including the only published lithologic map of the entire Farmville Basin.

William Barton Rodgers (1859) was the first person to describe the various lithologies in and around the Farmville Basin. Since that time, a majority of geologic studies in the vicinity have been reconnaissance in nature (Russell, 1892; Jonas, 1932; Espenshande and Potter, 1960). Two exceptions are the publications of Brown (1969) and Marr (1980).

A geologic map of the Dillwyn 15-minute quadrangle that includes the Gold Hill 7.5 minute quadrangle was prepared by Brown (1969). A geologic map of the Willis Mountain 7.5 minute quadrangle was prepared by Marr (1980). These two publications account for the majority of the known geology, within the study area. The stratigraphic columns presented in these two publications are different, and thus posed a problem as to the stratigraphic sequence of strata. Table 2 is a proposed stratigraphic column for the study area. This column is based on the publications by Brown (1969) and Marr (1980, 1981), as well as mapping conducted during this investigation. Rocks from oldest to youngest in the stratigraphic column are the Chopawamsic Formation, "Granitic" Gneiss Undifferentiated (Hatcher Complex (?)), Arvonian Formation, Triassic Rocks, Diabase/Granophyre dikes, and Quaternary alluvium.

Table 2: Tentative stratigraphic correlation of lithologies within the study area. The stratigraphic column used for this study is based on stratigraphy of Marr (1980, 1981), Brown (1969), and geologic mapping conducted during this investigation.

E R A	P E R I O D	Brown (1969)	Marr (1980)	Present Study
		C E N O Z O I C	Q A L	Alluvium
M E S O Z O I C	J R	Diabase Dikes	Diabase Dikes	Diabase/ Granophyric Diabase
	T R	Newark Supergroup	Newark Supergroup	Newark Supergroup
P A L E O Z O I C	O R D	Arvonja Formation	Arvonja Formation	Arvonja Formation
		Hatcher Complex	?	"Granitic" Gneisses (Hatcher Complex Equivalent ?)
	?	?	Pegmatite	Pegmatite
		Ultramafic Rocks & Hornblende Metadiorite	?	?
		C	Evington Group (?) & Rocks Of Uncertain Age	Chopawamsic Formation

Note: The letter abbreviations in this table are defined as follows: C-Cambrian, ORD-Ordovician, TR-Triassic, JR-Jurassic, and QAL-Quaternary. ?: Unknown

STRATIGRAPHY

The type section of the Chopawamsic Formation lies along Chopawamsic Creek near Quantico, Virginia (Southwick et al., 1971), and is estimated to be 1829 meters thick. Pavlidies (1980), and Conley and Johnson (1975) traced the formation from northern Virginia to the study area. Marr (1980) described the various lithologies within the Chopawamsic Formation, and defined a lower and upper member. Only the upper member is found within the study area. This formation has a maximum age of Early to Middle Cambrian (Tilton, 1970; Higgins, et al., 1977; Glover, 1975), and is comprised primarily of metavolcanic and metasedimentary rocks.

Chopawamsic Formation

The upper member of the Chopawamsic Formation is a biotite gneiss that ranges in thickness from 3 to 31 meters. The unit is interlayered with amphibolite gneiss. The biotite and amphibolite gneisses compose nearly 90 percent of this member. The remaining 10 percent of the upper member is comprised of felsic volcanics (rhyodacites), talc-tremolite schists, and ferruginous quartzites. These rocks are primarily found along the western margin of the basin; although, numerous outcrops are found farther to the south. The following descriptions of the above rocks units were taken from Marr (1980, and 1981) with modifications.

Table 3: General geophysical characteristics of lithologies in the area.

P E R O I D		GEOPHYSICAL CHARACTERISTICS OF LITHOLOGIES WITHIN STUDY AREA	
M E S O Z O I C	T R J	<u>DIABASE/GRANOPHYRIC DIKE</u>	<ul style="list-style-type: none"> 1. High Magnetics 2. High Gravity 3. Low Radiometrics 4. density = 2.88 g/cm³
	T R	<u>TRIASSIC ROCKS</u>	<ul style="list-style-type: none"> 1. Low Magnetics 2. Low Gravity 3. Low Radiometrics 4. density = 2.55 g/cm³
P A L E O Z O I C	O R D	<u>"GRANITIC GNEISS"</u>	<ul style="list-style-type: none"> 1. Low Magnetics 2. Low Gravity 3. High Radiometric 4. density = 2.775 g/cm³
	C	<u>CHOPAWAMSIK FORMATION</u>	<ul style="list-style-type: none"> 1. High Magnetics 2. High Gravity 3. Low Radiometrics 4. density = 2.845

Note1: The letter abbreviations in this table are defined as follows: C-Cambrian, ORD-Ordovician, TR-Triassic, JR-Jurassic, and QAL-Quaternary.

Note2: The terms High, and Low are relative terms. In other words they are relative to the surrounding rock units. For example, if a Triassic Rocks were in lithologic contact with the Chopawamsic Formation then magnetic, gravity, and radiometric readings of the two units would display the characteristics in this figure.

The biotite gneiss is medium to fine-grained, moderately foliated, and light gray to gray in color. Quartzofeldspathic bands found within this unit are interlayered with biotite layers. Some of the biotite layers contain amphibole. Composition of this unit ranges from granitic gneiss to biotite-quartz-feldspar gneiss. This unit is not resistant to weathering and occupies areas of low topography. Outcrop of the biotite gneiss is predominately limited to the Willis Mountain and Farmville quadrangles. In the field this rock is usually highly weathered; however, fresh outcrops contain pegmatitic bands, ranging in size from a few centimeters to nearly a half a meter. The pegmatitic bands are a distinctive feature of this unit. Generally, quartz veins are absent from this unit; although, veins are concentrated in some areas. This unit usually displays low magnetic, intermediate gravity, and low radiometric values in comparison to the surrounding rocks (Johnson, 1981), Table 3, and grades into an amphibole gneiss.

The amphibole gneiss is medium to coarse-grained, banded, and greenish-black to black in color. The banding in this unit is composed of tremolite-cummingtonite or hornblende-cummingtonite and quartz calcic oligoclase, biotite, epidote, and garnet. Talc-tremolite schistose bodies range in composition from talc-tremolite schist to actinolite-chlorite schist. This unit is generally found west of the basin and is more resistant to weathering than the

biotite gneiss, occurring in areas of rolling topography. The outcrop of this unit is often unweathered. Minor folds are common. Banding is not as distinctive in this unit as in the biotite gneiss. Light-green, quartz-epidote lenses are also characteristic of this unit. High magnetic and gravity values, and low radiometric values are the geophysical characteristic of the unit. Unconformably overlying the Chopawamsic Formation is the undifferentiated "granitic" gneiss.

Granitic-Gneiss Undifferentiated

The "granitic" gneiss is thought to be the equivalent of the Hatcher Complex Undifferentiated (Brown, 1969). Brown (1969) and Mose (1980) assign an age of 454 ± 9 million years to the Hatcher Complex. Surface exposure of these rocks occur in the northern and eastern portions of the study area. Generally, these rocks are medium grained, strongly lineated, and light-gray to tan in color. The term "granitic" was used to describe a group of intrusive rocks ranging in composition from granite to quartz diorite. The gneisses have a low resistance to weathering; therefore, are found in areas of low topography. In the field this unit ranges from highly weathered to fresh, and is strongly banded and foliated. No distinguishing characteristics exist, except for the interlocking granular patterns associated with intrusive rocks. When weathered the unit looks very similar to the

granitic gneisses of the Chopawamsic Formation. Geophysical characteristics include low magnetic and gravity values, and high radiometric values. Brown (1969) indicates that basal conglomerates of the Arvonian Formation unconformably overlie the granitic intrusives; therefore, the Arvonian is the younger of the two lithologies.

Arvonian Formation

Fossils indicate that the Arvonian Formation ranges in age from 440 to 460 million years (Mose, 1980; Mose and Nagel, 1983). Within the study area, this formation consists of the following rock units: quartz-mica schist with interlayered micaceous quartzite and quartz mica conglomerate, quartzite and kyanite quartzite, and porphyroblastic garnet mica schist. These rocks are found in the extreme northwestern part of the study area. Marr (1980) describes the conglomeritic quartz-mica schist as medium to coarse grained, moderately foliated and lineated, light-gray to gray schist with blue quartz found in some conglomerates. Kyanite occurs locally as massive lenses and can make up as much as 30 percent of the unit. The quartzite/kyanite quartzite unit is medium to coarse-grained, banded and cross-bedded, and is light-yellow to gray in color (Marr, 1980). This unit is resistant to weathering and found in areas of higher relief. This unit is resistant to weathering and underlies along NE-SE trending linear ridges formed by isoclinal synclines. The highest

magnetic values within the study area are found within this formation. The Arvonian Formation has intermediate radiometric and gravity values as compared to other lithologies within the study area. This formation is not used as a unit in the gravity models, produced in this study, because it lies outside the range of the surveyed gravity lines. An unconformity exists between the Arvonian Formation and the Triassic age rocks.

Newark Group

Unconformably overlying the metamorphic basement are the Triassic rocks of the Newark Supergroup. Basal strata are Carnian in age as determined by Robbins (1985). This age date is based on palynoflora data found in the basin. This places rocks of the Farmville basin, along with rocks in the Richmond and Taylorsville basins, as the oldest rocks in the Newark Supergroup (based on palynoflora data; Cornet, 1978). The rocks show a general fining away from the basin perimeter (Plate 4). According to Smoot (1985), this is indicative of a closed basin. He defines a closed basin as having no drainage outlet. In other words, all surface drainage and groundwater entering the basin evaporates. This is not to say the basin remained closed throughout its entire depositional history, since the erosion of hitherto undetermined strata overlying the presently exposed basin is not known.

Czechowski (1982) suggested that the paleoenvironment

during deposition of these rocks was more arid than the present climate. His conclusions are based on relative percentage of feldspar and lithic fragments in the Triassic rocks as compared with Quaternary stream sands in the basin. He also showed rocks within the basin have undergone less than 45 kilometers of transportation. Breccia-conglomerate, arkosic conglomerate, arkosic sandstone, and siltstone/shale are the four lithologies found in the basin.

The breccia-conglomerate is a fine to medium-grained, brown to reddish-brown rock with angular to subangular clast ranging from pebble to boulder size. In general, clasts are comprised of metamorphic rocks from the Chopawamsic and Arvonian Formations, and "granitic" gneiss undifferentiated. Clast imbrication indicate transportation of sediment comprising this unit was from the northwest (Marr, 1981; Czechowski, 1982).

The arkosic conglomerate is medium-grained and light brown to light gray in color, and has an arkosic sandstone matrix. Clasts are subangular to subrounded ranging from pebble to boulder size, and are predominately metamorphic in composition (Johnson, et al., 1985). Czechowski (1982) suggested that the clasts were transported in a north-south direction with source rocks laying farther than 43 kilometers north of the basin.

The arkosic sandstone is medium-grained, thick-bedded, and brown to light-brown in color with interlayers of

red-brown sandstone, siltstone, and shale (Johnson, et al., 1975). Source of this unit is thought to lie east of the basin (Cezchowski, 1982). Siltstone-shale is the youngest sedimentary unit in the basin. These rocks are light-gray in color and are interbedded with red-brown sandstone, quartz-pebble conglomerate, and dark-gray mudstone and coal. This unit is thought to have been deposited in a lacustrine environment (Cezchowski, 1982). The Mesozoic rocks are distinctive because of their low gravity, magnetic, and intermediate radiometric values. These rocks are cross-cut by diabase/granophyre dikes.

Dikes

The diabase dikes are the youngest rocks of interest in the area and are thought to be late Triassic to Jurassic in age (Marr, 1981). These dikes are medium to fine-grained, and light-gray to dark-gray in color. Several dikes have been found to contain granophyres (Rogan, pers. comm.). The granophyres are found predominately in larger (thicker) dikes. Compositionally, larger dikes seem to be of diabase composition along their margins with granophyre percentages increasing as one progresses towards their center. Two sets of dike trends are recognizable in the area. A majority of the dikes trend between N12°W and N25°W, with a second minor set trending between N and N20°E. Dikes in the area cross-cut Triassic Rocks, and the basin margin. This puts a cross

cutting relationship time constraint on sedimentation.

GEOLOGICAL DATA

The known structures from publications of Brown (1969) and Marr (1980), as well as structural data gained from this study give valuable information as to structures within and outside the basin. Knowing the structural regime of the area puts constraints on gravity models.

Folds

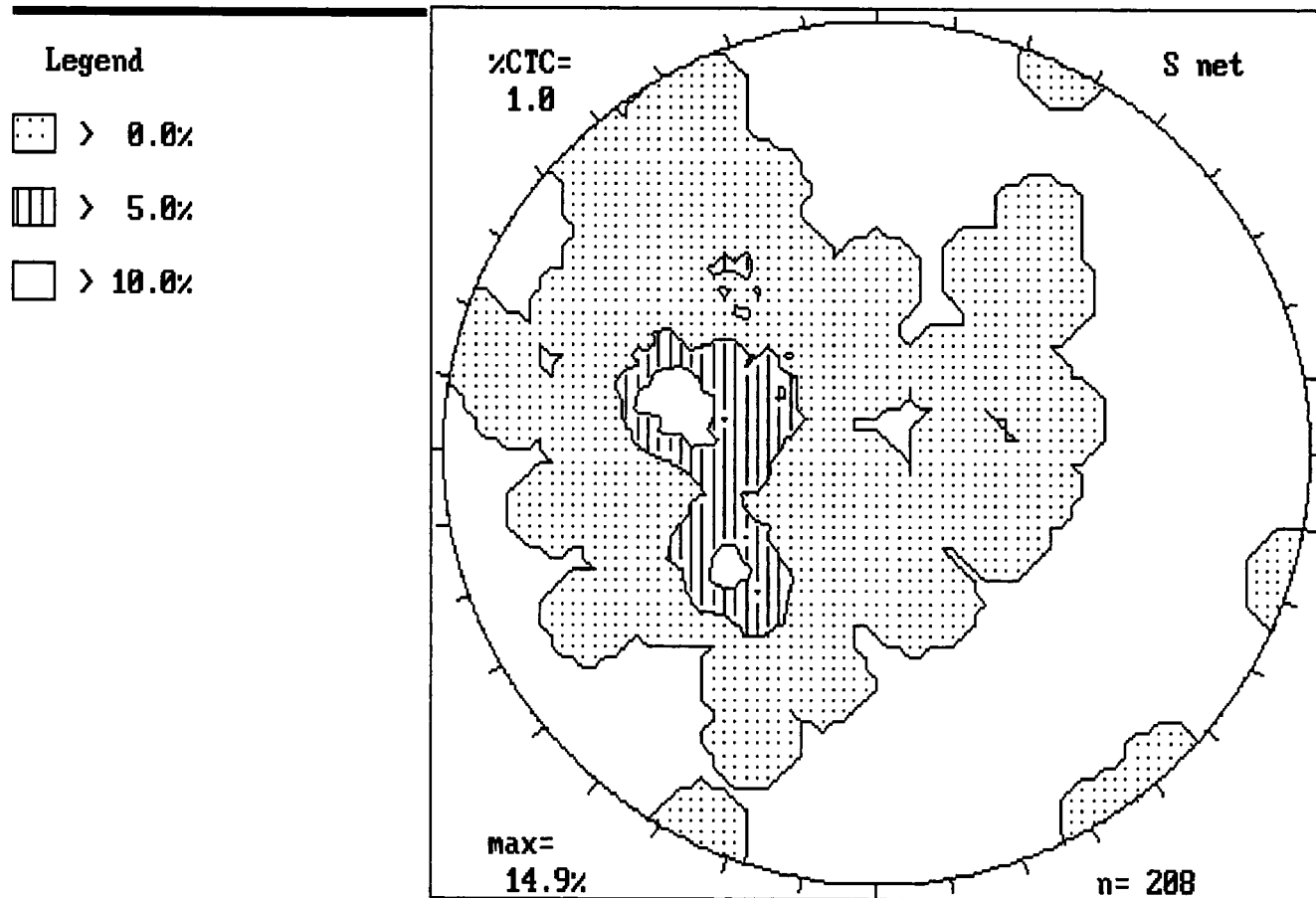
The scope of this thesis is limited to understanding the structural control of Mesozoic events imposed by Pre-Mesozoic structures. Previous studies discuss three phases of folding (Marr, 1980). The cumulative effect of these folding phases is the NE regional trend. Therefore, the geologic information collected during this study is limited in scope.

Foliation

Figure 3 is a compilation of 208 foliation measurements throughout the study area. Two foliation pole maxima are shown on the stereo net. The two maxima are separated by 35 degrees. The dominant pole concentration ('A') is in the NW quadrant of the net. This group of poles are representative of foliation that has an average strike of N15°E and dip of 35 degrees southeast. The secondary concentration of poles ('B')

Figure 3: Contour plot of 208 poles to foliation from this study and the geologic map of Marr (1980). The graph is a contour plot of foliation poles. The maxima represent foliation planes located at N15E 35 degrees SE, and N40W 35 degrees NE. Pole maxima are separated by 35 degrees. The distribution of pole clusters shows that the general modal average foliation plane strikes north-north east and dips to the south east.

One Percent Total Area Contour Of Poles To Foliation



is representative of foliation that has an average strike of N40W and dip of 35 degrees northeast.

Bedding

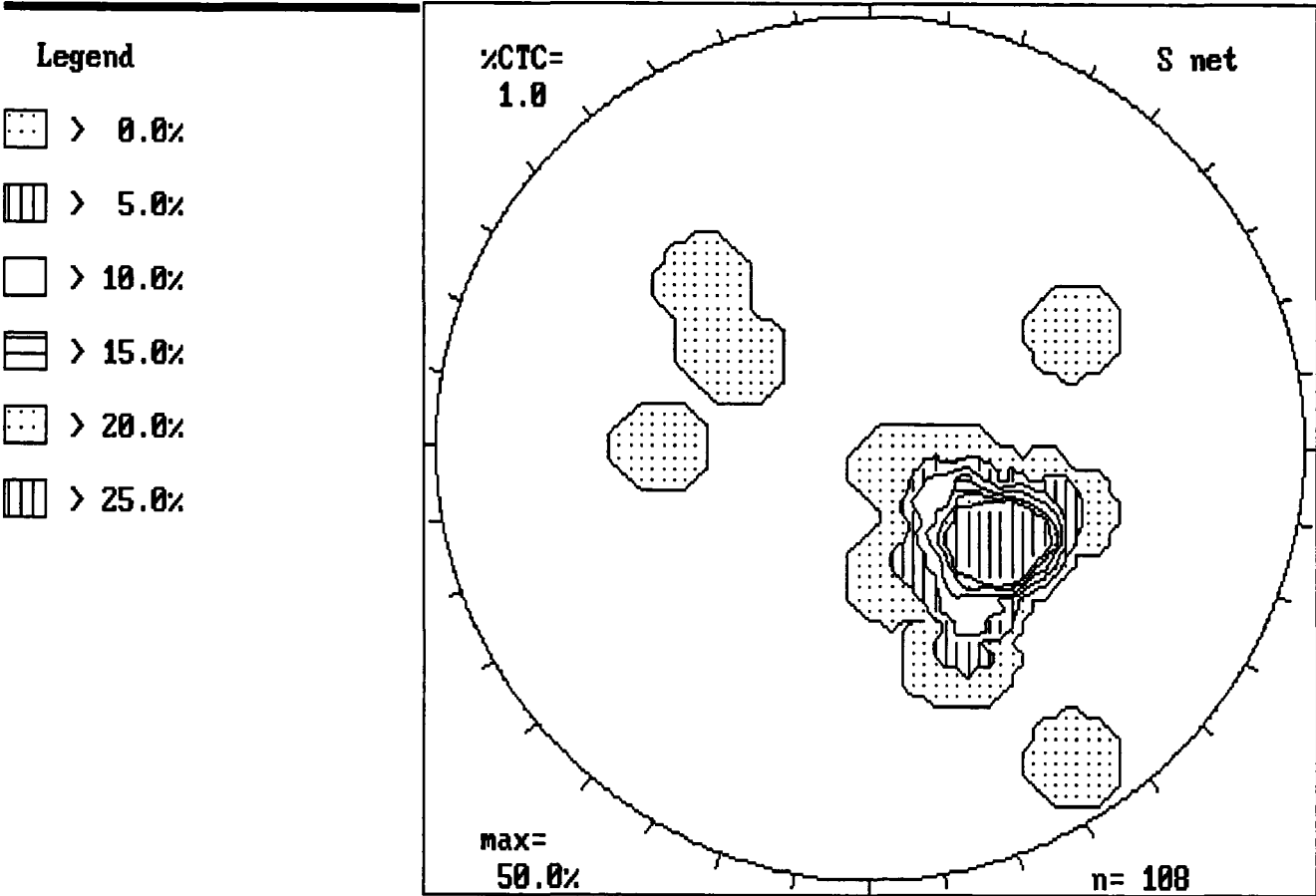
Poles of bedding within the basin show little variance (Figure 4). Bedding within the basin has an average strike of N45E and dip of 30 degrees northwest. Dips within the basin generally decrease from east to west. It should be noted that these dips vary along profile sections. A pattern of steep to shallow to steep is recognizable. This is best documented along the profile on State Road 636 (Plate 4).

Joints

Two systematic joint sets are found within the area (Figure 5). The joint set with poles in the NE quadrant of the stereo net have an average strike of N40W and an average dip of 50 degrees southwest ('A'). A second cluster of joint poles lay near the perimeter of the net in the NW quadrant ('B'). This joint set has an average strike of N70°E and dip of 80 degrees southeast. The contour projection indicates a third joint set may be present. In the NE and SW quadrants of the stereo net there are a group of poles that lie on the net's perimeter. This joint set has an average strike of N20°W and near vertical dips.

Figure 4: Contour plot of 108 poles to bedding taken in the Farmville Basin, during the course of this investigation. The stereo graphic projection is a contour plot of the poles to bedding and indicates that bedding in the basin has an average strike of N45E and dips 30 degrees northwest.

One Percent Total Area Contour Of Poles To Bedding



Rectified Stream Patterns

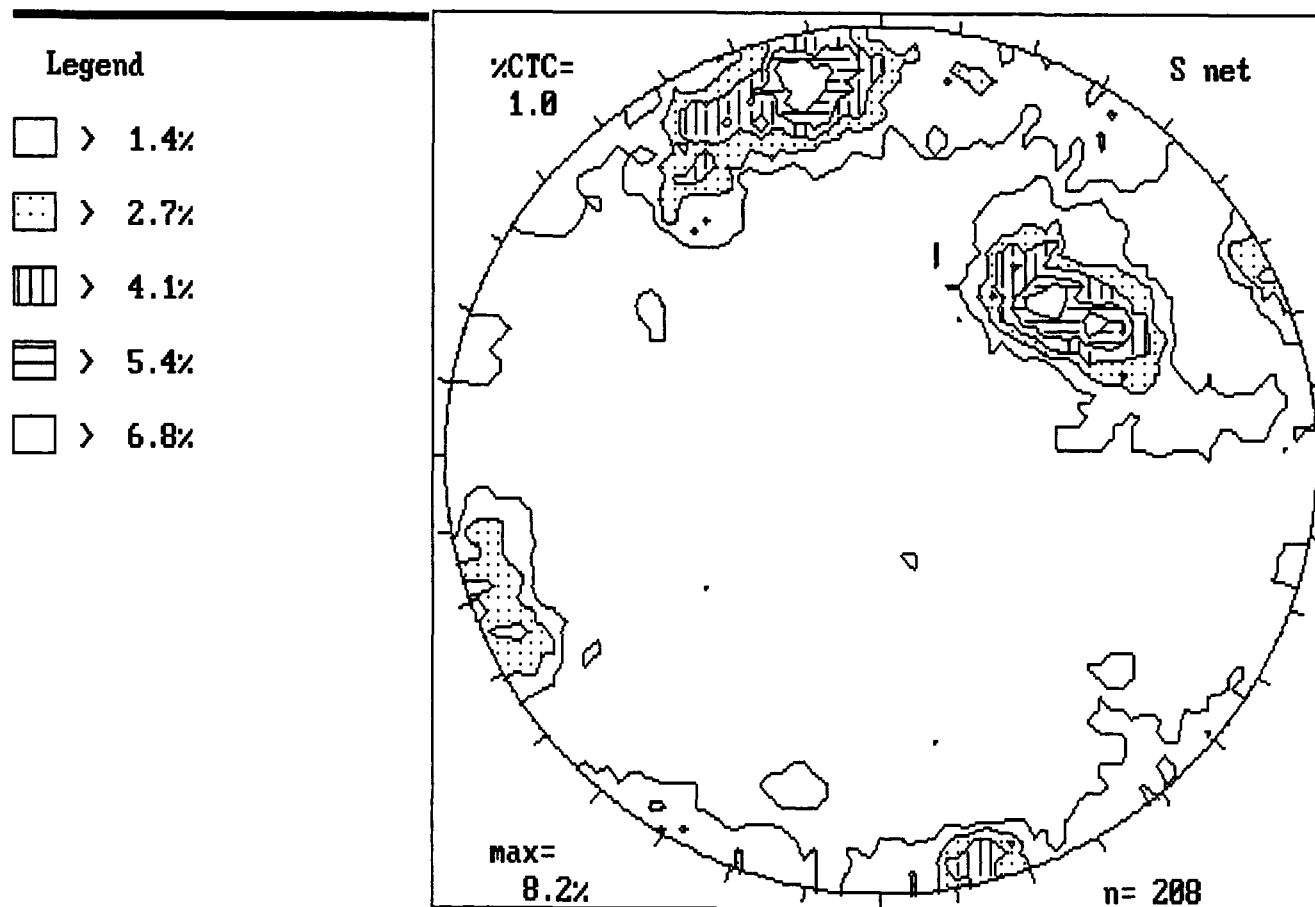
A rectified stream analysis was correlated with geological and geophysical trends to identify significant drainage trends, and to aid in the development of a kinematic model (Plate 5). This analysis is based on the underlying assumption that the stream drainage is structurally controlled. There is no validity to conclusions drawn from this type of analysis without this assumption. In this study, it is assumed streams are structurally controlled because of the near rectilinear stream segments.

Studies of stream patterns have been used in the identification of drainage trends and associated geologic and/or geophysical trends. This enables past geologic events to be reconstructed (Scheidegger, 1980 a, 1980 b; Cox and Harrison, 1979; Venkatakrisnan, 1984).

At least three significant trends have been identified from analysis of rectified stream data (Figure 6). These trends, listed in order of prominence, are NNW to SSE (160 to 180 degrees), NW to SE (120 to 130 degrees), and NE to SW (030 to 040 degrees) The most prominent trend occurs in the azimuthal range of 160 to 180 degrees.

Figure 5: Contour plot of 208 joint poles taken in this study from various areas within the area. From this plot one may interpret two joint sets; one at $N40^{\circ}W-50$ degrees SW, and the other at $N70^{\circ}E-80$ degrees SE.

One Percent Total Area Contour Of Poles To Joints



GEOPHYSICAL DATA

Gravity Data

The Bouguer Gravity anomaly map of the Farmville Basin (Plate 1) is prepared from two sets of gravity data. The first contains 700 detailed gravity readings taken along six roads at station spacings of 61 meters (Figure 2). All readings from this set either lie within the basin or within a 1.609 kilometers circumference of the basin's border. An additional 700 gravity readings were obtained from data of Johnson and others (1975). These readings lie outside the 1.609 km circumference of the basin's border.

The gravity map (Plate 1) defines both regional and local anomalies. Regionally, a general pattern of high gravity anomalies is evident on the west, and low anomalies occur on the east side of the basin. A strong NE-SW regional trend is evident on the gravity map. An E-W orientation of the regional trend becomes dominant in the southern portion of the map. Letters A-E, on the map designate local gravity anomalies.

Magnetic Data

The aeromagnetic map (Plate 2) show distinct regional and local trends (Virginia Division Of Mineral Resources Aeromagnetic 15-minute Maps; Dillwyn, 1970; Farmville, 1970). Magnetic anomalies in the area decrease in a NW-SE transverse. In addition, the anomalies indicate a strong NE-SW trend.

Figure 6: Plot of significant stream trends within the study area. The plots were generated for each 7.5 minute quadrangle within the study area. In addition, one plot has been generated to show the sum total of drainage trends. The degrees at the bottom of plots is the azimuthal range of streams. If peaks lie above the upper deviation bar it is deemed to be significant (Red Bar). Significant troughs lie below the lower deviation bar (Blue Bar).

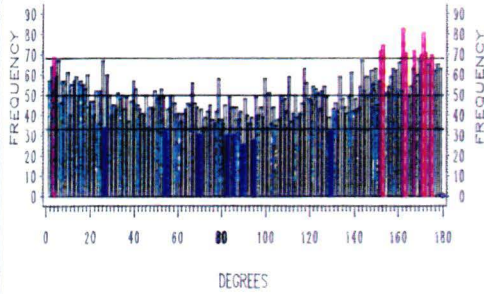
Upper Bar : Upper Third Deviation (Red Bar)

Middle Bar: Zero Deviation (Hollow Bar)

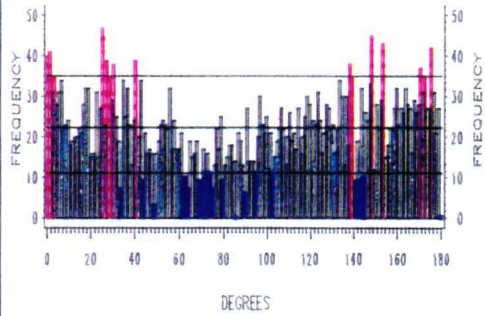
Lower Bar : Lower Third Deviation (Blue Bar)

STREAM TREND ANALYSIS

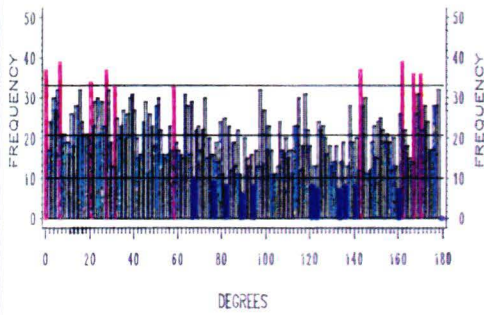
COMBINED



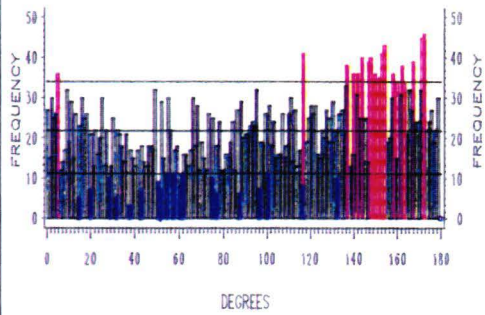
GOLD HILL



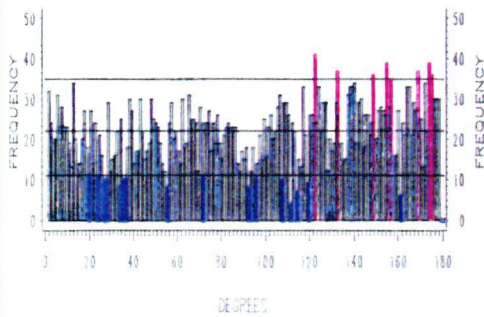
WILLIS MOUNTAIN



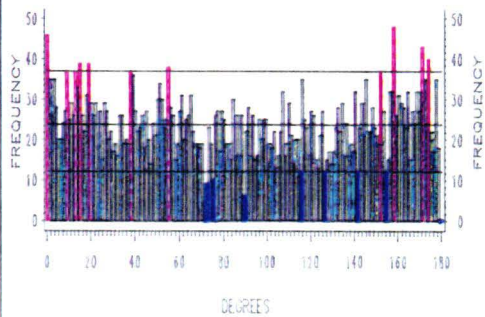
HILLCREST



FARMVILLE



RICE



Linear features and low closures, designated A-C on Plate 2, are the local anomalies identified on the magnetic map.

Radiometric Data

Three domains can be identified on the Radiometric Anomaly map (Plate 3). NW-SE profiles across the basin indicate radiometric anomalies west of the basin have a range of 100 to 200 count-per-second (cps). Radiometric anomalies generally have a range of 300 to 400 cps in the basin, and are higher than 400 cps east of the basin (Virginia Division Of Mineral Resources Aeroradiometric 15 minute Maps (Dillwyn, 1978; Farmville, 1978)).

PRELIMINARY GEOLOGIC INTERPRETATION

Before gravity modelling, a geologic interpretation is necessary, using the information presented in this chapter, to properly constrain the models. Without these constraints the gravity models could have an infinite number of solutions. The geologic interpretation will start with regional features, and terminate with a discussion of local features.

Regional Features

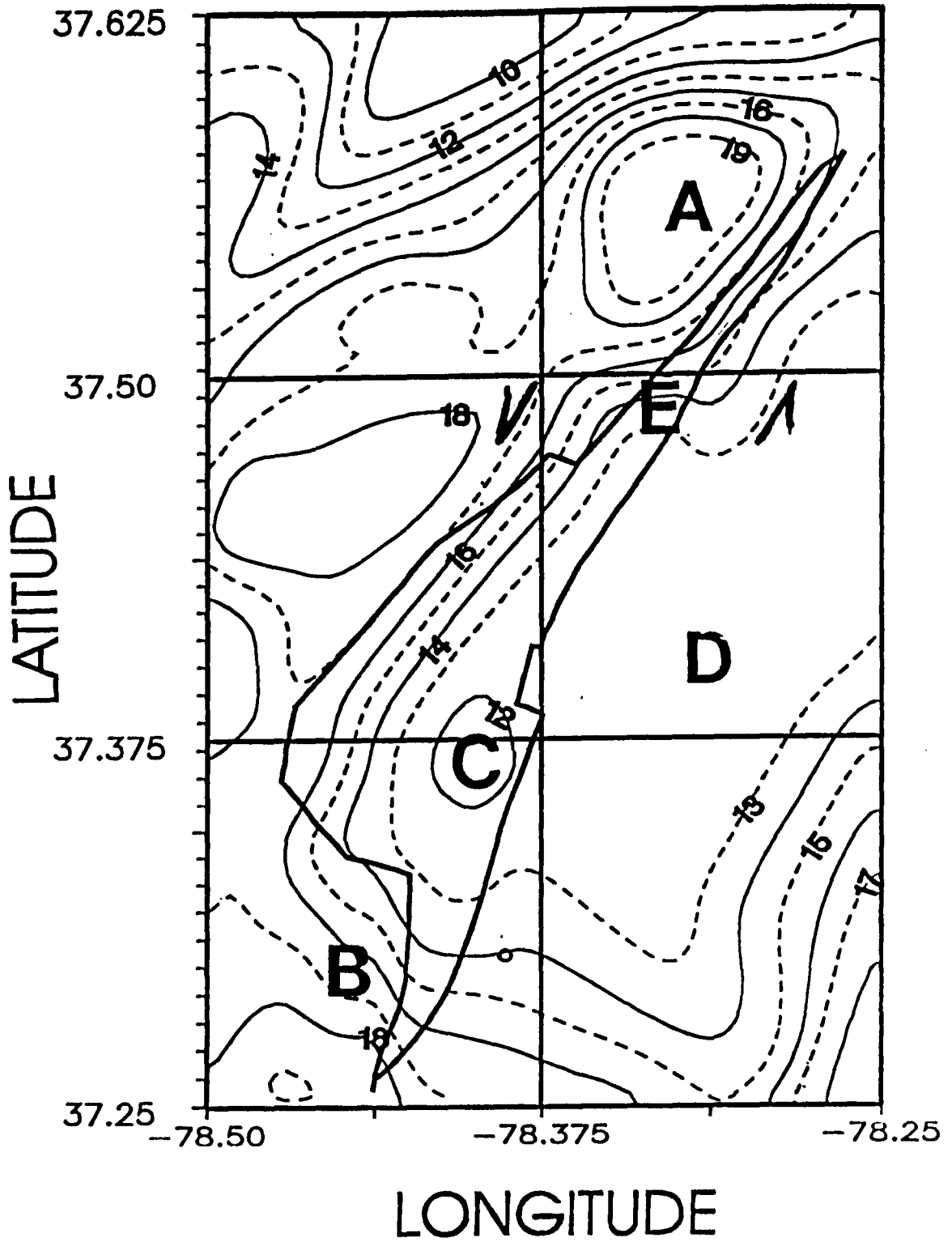
The regional NE-SW trend is the one feature common to all the geophysical anomalies, and geologic structures of the area (Plate 1,2,3; Figures 3, 4, 5). No other feature is common to both the geophysical and geological data. By closely examining

Figure 7: This is the Bouguer gravity field, shown on Plate 1, at the continuation level of +0.64 kilometers. The letters on this figure show the location of the following geologic features:

- A: Whispering Creek Anticline
- B: Diabase/Granophyre Dike
- C: Deepest Part Of Basin
- D: "Granitic" Gneiss Undifferentiated
- E: Possible Shear Zone (direction of shear shown
by arrows)

Note: Variation in gravity anomalies indicate that differences in density of the rocks can be seen at this level.

GRAVITY FIELD AT 0.64 KILOMETERS



the geophysical and geological data conclusions pertaining to the regional geology become apparent. Gravity and Magnetic maps are potential field data. This means that they measure the horizontal difference between densities (gravity), or magnetic susceptibilities (magnetic) of the lithology. A difference between two potential field readings indicates differences exist in the property of those rocks.

A wealth of information about the regional geology is contained on the gravity map (Plate 1). By drawing any NW-SE (X-X') profile on the gravity map, it is apparent that there are distinct differences in gravity values, leading to the conclusion that densities of lithologies along such a profile vary. This poses the question, whether the density variations are a result of shallow (< 10 km), or subcrustal features ?

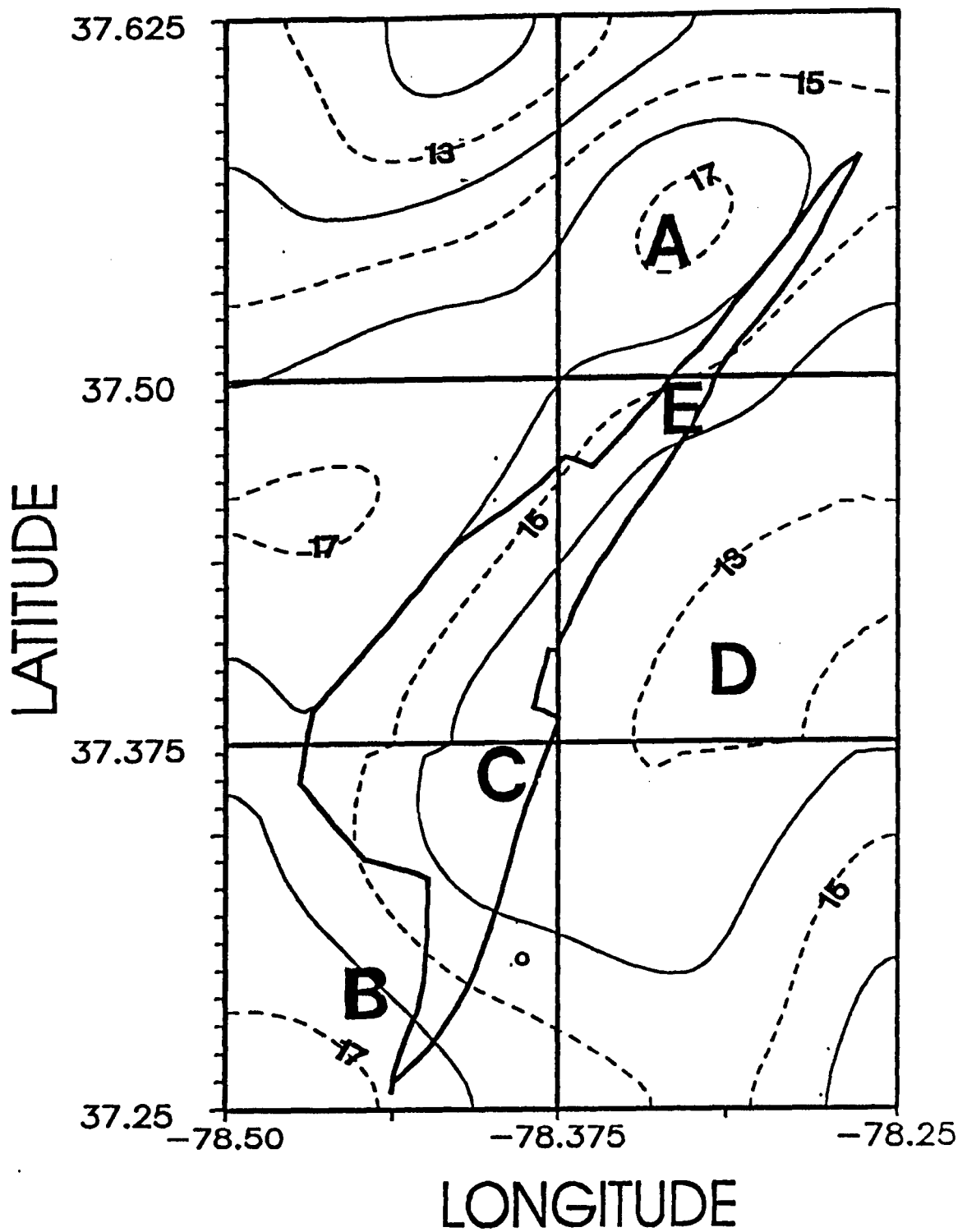
To address this problem, upward continuation of the gravity field (Plate 1) was performed. The upward continuation was done at various levels up to 8 kilometers (Figures 7, 8, 9). This resulted in the isolation of gravity anomalies attributed to density variations at the specified continuation level. This means that an upward continuation performed at 2 kilometers is providing a map of the variation in densities of rocks at a depth of 2 kilometers and higher, while upward continuation at 8 kilometers is providing data on the density of rocks at depth of 8 kilometers and more. It is apparent, from Figures 7, 8, and 9, that most of the gravity anomalies shown on Plate 1 are a result of density variations

Figure 8: This is the Bouguer gravity field, shown on Plate 1, at the continuation level of +2.89 kilometers. The letters on this figure show the location of the following geologic features:

- A: Whispering Creek Anticline
- B: Diabase/Granophyre Dike
- C: Deepest Part Of Basin
- D: "Granitic" Gneiss Undifferentiated
- E: Possible Shear Zone

Note: Variation in gravity anomalies indicate that differences in density of the rocks can be seen at this level.

GRAVITY FIELD AT 2.89 KILOMETERS



within the upper 8 kilometers of crust. At 8 kilometers, the NE-SW trend is apparent; although, the E-W trend (Plate 1) is no longer apparent in the southern portion of this map.

Magnetic anomalies, like gravity anomalies, show a strong NE-SW trend (Plate 2). In addition, the magnetic values generally decrease along NW-SE (X-X') profiles. This implies that the magnetic susceptibilities of the rocks, along such a profile, are different. With this information it can confidently be concluded that there are distinct lithologic breaks underneath and outside of the basin.

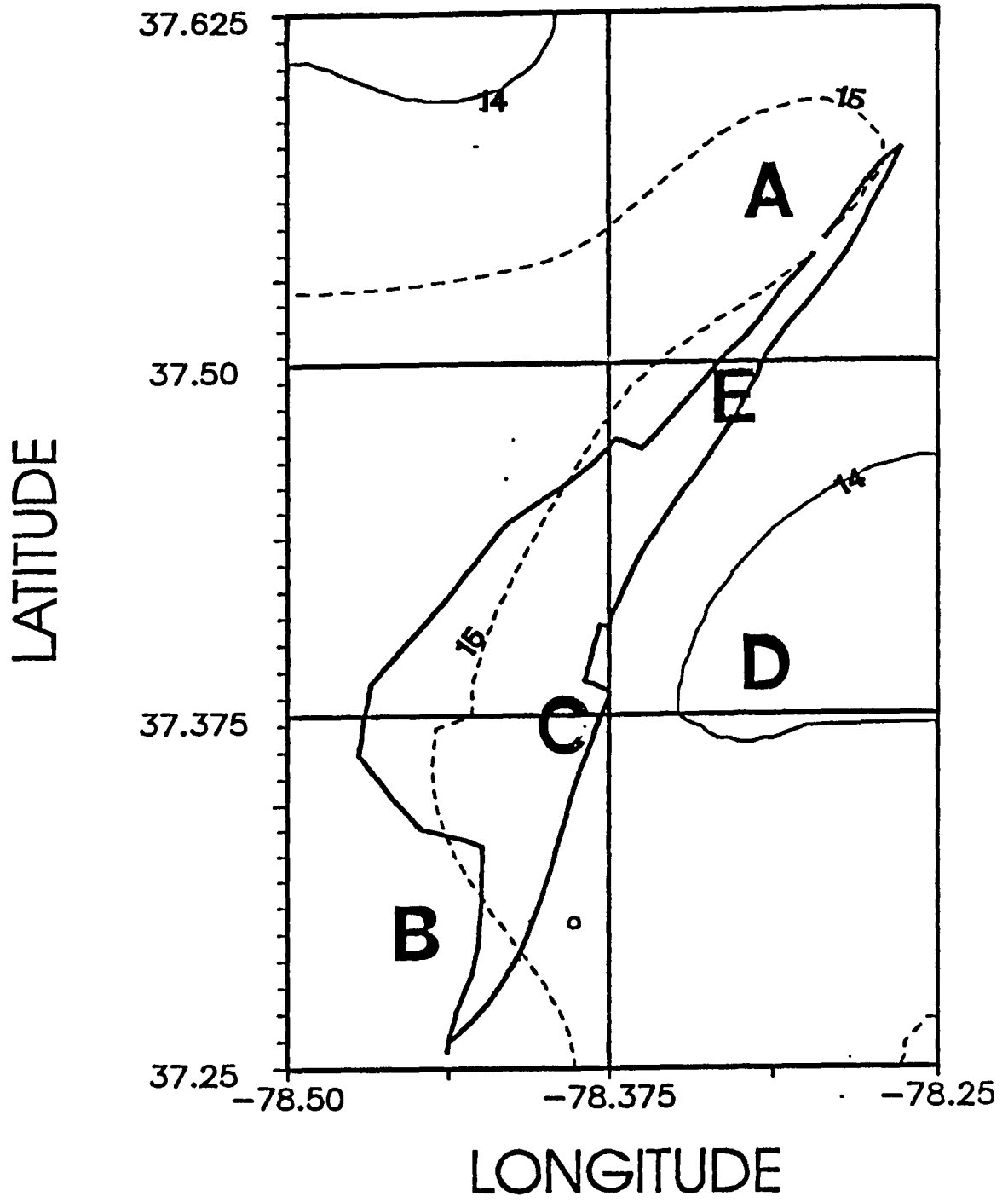
Both gravity and magnetic anomaly maps (Plates 1 and 2) show a definite change in the density and magnetic susceptibilities of rocks along NW-SE profiles. This is supported by the geology. Table 2, shows that there are several distinct lithologies in the study area. The geophysical properties of these rocks are listed in Table 3. The values in Table 3 are useful in approximating the regional surface geology. For example, using the gravity map (Plate 1) a general set of lithologic boundaries can be drawn, using the 15 milligal contour as a lithology break (Figure 10). The 15 milligal contour was chosen as the reference contour because it was present on the 8.00 kilometer continuation map (Figure 9), meaning it is a regional phenomenon. Figure 10 shows four distinct lithologic groups. These groups are from oldest to youngest: Chopawamsic Formation, "Granitic" Gneiss, Arvonian Formation, and Triassic rocks. This map is very close to the

Figure 9: This is the Bouguer gravity field, shown on Plate 1, at the continuation level of +8.00 kilometers. The letters on this figure show the location of the following geologic features:

- A: Whispering Creek Anticline
- B: Diabase/Granophyre Dike
- C: Deepest Part Of Basin
- D: "Granitic" Gneiss Undifferentiated
- E: Possible Shear Zone

Note: Variation in gravity anomalies indicate that differences in density of the rocks can be seen at this level.

GRAVITY FIELD AT 8.00 KILOMETERS



detail maps of Marr (1980) and Brown (1969). Because of the good correlation, geophysical data was used to make inferences about lithologies shown on Plate 4.

Radiometric data provides further proof that the study area is comprised of the lithologic units defined above (Plate 3). These domains correlate with lithologic units in the area. NW-SE profiles across the basin indicate radiometric anomalies west of the basin have a range of 100 to 200 counts-per-second (cps). Radiometric anomalies generally have a range of 300 to 400 cps in the basin, and are generally higher than 400 cps, east of the basin.

Structurally, foliation, bedding, and joint measurements all have concentration of poles whose average plane strike lies within 25 degrees of the NE-SW regional trend. The dominant foliation pole concentration, has an average strike of N15°E and dip of 35 degrees southeast (Figure 3). The average bedding strike is N45°E and dips 30 degrees northwest (Figure 4). The secondary joint set has an average strike of N70°E and dips 80 degrees southeast (Figure 5). In addition, the rectified stream analysis identified a significant drainage trend in the azimuthal range of 030 to 040 degrees.

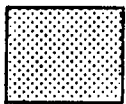
Local Analysis

An examination of local geophysical and geological anomalies is necessary to complete the preliminary geological analysis of the area. Once again, examination of the gravity

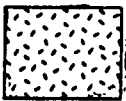
Figure 10: This is the Bouguer gravity field, shown on Plate 1, at the continuation level of +0.64 kilometers. This maps show the four lithologies based on gravity values. The reference line for dividing the lithologies is 15 milligals.

Note: Variation in gravity anomalies indicate that differences in density of the rocks can be seen at this level.

LITHOLOGIES:



CHOPAWAMSIC FORMATION



"GRANITIC" GNEISS UNDIFFERENTIATED

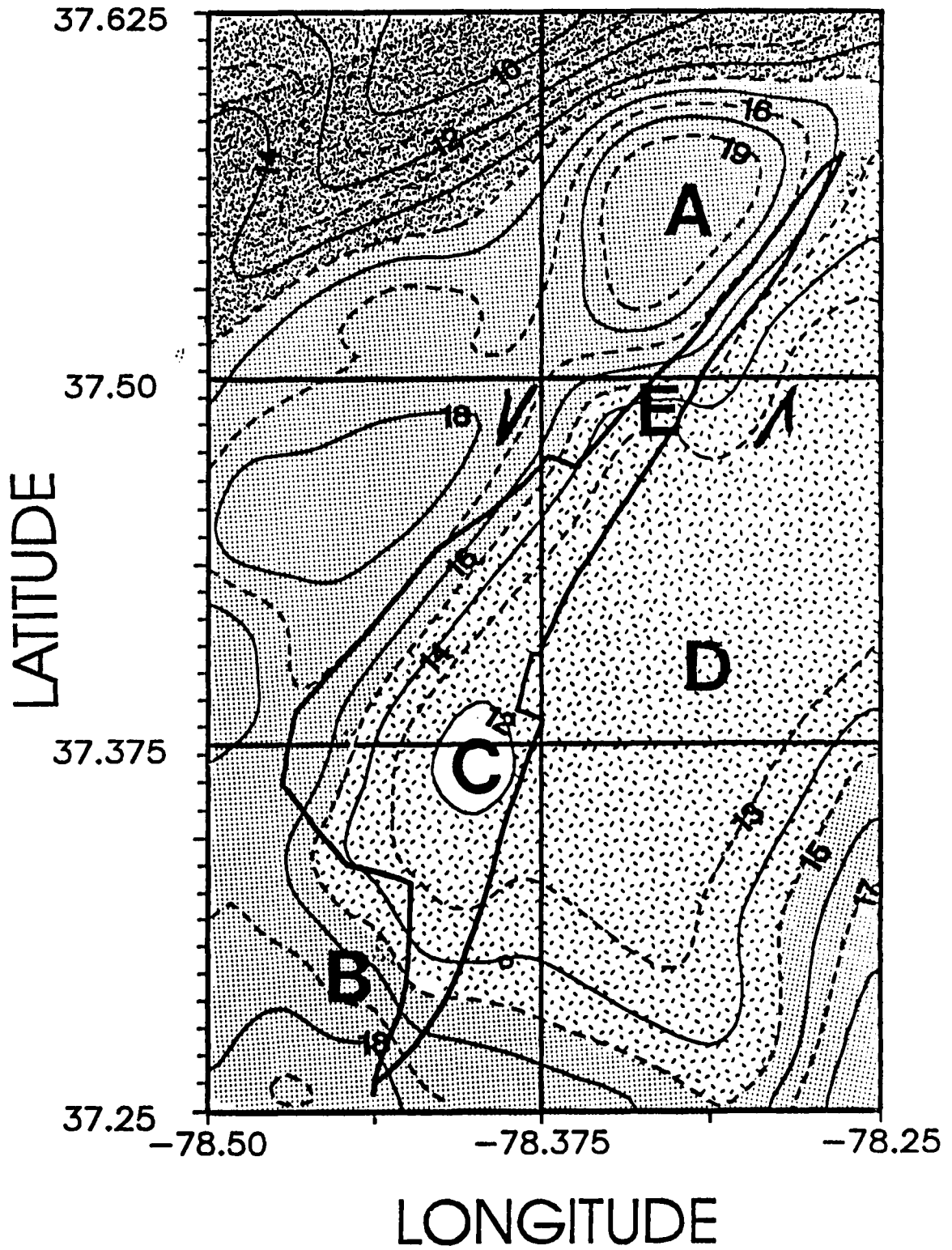


ARVONIA FORMATION



TRIASSIC ROCKS

GRAVITY FIELD AT 0.64 KILOMETERS



and magnetic maps indicate localized features. Two local anomalies are common to both the gravity (Plate 1) and magnetic (Plate 2) maps. The first feature is the gravity and magnetic lows found on the eastern margin of the Farmville Basin, marked 'C' respectively. Another common feature to both maps is a NNW-SSE diabase/granophyre dike marked 'B' on both maps.

Labels A-E, on the gravity map (Plate 1), are the locations of localized gravity anomalies. The circular high marked 'A' (Plate 1) is in excess of 21 milligals. This high is attributed to the Whispering Creek Anticline (Brown, 1969). A sharp high amplitude feature marked 'B' on the gravity map is a diabase/granophyre dike that exceeds 488 meters in width, across U.S. Highway 460E. At location 'C' the gravity values decrease below 10.5 milligals. It is at this point where the deepest portion of the basin is believed to exist. The elliptical gravity low 'D' is typical of intrusive bodies (Griffin, 1949). An unusual gravitational anomaly, marked 'E' (Plate 1) is thought to be a remnant of a shear zone. This conclusion is made from the 'Z' pattern displayed by the gravity contours (Plate 1). The 'Z' pattern indicates a left-lateral sense of shear has occurred. If this is a shear zone, then projecting it south indicates it continues underneath the basin.

The upward continuation maps (Figures 7, 8, and 9) give an approximate depth of the local features. As the gravity

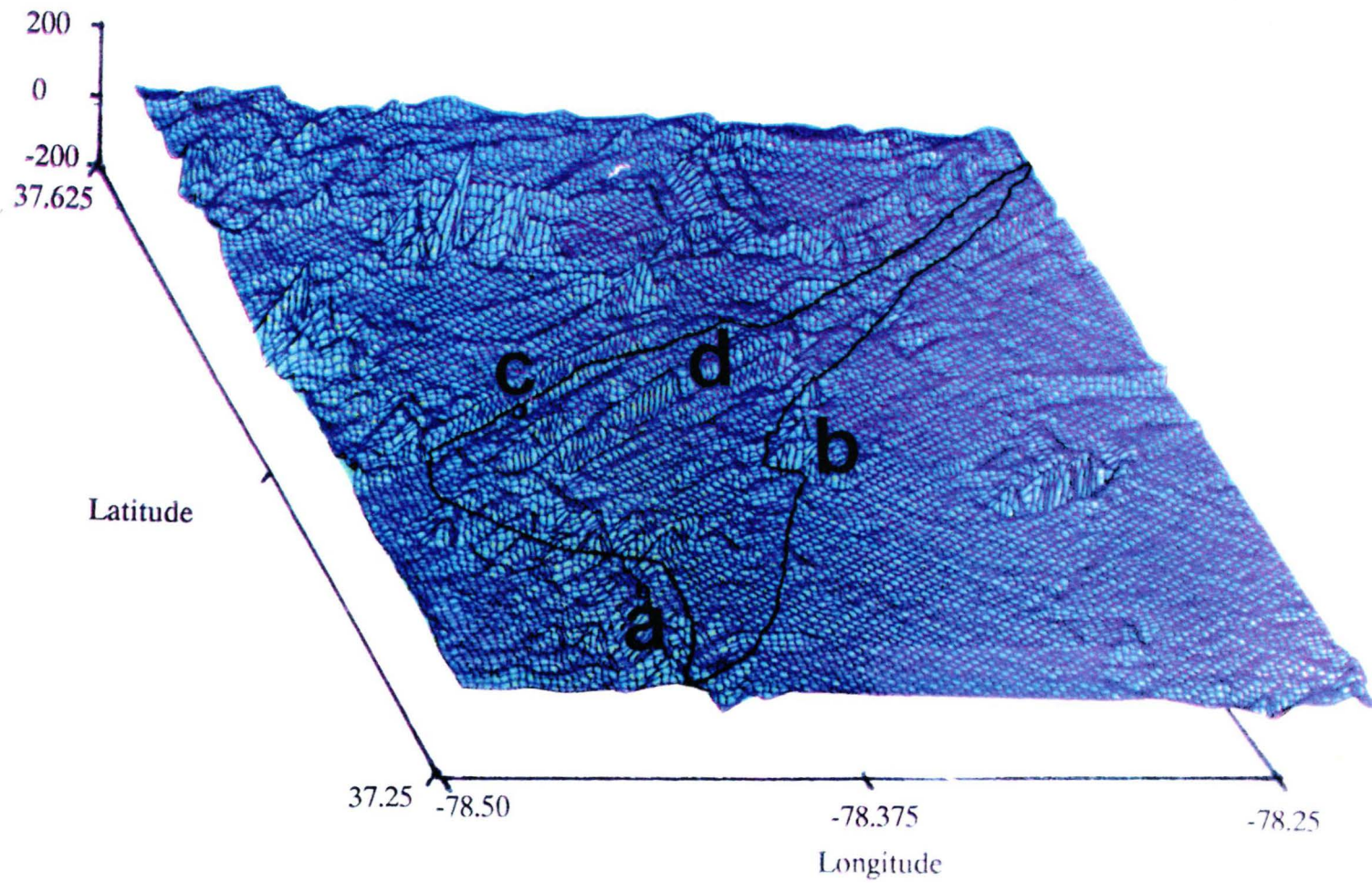
field is continued upward regional features are emphasized, as previously discussed. Remember, the upward continuation is a sampling of the variation of densities at the continuation level; therefore, if a local anomaly is no longer present at a continuation level then the horizontal variation in rocks that caused that anomaly is no longer present. The result is that the maximum depth of a local anomaly can be determined using upward continuation.

At the continuation level of 0.64 kilometers all the localized anomalies are still definable; although, the diabase/granophyre dike ('B', Plate 1) is barely discernable. After the 1 kilometer continuation the circular gravity anomaly, 'C' Plate 1, is no longer present. This suggest that the basin is less than 1.00 kilometer in thickness. If this is the case then no gravity model can have the basin exceeding 1.00 kilometers in depth. Continuing the gravity field to 2.89 kilometers eliminates the dike anomaly, 'B' Plate 1. At the continuation level of 8 kilometers, the gravity map is less sinuous, the Whispering Creek gravity high ('A', Plate 1) is no longer present, and the strong E-W trend in the southern portion of the study area is not present (Figure 9).

Figure 11 is the second vertical derivative of the gravity field. This map has several interesting features. The linear features that lie outside the basin are diabase dikes ('a' and 'b'). On the basin margin and inside the basin are linear highs adjacent to lows ('c' and 'd') which are

Figure 11: Second vertical derivative of the study area gravity field. Locations 'a' and 'b' mark the location of diabase dikes, while the locations 'c' and 'd' mark the location of possible mylonite zones.

Second Vertical Derivative Map



thought to be mylonite zones. This is supported by field evidence at location 'c'. Inside the basin these features are believed to mylonite zones; however, no field evidence was found to support or disprove this hypothesis. No diabase outcrop was found in the vicinity of these highs, eliminating possibility that the linear highs in the basin are a result of diking. Gravity modelling should take into account all features shown on this map.

High frequency magnetic values indicates the presence of dikes and a basin that is relatively shallow. Linear magnetic features present on the magnetic map (Plate 2) are diabase/granophyre dikes. The area marked 'B' and the linear high east of 'C' on the magnetic map are large dikes. The dike marked 'B' exceeds 488 meters in width across U.S. Highway 460E. The low marked 'C' on the magnetic map (Plate 2) is attributed to the deepest part of the basin.

Field data provides limited insight into local structures of the area, because of the large scale on which it was conducted. One exception is the variation of bedding dips within the basin. Mapping conducted along State Road 636 (Plate 4) shows a variance in dips from shallow to steep to shallow. This phenomenon is a result of some type of localized displacement. The cause of this displacement has to be addressed in any gravity model.

SUMMARY

The study area is dominated by a NE-SW regional trend. This trend is present in the basement structural grain of the rock, as well as the local lithologies. As a result, this trend can be identified on all geophysical and geological maps, data, and analyzes. One implication of this finding is that most of the structures in the area are dependent on this feature.

The relationship of the various lithologies in the area are a second factor to consider in defining the structural controls on the basin geometry. There are five lithologic units in the area; however, only the Chopawamsic Formation, "Granitic" Gneiss Undifferentiated, and Dikes are in surficial contact with the Triassic rocks. Each of these lithologies have unique physical properties (i.e. densities, magnetic susceptibilities, and radioactive elements). It is the unique physical properties of these lithologies that cause a majority of the local anomalies found on the geophysical maps (Plates 1, 2, and 3). These anomalies support the hypothesis that the Farmville Basin covers the lithologic contact between the Chopawamsic Formation and the "Granitic" Gneiss. If this is the case, then the lithologic contact is a possible plane of weakness along which faults could form. Only subsurface modelling can verify this hypothesis.

CHAPTER 4



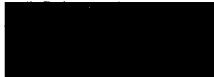
GRAVITY MODELLING

INTRODUCTION

Gravity models are based on data obtained from six profiles that cross-cut the Farmville Basin nearly perpendicular to the regional geophysical and geological trends. Four lithologic units were used to create the gravity models. The modelled lithologies from oldest to youngest are the Chopawamsic Formation, "Granitic" Gneiss Undifferentiated, Triassic rocks, and Diabase/Granophyre dikes. Density listing of the Arvonian Formation is not given because it is not present in the gravity models. Densities for the modelled lithologies are listed in Table 4. These values were calculated from a series of density measurements. The density values for the Triassic rocks were obtained by taking the mean of the density measurements along the southern traverse across the basin (Wilkes and Lasch, 1979). Density measurements were not taken for basin rocks because most of the outcrops were highly weathered. Two categories of dikes are distinguished based on densities. One group of dikes have an average density of 2.99 g/cm^3 and the second group have an average density of 2.89 g/cm_3 . Most dikes that cross the gravity profiles contained granophyres; therefore, the density value of 2.89 g/cm^3 was used for modelling.

Table 4: Densities of the lithologies used in the gravity models. This legend is referenced in the gravity models that follow.

LEGEND

	UNIT	DENSITY (g/cm ³)
	CHOPAWAMSI FORMATION	2.845
	GRANITIC GNEISSES	2.775
	TRIASSIC ROCKS	2.55
	MESOZOIC DIKES	2.88

- + : OBSERVED GRAVITY CURVE**
- * : THEORETICAL GRAVITY CURVE**
- : REGIONAL GRAVITY GRADIENT**

The assigned density when modelling the "granitic" gneiss is much higher than the measured densities. The density value used for the "granitic" gneiss is from the density values of the Columbia Granite (Keller and others, 1985). The densities assigned to the modelled lithologies remained constant in all profiles. This gave additional constraints to the gravity models.

PROFILES

Figure 2 shows the location of the modelled gravity profiles. Discussion of these models will begin with U.S. Highway 460E continuing north and ending with State Road 622. A description of the lithologies used in the models is given in Table 4. Each of the modelled profiles is comprised of two graphs. The upper graph is a plot of the observed and theoretical Bouguer anomalies. The lower graph is the gravity model that produced the theoretical curve, shown on the upper graph. The regional gravity gradient is represented by the solid line on the upper graph. The regional gradients are related to the deeper structure, and are used to identify local gravitational anomalies. The term "residual" is used to describe the variation of the observed gravity with respect to the regional gradient. In modeling one must keep in mind the basin's geometry, strike and dip orientations of faults and dikes, as well as the density contrast of the various lithologies.

Models indicate two sets of faults are present in the study area. Master faults (solid lines in lower graph on Figures 13-16) are believed to be reactivated Paleozoic faults. The greatest displacement occurred along such faults in the study area. Splay faults (dashed line in lower graph) are believed to be Mesozoic in age, and are thought to have formed along existing planes of weakness (other than faults) in the structural grain of the basement rocks. All faults were drawn on the models after each model was completed. The relative displacement of each fault is shown by the arrows. Each fault is drawn so that the models were as close to being a balanced cross-section, as possible.

U.S. Highway 460E Profile

U.S. Highway 460E crosses the southern portion of the basin. Figure 12 is the gravity model produced for this profile. The profile is 6705 meters in length and modelled to a depth of 3657 meters. A model depth of 2800 meters is shown for this profile to keep uniformity between each profile. A model depth of 2800 meters is possible with this profile because the lithology appear to be homogenous below 2800 meters. The anomaly marked on the profile is attributed to a diabase/granophyre dike, as shown in the model. Location of a dike at this location is supported by outcrop found along U.S. 460E (Plate 4), as well as the geophysical evidence previously discussed. In outcrop, the dike is at least 305

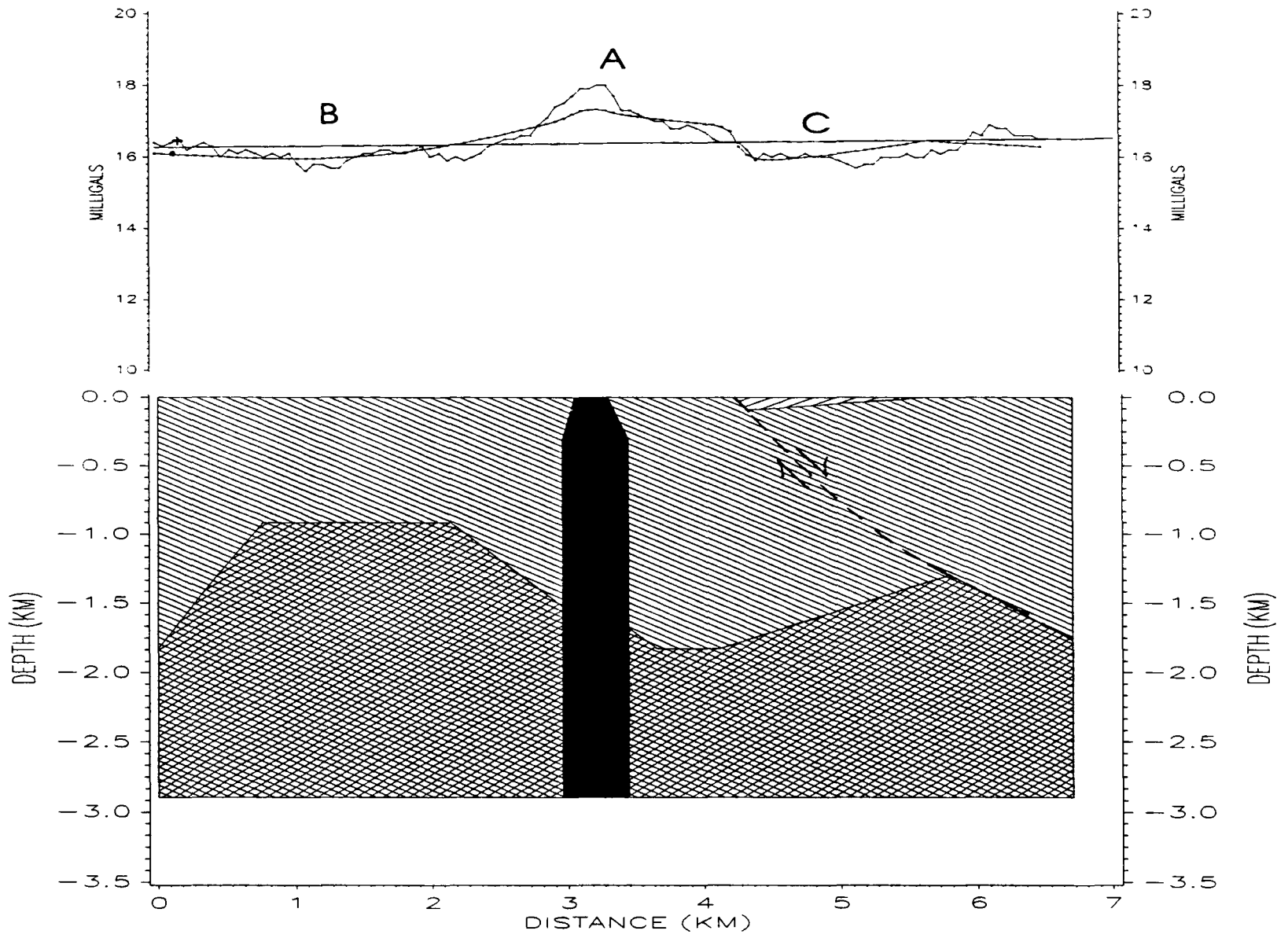
Figure 12: The gravity model developed for the profile U.S. 460E. The lower graph is the geologic model that generated the calculated Bouguer anomalies shown on the upper plot. Letters shown on the gravity profile are representative of the geologic features:

- A: "Massive" Diabase/Granophyre Dike Anomaly
- B: "Granitic" Gneiss Anomaly
- C: Triassic Basin Anomaly

Arrows: Indicate direction of displacement along fault

Dashed Line: Secondary listric normal faulting

Note: Refer to Table 4 for description of lithologies in models.



meters in width. This width increases to 488 meters at depth. Residual lows, marked 'B' and 'C', occur on both sides of the two milligal high. The residual low 'B' is interpreted to be the result of the "granitic" gneiss undifferentiated lying 305 meters below the surface. Triassic rocks of the basin are responsible for the low marked 'C'. Modelling indicates the Chopawamsic Formation is present east of the basin. Length and depth of the basin is 1402 meters, and 91 meters, respectively. The length of the modelled basin is greater than suggested by Johnson and others (1975). Basin width, along this profile, is based on the soil map of Prince Edward County (Henery et. al, 1949). The western border fault, of the basin is defined as a splay fault. This fault dips 35 degrees SE, at the surface, and decreases with depth. A 10 to 15 degree difference exist between the average dip of foliation (45 degrees) and the splay fault. The fault is shown to have normal slip displacement. Palinspastic reconstruction of this profile suggests 5 percent extension has occurred.

State Road 637 Profile

State Road 637 is 3.2 kilometers north of U.S. Highway 460E (Figure 13). This profile is 9448 meters in length and modelled to a depth of 2743 meters. Observed Bouguer gravity values indicated there are several residual highs interpreted. These highs are interpreted as dikes. Outcrop and float found along the profile support this interpretation. Corresponding

Figure 13: The gravity model developed for the profile State Road 637. The lower graph is the geologic model that generated the calculated Bouguer anomalies shown on the upper plot. Letters shown on the gravity profile are representative of the geologic features:

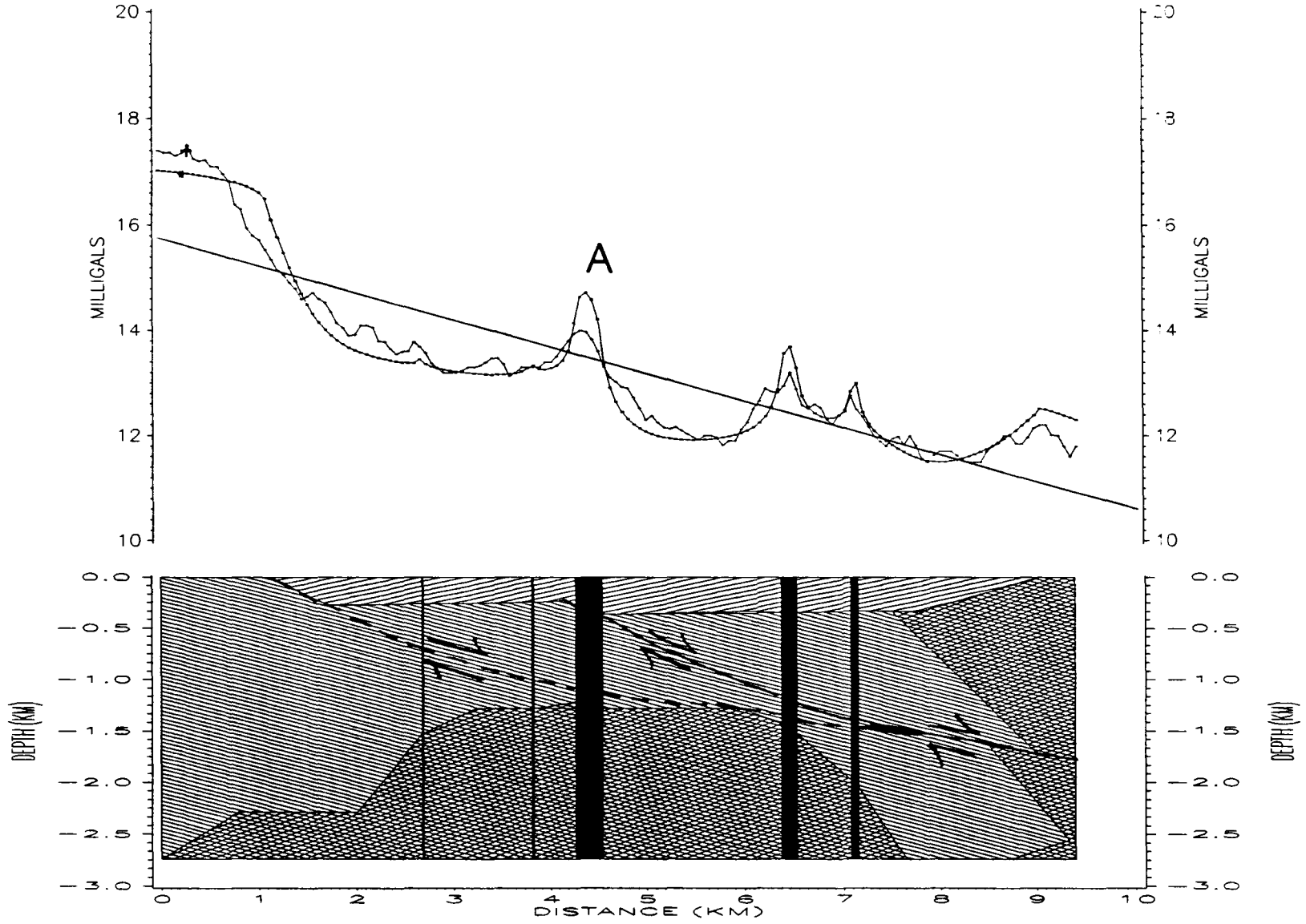
A: "Massive" Diabase/Granophyre Dike Anomaly

Arrows: Indicate direction of displacement along fault

Dashed Line: Secondary listric normal faulting

Solid Line: Primary listric normal faulting

Note: Refer to Table 4 for description of lithologies in models.



dike locations are shown on the model. The largest dike is 274 meters in width ('A'), and is the same dike found along profile U.S. 460E. Dike width has decreased 61 meters within 3.2 kilometers. Basin length, along profile State Road 637, is 7925 meters, and is modelled to a depth of 343 meters. Rotational listric type faulting (Wernicke and Burchfield, 1982) is clearly indicated on the model. Both master (solid line) and splay faults (dashed line) are identified in the model, each shows normal slip displacement. Splay faults form the western margin of the basin. At the surface the splay fault dips 24 degrees to the southeast. The master fault is covered by the Triassic rocks. The greatest displacement occurs along the master. Ten percent extension is estimated for this profile, as a result of palinspastic reconstruction.

State Road 636 Profile

State Road 636 is the longest of all modelled profiles. It is 10896 meters in length and is modelled to a depth of 2743 meters (Figure 14). Two broad residual highs, marked 'A' and 'B' on the profile represent high density country rocks occurring along the basins' margin and a 61 meter dike, respectively. This dike contains granophyres and is a continuation of the dike present on profile U.S. Highway 460E and State Road 637. The low, marked 'C', is caused by the Triassic rocks. Basin length is 8229 meters, and is modelled to a depth of 617 meters making it the deepest part of the

Figure 14: The gravity model developed for the profile State Road 636. The lower graph is the geologic model that generated the calculated Bouguer anomalies shown on the upper plot. Letters shown on the gravity profile are representative of the geologic features:

A: Chopawamsic Formation Anomaly

B: "Massive" Diabase/Granophyre Dike Anomaly

C: Triassic Basin Anomaly

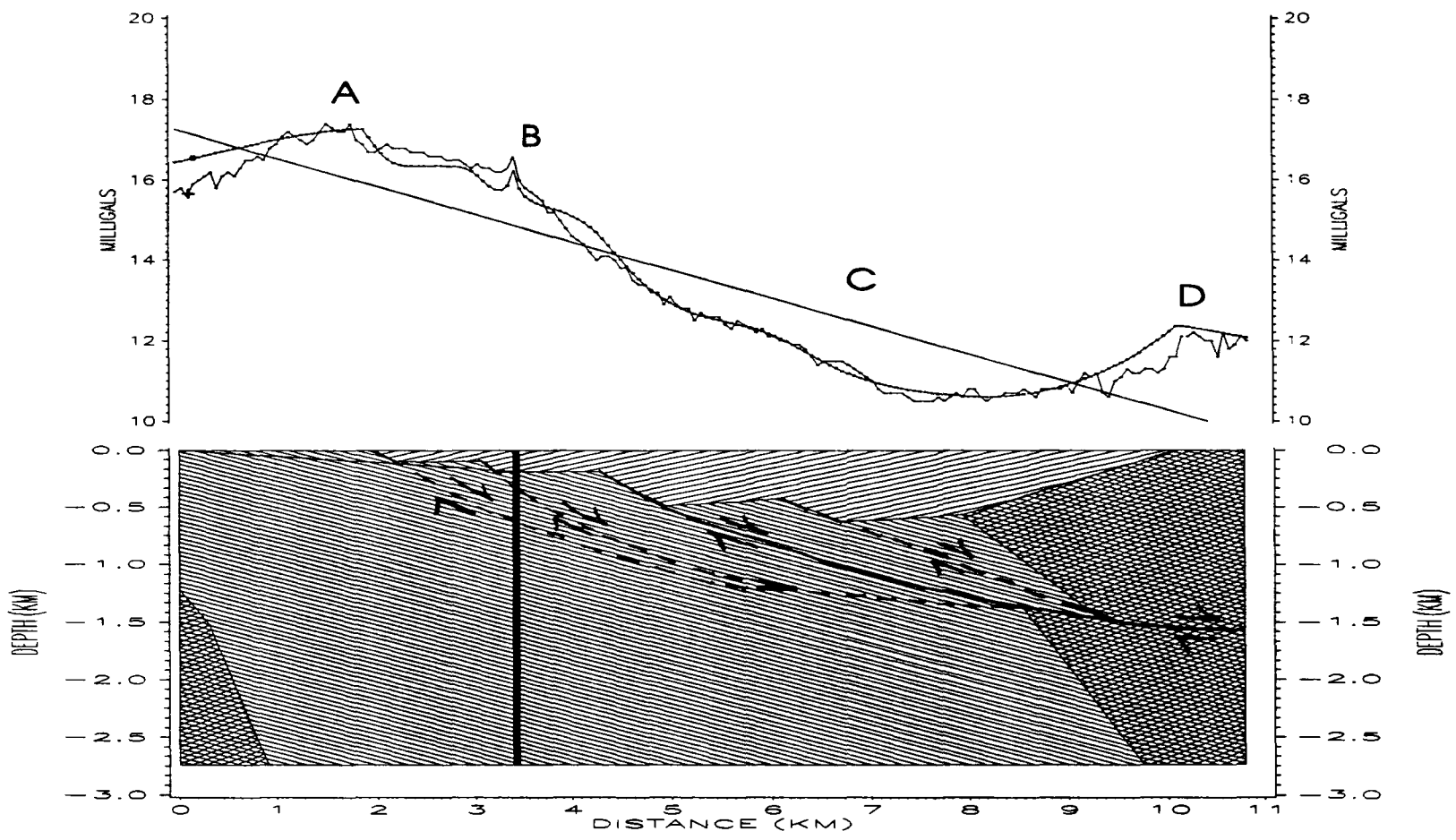
D: "Granitic" Gneiss Anomaly

Arrows: Indicate direction of displacement along fault

Dashed Line: Secondary listric normal faulting

Solid Line: Primary listric normal faulting

Note: Refer to Table 4 for description of lithologies in models.



basin. Unlike existing Mesozoic basin models, the deepest section of the Farmville basin lies along its' eastern margin. This conclusion is supported by the low closures found on both gravity and magnetic contour maps (Plates 1 and 2). Rotational listric normal slip movement is displayed by both the master and splay faults. A splay fault forms the western margin of the basin, dipping 28 degrees to the southeast, on the surface. All faults shallow with depth cross-cutting the foliation. Extension of 15 percent was calculated for this model after palinspastic reconstruction.

State Road 634 Profile

Figure 15 is the gravity model of State Road 634. The profile is 8500 meters in length and is modelled to a depth of 2743 meters. No sharp high amplitude residuals are present on this profile, meaning that no dikes greater than 50 meters cross the profile. Field evidence supports this aspect of the model. A broad residual low, marked 'A', is caused by the basin. Along this profile the basin is 3554 meters in length and 427 meters in depth. As in previous profiles the deepest part of the basin lies along its eastern margin. Both splay and master faults are present along this profile. The western margin of the basin is bounded by a splay fault with the master fault laying underneath the basin rocks. All faults are listric normal slip with the western border fault dipping to the SE at 28 degrees. The palinspastic

Figure 15: The gravity model developed for the profile State Road 634. The lower graph is the geologic model that generated the calculated Bouguer anomaly shown on the upper gravity profile. Letters shown on the gravity profile are representative of the geologic features:

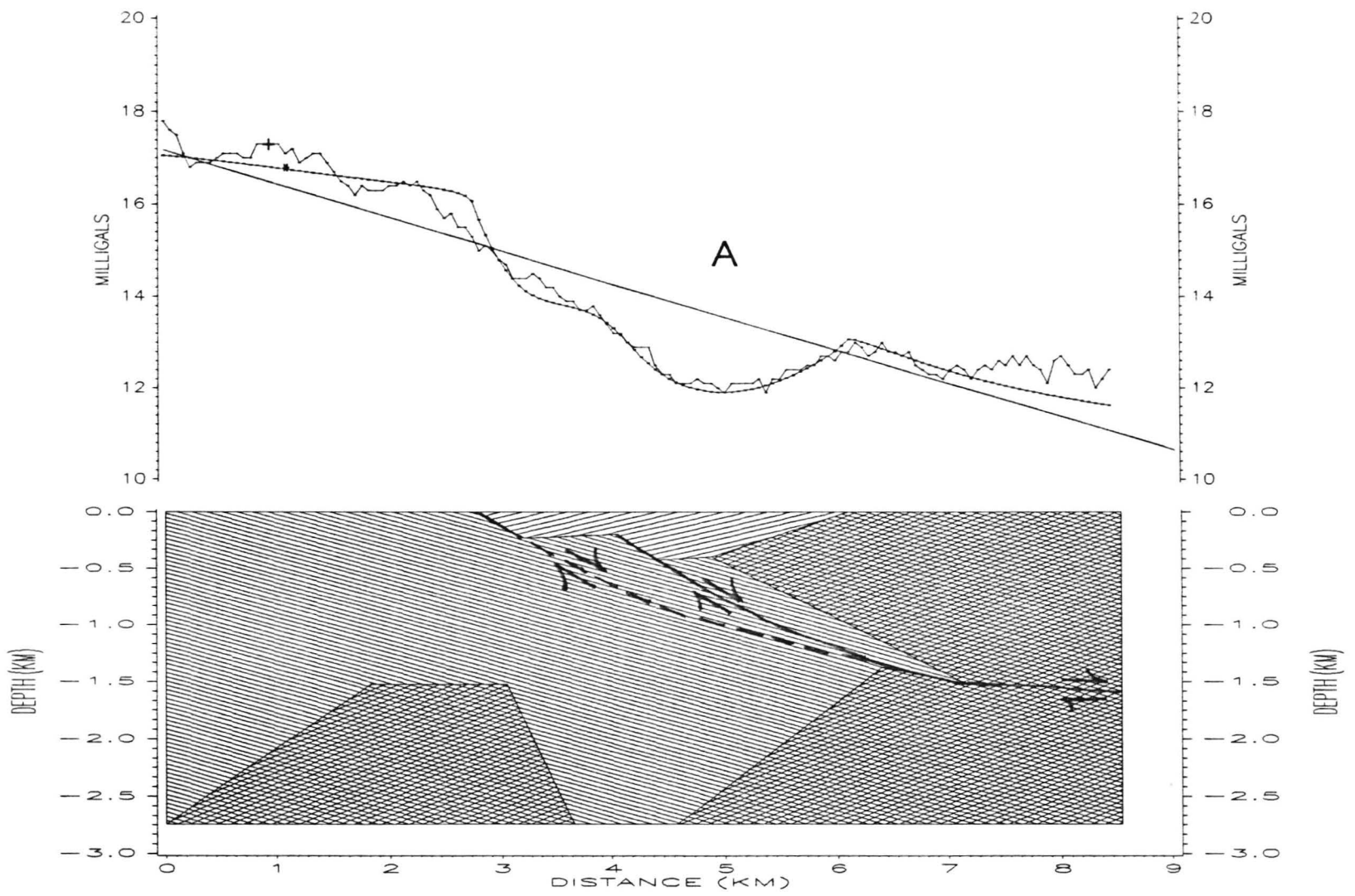
A: Triassic Basin

Arrows: Indicate direction of displacement along fault

Dashed Line: Secondary listric normal faulting

Solid Line: Primary listric normal faulting

Note: Refer to Table 4 for description of lithologies in models.



reconstruction of this model indicates a maximum of 10 percent extension has occurred along this profile.

U.S. Highway 60 Profile

The gravity profile and model for U.S. Highway 60 is shown in Figure 16. Profile length is 3353 meters with a modelled depth of 2591 meters. Residual highs are found at the NW and SE ends of this profile. These highs are attributed to the higher density country rocks that surround the basin. The residual low, marked 'A', is a typical pattern of a full graben basin; however, modelling indicates the basin is a true half graben with listric type fault geometry. The basin is 2591 meters in length and 259 meters in depth along this profile. As in the four previous profiles, a splay fault forms the western margin of the basin. The border fault dips 25 degrees to the southeast, decreasing at depth. Unlike the four previous profiles, evidence suggests the master fault lies east of the basin. Palinspastic reconstruction of the profile was difficult because of the individual unit shapes; however, it is estimated that 11 percent of extension has occurred.

State Road 622

The northern most of the modelled profiles is State Road 622 (Figure 17). This profile has a length of 3231 meters and is modelled to a depth of 3231 meters. The basin is 914

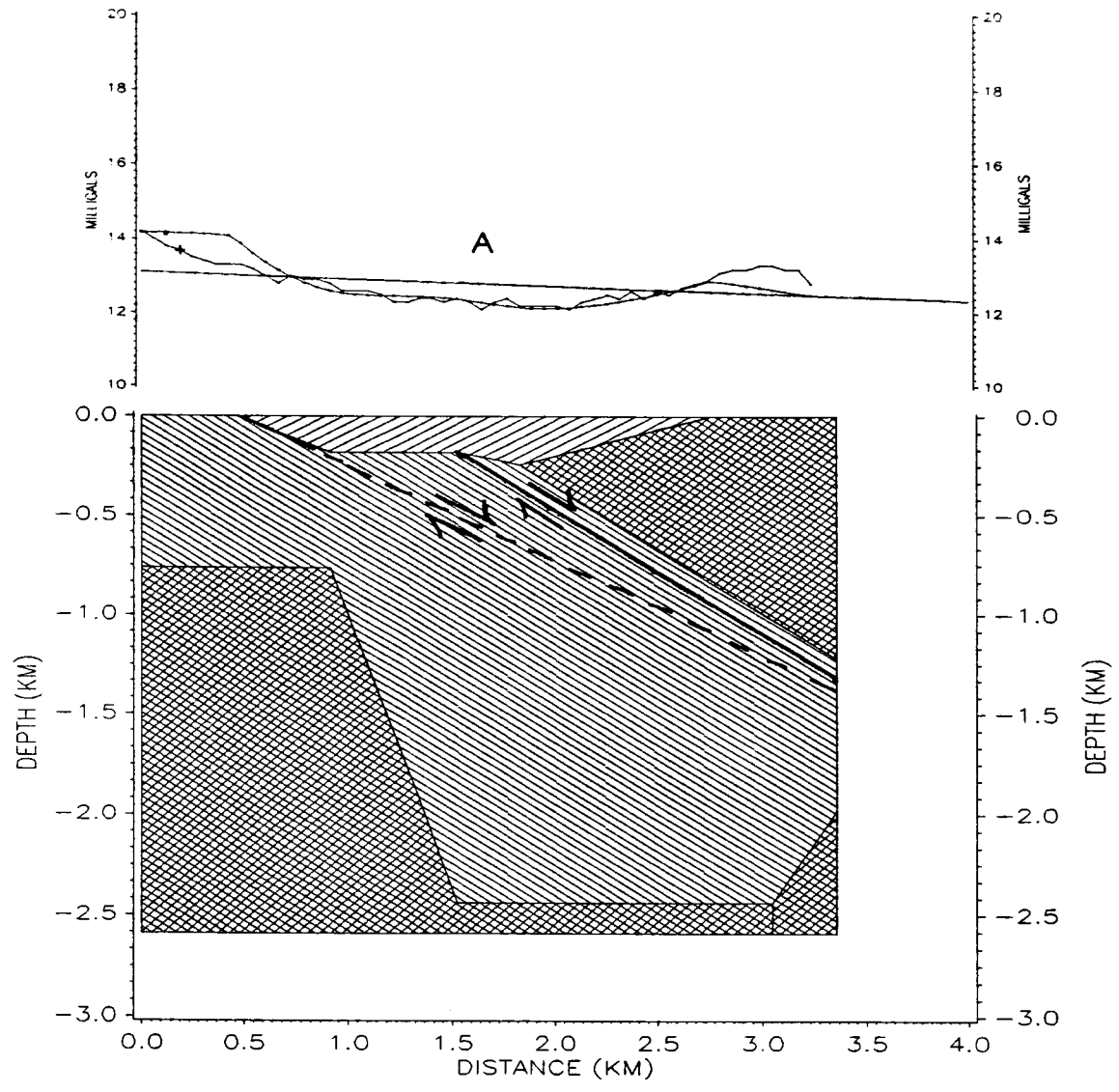
Figure 16: The gravity model developed for the profile U.S. Highway 60. The lower graph is the geologic model that generated the calculated Bouguer anomaly shown on the upper gravity profile. Letters shown on the gravity profile are representative of the geologic features:

A: Triassic Basin

Dashed Line: Secondary listric normal faulting

Solid Line: Primary listric normal faulting

Note: Refer to Table 4 for description of lithologies in models.



meters and is 122 meters in depth at this location. A splay fault forms the basin's western margin, dipping to the southeast at 26 degrees. The fault indicates normal displacement has occurred. As the fault shallows with depth it cross-cuts the foliation. It is believed that the master fault lies east of the profile section. Outcrop east of this profile showed mylonitic signs; although the highly weathered condition of the rocks proved inconclusive. Reconstruction of this profile indicates this area of the basin has undergone 8 percent extension.

SUMMARY

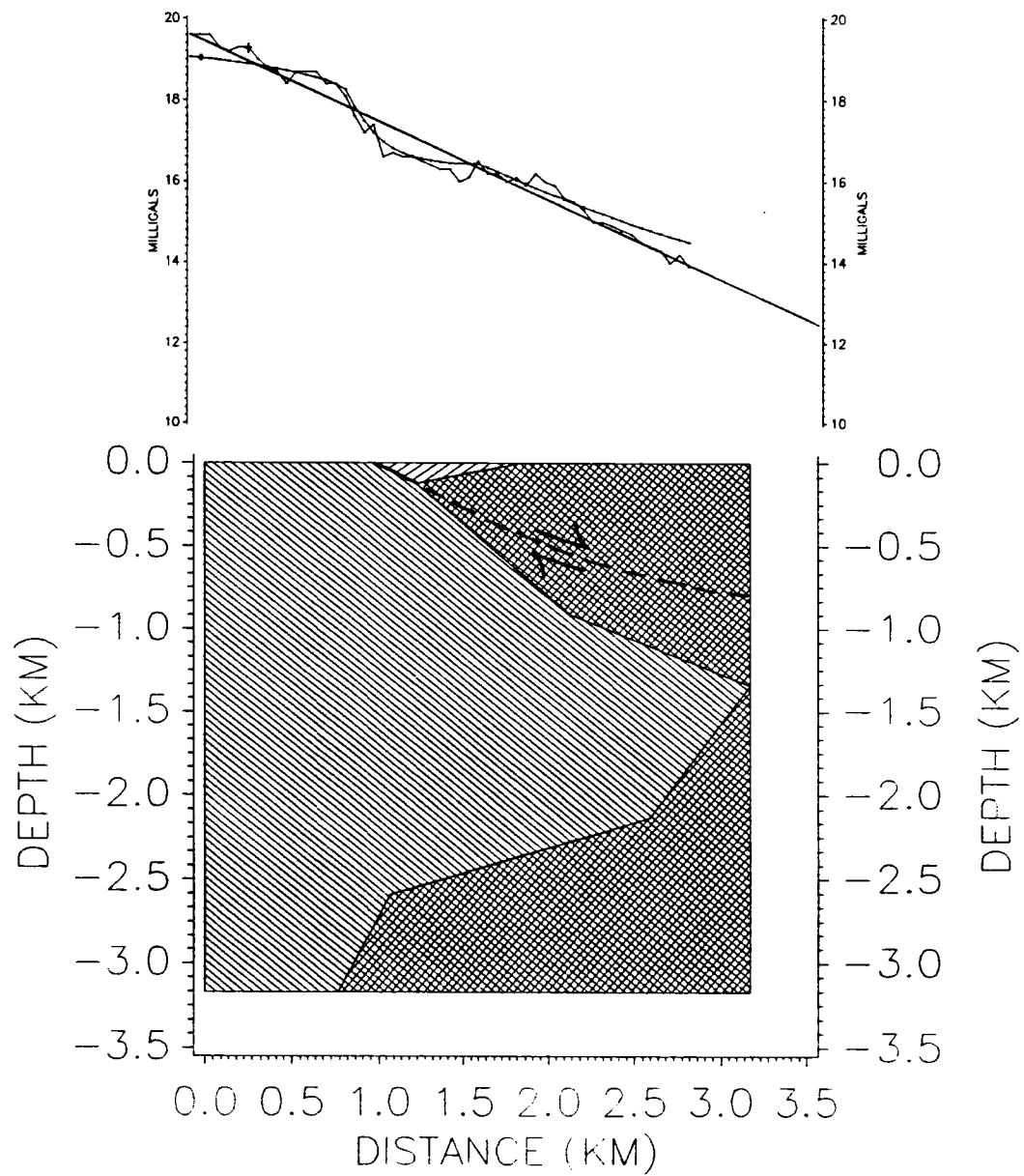
Gravity models show the subsurface relationship of the lithologies present in the area. All models indicate the western margin of the Farmville Basin is bounded by splay faults with the master fault(s) lying beneath or east of the basin. Along U.S. Highway 460E and State Road 622 the master fault lies to the east of the profiles. Modelling further indicates the basin's geometry is of normal, listric, rotational-type faulting described by Wernicke and Burchfield (1982). When averaged, the calculated extension of the individual profiles is 9.8 percent. Indicating that at least 9.8 percent extension has occurred in the study area. It is to be noted that the total extension does not include extension caused by dilation as a result of dike emplacement. Extension

Figure 17: The gravity model developed for the profile State Road 622. The lower graph is the geologic model that generated the calculated Bouguer anomaly shown on the upper gravity profile. Letters shown on the gravity profile are representative of the geologic features:

A: Triassic Basin

Solid Line: Primary listric normal faulting

Note: Refer to Table 4 for description of lithologies in models.



as noted only measures fault slip or horizontal heave.

CHAPTER 5

INTERPRETATION

To explain the geologic processes responsible for the structure and formation of the Farmville Basin, a kinematic model was developed. This model is based on geological and geophysical data presented in this study. The past century has seen the development of numerous theories explaining the formation of Mesozoic basins. "Unifying" theories explaining the formation of the Newark Supergroup are grouped into rift, structural grain, and fault reactivation categories.

PREEXISTING THEORIES

Russell (1892) proposed what is known as the Broad Terrane hypothesis, to explain the formation of the Newark Supergroup. He summarized his hypothesis by stating the Newark system of basins are remnants of a broader terrane that, at one time, united all the Newark basins. Russell suggested that sedimentation, orogenic movements, and upheaval occurred. These processes were followed by faulting and dike emplacement.

The theory of continental drift lead Sanders (1963) to propose the broad terrane of Russell was a failed rift. Sanders suggested development of the present day Newark basin is a result of three phases. During phase 1, Pangea began to break-up forming a rift basin along the present day North

American east coast. Sediments from the surrounding terranes filled the basin. As rifting continued the center of the rift was gradually heaved upward because of thermal processes. This upheaval defines the second phase of the Newark Supergroup evolution. As upheaval continued a central ridge developed within the rift. Sediments west of the central dipped west, and sediments east of the ridge dipped east. When the rift failed, 160 million year of erosion began. This period of erosion defines the third phase. During this third phase, the rift was eroded to a point where the only distinguishable features left are the remnant basins of today. Sander suggested that basins with a western border fault lay west of the central ridge and basins with an eastern border fault lay east of the ridge.

STRUCTURAL GRAIN

Lindholm (1978) proposed that the structural grain of basement rocks and their orientation to tensional stresses is the primary mechanism controlling the occurrence and formation of Mesozoic basins. The present day foliation is representative of the ancient structural grain, according to Lindholm (1978). Making this assumption Lindholm discovered that a majority of the Mesozoic basins have border faults dipping the same direction as the surrounding basement foliation. After extensive analysis Lindholm postulated that basins formed in areas where the basement structural grain was nearly perpendicular to tensional stresses. He related this

to the separation of Pangea. Erratic foliation, foliation not suitably oriented to tensional stresses, and/or the dip of the foliation was either too high or too low are the three reasons given to explain why basins did not form.

FAULT REACTIVATION

Ratcliffe and Burton (1985) proposed that the formation of the Newark basin was the result of duplex fault reactivation. They stated that asymmetry, width, and thickness of sediments within some eastern North American Mesozoic half-grabens may be related to the position and attitude of Paleozoic fault systems, in basement rocks, formed by tensional stresses. This theory concludes that all west dipping asymmetric basins, like the Newark basin, formed from reactivation of either concave listric foreland thrust, or convex ramp systems. As an example they chose the Newark basin, and explained that by simple extensional reactivation of a complex system of curvilinear thrust ramp structures one could explain present structures of the basin. The widest and deepest part of the basin occurs where SE extension was normal to the strike of the ancestral thrust ramp complex, according to this theory.

A similar hypothesis was proposed by Swanson (1986). This hypothesis states reactivation of preexisting fault systems of late Paleozoic age is the primary control for Mesozoic basin formation. His sites as examples in Virginia,

the Lakeside fault controlling the formation of the Farmville basin and it's stringers (this fault lies to the east of the basin), the Hylas fault controlling the formation of the Richmond and Taylorsville basins, and the Chatham fault controlling formation of the Danville basin and possibly the Scottsville and Culpeper basins.

STRUCTURAL MODEL

The structural model presented in Figure 18 illustrates several structural and lithologic relationships. The models indicate the "granitic" gneiss undifferentiated varies in depth and form between profile sections. Another conclusion drawn from this model is that rocks of the "granitic" gneiss undifferentiated generally lie east, and rocks of the Chopawamsic Formation generally lie west of the basin's margin, at the surface. The contact between the "granitic" gneisses and Chopawamsic Formation is not exposed at the surface. This contact is covered by the Carnian aged rocks of the Farmville Basin. The model further shows the Farmville basin has a block fault geometry similar to the models published by Wernicke and Burchfield (1982). All the observations presented in this model have supporting geological and geophysical evidence.

An igneous origin explains the variance in depth and form of the "granitic" gneisses. It is often assumed that an

Figure 18: Structural model of the Farmville Basin. This model is intended to show the subsurface relationship of the modelled lithologies.

LITHOLOGIES



Chopawamsic Formation



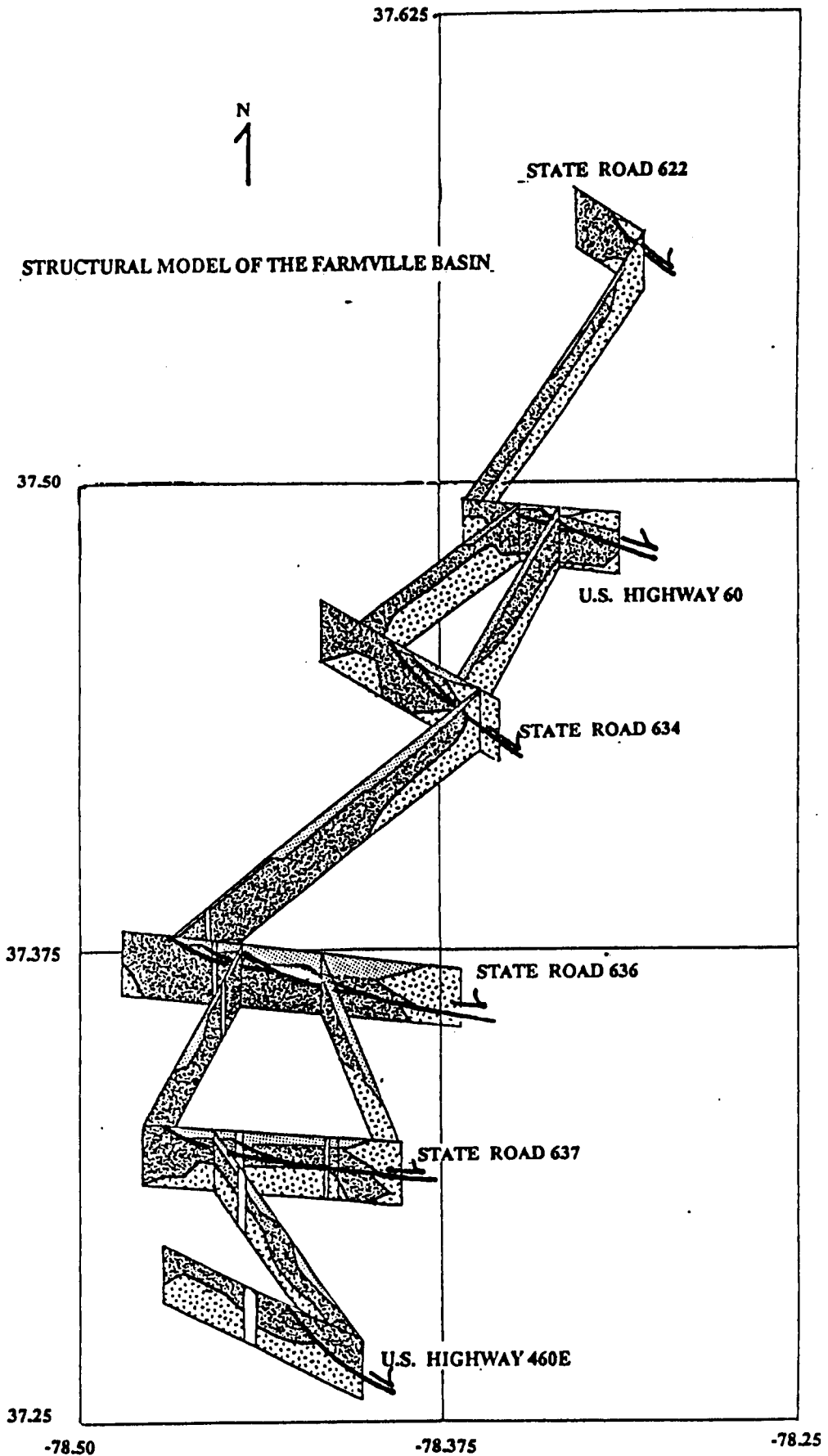
"Granitic" Gneiss Undifferentiated



Triassic Rocks



Diabase/Granophyre Dikes



intrusive body forms a smooth surface with the country rock. In reality, the contact surface between an intrusive body and the country rock is highly irregular. Only indirect evidence supports the proposed subsurface relationship between the "granitic" gneisses and the Chopawamsic Formation. Although there are an infinite number of solutions in gravity modelling, there are enough geologic constraints on the modelled profiles to ensure a close approximation of the actual subsurface geology.

Geologic and geophysical evidence support that the rocks of the Chopawamsic Formation lie to the west and that the "granitic" gneisses lie to the east of the basin, at the surface. Plate 4 shows these lithologies and their relationship to the basin. Supporting geophysical evidence includes high gravity and magnetic, and low radiometric values west of the basin. East of the basin, geophysical signatures include low gravity and magnetic values, and high radiometric values (Plates 1, 2, 3). The geophysical pattern changes in the southern portion of the study area. In the vicinity of profile U.S. Highway 460E it is known that the Chopawamsic Formation occurs on both sides of the basin, based on field mapping. However, the radiometric anomalies are greater than 400 CPS (indicative of the "granitic" gneisses). In addition, there is a change in the regional gravity gradient from NE-SW to E-W, along the same profile. Based on geophysical evidence, rocks of the "granitic" gneiss undifferentiated should be

present. The structural model indicates the "granitic" gneisses are present, but lie 1000 to 1200 meters below the surface. The model suggest the "granitic" gneisses taper off in a southern direction causing the change in the regional gravity gradient.

The structural model indicates that the Farmville Basin's geometry is controlled by a series of down faulted blocks. Using the classification of Wernicke and Burchfield (1982), this basin is defined as having a listric normal rotational-type fault geometry. Several geological and geophysical relationships would be expected with this type of geometry. Expected geological relationships include near vertical border faults, variations in dips across the basin, and a general trend of dips decreasing toward the shallow part of the basin. Circular gravity and magnetic lows over the deepest part of the basin would be expected. In addition, large mylonite zones, if present, should be recognizable on gravity maps due to their high density.

A listric fault defined by Shelton (1984) should have near vertical dips at the surface and decrease with depth. His definition is based on Basin and Range structures in the western United States. Many of these structures are young relative to Triassic times. If these structures were uplifted and eroded, faults at the erosion surface would begin to shallow; therefore, the more uplift and erosion, the less the dip of the border fault at the surface. This is believed to

be the case for the Farmville Basin where the border fault at the surface generally dips to the SE between 24 and 35 degrees.

The structural model developed indicates that the basin is comprised of a series of down-faulted blocks, separated by what are believed to be mylonite zones. The mylonite zones are reactivated Paleozoic faults and possibly Mesozoic splay faults. The Paleozoic faults lie beneath the basin, and the Mesozoic faults form the basin's western border. Since the deepest part of the basin lies along the eastern portion part of the basin it is concluded that larger displacements occurred along the reactivated Paleozoic faults. This is shown in all the models, and is supported by the low gravity and magnetic closures along State Road 636.

Geological evidence strongly supports this aspect of the model. Strike and dip of bedding within the basin is generally NE-SW at 30 degrees NE; however, there is a large variation in dips across the basin. Three basins with listric rotational type geometry and east dipping border faults are shown in Figures 19, 20, and 21. The first model shows a basin with a rotational geometry soled on one fault. The second and third models show basins with a listric rotational type of geometry. Model 2 shows the deepest part to be nearest the western border fault while Model 3 is representative of a basin that is deepest nearest its eastern margin. Each model has unique features and these are discussed below.

Figure 19: Model 1 shows a basin comprised of a single fault that shallows with depth. Distinguishing characteristics of this model are the dip of basin rocks and the age of the basin rocks increases away from the border.

Legend:

Dark Solid Lines : Dip of Triassic Beds

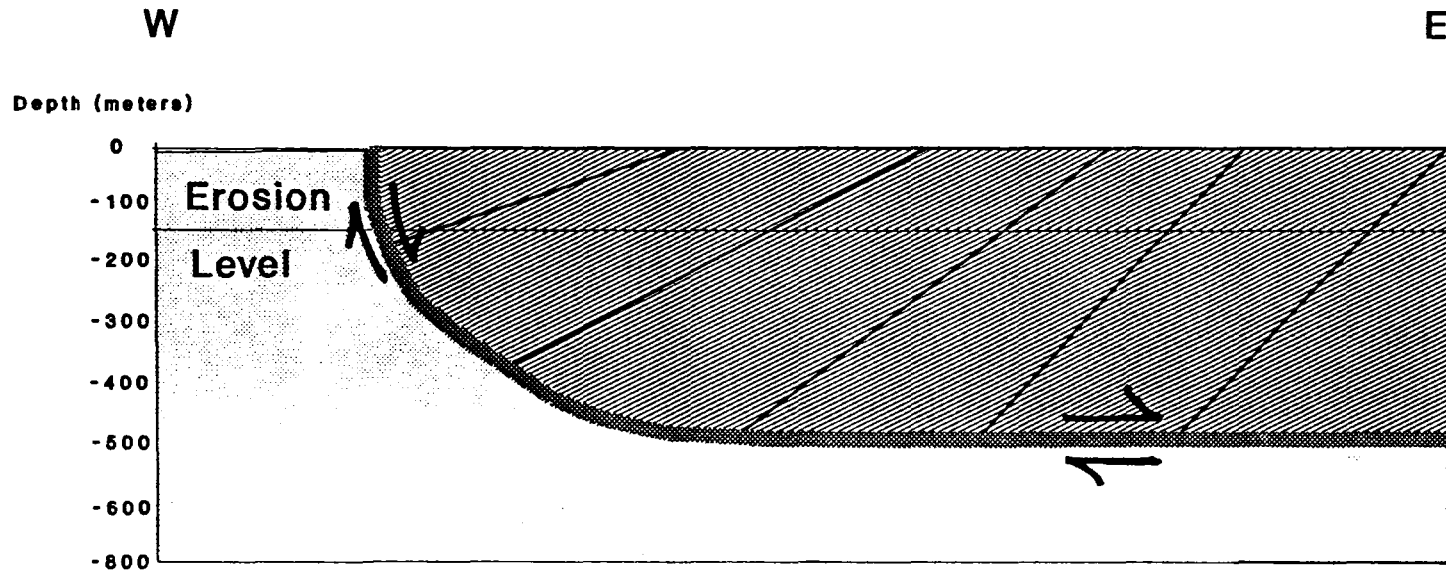
Light Solid Lines: Triassic Rocks

Dotted Area : Country Rock

Angle Cross-Hatch: Master Fault

Arrows : Indicate Fault Displacement

MODEL 1: SINGLE MASTER FAULT



Basins with the geometry shown in model 1 have two distinguishing features (Figure 19). The most recognizable feature of a basin having this geometry is the dip of rocks within the basin increase away from the border fault. The second distinguishing feature is rocks are older in age as one proceeds away from the border fault. As a basin of this type is eroded the dips of rocks become steeper at the surface. Geophysical anomalies of this type of basin are unique. Residual values of the Bouguer and magnetic anomalies would have minimums near the basins' center. Neither rocks of the Farmville Basin nor the gravity data indicate the basin has the geometry of model 1.

Model 2 is the geometric scenario presented for all modelled Mesozoic Basins to date (Figure 20). In this model, the primary fault bounds the basins' western border, with secondary faults covered by the Triassic rocks. Faults divide the basin into a series of blocks that join the master fault. Dip patterns of rocks in such a basin are unique. The dips alternate from shallow to steep to shallow. Overall the dips in the basin decrease away from the border fault. If a mylonite zone bounds the basin then the gravity values sharply decrease at the basins' border fault. Gravity values gradually increase away from the basin border fault. This is attributed to the decrease in basin thickness away from the master fault.

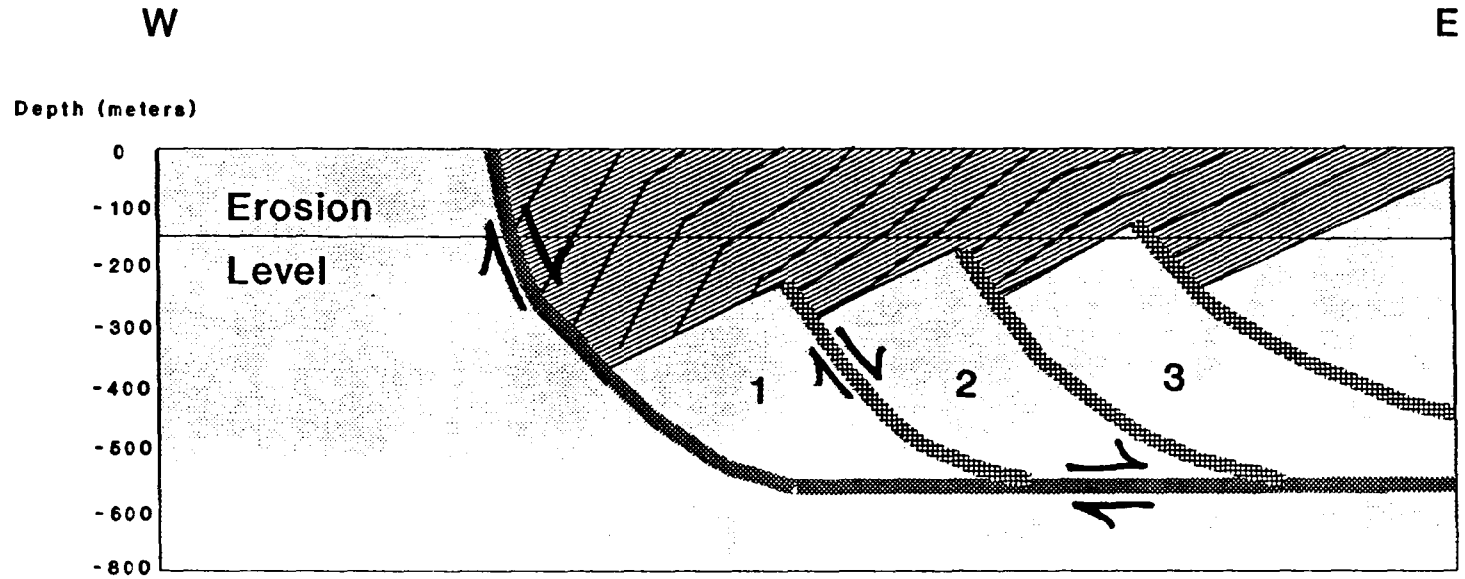
Figure 20: Model 2 shows a basin comprised of a two fault system. The master fault forms the western border of the basin, while splay faults (secondary) are found underneath the basin rocks. All faults shallow with depth. The splay faults eventually join the master fault at depth. The shallow to steep to shallow change in dip patterns along profile section is typical of such basins. The dips generally steepen toward the master fault. If a mylonite zone is present then the Bouguer curve may displays a peak near the border fault perimeter, at the surface.

Legend:

Dark Solid Lines	: Dip of Triassic Beds
Light Solid Lines	: Triassic Rocks
Dotted Area	: Country Rock
Angled Cross-Hatch	: Master Fault
Vertical Cross-Hatch	: Splay Fault
1, 2, 3	: Fault Blocks
Arrows	: Direction Of Displacement

MODEL 2: LISTRIC FAULTING

Multiple Faults with Primary on Western Border



Model 3 is believed to be representative of the Farmville Basin (Figure 21). In this model, the primary fault lies near the basins' center while secondary faults bound the basin. With this geometry the deepest part of the basin lies on the opposite side of the basins' western border fault. Distinguishing geologic characteristics of this model include dip variations, and a general decrease in dips toward the basin border fault. The lowest gravity anomalies are found over the deepest part of the basin, or nearest the eastern margin.

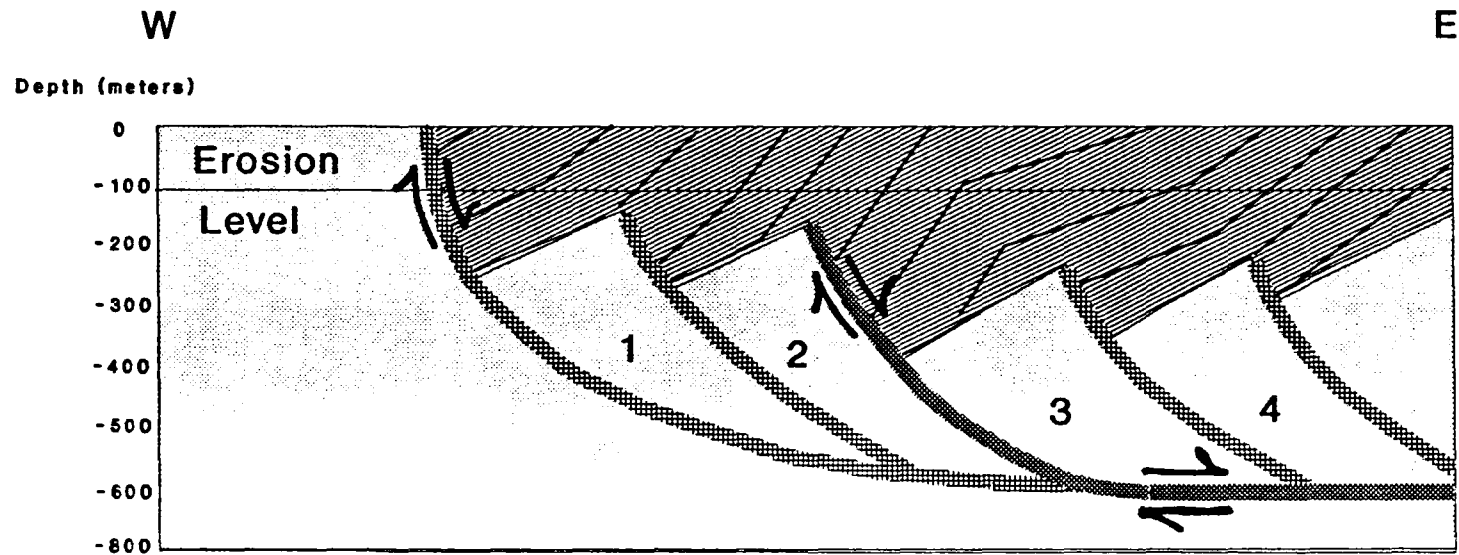
Figure 21: Model 3 shows a basin comprised of a two fault system. A splay fault forms the western border of the basin, while the master fault(s) are found underneath the basin rocks. All faults shallow with depth. The splay faults eventually join the master fault at depth. The shallow to steep to shallow change in dip patterns along profile section is typical of such basins; however, unlike Model 2 the dips generally steepen toward the eastern portion of the basin (master fault).

Legend:

Dark Solid Lines	: Dip of Triassic Beds
Light Solid Lines	: Triassic Rocks
Dotted Area	: Country Rock
Angled Cross-Hatch	: Master Fault
Vertical Cross-Hatch	: Splay Fault(s)
1, 2, 3, 4	: Fault Blocks

MODEL 3: LISTRIC FAULTING

Multiple Faults with Primary Underneath Basin



CHAPTER 6

KINEMATIC MODEL

Geologic Evolution

All evidence gathered and analyzed during this study indicates that the present day geometry of the Farmville Basin is a result of Alleghanian, Triassic, and Jurassic structures. The kinematic model developed for the Farmville Basin attempts to explain the evolution of the basin and how the various structures interacted to form the present day basin. Stresses that apparently controlled basin evolution are also examined.

Alleghanian or Preexisting Structures

The Alleghanian orogeny occurred during the Middle Carboniferous to Late Permian (Lefort and Van derVoo, 1980). This orogeny was the result of a collision between North America and Africa. A majority of the regional structural trends found in the study area, are thought to be a result of this orogeny and these are the NE-SW orientation of foliation and folds, as well as the NW-SE orientation of master joints. Foliation and folds were formed as a result of NW-SE directed primary stress or shortening (P1), during the Alleghanian orogeny. A majority of the folds plunge to the SE and are classified as tight isoclinal (Fluety, 1964). In general, foliation dips to the SE between 35 and 45 degrees. Crustal cooling occurred during Post-Alleghanian times, and is

believed to be responsible for the NW-SE joints. This joint set is related to extension or release fracturing, as a result of the cooling. Features formed during the Alleghanian and Post-Alleghanian were the primary structures in determining the geometry of the Farmville Basin.

Basin Formation

Manspeizer and others (1982) suggested the breakup of Pangea began sometime during the Late Permian to Middle Triassic, with the onset of continental uplift. The uplift caused tensional stresses, resulting in graben type structures on both continents. Dooley and Smith (1982) cited evidence to support the conclusions of Manspeizer and others (1982). Van der Voo and others (1976) concluded a counter-clockwise rotation of Africa relative to North America occurred during the Triassic. Venkatarishnan and Lutz (1989) presented a kinematic model of the Richmond basin based on the model of Van der Voo (1976).

Field evidence, basin shape and geophysical modelling suggests that extension was in a NW-SE direction during the formation of the Farmville Basin (Figure 22). This study places P1 in an E15S orientation. This implies P1 (tensional maximum stress) was nearly perpendicular to the NE-SW strike of the foliation, and less than 30 degrees from being parallel with the NW-SE joint set. As extension continued through the

Figure 22: Simplified block diagram illustrates the major structural features and associated stereograms of these structures. Large converging arrows mark the directions of shortening (P_1) during the Alleghanian and large diverging arrows mark principal extensional stress (P_3) during the Mesozoic times (see text for further details).

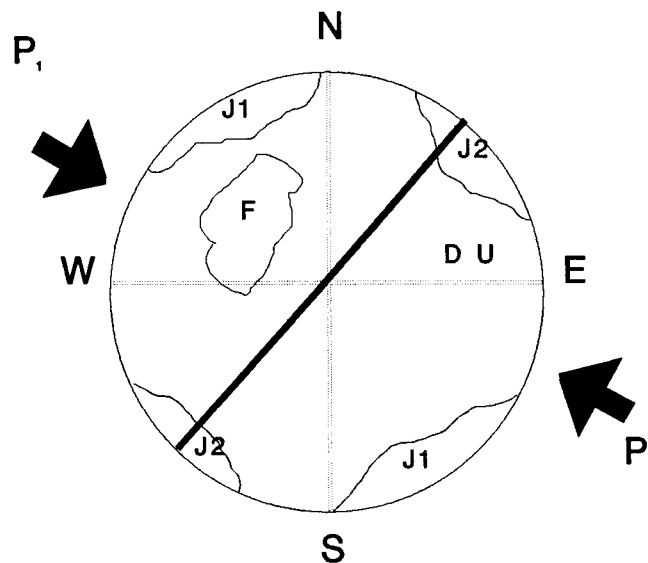
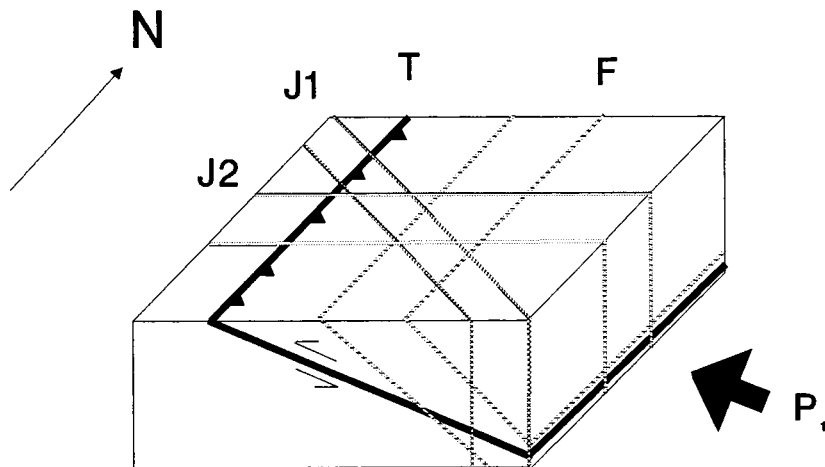
STRESSES

- P_1 : Primary Stress (convergent arrows - shortening stress)
- P_2 : Intermediate Stress
- P_3 : Minimum Stress (divergent arrows - extensional stress)
- P'_3 : Minimum Stress During Dike Emplacement (extensional stress during dike emplacement)

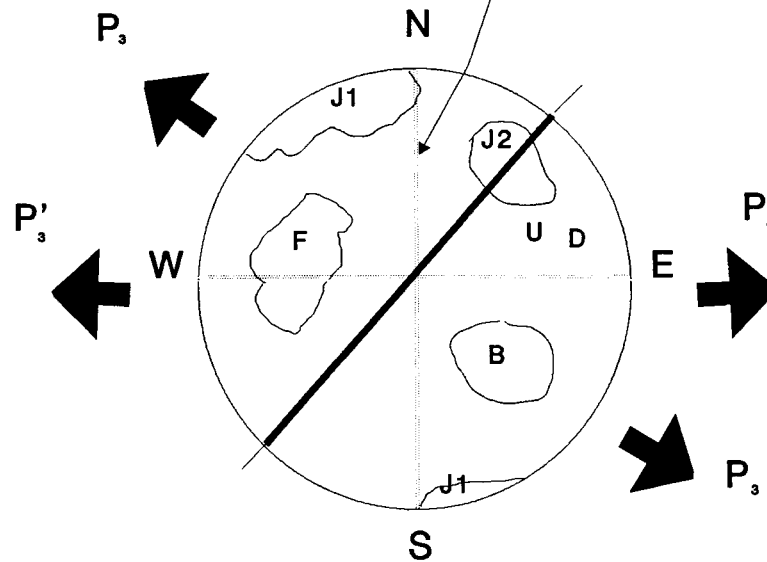
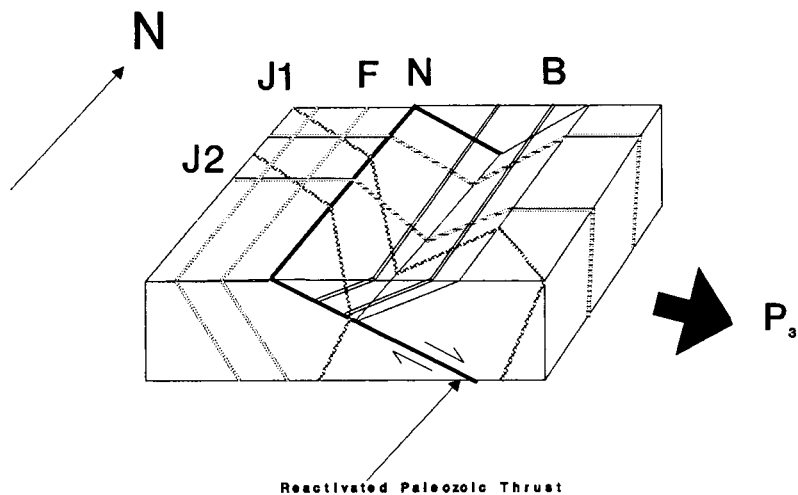
STRUCTURES

- T : Thrust Fault
- N : Reactivated Thrust Fault
- F : Foliation
- J1 : NE-SW Release Fractures
- J2 : E-W Extension Joints
- B : Bedding

A. POST ALLEGHANIAN STRUCTURES



B. LARNIAN STRUCTURES (BASIN FORMATION)



Carnian, reactivation of the NE-SW fabric occurred forming listric faults. During Mesozoic extension, the NW-SE directed principal extensional stress (P3, corresponding to maximum shortening axis during the Alleghanian) resulted in the reactivation of favorably oriented Paleozoic structures. Alleghanian thrust faults appear to have been reactivated as listric-normal, down-to-the east step faults. Even-though there is no kinematic explanation presently available to suggest why the western most normal fault does not form the basin marginal fault, field evidence suggest that the "master" fault may indeed lie beneath the basin. If this model (Figure 21) is accepted then it is suggested that the basin oversteps the western marginal fault (see also Wernicke and Burchfield, 1982). The geophysical models also support the above interpretation.

Jurassic

As extension continued, changing orientations of the principal extensional stress appears to have resulted in the emplacement of dikes that trend about north-south. Dike orientations range from NNW-SSE to NE-SW. These dikes were part of a "major" igneous event(s) that occurred along eastern North America, Europe, Africa, and South America, during the Jurassic (Dooley and Smith, 1983). It is believed that dikes within the study area were emplaced during the Jurassic; however, radiometric dating of these dikes has not been conducted. Dikes striking in a NE-SW direction parallel the

strike of regional foliation. This indicates that foliation was the structural feature responsible for the NE-SW oriented dike group. The NNW-SSE dike group is thought to have formed along N-S fractures formed as a result of sea-floor spreading. Dikes in the NNW-SSE group were found to have a high concentration of granophyres (Rogan, personal communication, 1987). This lead to the conclusion that the two dike groups were emplaced at different times. Granophyres found in the NNW-SSE dike group indicated the parent magma of this dike group was chemically mature compared to the parent magma of the NE-SW dike group. This implies the NE-SW dike group was emplaced before the NNW-SSE dike group, and lends support to the two phase igneous event suggested by Smith and Noltier (1979). They claim an igneous event occurred at 190 million years and a second igneous event occurred at 170-175 million years. Further field and laboratory analysis is needed to confirm the proposed two phase igneous events proposed in this study.

Post Jurassic

From the Cretaceous to the Holocene tectonic, stresses in the study area are generally attributed to isostatic rebound. This conclusion is supported by the lack of structural features cross-cutting dikes in the area. To test this reasoning, a rectified stream analysis was conducted to determine structural trends. The results of the stream analysis indicates there are three significant trends within

the study area, including a N-S, a NE-SW, and a NW- SE trend. These trends approximate the Pre-Jurassic NE-SW foliation, N-S dikes, and NW-SE joint set. From the evidence gathered during this study it is believed that the present Farmville Basin is a remanent of a much larger basin. It is commonly accepted that as much as 2 kilometers of erosion has occurred in the Piedmont of Virginia (Dooley and Smith, 1982).

COMPARISON WITH OTHER MODELS

One purpose of this study was to compare and contrast the kinematic model of the Farmville Basin with existing models that explain the formation of the Newark-Supergroup. Of existing models, this study presents data to support some aspect of every model with the exception of the Broad Terrane hypothesis (Russell, 1892).

Foliation Control

Strong evidence exist to support the Foliation Control theory of Lindholm (1978). As Lindholm stated, the geometry of a basin and its location was dependent on the Paleozoic foliation, and its orientation to p_1 , during the break-up of Pangea. This study definitely indicates that preexisting foliation was one factor contributing to the Farmville Basins' geometry. This foliation is thought to have formed during the Alleghanian orogeny. The difference between Lindholm's theory and the kinematic model is that structural features, besides

foliation, contributed to the present day geometry of the Farmville Basin. In addition, mapping in the Farmville Quadrangle showed that the foliation strikes are perpendicular to the western border of the basin (Plate 4). This is a direct contradiction to Lindholm's model.

Paleozoic Fault Control

Swanson (1982) believes the primary factor controlling a basins' geometry and location are Paleozoic Mylonite zones. Though Swanson's model is vague, he believes that the Newark-Supergroup of basins formed along Paleozoic Fault zones. Evidence from this study indicates that Paleozoic age mylonitic zones were critical in determining the Farmville Basins' geometry; however, this was not the only factor contributing to the formation of the basin.

Ratcliffe And Burton (1985)

The strongest similarity between the model of Ratcliffe and Burton (1985), and the model presented in this study is that the geometry of the Farmville basin is a direct result of Paleozoic structures. This study concludes that foliation, joints, and Alleghanian thrust are the structural features most strongly controlling the geometry of the Farmville Basin. In contrast, the duplex reactivation model of Ratcliffe and Burton (1985) proposes reactivation of concave and convex Paleozoic thrust systems as the primary factor controlling a

basin's geometry. The geophysical model does not support a duplex model. Ratcliffe and Burton (1985) proposed the duplex reactivation model can explain the geometry of all Mesozoic Basin in eastern North America. Differences explained above between the duplex reactivation and kinematic model raise doubts as to whether the model of Ratcliffe and Burton (1985) is a unifying model for the formation of basins of the Newark Supergroup. One primary difference is that the geometry of the Farmville Basin is of rotational listric type as defined by Wernicke and Burchfield (1982) and convex and concave fault geometry does not appear to be present.. In other words, the basin is comprised of a series of block faults joining a master decollement at depth. The fault with maximum displacement in the Farmville Basin is believed to lie underneath the basin as opposed to the western margin of a basin (as is the case in the duplex reactivation model). Ratcliffe and Burton (1985) suggest the deepest part of a basin occurs immediately to that east of the border fault. The results of this study and evidence presented in this study clearly shows that the deepest part of the Farmville Basin lies farther to the east of the border thrust (eastern part of the basin). Geophysical evidence from this study suggests that block faults were displaced by cross-faults while no evidence was presented indicating that similar displacements were expected in duplex reactivation model.

CHAPTER 7

CONCLUSIONS

Field geological and geophysical data obtained during the course of this study show that the Farmville basin is indeed a true half graben. The half graben was formed during NW-SE directional Mesozoic extension. However, unlike the generally accepted and existing models suggesting that basin formation nucleates on one common marginal border fault, this study shows that the fault displays maximum down-dip movement and hence controlling the deepest part of the basin may indeed lie within the central part of the basin. In other words, the Newark Group of Triassic basins need not all be nucleated on a western, down-to-the-east marginal fault. The geophysical models presented also clearly displayed the staircase geometry of reactivated Paleozoic faults. However, amounts of down-dip (to the east) movement varied. The deepest part of the Farmville basin is clearly along the eastern margin of the basin.

Future study would be extremely helpful in clarifying some of the more obscure points in this study. A detailed structural analysis is needed of the basin rocks to determine if cross-faults do exist in the basin. Proving the presence of cross-faults would lend more support to the structural and

kinematic models presented in this study. Other areas of study that would be useful in understanding the formation of the Farmville Basin include, a detailed analysis of dike morphology, and seismic profiles across the modelled gravity profiles.

REFERENCES CITED

- Abdel-Rahman, M.A., Hay, A.M., 1978. Sampling and Statistical Analysis Of Mult-Modal Data. Contribution 12 in: Basement Tectonic Contributions, p.73-85.
- Agarwal R. G., 1968. Double Harmonic Analysis for Upward and Downward Continuation: Unpublished Dissertation From Dept. of Physics, Edmonton, Alberta.
- Bhattacharyya, B.K., 1965. Two-Dimensional Harmonic Analysis As a Tool For Magnetic Interpretation: Geophysics, Vol. 20, p. 829-857.
- Brown, W.R., 1969. Geology of the Dillwyn quadrangle, Virginia: Virginia Division of Mineral Resources Rept. Inv. 10, 77 p.
- Conley, J.F. and Johnson, S.S., 1975. Road log of the geology from Madison to Cumberland counties in the Piedmont, central Virginia: Virginia Minerals Vol. 21, No. 4, p. 29-38.
- Cornet, B., 1977. The palynostratigraphy and age of the Newark Supergroup: University Park, Penn. State University, Unpublished PhD Dissertation, p. 501.
- Cox, J.C., and Harrison, S.S., 1979. Fracture-trace influenced stream orientation in glacial drift, North Western Pennsylvania: Canadian Journal Earth Science, Vol. 16, p. 1511-1514.
- Czechowski, D.A., 1982. Petrologic Comparison of Holocene Stream Sands and Triassic Sandstones in The Central Piedmont of Virginia: Evidence For Triassic Paleoclimate: Unpublished Masters Thesis, Southern Illinois University., 96p.
- Decker, E.W., 1987. DIGIT.EXE: A digitizing program for the Numonics 2400 series digitizer (Personal Communication).
- Decker, E.W., 1988. RECTIFY.EXE: A program to break stream segments into straight line segments (Personal Communication).
- Decker, E.W., 1988. SNET.EXE: A program for maintaining and analyzing geologic structural data (Personal Communication).

- Decker, E.W., and James Jr., C.G., QUAD.EXE: A program designed to analyze multimodal data (i.e. rectified stream data) (Personal Communication).
- Dooley, R.E., and Smith, W.A., 1982. Age and magnetism of diabase dykes and tilting of the Piedmont: *Tectonophysics*, 90., p. 283-307.
- Espenshade, G. H., and Potter, D. B., 1960. Kyanite, sillimanite, and andalusite deposits of the southern-eastern states: U.S. Geol. Survey Prof. Paper 336, 121 p.
- Fleuty, M. J., 1964. The description of folds, *Proc. Geol. Assoc.*, 75, Pt 4, p. 461-489.
- Glover, L. III, Pratt, T.L., Costain, J.K., Coruh, C., Mose, D.G., Gates, A.E., Evans, N.H., 1987. Tectonics and Crustal Structure In The Central Appalachians of Virginia: Reinterpretation From USGS I-64 Reflection Seismic Profile: Abstract GSA SE Regional Meeting, Norfolk, Virginia.
- Griffin, W.R., 1949. Residual Gravity in Theory and Practice: *Geophysics*, Vol. 14, p. 39-56.
- Henderson, R.G., 1960. A Comprehensive System of automatic Computation in Magnetic and Gravity Interpretation: *Geophysics*, Vol. 25, p. 569-585.
- Henery, E.F., Welch, W.J., Fussell, K.E., Bailey, H.H., and Smith, G.K., 1958. Soil survey of Prince Edward County Virginia: United States Dept. of Agriculture, Series 1949, No. 4.
- Higgins, M.W., Sinha, A.K., Zartman, R.E., and Kirk, W.S., 1977. U-Pb zircon dates from Central Appalachian Piedmont: A possible case of inherited radiogenic lead: *Geol. Soc. America Bull.*, Vol. 88, p. 124-132.
- Johnson, S.S., 1981. Regional geophysics, in *Geologic investigations in the Willis Mountain and Andersonville quadrangles: Virginia Division of Mineral Resources Publication 29*, p. 9-16.
- Johnson, S.S., Wilkes, G.P., and Zeigler, T.L., 1985. Simple Bouger gravity anomaly map of the Farmville, Briery Creek, Roanoke Creek, Randolph, and Scottsburg basins and vicinity, Virginia: Virginia Division of Mineral Resources, Publication 47, one sheet.

- Johnson, S.S, and Zeigler, R.E., 1972. Virginia gravity base net: Virginia Division of Mineral Resources, Inf. Circ. 17, 22 p.
- Jonas, A.I., 1932. Geology of the kyanite belt of Virginia, in Kyanite in Virginia: Virginia Geol. Survey Bull. 38, p. 1-38
- Klein, G. deV., 1969. Deposition of Triassic sedimentary rocks in separate basins, eastern North America: Geol. Society of America Bull., Vol. 80, p. 1825-1831.
- Lefort, J. P., and R. Van der Voo, 1981. A kinetic model for the collision and complete suturing between Gondwana and Laurussia in the Carboniferous: Journal of Geology, Vol. 84, p. 537-550.
- Linholt, R.C., 1978. Triassic-Jurassic faulting in eastern North America-A model based on pre-Triassic structures: Geology, Vol. 6, p. 365-368.
- Lacoste and Romberg, 1980. Model G Instruction Manual: Lacoste and Romberg Inc.
- Manspeizer, W., 1981, Early Mesozoic Basins of the Central Atlantic Passive Margins, in: Geology of Passive Continental Margins, AAPG Eastern Sectional Meeting, Education Course Note Series #19, p. 4:1-4:60.
- Marr, J. D., Jr., 1980A. The geology of the Willis Mountain quadrangle, Virginia: Virginia Division of Mineral Resources Publication 25, text and 1:24,000 scale map.
- Marr, J.D., Jr., 1981. Stratigraphy and structure (Triassic System by M.B. McCollum), in Geologic investigations in the Willis Mountain and Andersonville quadrangles, Virginia: Virginia Division of Mineral Resources Publication 29, p. 3-8.
- Mose, D.G., and Nagel, M.S., 1983. Plutonic Events in The Piedmont of Virginia: South Eastern Geol., Vol. 23, p. 25-39.
- Mose, D.G., 1980. Rb-Sr Whole-Rock Studies: Virginia Piedmont II: Year Book, Carnegie Institution of Washington, p. 483-485.
- Nettleton, L.L., 1954. Regionals, Residuals, and Structures: Geophysics, Vol. 9, p. 1-22.

- Ratcliffe, N.M., and Burton, W.S., 1985. Fault reactivation models for origin of the Newark basin and studies related to Eastern U.S. seismicity: U.S. Geol. Survey Cir. 946, p. 36-44.
- Robbins, E.I., 1985. Palynostratigraphy of coal-bearing sequences in early Mesozoic Basins of the eastern United States: U.S. Geol. Survey Cir. 946, p. 27-28.
- Rogan, P., 1988. personal communication
- Rodgers, W.B., 1840. Report of the progress of the geological survey of the state of Virginia for the year 1839. Richmond, 1840. Pp. 1-161, pls.1-2. (Reprinted in a reprint of annual reports and other papers on the geology of the Virginians, by the late William Barton Rogers. New York, 1889, p. 285-410, pl. op. 276, and pl.1)
- Russell, I.C., 1892. Correlation papers-the Newark System: U.S. Geol. Survey Bull. 85, p.344.
- Sanders, J.E., 1963. Late Triassic tectonic history of northeastern United States: American Journal of Science, Vol.261, p. 501-524.
- Scheidegger, A.E., 1980b. The Geotectonics stress field and crustal movements: Tectonophysics, Vol. 71, p. 217-226.
- Shelton, J.W., 1984. Listric normal faults: An illustrated summary: American Assoc. of Petroleum Geol. Bull., Vol. 68, No. 7, p. 801-815.
- Smoot, J.P., 1985. The closed-basin hypothesis and it's use in facies analysis of the Newark Supergroup: U.S. Geol. Survey Cir. 946, p. 4-9.
- Southwick, D.L., Reed, J.C., Jr., and Mixon, R.B., 1971. The Chopawamsic Formation-A new stratigraphic unit in the Piedmont of northern Virginia: U.S. Geol. Survey Bull. 1324-D, 11 p.
- Swanson, M.T., 1986. Preexisting fault control for Mesozoic basin formation in eastern North America: Geology, Vol. 14, No. 5, p 36-38.
- Tilton, G.R., 1970. Zircon age measurements in the Maryland Piedmont with special reference to Baltimore Gneiss problems; in Fisher, G.W., eds. Studies of Appalachian Geology-central and southern: New York, Interscience, p. 429-434.

- Talwani, M., Heirtzler, J.R., 1964. Computation of magnetic anomalies caused by two-dimensional structures of arbitrary shape, in Computers in the Mineral Industries, Part 1: Stanford University Publications, Geological Sciences Vol. 9, No. 1, p. 464-480.
- Talwani, M., 1965. Computation with the help of a digital computer of magnetic anomalies caused by bodies of arbitrary shape: Geophysics, Vol. 30, p. 797.
- Tasubi, C., 1959. Applications of Double Fourier Series to Computing Gravity anomalies and other Gravimetric Quantities at higher Elevations from Surface Anomalies: Report No.2 Institute Geodesy, Photogrammetry, and Cartography, Ohio St. University.
- Venkatakrishnan, R., 1984. A remote sensing-based study of lineament block tectonics in the Coastal Plain of Virginia: (Personal Communication).
- Venkatakrishnan, R. and Lutz, R., 1989. Chapter 13: A Kinematic Model For The Richmond Triassic Basin, Virginia in: Triassic-Jurassic Rifting, Manzpeizer, W.. Elseir Publications, The Netherlands.
- Virginia Division Of Mineral Resources, 1970A. Aeromagnetic contour map of the Farmville quadrangle (15-minute map; scale 1:62,500): Open file report, Virginia Division Of Mineral Resources.
- Virginia Division Of Mineral Resources, 1970. Aeromagnetic contour map of the Dillwyn quadrangle (15-minute map; scale 1:62,500): Open file report, Virginia Division Of Mineral Resources.
- Virginia Division Of Mineral Resources, 1978. Aero-radiometric contour map of the Farmville quadrangle (15-minute map; scale 1:62,500): Open file report, Virginia Division Of Mineral Resources.
- Virginia Division Of Mineral Resources, 1978. Aero-radiometric contour map of the Dillwyn quadrangle (15-minute map; scale 1:62,500): Open file report, Virginia Division Of Mineral Resources.
- Wernicke, B., and Burchfiel, B.C., 1982. Modes of extensional tectonics: Journal of Struc. Geol., No. 4, p. 105-115.

Wilkes, G.P., and Lasch, D.K., 1979. The Farmville Triassic Basin: an integrated geological/geophysical study: Va. J. Sci., Vol. 30, No.2.

APPENDIX I-A

GRAVAS FORTRAN

Gravas Fortran is a used to reduced the gravimetric dial readings to Free Air and Bouguer Anomalies. The algorithm first converts the dial readings from a LaCoste Romberg gravity meter (Model G, #289) to observed gravity values. The program converts observed gravity values for elevation and mass differences between stations, as well as solar and lunar fluctuations (tides), and instrumental drift. Finally, the algorithm applies Free Air and Bouguer corrections to the observed data yielding the Free Air and Bouguer anomalies for each station. This program was originally written by Virginia Division of Mineral Resources, Charlottesville Virginia. The program is listed below:

GRAVAS FORTRAN:

Written By: Virginia Division Of Mineral Resources

C	ROUTINE GRAVAS (AFTER SNOWDEN; FROM VDMR)	GRA00010
C		GRA00020
	DIMENSION VIM(72),NBASE(30),BASEG(30)	GRA00030
	DIMENSION DELT(100),DELG(100),RES(100)	GRA00040
	DIMENSIONIDATE(190),PHI(190),ALON(190),OBSG(190),H(190),NUM(190)	GRA00050

```

DIMENSION HS(190),SURNAM(21)                                GRA00060
CHARACTER*6TAG(13),STA1(190),STA2(190),A,B,C,D,E,F,G,Q,R,S,T,U,VGRA00070
CHARACTER *6 CONVER                                          GRA00080
CHARACTER * 1 TITLE(67)                                      GRA00090
C OPEN (UNIT=1,ACCESS='SEQUENTIAL',FILE='CAL')              GRA00100
C OPEN (UNIT=2,ACCESS='SEQUENTIAL',FILE='GRAVAS')           GRA00110
C OPEN (UNIT=4,ACCESS='SEQUENTIAL',FILE='FINAL')           GRA00120
JIMMY=0                                                       GRA00130
WRITE(6,1141)                                                GRA00140
1141 FORMAT(10X,44HENTER DESIRED DISTANCE TO START FOR PLOTTING,/, GRA00150
+20X,49HIF DISTANCE DESIRED IS 0.0 FEET ENTER -400.0 FEET,/) GRA00160
READ(5,*) DIST                                               GRA00170
C IF JAG =                                                    GRA00180
C     0 TERMINATE RUN                                         GRA00190
C     1 DO NOT READ CALIBRATION                               GRA00200
C     2 READ CALIBRATION TABLE                               GRA00210
C IF KAG =                                                    GRA00220
C     1 DO NOT READ BASE STNS                                 GRA00230
C     2 READ BASE STNS                                       GRA00240
C IF LAG =                                                    GRA00250
C     1 OMIT OPTION                                           GRA00260
C     2 READ GMT REJKT CALIM RHO                              GRA00270
C IF MAG =                                                    GRA00280
C     1 LOOP DRIFT COMPUTATION                                GRA00290
C     2 LINE DRIFT COMPUTATION                                GRA00300
C IF NAG =                                                    GRA00310
C     1 INDIVIDUAL LOOP(LINE) COMPUTATION                     GRA00320
C     2 STORE LOOP PENDING INTERLOOP COMPARISON              GRA00330
C     3 LAST LOOP,STORE,EXECUIT COMPARISON                    GRA00340
C IF IAG =                                                    GRA00350
C     1 IGNORE OPTION                                         GRA00360
C     2 PUNCH ACIC CARDS                                       GRA00370
C     3 PUNCH NON-ACIC CARDS                                   GRA00380
C IF IFOR =                                                  GRA00390
C     0 PRINT STANDARD TITLE                                   GRA00400
C     1 PRINT ALTERNATE TITLE                                   GRA00410
90 READ (1,100) JAG,KAG,LAG,MAG,NAG,IAG,IFOR                GRA00420
100 FORMAT(7I1)                                               GRA00430
NOMTYP=0                                                       GRA00440
IF(JAG) 700,700,150                                           GRA00450
150 GO TO (300,200),JAG                                       GRA00460
C TAG IS CALIBRATION TABLE TITLE                             GRA00470
200 READ (1,225) (TAG(I),I=1,13)                               GRA00480
225 FORMAT(13A6)                                               GRA00490
READ (1,230) SCALE                                             GRA00500
230 FORMAT(F8.6)                                               GRA00510
DO 250 I=1,9                                                   GRA00520
C VIM (VALUE IN MILLIGALS) IS CALIBRATION TABLE            GRA00530
K=I*8                                                           GRA00540
J=K-7                                                           GRA00550
250 READ (1,260) (VIM(L),L=J,K)                                GRA00560
260 FORMAT(8F10.2)                                             GRA00570
IF(SCALE) 285,300,285                                          GRA00580
285 DO 290 I=1,72                                             GRA00590
290 VIM(I)=VIM(I)*SCALE                                        GRA00600
300 GO TO (400,310),KAG                                        GRA00610
C NBASE AND BASEG ARE NUMBER AND MGAL VALUE OF BASE STATIONS GRA00620
310 READ (1,320) NNBASE                                        GRA00630
320 FORMAT(I2)                                                 GRA00640
DO 330 I=1,NNBASE                                             GRA00650
IF(IFOR.NE.0) GO TO 345                                        GRA00660
READ (2,340) NBASE(I),BASEG(I)                                GRA00670

```

```

340 FORMAT(I4,2X,F9.3)
GO TO 330
345 READ (2,346) NBASE(I),BASEG(I)
346 FORMAT(I5,F9.3)
330 BASEG(I)=BASEG(I)-976000.
400 GO TO (500,410),LAG
C      LCT+GMT=GCT
C      REJKT IS REJECTION LIMIT
C      CALIM IS CALIBRATION REJECTION LIMIT
410 READ (1,420) GMT,REJKT,CALIM
420 FORMAT(F6.2,2F5.3)
IF(CALIM.LE.0.) CALIM=.15
IF(REJKT.LE.0.) REJKT=.05
C      READ LOOP (LINE) TITLE
500 IF(IFOR.NE.0) GO TO 511
READ(2,505) (TITLE(II),II=1,67)
505 FORMAT(67A1)
WRITE(4,510) (TITLE(II),II=1,67)
510 FORMAT(1X,67A1)
GO TO 519
511 READ (2,512) (SURNAM(I),I=1,8),TYPINS,INSNO,SURNAM(9),SURNAM(10),
1NOMTYP,(SURNAM(I),I=11,21)
512 FORMAT(8A6,A3,I3,2A6,I3,11A1)
WRITE (4,513) (SURNAM(I),I=1,8),TYPINS,INSNO,(SURNAM(I),I=9,21)
513 FORMAT(1H1,45X,5A6/2X,10HLOOP/LINE,A6,7X,5HDATE,2A6,7X,11HGRAVIMGRAO0920
1ETER,A3,I3,7X,9HOBSERVER,2A6,7X,8HCOMMENT,11A1)
519 WRITE (4,225) (TAG(I),I=1,13)
520 CALL STORE(IDATE,PHI,ALON,OBSG,H,NUM,VIM,GMT,ICOUNT,STA1,STA2GRAO0950
1,IYEAR,HS,IFOR)
530 CALL TIDE(ICOUNT,NUM,IDATE,OBSG,PHI,ALON,H)
CALL DRIFT(ICOUNT,NUM,OBSG,IDATE,REJKT,MAG,NNBASE,NBASE,BASEG,
1DELTA,DELTA,RES,RR,DD)
GO TO (550,560,550,550),NAG
550 IF(IFOR.NE.0) GO TO 552
WRITE (4,551) A,B,C,D,E,G,Q
551 FORMAT(1H1,9X,5A6,2X,2A6)
GO TO 554
552 WRITE (4,553) (SURNAM(I),I=1,5)
553 FORMAT(1H1,45X,5A6)
554 GO TO (555,560,560,555),NAG
555 WRITE (4,225) (TAG(I),I=1,13)
560CALLGRANET(ICOUNT,NUM,STA1,STA2,OBSG,PHI,ALON,H,NNBASE,NBASE,BASEGRAO1090
1G,NOMTYP,JIMMY,NAG,IAG,HS,RR,DD,DIST)
IF(NAG.EQ.4)CALLCALIB(ICOUNT,NUM,OBSG,NNBASE,NBASE,BASEG,STA1,STGRAO1110
1A2,NAG,PHI,ALON,H,CALIM,DELTA,DELTA,RES)
IF(NAG.EQ.5) GO TO 560
C      GO TO 90
C      CLOSE (UNIT=20)
C      CLOSE (UNIT=21)
C      CLOSE (UNIT=41)
C      CLOSE (UNIT=42)
700 STOP
END
C
C
C      SUBROUTINE STORE(IDATE,PHI,ALON,OBSG,H,NUM,VIM,GMT,ICOUNT,STAGRAO1240
1 1,STA2,JYEAR,HS,IFOR)
C      IDATE = DATE AND TIME OF OBSERVATION
C      CONVERTS YEAR, DAY, HOUR, MINUTES TO ONE VARIABLE IDATE IN MINUGRAO1270
C      LEAP YEAR TAKEN INTO ACCOUNT, CONVERSION TO GMT

```

C	LATITUDE , LONGITUDE CONVERTED TO RADIANS	GRA01290
C	DIAL READING CONVERTED TO MGALS	GRA01300
C	*****NUMBER,DATE,TIME,OBS.G,PHI,LAMBDA,HEIGHT ARE STORED	GRA01310
	DIMENSION IDATE(1),PHI(1),ALON(1),OBSG(1),NUM(1),VIM(1)	GRA01320
	DIMENSION HS(1),H(1)	GRA01330
	CHARACTER *6 CONVER,CON,CKF, STA1(1),STA2(1)	GRA01340
	I=1	GRA01350
	CKF='F'	GRA01360
1000	IF(IFOR.NE.0) GO TO 50	GRA01370
	READ (2,1001) NUM(I),STA1(I),STA2(I),IDAY,MONTH,IYEAR,IHOUR,DIA	GRA01380
	1L,IPHI,JPHI,PHI(I),LON,ILON,ALON(I),CONVER,H(I)	GRA01390
1001	FORMAT(I5,2A6,I2,I2,I4,I4,F7.3,2I3,F2.0,I4,I3,F2.0,A1,F8.2)	GRA01400
	WRITE (9,1002) STA1(I),STA2(I)	GRA01410
1002	FORMAT (5X,2A6)	GRA01420
	GO TO 99	GRA01430
999	PHI(I)=PHI(I)*0.6	GRA01440
	ALON(I)=ALON(I)*0.6	GRA01450
50	READ (2,51) NUM(I),STA1(I),STA2(I),IDAY,MONTH,IYEAR,IHOUR,MINUTE ,	GRA01460
	1IPHI,PHI(I),LON,ALON(I),CONVER,H(I)	GRA01470
51	FORMAT(I5,2A6,2I2,I4,2I2,F7.3,I3,F5.2,I4,F5.2,A1,F8.2)	GRA01480
	WRITE (9,1002) STA1(I),STA2(I)	GRA01490
99	IF(IYEAR) 105,100,105	GRA01500
100	ICOUNT=I-1	GRA01510
	RETURN	GRA01520
105	GO TO (110,111,112,113,114,115,116,117,118,119,120,121),MONTH	GRA01530
110	IDATE(I)=IDAY	GRA01540
	GO TO 125	GRA01550
111	IDATE(I)=IDAY+31	GRA01560
	GO TO 125	GRA01570
112	IDATE(I)=IDAY+59	GRA01580
	GO TO 125	GRA01590
113	IDATE(I)=IDAY+90	GRA01600
	GO TO 125	GRA01610
114	IDATE(I)=IDAY+120	GRA01620
	GO TO 125	GRA01630
115	IDATE(I)=IDAY+151	GRA01640
	GO TO 125	GRA01650
116	IDATE(I)=IDAY+181	GRA01660
	GO TO 125	GRA01670
117	IDATE(I)=IDAY+212	GRA01680
	GO TO 125	GRA01690
118	IDATE(I)=IDAY+243	GRA01700
	GO TO 125	GRA01710
119	IDATE(I)=IDAY+273	GRA01720
	GO TO 125	GRA01730
120	IDATE(I)=IDAY+304	GRA01740
	GO TO 125	GRA01750
121	IDATE(I)=IDAY+334	GRA01760
125	YEAR=IYEAR	GRA01770
	IDATE(I)=IDATE(I)+(IYEAR-1900)/4+1	GRA01780
	IF(YEAR/4.-FLOAT(IYEAR/4)) 145,135,145	GRA01790
135	IF(MONTH-3) 140,145,145	GRA01800
140	IDATE(I)=IDATE(I)-1	GRA01810
145	TIME=(FLOAT(IHOUR)/100.0)+0.001	GRA01820
	JHR=IFIX(TIME)	GRA01830
	MINUTE=IFIX((TIME-FLOAT(JHR))*100.0)	GRA01840
	IHOUR=JHR	GRA01850
	IDATE(I)=(IYEAR-1900)*525600+(IDATE(I)-2)*1440+IHOUR*60+IFIX(GMT*6	GRA01860
	10.)+720+MINUTE	GRA01870
	IF(CONVER.EQ.CKF) H(I)=H(I)/3.280833	GRA01880
	IF(IFOR.EQ.0) GO TO 180	GRA01890
	IF(CON.EQ.CKF) HS(I)=HS(I)/3.280833	GRA01900

```

180 PHI(I)=DERAD2(IPHI,JPHI,PHI(I))          GRAO1910
ALON(I)=DERAD2(LON,ILON,ALON(I))          GRAO1920
J=IFIX(DIAL/100.0)                        GRAO1930
CR=FLOAT(J)*100.0                         GRAO1940
R=DIAL-CR                                  GRAO1950
J=J+1                                      GRAO1960
OBSG(I)=VIM(J)+R*(VIM(J+1)-VIM(J))/100.  GRAO1970
JYEAR=IYEAR                                GRAO1980
I=I+1                                      GRAO1990
GO TO 1000                                  GRAO2000
END                                          GRAO2010

C                                          GRAO2020
C                                          GRAO2030
C                                          GRAO2040
SUBROUTINE TIDE(ICOUNT,NUM,IDATE,OBSG,PHI,ALON,H) GRAO2050
C COMPUTES TIDAL CORRECTION BY LONGMAN METHOD. JGR,VOL.64,NO.12,P.23GRAO2060
  DIMENSION PHI(1),IDATE(1),H(1),ALON(1),OBSG(1),NUM(1) GRAO2070
  DATA SMLA,SMLC1,SMLE,SMLM,OMEGA,AMU,BIGM,BIGS,SMLC,SMLI,SMLAP,CON1GRAO2080
1,CON2,CON3,CON4,CON5,CON6,CON7,CON8,CON9,CON10,CON11,CON12,CON13, GRAO2090
2CON14,CON15,CON16,CON17,CON18,CON19,CON20,CON21,CON22,CON23,CON24/GRAO2100
36.37827E8,1.495E13,5.489972E-2,7.4804E-2,4.09314616E-1,6.670E-8,GRAO2110
47.3537E25,1.993E33,3.84402E10,8.979719E-2,.260931E-10,.006738,.016GRAO2120
575104,.00004180,.126E-6,4.90822947,3.00052642E-2,7.90246E-6,5.818EGRAO2130
6-8,4.71996657,8399.70914,-1.97803982E-5,3.29673303E-8,5.83515153, GRAO2140
771.0180412,1.80205245E-4,2.18166156E-7,4.88162793,628.331951,5.279GRAO2150
862E-6,.261799388,4.52360045,33.7571462,3.62640633E-5,3.87850945E-8GRAO2160
9/
  WRITE (4,71)                              GRAO2170
71 FORMAT(///5X,6HSTA NO,14X,4HDATE,10X,12HUNCORR OBS G,10X,9HTIDE COGRAO2190
1RR//20X,14HJULIAN MINUTES,9X,5HMGALS,15X,5HMGALS//) GRAO2200
200 DO 300 I=1,ICOUNT                       GRAO2210
  SNPHI=SIN(PHI(I))                         GRAO2220
  CSPHI=COS(PHI(I))                         GRAO2230
205 T=FLOAT(IDATE(I))/52596000.            GRAO2240
  T2=T**2                                    GRAO2250
  T3=T*T2                                    GRAO2260
210 BIGC=SQRT(1.0/(1.0+CON1*SNPHI**2))     GRAO2270
  SMLR=BIGC*SMLA+H(I)*100.0                GRAO2280
  SMLE1= CON2-CON3*T-CON4*T2               GRAO2290
  SMLAP1=1.0/(SMLC1*(1.0-SMLE1**2))        GRAO2300
  SMLP1=CON5+CON6*T+CON7*T2+CON8*T3        GRAO2310
  SMLS=CON9+CON10*T+CON11*T2+CON12*T3      GRAO2320
  SMLP=CON13+CON14*T-CON15*T2-CON16*T3     GRAO2330
  SMLH=CON17+CON18*T+CON19*T2              GRAO2340
220 BIGRD=1.0/SMLC1+SMLAP1*SMLE1*COS(SMLH-SMLP1) GRAO2350
  SMLRD=1.0/SMLC+SMLAP*SMLE*COS(SMLS-SMLP)+SMLAP*SMLE**2*COS(2.0*GRAO2360
1(SMLS-SMLP))+ (15.0/8.0)*SMLAP*SMLM*SMLE*COS(SMLS-2.0*SMLH+SMLP)+GRAO2370
2 SMLAP*SMLM**2*COS(2.0*(SMLS-SMLH))      GRAO2380
225 SMLTO=FLOAT(IDATE(I)-(IDATE(I)/1440)*1440)/60.0 GRAO2390
  SMLT=CON20*(SMLTO )+ALON(I)             GRAO2400
  CHI1=SMLT+SMLH                           GRAO2410
  SMLL1=SMLH+2.0*SMLE1*SIN(SMLH-SMLP1)    GRAO2420
230 BIGN=CON21-CON22*T+CON23*T2+CON24*T3   GRAO2430
  CSBIGI=COS(OMEGA)*COS(SMLI)-SIN(OMEGA)*SIN(SMLI)*COS(BIGN) GRAO2440
  SNBIGI=SQRT(1.0-CSBIGI**2)              GRAO2450
  BIGI=ATAN2(SNBIGI,CSBIGI)               GRAO2460
235 SNGNU=SIN(SMLI)*SIN(BIGN)/SNBIGI      GRAO2470
  CSGNU=SQRT(1.0-SNGNU**2)               GRAO2480
  GNU=ATAN2(SNGNU,CSGNU)                  GRAO2490
  CHI=SMLT+SMLH-GNU                        GRAO2500
  CSALFA=COS(BIGN)*CSGNU+SIN(BIGN)*SNGNU*COS(OMEGA) GRAO2510

```



```

        SNALFA=SIN(OMEGA)*SIN(BIGN)/SNBIGI                                GRA02520
        ALFA=2.0*ATAN(SNALFA/(1.0+CSALFA))                                GRA02530
240    ETA=BIGN-ALFA                                                    GRA02540
        SIGMA=SMLS-ETA                                                  GRA02550
        SMLL=SIGMA+2.0*SMLE*SIN(SMLS-SMLP)+1.25*SMLE**2*SIN(2.0*(SMLS-
1    SMLP))+3.75*SMLM*SMLE*SIN(SMLS-2.0*SMLH+SMLP)+(11.0/8.0)*SMLM**2*GRA02570
2    SIN(2.0*(SMLS-SMLH))                                              GRA02580
245    CSFEE=SNPHI*SIN(OMEGA)*SIN(SMLL1)+CSPHI*(COS(OMEGA/2.0)**2*COS  GRA02590
1    (SMLL1-CHI1)+SIN(OMEGA/2.0)**2*COS(SMLL1+CHI1))                  GRA02600
250    CSTHET=SNPHI*SNBIGI*SIN(SMLL)+CSPHI*(COS(BIGI/2.0)**2*COS(SMLL-
1    CHI)+SIN(BIGI/2.0)**2*COS(SMLL+CHI))                              GRA02620
C THE NEXT TWO STATEMENTS ARE WRITTEN TO TAKE ADVANTAGE OF MACHINES WITHGRA02630
C LIMITATIONS AS TO THE SIZE OF LARGE NEGATIVE EXPONENTS              GRA02640
255    GS=AMU*BIGS*SMLR*BIGRD**2*BIGRD*(3.0*CSFEE**2-1.0)             GRA02650
260    GM=AMU*BIGM*SMLR*SMLRD**3*(3.0*CSTHET**2-1.0)+1.5*AMU*BIGM*SMLRD GRA02660
1**2*SMLR**2*SMLRD**2*(5.0*CSTHET**3-3.0*CSTHET)                     GRA02670
270    GOO=(GM+GS)*1200.0                                              GRA02680
        WRITE (4,3000) NUM(I),IDATE(I),OBSG(I),GOO                     GRA02690
3000   FORMAT(5X,I5,10X,I10,8X,F10.3,13X,F6.3)                         GRA02700
300    OBSG(I)=OBSG(I)+GOO                                             GRA02710
        RETURN                                                            GRA02720
        END                                                                GRA02730
C                                                                           GRA02740

C                                                                           GRA02750
C                                                                           GRA02760
C                                                                           GRA02770
        SUBROUTINE DRIFT(ICOUNT,NUM,OBSG,IDATE,REJKT,MAG,NNBASE,NBASE,
1BASEG,DELTA,DELTA,RES,ZSUM,ZENO)
        DIMENSION NUM(1),OBSG(1),IDATE(1),NBASE(1),BASEG(1)
        DIMENSION DELTA(1),DELTA(1),RES(1),LUM(100)
C IF MAG=@
C     1,LOOP COMPUTATION
C     2,LINE COMPUTATION
        KDAT=IDATE(1)
C     REFERANCE ALL TIMES TO INITAL TIME
        WRITE (4,69)
69    FORMAT(//5X,6HSTA NO,14X,4HTIME,14X,4HOBSG,15X,' (CORRECTED FOR
1    TIDE) ' /)
        WRITE (4,1)
1    FORMAT(10H
        )
        DO 10 J=1,ICOUNT
10    IDATE(J)=IDATE(J)-KDAT
        DO 12 I=1,ICOUNT
        WRITE (4,15) NUM(I),IDATE(I),OBSG(I)
15    FORMAT(5X,I5,13X,I6,11X,F9.3)
12    CONTINUE
        JC=ICOUNT-1
C     REMOVE DRIFT STNS
        DO 19 J=1,JC
        IF(NUM(J).NE.0) GO TO 19
        IF(NUM(J)-NUM(J+1)) 19,16,19
16    GLAY=OBSG(J+1)-OBSG(J)
        LAYT=IDATE(J+1)-IDATE(J)
        KK=J+1
        DO 18 K=KK,ICOUNT
        OBSG(K)=OBSG(K)-GLAY
18    IDATE(K)=IDATE(K)-LAYT
19    CONTINUE
C     TEST FOR AND REMOVE ANY LAY-OVERS
        DO 30 J=1,JC
        IF(NUM(J).EQ.0) GO TO 30
        IF(NUM(J)-NUM(J+1)) 30,20,30

```

20	GLAY=OBSG(J+1)-OBSG(J)	GRA03130
	LAYT=IDATE(J+1)-IDATE(J)	GRA03140
	KK=J+1	GRA03150
	NUM(KK)=0	GRA03160
	DO 25 K=KK, ICOUNT	GRA03170
	OBSG(K)=OBSG(K)-GLAY	GRA03180
25	IDATE(K)=IDATE(K)-LAYT	GRA03190
30	CONTINUE	GRA03200
	GO TO(31,150),MAG	GRA03210
C	TEST FOR REOCCUPATIONS, FORM DELTA G2S AND DELTA T2S	GRA03220
31	XYSUM=0.	GRA03230
	X2SUM=0.	GRA03240
	XSUM=0.	GRA03250
	YSUM=0.	GRA03260
	L=0	GRA03270
	WRITE (4,39)	GRA03280
39	FORMAT(///)	GRA03290
	DO 50 I=1, JC	GRA03300
	IF(NUM(I)) 50,50,32	GRA03310
32	K=I+1	GRA03320
	DO 45 J=K, ICOUNT	GRA03330
35	IF(NUM(I)-NUM(J)) 45,40,45	GRA03340
40	L=L+1	GRA03350
	LUM(L)=NUM(J)	GRA03360
	DELG(L)=OBSG(J)-OBSG(I)	GRA03370
	DELT(L)=IDATE(J)-IDATE(I)	GRA03380
	WRITE (4,941) L,DELG(L),L,DELT(L)	GRA03390
941	FORMAT(1H ,5HDELG(,I2,2H)=,F7.3,8X,5HDELT(,I2,2H)=,F8.1)	GRA03400
	XYSUM=XYSUM+DELG(L)*DELT(L)	GRA03410
	X2SUM=X2SUM+DELT(L)**2	GRA03420
	XSUM=XSUM+DELT(L)	GRA03430
	YSUM=YSUM+DELG(L)	GRA03440
45	CONTINUE	GRA03450
50	CONTINUE	GRA03460
	WRITE (4,600)	GRA03470
600	FORMAT(1H1,50X,20HD R I F T P L O T//)	GRA03480
	CALL PLOT2D(L,DELT,DELG)	GRA03490
C	SOLVE FOR BEST FIT LINEAR DRIFT	GRA03500
	WRITE (4,68)	GRA03510
68	FORMAT(1H1)	GRA03520
	IPASS=1	GRA03530
	DENO = L+1	GRA03540
	ZENO=DENO	GRA03550
70	DENOM= DENO*X2SUM-XSUM**2	GRA03560
	AC=(DENO*XYSUM-XSUM*YSUM)/DENOM	GRA03570
	BINT=(YSUM*X2SUM-XYSUM*XSUM)/DENOM	GRA03580
C	COMPUTE RESIDUALS , TEST AGAINST REJECTION LIMIT	GRA03590
	II=1	GRA03600
	RSUM=0.	GRA03610
	WRITE (4,800) IPASS,REJKT	GRA03620
800	FORMAT(////13H FIT NUMBER ,I1,37H REJECTED VALUES REJECTION LIM	GRA03630
	1IT = ,F5.3,5HMGALS/)	GRA03640
	DO 72 I=1,L	GRA03650
	IF(LUM(I)) 72,72,71	GRA03660
71	RES(I)=BINT+AC*DELT(I)-DELG(I)	GRA03670
	RSUM=RSUM+RES(I)**2	GRA03680
72	CONTINUE	GRA03690
	IF(IPASS.EQ.1) ZSUM=RSUM	GRA03700
	SIGMA=SQRT(RSUM/DENO)	GRA03710
	RESMAX=0.	GRA03720
	DO 74 I=1,L	GRA03730
	IF(LUM(I)) 74,74,73	GRA03740

```

73 RESMAX=AMAX1 (RESMAX,ABS (RES (I)))
74 CONTINUE
  DO 76 I=1,L
    IF (LUM (I)) 76,76,75
75 IF (ABS (RES (I))-RESMAX) 76,77,77
77 IF (ABS (RES (I))-REJKT) 76,76,80
80 II=2
  XYSUM=XYSUM-DELG (I)*DELT (I)
  X2SUM=X2SUM-DELT (I)**2
  XSUM=XSUM-DELT (I)
  YSUM=YSUM-DELG (I)
  KDELT=DELT (I)
  WRITE (4,900) LUM (I),KDELT,RES (I)
900 FORMAT (1H0,11HSTA NUMBER ,I5,4X,6HTIME = ,I5,5X,11HRESIDUAL = ,F7.3
1)
  LUM (I)=0
  DENO=DENO-1.
76 CONTINUE
  WRITE (4,1000) IPASS,SIGMA
1000 FORMAT (1H0,14HSIGMA FOR FIT ,I1,3H = ,F8.4)
C   IF ANY VALUES REJECTED REFIT DRIFT
  GO TO (120,85),II
85 IPASS=IPASS+1
  GO TO 70
C   DRIFT COMPUTATION FOR LINE
150 DO 170 I=1,NNBASE
  IF (NUM (1)-NBASE (I)) 160,155,160
155 FIRST=BASEG (I)
160 IF (NUM (ICOUNT)-NBASE (I)) 170,165,170
165 BLAST=BASEG (I)
170 CONTINUE
  REFDIF=FIRST-BLAST
  DIF=OBSEG (1)-OBSEG (ICOUNT)
  AC=(REFDIF-DIF)/FLOAT (IDATE (ICOUNT))
120 AII=AC*60.
  WRITE (4,1200) AII
1200 FORMAT (1H0,19HFINAL DRIFT RATE = ,F8.4,16HMILLIGALS / HOUR)
  IF (MAG.NE.1) GO TO 121
  WRITE (4,1250) BINT
1250 FORMAT (1X,12HINTERCEPT = ,F8.4,5H MGAL)
C   APPLY DRIFT CORRECTION AND FORM DELTA G2S WITH RESPECT TO FIGRAO4150
121 DO 125 I=1,ICOUNT
  IF (NUM (I)/1000.GT.0) GO TO 126
125 CONTINUE
126 GEE=OBSEG (I)
  DO 130 I=1,ICOUNT
130 OBSEG (I)=OBSEG (I)-GEE -AC*FLOAT (IDATE (I))
  WRITE (4,1300)
1300 FORMAT (///6X,17HCORRECTED DELTA G//)
  WRITE (4,1400)
1400 FORMAT (6X,3HSTA,13X,1HG,11X,8HINTERVAL)
  DO 1700 I=1,ICOUNT
  IF (NUM (I)) 1700,1700,1450
1450 WRITE (4,1500) NUM (I),OBSEG (I)
1500 FORMAT (5X,I5,5X,F11.3)
  J=I+1
1505 IF (J.GT.ICOUNT) GO TO 1700
  IF (NUM (J).GT.0) GO TO 1550
1510 J=J+1
  GO TO 1505
1550 XINT=OBSEG (J)-OBSEG (I)
  WRITE (4,1600) XINT

```

1600	FORMAT(31X,F11.3)	GRA04370
1700	CONTINUE	GRA04380
	RETURN	GRA04390
	END	GRA04400
C		GRA04410
C		GRA04420
C		GRA04430
	SUBROUTINE GRANET(ICOUNT,NUM,STA1,STA2,OBSEG,PHI,ALON,H,NNBASE,NBASE,NUMI,PHI,ALON,HS,RR,DD,DIST)	GRA04440
	1E,BASEG,NOMTYP,JIMMY,NAG,IAG,HS,RR,DD,DIST)	GRA04450
C	COMPUTES MEAN VALUES FOR REOBSERVATIONS	GRA04460
C	ADDS REFERENCE STATION VALUE TO DELTA G	GRA04470
	DIMENSION NUM(1),PHI(1),ALON(1),H(1),HS(1),OBSEG(1),NBASE(1)	GRA04480
	DIMENSION NUMI(500),PHI(500),ALONI(500),HI(500),STA1I(500),	GRA04490
	1STA2I(500),BASEG(1),OBSEG(500),HSI(500)	GRA04500
	DIMENSION STA1(1),STA2(1)	GRA04510
39	GO TO(310,400,400,310,15),NAG	GRA04520
C	AVERAGING FOR SINGLE LOOP	GRA04530
310	IC=ICOUNT-1	GRA04540
	II=ICOUNT	GRA04550
	DO330 I=1,IC	GRA04560
	IF(NUM(I)) 330,330,315	GRA04570
315	K=I+1	GRA04580
	CN=1.	GRA04590
	SUM=OBSEG(I)	GRA04600
	DO325 J=K,ICOUNT	GRA04610
	IF(NUM(I)-NUM(J)) 325,320,325	GRA04620
320	NUM(J)=0	GRA04630
	CN=CN+1.	GRA04640
	SUM=SUM+OBSEG(J)	GRA04650
325	CONTINUE	GRA04660
	OBSEG(I)=SUM/CN	GRA04670
330	CONTINUE	GRA04680
C	ZERO DELTA G	GRA04690
	DO 6 I=1,ICOUNT	GRA04700
	IF(NUM(I)/1000) 6,6,8	GRA04710
6	CONTINUE	GRA04720
8	GEE=OBSEG(I)	GRA04730
	DO 14 J=1,ICOUNT	GRA04740
	HSI(J)=HS(J)	GRA04750
	HI(J)=H(J)	GRA04760
14	OBSEG(J)=OBSEG(J)-GEE	GRA04770
C	ADD BASE VALUE	GRA04780
16	DO 30 I=1,ICOUNT	GRA04790
	IF(NUM(I)/1000.LE.0) GO TO 30	GRA04800
	DO 25 JA=1,NNBASE	GRA04810
	IF(NUM(I)-NBASE(JA))25,10,25	GRA04820
10	DO 20 J=1,ICOUNT	GRA04830
20	OBSEG(J)=OBSEG(J)+BASEG(JA)	GRA04840
	GO TO 40	GRA04850
25	CONTINUE	GRA04860
30	CONTINUE	GRA04870
40	GO TO(300,100,100,300),NAG	GRA04880
C	STORE DATA FOR COMPARISON	GRA04890
100	JIMMY=JIMMY+1	GRA04900
	IF(JIMMY.NE.1) GO TO 105	GRA04910
	SR=0.	GRA04920
	SD=0.	GRA04930
	RM=0.	GRA04940
	II=0	GRA04950
105	IF(SQRT(RR/DD).GT.RM) RM=SQRT(RR/DD)	GRA04960
	SR=SR+RR	GRA04970

SD=SD+DD	GRA04980
DO 190 I=1,ICOUNT	GRA04990
IF(NUM(I)) 190,190,110	GRA05000
110 DO 140 J=1,500	GRA05010
IF(NUMI(J)) 120,120,130	GRA05020
120 NUMI(J)=NUM(I)+100000	GRA05030
II=II+1	GRA05040
PHII(J)=PHI(I)	GRA05050
ALONI(J)=ALON(I)	GRA05060
HI(J)=H(I)	GRA05070
HSI(J)=HS(I)	GRA05080
STA1I(J)=STA1(I)	GRA05090
STA2I(J)=STA2(I)	GRA05100
OBSGI(J)=OBSG(I)	GRA05110
GO TO 190	GRA05120
130 IF(NUMI(J)-(NUMI(J)/100000)*100000.EQ.NUM(I)) GO TO 150	GRA05130
140 CONTINUE	GRA05140
WRITE (4,1000)	GRA05150
1000 FORMAT(1H1,33X,54HOBSERVATION ARRAYS FILLED,EXECUTE MEANING AND CO	GRA05160
INTINUE)	GRA05170
GO TO 200	GRA05180
150 OBSGI(J)=OBSGI(J)+OBSG(I)	GRA05190
NUMI(J)=NUMI(J)+100000	GRA05200
190 CONTINUE	GRA05210
GO TO (310, 90,200),NAG	GRA05220
200 NSUM=0	GRA05230
DO 260 I=1,II	GRA05240
NSUM=NSUM+NUMI(I)/100000	GRA05250
OBSGI(I)=OBSGI(I)/FLOAT(NUMI(I)/100000)	GRA05260
260 NUMI(I)=NUMI(I)-(NUMI(I)/100000)*100000	GRA05270
SIG=SQRT(SR/SD)	GRA05280
WRITE (4,2000) NSUM,II,SIG,RM,JIMMY	GRA05290
2000 FORMAT(1H1,I10,2X,12HOBSERVATIONS,10X,I4,2X,8HSTATIONS,10X,13HMEANGRA05300	GRA05300
1 SIGMA = ,F6.3,10X,16HMAXIMUM SIGMA = ,F6.3/60X,I5,2X,5HLOOPS)	GRA05310
JIMMY=0	GRA05320
CALL NOMALY(II,NUMI,STA1I,STA2I,OBSGI,PHII,ALONI,HI,NOMTYP,IAG,HSIGRA05330	GRA05330
1,DIST)	GRA05340
NAG=0	GRA05350
DO 270 J=1,II	GRA05360
270 NUMI(J)=0	GRA05370
RETURN	GRA05380
300 IF(NAG.EQ.4) RETURN	GRA05390
15 CONTINUE	GRA05400
CALL NOMALY(II,NUM,STA1,STA2,OBSG,PHI,ALON,HI,NOMTYP,IAG,HSI,DIST)GRA05410	GRA05410
90 NAG=0	GRA05420
RETURN	GRA05430
400 DO 405 I=1,ICOUNT	GRA05440
IF(NUM(I)/1000.GT.0) GO TO 410	GRA05450
405 CONTINUE	GRA05460
410 LN=NUM(I)	GRA05470
GS=0.	GRA05480
CN=0.	GRA05490
DO 415 I=1,ICOUNT	GRA05500
IF(NUM(I).NE.LN) GO TO 415	GRA05510
GS=GS+OBSG(I)	GRA05520
CN=CN+1.	GRA05530
415 CONTINUE	GRA05540
GS=GS/CN	GRA05550
DO 420 I=1,ICOUNT	GRA05560
IF(NUM(I).EQ.LN) GO TO 418	GRA05570
OBSG(I)=OBSG(I)-GS	GRA05580
GO TO 420	GRA05590

```

      418 OBSG(I)=0.
GRA05600
      420 CONTINUE
            GO TO 16
            END
C
C
C
      SUBROUTINE NOMALY(ICOUNT,NUM,STA1,STA2,OBSG,PHI,ALON,HI,NOMTYP,
1IAG,HSI,DIST)
C      COMPUTES FREE AIR AND BOUGUER ANOMALIES
C      PRINTS FINAL OUTPUT TAB
C      PUNCHES CARDS
      DIMENSION NUM(1),PHI(1),ALON(1),H(1),OBSG(1)
      DIMENSION HS(1),HI(1),HSI(1)
      DIMENSION COEF(11)
      CHARACTER *6 SECCON(2),TYP(13), STA1(1),STA2(1)
      DATA(COEF(I),I=1,11)/.3086,.1119,.2238,.06886,.2225,.04191,.08382,
1.06999,.2248,.03843,.07347/, (TYP(I),I=1,13)/'1','2','3','4','5','
26','7','8','9','A','B','C','D'/
      WRITE (4,1000)
1000 FORMAT(/25X,69HP R I N C I P A L   F A C T S   A T   G R A V I T YGRA05800
1   S T A T I O N S//6X,16HSTA NAME AND NUM,5X,8HLATITUDE,3X,9HLONGGRA05810
2ITUDE,3X,9HELEVATION,2X,9HSUPP ELEV,2X,10HOBSERVED G,2X,8HFREE AIRGRA05820
3,3X,7HBOUGUER,3X,7HTHEOR G/28X,7HNORTH +,5X,6HEAST +,6X,6H FEET , GRA05830
45X,6HMETERS,6X,4HMGAL,7X,4HMGAL,6X,4HMGAL,6X,4HMGAL/)
      SECCON(1)='2'
      SECCON(2)=' '
      NOMTYP=NOMTYP+1
      IPAGE=0
      I=1
      DO 500 J=1,ICOUNT
      IF(NUM(J).EQ.0)GO TO 500
      CALL RADEG(PHI(J),KDEG,XMIN)
      CALL RADEG(ALON(J),JDEG,TMIN)
      H(1)=HI(J)
      HS(1)=HSI(J)
      GAMMA=2049.+978049.*(.0052884*SIN(PHI(J))**2-.0000059*SIN(2.*PHI(J)GRA05960
1))**2)
      GO TO (10,15,20,25,30,35,40,45,50,55,60,65,70),NOMTYP
      GRA05980
10 FA=OBSG(J)+COEF(NOMTYP)*H(I)-GAMMA
      BA=FA-COEF(NOMTYP+1)*H(I)
      GRA05990
      GO TO 100
      GRA06000
15FA=OBSG(J)+COEF(NOMTYP+1)*HS(I)+COEF(NOMTYP-1)*(H(I)-HS(I))-GAMMAGRA06020
      BA=FA-COEF(NOMTYP)*H(I)
      GRA06030
      GO TO 100
      GRA06040
20 FA=OBSG(J)-GAMMA
      BA=FA+COEF(NOMTYP+1)*H(I)
      GRA06050
      GO TO 100
      GRA06060
25 FA=OBSG(J)-COEF(NOMTYP+1)*HS(I)-GAMMA
      BA=FA+COEF(NOMTYP)*H(I)
      GRA06070
      GO TO 100
      GRA06080
30 FA=OBSG(J)-COEF(NOMTYP)*HS(I)-GAMMA
      BA=FA+COEF(NOMTYP-1)*HS(I)
      GRA06090
      GO TO 100
      GRA06100
35 FA=OBSG(J)+COEF(NOMTYP-5)*H(I)-GAMMA
      BA=FA-COEF(NOMTYP)*HS(I)-COEF(NOMTYP-4)*(H(I)-HS(I))
      GRA06110
      GO TO 100
      GRA06120
40 FA=OBSG(J)+COEF(NOMTYP)*HS(I)+COEF(NOMTYP-6)*(H(I)-HS(I))-GAMMA
      BA=FA-COEF(NOMTYP-1)*HS(I)-COEF(NOMTYP-5)*(H(I)-HS(I))
      GRA06130
      GO TO 100
      GRA06140
      GRA06150
      GRA06160
      GRA06170
      GRA06180
      GRA06190

```

```

45 FA=OBSG(J)+COEF(NOMTYP-1)+COEF(NOMTYP-7)*(H(I)-HS(I))-GAMMA      GRA06200
   BA=FA-COEF(NOMTYP-2)*H(I)-COEF(NOMTYP)*(H(I)-HS(I))              GRA06210
   GO TO 100                                                            GRA06220
50 FA=OBSG(J)+COEF(NOMTYP-8)-GAMMA                                    GRA06230
   BA=FA-COEF(NOMTYP-3)*H(I)-COEF(NOMTYP-1)*(H(I)-HS(I))            GRA06240
   GO TO 100                                                            GRA06250
55 FA=OBSG(J)+COEF(NOMTYP-9)*H(I)-GAMMA                              GRA06260
   BA=FA-COEF(NOMTYP-8)*H(I)+COEF(NOMTYP-2)*HS(I)                   GRA06270
   GO TO 100                                                            GRA06280
60 FA=OBSG(J)+COEF(NOMTYP-10)*H(I)-COEF(NOMTYP-2)*HS(I)-GAMMA      GRA06290
   BA=FA-COEF(NOMTYP-9)*H(I)+COEF(NOMTYP-3)*HS(I)                   GRA06300
   GO TO 100                                                            GRA06310
65 FA=OBSG(J)+COEF(NOMTYP-11)*H(I)-GAMMA                            GRA06320
   BA=FA-COEF(NOMTYP-2)*H(I)-COEF(NOMTYP-1)*(H(I)-HS(I))            GRA06330
   GO TO 100                                                            GRA06340
70 FA=OBSG(J)+COEF(NOMTYP-12)*H(I)-GAMMA                            GRA06350
   BA=FA-COEF(NOMTYP-3)*HS(I)-COEF(NOMTYP-11)*(H(I)-HS(I))          GRA06360
100 OBSG(J)=OBSG(J)+976000.                                           GRA06370
    GAMMA=GAMMA+976000.                                               GRA06380
    H(I)=H(I)*3.280833                                               GRA06390
    WRITE(4,2000) STA1(J),STA2(J),NUM(J),KDEG,XMIN,JDEG,TMIN,H(I),    GRA06400
    1HS(I),OBSG(J),FA,BA,GAMMA                                       GRA06410
2000 FORMAT(5X,2A6,1X,I5,3X,I3,F6.2,2X,I4,F6.2,2X,F10.3,2X,F9.3,1X,F11. GRA06420
    13,2X,F10.3,2X,F10.3,1X,F11.3)                                     GRA06430
    WRITE(6,2001) STA1(J),STA2(J),KDEG,XMIN,JDEG,TMIN,H(I),OBSG(J),  GRA06440
    *FA,BA                                                            GRA06450
    WRITE(6,*) FA,BA                                                  GRA06460
2001 FORMAT(4X,2A6,1X,I3,F6.2,1X,I4,F6.2,F10.3,1X,F11.3,2X,E9.3,1X,  GRA06470
    *E9.3)                                                            GRA06480
    DIST=DIST+200.                                                    GRA06490
C    IF (BA.EQ.13.3262033) THEN                                       GRA06500
C    PRINT *, 'HELLO'                                                GRA06510
C    DIST=DIST+200.                                                  GRA06520
C    END IF                                                            GRA06530
    TLAT1=KDEG - (XMIN/60.)                                           GRA06540
    TLONG1=JDEG + (TMIN/60.)                                          GRA06550
    WRITE(3,1234) DIST,BA                                             GRA06560
1234 FORMAT(F9.2,2X,F6.2)                                             GRA06570
    IPAGE=IPAGE+1                                                     GRA06580
    IF(IPAGE.LT.50) GO TO 200                                         GRA06590
    IPAGE=0                                                            GRA06600
    WRITE(4,4000)                                                      GRA06610
4000 FORMAT('1')                                                      GRA06620
    WRITE(4,1000)                                                      GRA06630
    200 CONTINUE                                                       GRA06640
    IF(IAG.EQ.1) GO TO 500                                             GRA06650
    KMIN=IPUNIX(XMIN,2)                                               GRA06660
    JMIN=IPUNIX(TMIN,2)                                               GRA06670
    IH=IPUNIX(H(I),1)                                                 GRA06680
    IHS=IPUNIX(HS(I),1)                                              GRA06690
    OBSG(J)=OBSG(J)-976000.                                           GRA06700
    IG=IPUNIX(OBSG(J),2)                                             GRA06710
    IFA=IPUNIX(FA,1)                                                 GRA06720
    IBA=IPUNIX(BA,1)                                                 GRA06730
    IF(IAG.EQ.3) GO TO 300                                             GRA06740
    WRITE(6,3000) SECCON(1),SECCON(2),KDEG,KMIN,JDEG,JMIN,TYP(NOMTYP) GRA06750
    1,IH,IHS,IG,IFA,IBA,NUM(J)                                       GRA06760
3000 FORMAT(2A1,I3,I4,2X,I4,I4,1X,A1,1X,I7,1X,I5,1X,I6,1X,I5,1X,I5,14X, GRA06770
    1I4)                                                                GRA06780
    GO TO 500                                                          GRA06790
300 OBSG(J)=OBSG(J)+976000.                                           GRA06800
    WRITE(6,5000) STA1(J),STA2(J),KDEG,XMIN,JDEG,TMIN,H(I),OBSG(J),FAGRA06810

```

```

1,BA
5000 FORMAT(2A6,2X,I3,F6.2,2X,I4,F6.2,2X,F8.2,2X,F10.3,4X,F7.2,4X,F7.2)
500 CONTINUE
RETURN
END
C
C
C
SUBROUTINE CALIB(ICOUNT,NUM,OSBG,NNBASE,NBASE,BASEG,STA1,STA2,NAG,
1PHI,ALON,H,CALIM,PUBG,Y,V)
DIMENSION NUM(1),OSBG(1),NBASE(1),BASEG(1),STA1(1),STA2(1)
DIMENSION PHI(1),ALON(1),H(1)
DIMENSION PUBG(1),Y(1),V(1)
WRITE (4,1000)
1000 FORMAT(46X,38H CALIB IS A DUMMY,NO SCALE WAS COMPUTED)
NAG=NAG+1
RETURN
END
C
C
C
SUBROUTINE PLOT2D(N,X,Y)
C PLOTS Y AGAINST X. N IS NUMBER OF POINTS
C Y AND X ARE SCALED AGAINST THEIR MAX AND MIN VALUES
C THE ELEMENTS OF X AND Y ARRAYS ARE NOT ALTERED
DIMENSION X(1),Y(1)
CHARACTER *6 P(100)
DO 10 I=1,100
10 P(I)=' '
XMIN=0.0
XMAX=0.0
YMIN=0.0
YMAX=0.0
DO 20 I=1,N
IF(XMIN.GT.X(I)) XMIN=X(I)
IF(X(I).GT.XMAX) XMAX=X(I)
IF(YMIN.GT.Y(I)) YMIN=Y(I)
IF(Y(I).GT.YMAX) YMAX=Y(I)
20 CONTINUE
WRITE (4,200) XMIN,XMAX
200 FORMAT(3X,F7.0,92X,F7.0)
XSCALE=(XMAX-XMIN)/99.0
YSCALE=(YMAX-YMIN)/49.0
IF(YMAX) 25,25,27
27 IF(YMIN) 28,25,25
28 JYO=-YMIN/YSCALE+1.0
GO TO 26
25 JYO=0
26 DO 95 I=1,50
IF(I.EQ.1) P(1)='+'
IF(I.EQ.1) P(100)='+'
IF(I.EQ.50) P(100)='+'
IF(I.EQ.50) P(1)='+'
IYREF=51-I
DO 60 J=1,N
JYTEM=(Y(J)-YMIN)/YSCALE+1.0
IF(JYTEM-IYREF) 60,30,60
30 KJ=(X(J)-XMIN)/XSCALE+1.0
35 P(KJ)='*'
60 CONTINUE
IF(IYREF-50) 65,70,65

```

GRA06820

GRA06830

GRA06840

GRA06850

GRA06860

GRA06870

GRA06880

GRA06890

GRA06900

GRA06910

GRA06920

GRA06930

GRA06940

GRA06950

GRA06960

GRA06970

GRA06980

GRA06990

GRA07000

GRA07010

GRA07020

GRA07030

GRA07040

GRA07050

GRA07060

GRA07070

GRA07080

GRA07090

GRA07100

GRA07110

GRA07120

GRA07130

GRA07140

GRA07150

GRA07160

GRA07170

GRA07180

GRA07190

GRA07200

GRA07210

GRA07220

GRA07230

GRA07240

GRA07250

GRA07260

GRA07270

GRA07280

GRA07290

GRA07300

GRA07310

GRA07320

GRA07330

GRA07340

GRA07350

GRA07360

GRA07370

GRA07380

GRA07390

GRA07400

GRA07410

GRA07420

65	IF(IYREF-1) 66,75,66	GRA07430
66	IF(JYO) 80,80,67	GRA07440
67	IF(JYO-IYREF) 80,68,80	GRA07450
68	P(1)='+'	GRA07460
	WRITE (4,690) P	GRA07470
690	FORMAT(2X,5H0.000,2(50A1))	GRA07480
	GO TO 85	GRA07490
70	WRITE (4,700) YMAX,P	GRA07500
700	FORMAT(F7.3,2(50A1))	GRA07510
	GO TO 85	GRA07520
75	WRITE (4,700) YMIN,P	GRA07530
	GO TO 85	GRA07540
80	WRITE (4,800) P	GRA07550
800	FORMAT(7X,2(50A1))	GRA07560
85	DO 90 J=1,100	GRA07570
90	P(J)=' '	GRA07580
95	CONTINUE	GRA07590
	RETURN	GRA07600
	END	GRA07610
C		GRA07620
C		GRA07630
C		GRA07640
	FUNCTION DEGRAD(JDEG,AMIN)	GRA07650
C	* * * * DEGRAD CONVERTS DEGREES + MINUTES (1/102S) TO RADIANS	GRA07660
	ALFA= .174532925199 E-1	GRA07670
	BETA=.290888208666 E-3	GRA07680
	A=JDEG	GRA07690
	IF(A) 100,200,300	GRA07700
100	DEGRAD=A*ALFA-AMIN*BETA	GRA07710
	GO TO 400	GRA07720
200	DEGRAD=AMIN*BETA	GRA07730
	GO TO 400	GRA07740
300	DEGRAD=A*ALFA+AMIN*BETA	GRA07750
400	RETURN	GRA07760
	END	GRA07770
C		GRA07780
C		GRA07790
C		GRA07800
	SUBROUTINE RADEG(RAD,JDEG,TMIN)	GRA07810
C	CONVERTS RADIANS TO DEGREES(SIGNED) AND MINUTES	GRA07820
	TMIN=3437.74677078*RAD	GRA07830
	JDEG=TMIN/60.	GRA07840
	TMIN=TMIN-FLOAT(JDEG*60)	GRA07850
	IF(JDEG.LT.0) TMIN=-TMIN	GRA07860
	RETURN	GRA07870
	END	GRA07880
	FUNCTION IPUNIX(VAL,IDEC)	GRA07890
C	CONVERTS REAL VALUE(VAL) TO ROUNDED INTEGER RETAINING	GRA07900
C	SPECIFIED(IDEC) NO. OF DECIMAL PLACES	GRA07910
C	USE FOR PUNCHED OUTPUT WITH NO DECIMAL POINT	GRA07920
	P=VAL*10.**IDEC	GRA07930
	IP=P	GRA07940
	FRACT=P-FLOAT(IP)	GRA07950
	IPUNIX=P	GRA07960
	IF(FRACT) 10,30,20	GRA07970
10	IF(FRACT+.5) 15,15,30	GRA07980
15	IPUNIX=P-1.	GRA07990
	GO TO 30	GRA08000
20	IF(FRACT-.5) 30,25,25	GRA08010
25	IPUNIX=P+1.	GRA08020
30	RETURN	GRA08030

	END	GRA08040
C		GRA08050
C		GRA08060
C		GRA08070
	FUNCTION DERAD2(J,K,C)	GRA08080
C	CONVERTS WHOLE DEG,MIN AND FRACTIONAL SEC TO RADIANS	GRA08090
	DATA X,Y,Z/.174532925199E-1,.290888208666E-3,.4848136811E-5/	GRA08100
	A=J	GRA08110
	B=K	GRA08120
	IF(J.LT.0) GO TO 1	GRA08130
	IF(K.LT.0) GO TO 2	GRA08140
	DERAD2=X*A+Y*B+Z*C	GRA08150
	RETURN	GRA08160
1	DERAD2=X*A-Y*B-Z*C	GRA08170
	RETURN	GRA08180
2	DERAD2=Y*B-Z*C	GRA08190
	RETURN	GRA08200
	END	GRA08210

APPENDIX I-B

STATION FORTRAN

STATION FORTRAN converts station foresight and backsight level readings to elevations. In addition, the program calculates station spacing, total elevation change, and total elevation error for each line. The program source listing is given below:

```

C Title : Title of Line
C   NA: Total Number Of Station
C BENCH: Bench Mark Elevation
C CORR1 : Correction Factor 1
C CORR2 : Correction Factor 2
      CHARACTER * 80 TITLE
      INTEGER SUM
      WRITE(6,*) 'TYPE TITLE NAME'
      READ(5,1011) TITLE
1011  FORMAT(A80)
      WRITE(2,1012) TITLE
1012  FORMAT(//,A80,/)
      READ(1,*) NA,BENCH,CORR1,CORR2
      SUMB=0.0
      SUMF=0.0
      BSUM=0.0
      FSUM=0.0
C
C
C   ELEV=BENCH
      DO 100 I=1,NA
C
      WRITE(2,1000)
1000  FORMAT(1X,'BACKSIGHT',4X,'MEAN',2X,'INTERVAL',4X,'FORESIGHT',4X,
+ 'MEAN',4X,'INTERVAL',/,1X,'-----',4X,'----',2X,'-----',4X,
+ '-----',5X,'----',4X,'-----',/)
C
C B1, B2, B3 : Corresponds To Top-Middle-Bottom Backsight Readings
C F1, F2, F3 : Corresponds To Top-Middle-Bottom Foresight Readings
C
C
      READ(1,*) B1,B2,B3,F1,F2,F3
C
      BMEAN=(B1+B2+B3)/3.0

```

STA00010
 STA00020
 STA00030
 STA00040
 STA00050
 STA00060
 STA00070
 STA00080
 STA00090
 STA00100
 STA00110
 STA00120
 STA00130
 STA00140
 STA00150
 STA00160
 STA00170
 STA00180
 STA00190
 STA00200
 STA00210
 STA00220
 STA00230
 STA00240
 STA00250
 STA00260

APPENDIX I-C

COMPARISON OF UPDW/UDD FORTRAN ALGORITHMS

UPDW FORTRAN algorithm is based on the two-dimensional harmonic analysis method of Bhattacharyya (1965). This program was written by Agrwal (1968). It was used to differentiate local and regional gravitational trends. A comparison between the algorithms used in the programs UPDW FORTRAN and UDD FORTRAN (Ruddman and Blakley, 1983) was conducted at the onset of this study. The purpose of this comparison was to determine which algorithm was best for this study. The algorithm used in UDD FORTRAN is based on a method developed by Henderson and Zietz (1949) while the algorithm used in UPDW FORTRAN is based on the method of Bhattacharyya (1965).

The algorithm used in UDD FORTRAN is based on:

Equation 1:

$$\Delta T(h) = \sum_{i=1}^{n-1} \Delta \bar{T}(r_i) K(r_i, h) + \Delta \bar{T}(r_n) K(r_n, h)$$

Figure 23: Contour map of vertical gravity component over a sphere. Contour interval is 0.40 milligals. This data was used in comparing the algorithms of the programs UPDW and UDD FORTRAN.

where

h : height above surface

$K(r_i, h)$: Continuation and vertical Derivative Coefficients

$T(h)$: Calculated field

$T(r^i)$: Average value of T on the i th circle of radius r

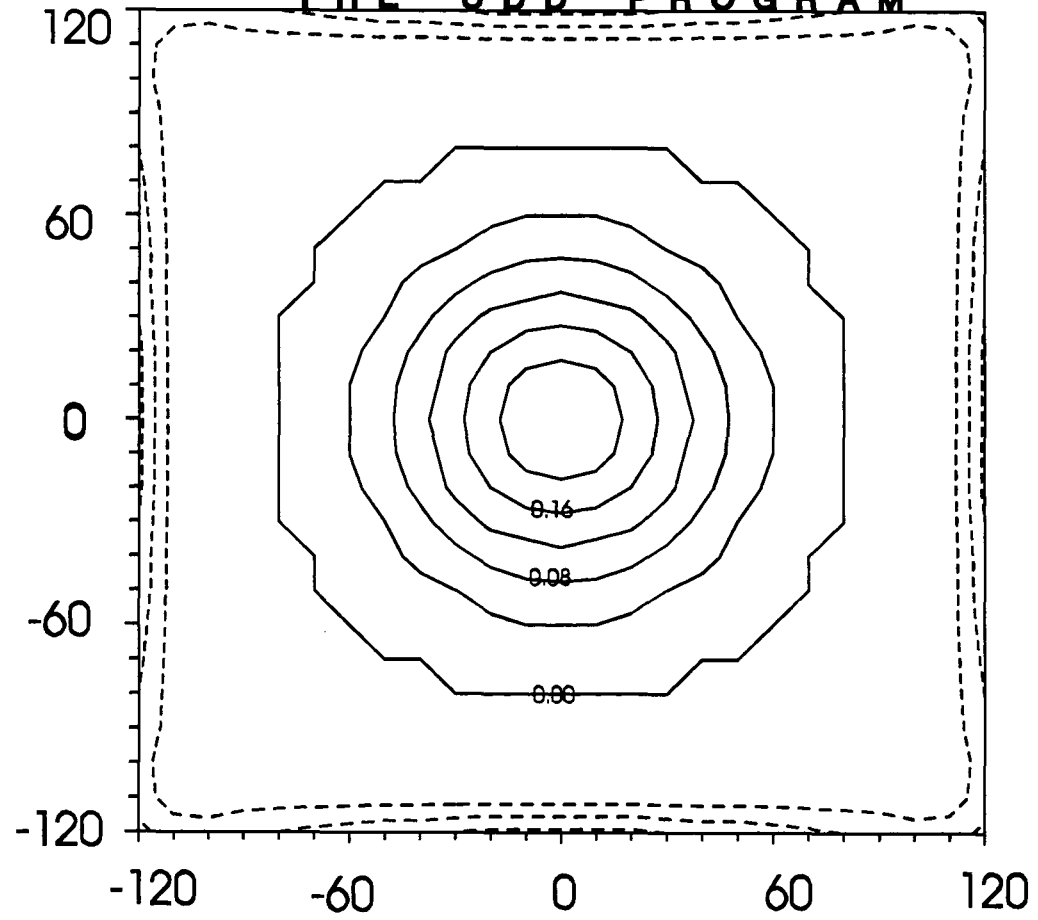
Using this equation Ruddman and Blackely (1983) developed a UDD FORTRAN that determined the upward and downward continuation of a potential field. In addition, the program can determine the second vertical derivative of a potential field. To use this program the data had to be gridded. Once gridded the potential field can be filtered by continuing it upward or downward, or by taking the 2nd vertical derivative. Filtering is accomplished by using a series concentric rings about each grid point. The radius of these rings is defined as follows:

$$r_i = \text{gridspacing} * n, \text{ where } n=1,2,3,\dots,k-1.$$

The potential field values that intersect the respective circles are multiplied by the appropriate table of coefficients (Henderson and Zietz, 1949). After this is done for each grid point, values of the operation are summed at the grid points resulting in filtered values.

Figure 24: Contour plot of the second vertical derivative field of the spherical gravity field, using UDD FORTRAN. Contour interval is 0.04 milligals.

SECOND DERIVATIVE OF
SPHERICAL BODY USING
THE UDD PROGRAM



The two-dimensional harmonic analysis method used in the program UPDW FORTRAN (Agarwal, 1968) is based on:

Equation 2:

$$T(x, y, z) = \sum_{m=0}^{m_0} \sum_{n=0}^{n_0} [A_{mn} \cos(2\Pi m \frac{x}{L_x}) \cos(2\Pi n \frac{y}{L_y}) + B_{mn} \cos(2\Pi m \frac{x}{L_x}) \sin(2\Pi n \frac{y}{L_y}) + E_{mn} \sin(2\Pi m \frac{x}{L_x}) \cos(2\Pi n \frac{y}{L_y}) + F_{mn} \sin(2\Pi m \frac{x}{L_x}) \sin(2\Pi n \frac{y}{L_y})] [e^{-2\Pi(\frac{m^2}{L_x^2} + \frac{n^2}{L_y^2}) \frac{1}{2} z}] [-2\Pi \frac{m^2}{L_x^2} + \frac{n^2}{L_y^2} \frac{1}{2}]^r$$

where

$A_{mn}, B_{mn}, E_{mn}, F_{mn}$: are coefficients of the solution to the partial differential equation.

m : number of values along x-axis

n : number of values along y-axis

S_x : Uniform spacing along x-axis

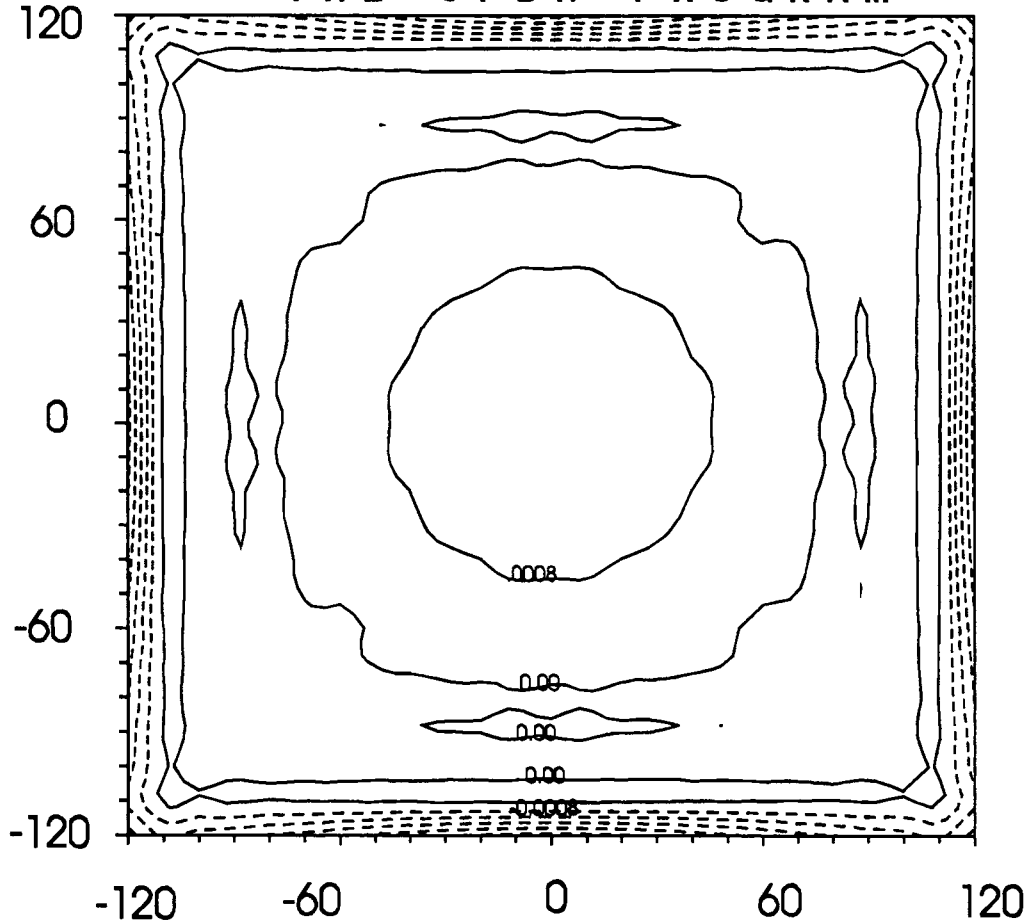
S_y : Uniform spacing along y-axis

$L_x = mS_x$: L_x is the Nyquist Frequency

$L_y = nS_y$: Uniform spacing along y-axis

Figure 25: Contour plot of the second vertical derivative of spherical gravity field, using UPDW FORTRAN. Contour interval is 0.04 milligals.

SECOND DERIVATIVE OF
SPHERICAL BODY USING
THE UPDW PROGRAM



Downward Continuation: $Z > 0$

Upward Continuation : $Z < 0$

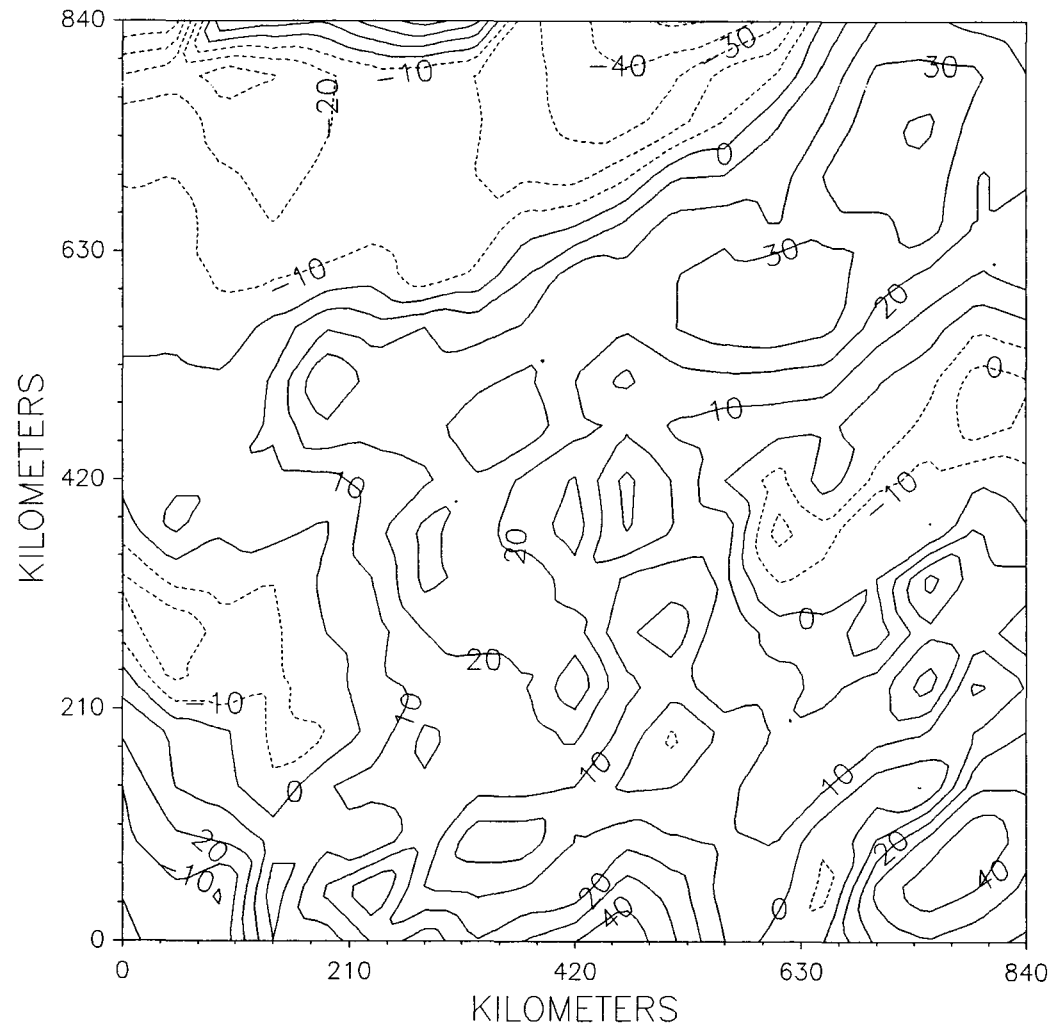
Vertical Derivative : $r = 0, 1, 2, 3, \dots, n$

The two dimensional harmonic analysis method allows the potential field to be continue upward or downward at any level. In addition, this method can determine the n TH vertical derivative of a potential field at the specified level. The coefficients A_{mn} , B_{mn} , E_{mn} , and F_{mn} in the equation 2 are first calculated by the algorithm. These coefficients are the solution to the partial differential equation. Once the coefficients are calculated the upward/downward continuation and/or the vertical derivative of the potential field can be calculated since the remaining values in the equation are known. To calculate the upward or downward continuation of a potential field at the surface assign the appropriate "Z" value and set r to zero. The n TH vertical derivative is calculated in a similar fashion; however, the value of r is greater than one. It is apparent the continuation and n TH vertical derivative use different terms of the same equation when calculating the respective fields.

A theoretically calculated data set was computed for a sphere. This output was used as input for UPDW FORTRAN and UDD FORTRAN, so that a comparison of these programs could

Figure 26: Contour plot of the potential field values listed in a paper by Tasubi (1959).

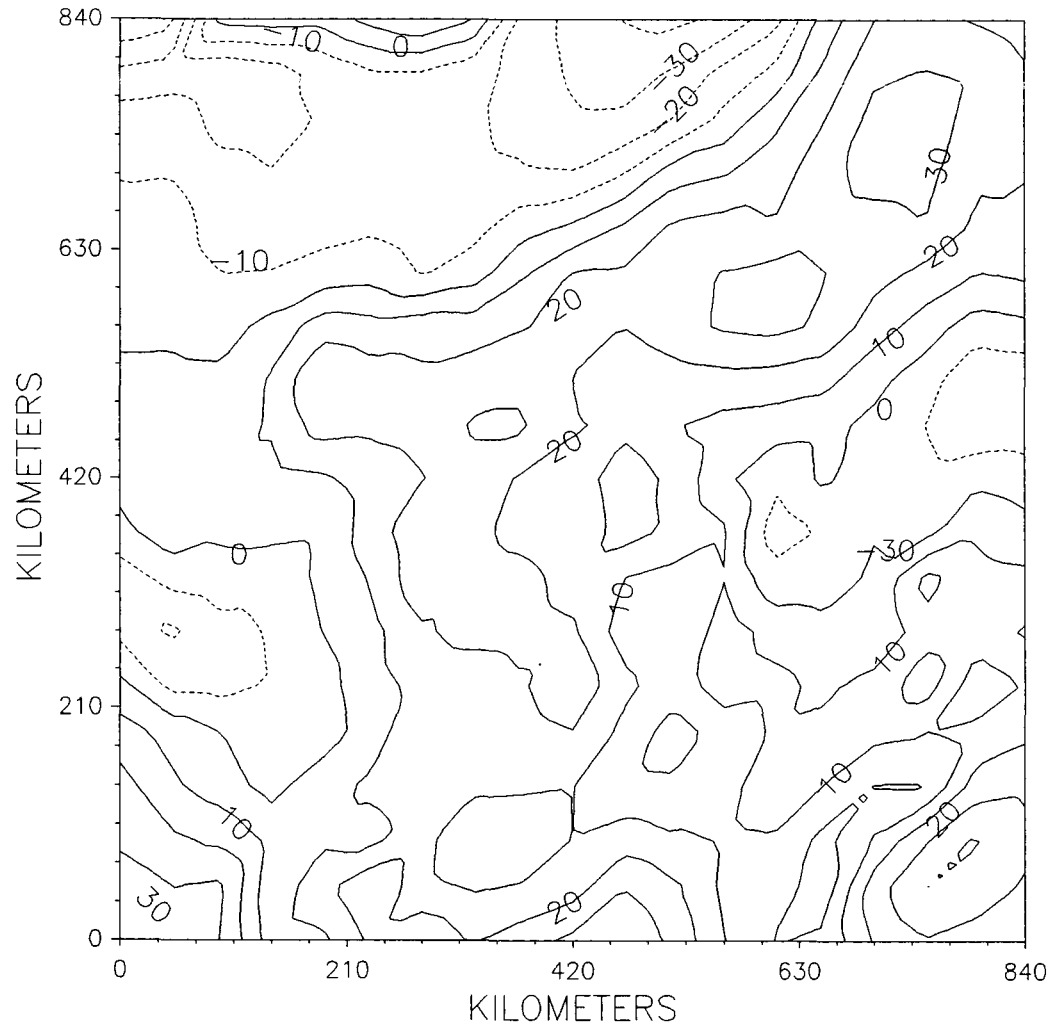
Tasubi Gravity Data (1959)



be conducted (Figure 23). The output from both programs was contoured with the results shown in Figures 24 and 25, respectively. Both maps have concentric rings about their centers. In fact, when the two maps are overlain, like contours, at the maps' center, closely approximate each other. The difference is at the maps edges. These differences are attributed to the algorithms being used. UDD FORTRAN output has a minimum edge effect, while UPDW FORTRAN values are effected at the edge. This aspect of the two methods is the only advantage UDD FORTRAN has over UPDW FORTRAN. A critical advantage UPDW FORTRAN has over UDD FORTRAN is that a continuation field can be continued upward or downward at any level. UDD FORTRAN can continue a field upward or downward only at grid spacing intervals. The maximum a field can be continued upward or downward with UDD FORTRAN is four grid levels. A second advantage of UPDW FORTRAN when compared to UDD FORTRAN is UPDW can process a matrix of potential field values up to 60x60 while UDD can process a maximum matrix of 25x25. The capability of UPDW to process a 60x60 was deemed important because it reduced the time in performing the potential field filtering. For the reasons listed above, UPDW FORTRAN was chosen to perform the analysis of the gravity data in this study. To compensate for the edge effects of UPDW the output was overlapped. A listing of both UPDW and UDD FORTRAN are given below:

Figure 27: Contour plot of the potential field values listed in a paper by Tasubi (1959), continued to a level of +15.9 kilometers.

Upward Continuation Of Tasubi Gravity Data at 15.9 Km.



To verify the output from UPDW FORTRAN the data of Tasubi (1959) was gridded and contoured for analysis (Figure 26). The potential field was continued upward 15.9 kilometers using UPDW FORTRAN. The contour plot of this operation (Figure 27) was compared to the values in Tasubi's paper (1959), and no discernable differences were identified.

UPDW FORTRAN:

Written by: Agarwal (1968)

```

C                                     UPD00010
C THIS PROGRAM CALCULATES THE UPWARD OR DOWNWARD CONTINUATION AT ANY UPD00020
C HEIGHT OR DEPTH IN A PARTICULAR LOCATION. IT ALSO OBTAINS FIRST,SECOND UPD00030
C OR HIGHEST SET OF DERIVATIVES. USES TWO DIMENSIONAL FOURIER ANALYSIS. UPD00040
C                                     UPD00050
C THIS PROGRAM ALSO OBTAINS 1ST, 2ND, OR HIGHEST SET OF DERIVATIVES. UPD00060
C                                     UPD00070
C THE GAUSSIAN DISTRIBUTION FOR THE CALCULATIONS USED IN THIS PROGRAM UPD00080
C IS AFTER TSUBOI(1959) UPD00090
C                                     UPD00100
C Z: UPWARD (-IVE) OR DOWNWARD (+IVE) HEIGHT. UPD00110
C                                     UPD00120
C ID=0 FOR NO DERIVITVE UPD00130
C ID=1 FOR FIRST DERIVITIVE UPD00140
C ID=2 FOR 2ND DERIVITIVE UPD00150
C ID=3 FOR 3RD DERIVITIVE AND SO ON UPD00160
C                                     UPD00170
C X1(I,J) IS THE REAL INPUT MATRIX IN SPACE DOMAIN. UPD00180
C                                     UPD00190
C X(J) IS THE FINAL SYMMETERIZED DATA, USING GYCLIC PROORTIES OF UPD00200
C FOURIER TRANSFORMS. UPD00210
C                                     UPD00220
C FOR COMPUTATION PROGRAM USES X(J)+IY(J) WHERE Y(J)=0.0 UPD00230
C OUTPUT RESULTS ARE GIVEN AS X(J)+IY(J) IN FREQUENCY DOMAIN UPD00240
C                                     UPD00250
C N(J,K,0) : ARRAY OF DATA IS TOW DIMENSIONAL WITH SIDE J BY K UPD00260
C NOPTS: NUMBER OF DATA POINTS (J*K) UPD00270
C DELT: THE DIGITIZING INTERVAL IN MILES. UPD00280
C                                     UPD00290
C                                     UPD00300
C         DIMENSION X(15000),Y(15000),S(15000),N(3),X1(76,76) UPD00310
C 20 FORMAT(5X,3I5) UPD00320
C 22 FORMAT(1HJ,31X,23HDEGREE OF DERIVATIVE = ,I5,23X,24HSIZE OF OUTPUT UPD00330
C 1 MATRIX = ,I5) UPD00340
C 23 FORMAT(1HJ,20X,34HELEVATION OF CONTINUATION FIELD = ,F10.5,5X,37HD UPD00350
C 1IGITIZING INTERVAL OF DATA POINTS = ,F10.5) UPD00360
C 30 FORMAT(5X,F10.5) UPD00370
C 35 FORMAT(1X,6E11.4) UPD00380
C 36 FORMAT(1X,10E13.4) UPD00390
C 45 FORMAT(1HJ) UPD00400
C 40 FORMAT(1H1,60X,10HINPUT DATA) UPD00410
C 42 FORMAT(1HT,60X,10H*****)) UPD00420
C 50 FORMAT(1HT,25X,80(1H*)) UPD00430
C 60 FORMAT(1X,6HDELT = ,F8.3,8X,18HNYQUIST FREQUENCY=,F8.3) UPD00440
C 70 FORMAT(1HJ,22X,15HFREQUENCY =2*J*,F10.6,1X,15HCYCLES PER MILE) UPD00450
C 316 FORMAT(1H1,40X,47HUPWARD OR DOWNWARD CONTINUATION AND DERIVATIVES) UPD00460
C 317 FORMAT(41X,47(1H*)) UPD00470
C 320 FORMAT(1HL,56X,17HREAL (SPACE) PART) UPD00480
C 325 FORMAT(1HT,56X,17H*****)) UPD00490
C
C XMIN : MINIMUM XMIN=MINX-TERV where MINX= minimum x value
C YMIN : MINIMUM YMIN=MINY-TERV where MINY= minimum y value
C TERV : Digitizing Interval
C

```

```

READ(1,*) ID,XMIN,YMIN,TERV
READ(1,*) DELT
READ(1,*) Z
READ(1,*) (N(J),J=1,3)
NOPTS=N(1)*N(2)
WRITE(6,*) NOPTS, N(1), N(2)
NN=N(1)
NNN=N(2)
DO 9 I=1,NN
READ(1,1235) (X1(I,J),J=1,NNN)
C Choose One Format: Current Format gives X, Y, and Z values
C WRITE(6,1235) (X1(I,J),J=1,NNN)
C235 FORMAT(23X,F10.2)
1235 FORMAT(F10.2)
9 CONTINUE
WRITE(2,40)
WRITE(2,42)
DO 10 I=1,NN
WRITE(2,36) (X1(I,J),J=1,NNN)
WRITE(2,45)
10 CONTINUE
WRITE(2,50)
C
C SETTING X AS THE FINAL SYMMERTIZED MATRIX OF SIZE (2N-2)*(2N-2). REMEMUP
C BER HERE X IS STORED IN A VECTOR FORM.
C
C
DO 1 I=1,NN
DO 2 J=1,NNN
J1=(2*NN-2)*(I-1)+J
X(J1)=X1(I,J)
2 CONTINUE
N1=NN-2
DO 3 J=1,N1
J2=J1+J
X(J2)=X1(I,NN-J)
3 CONTINUE
1 CONTINUE
N2=2*NN-2
DO 5 K=1,N1
DO 4 J=1,N2
J3=J2+J
X(J3)=X(J3-(4*NN-4)*K)
4 CONTINUE
J2=J3
5 CONTINUE
C
C END OF SYMMETRIZED VECTOR. NOW WE RESET N(1),N(2),NOPTS,ETC.....
C
N(1)=2*NN-2
N(2)=2*NNN-2
NN=N(1)
NNN=N(2)
NOPTS=N(1)*N(2)
FN=1./(2.*DELT)
WRITE(2,60) DELT, FN
PRINT *, 'FP=' , FP, 'NOPTS=' , NOPTS
FP=FN/(FLOAT(NOPTS))
WRITE(2,70) FP
CALL ZERO(Y,NOPTS)
CALL ZERO(S,NOPTS)
CALL ARMDFT(N,X,Y,S)

```

```

UPD00500
UPD00510
UPD00520
UPD00530
UPD00540
UPD00550
UPD00560
UPD00570
UPD00580
UPD00590
UPD00600
UPD00610
UPD00620
UPD00630
UPD00640
UPD00650
UPD00660
UPD00670
UPD00680
UPD00690
UPD00700
UPD00710
UPD00720
UPD00730
UPD00740
UPD00750
UPD00760
UPD00770
UPD00780
UPD00790
UPD00800
UPD00810
UPD00820
UPD00830
UPD00840
UPD00850
UPD00860
UPD00870
UPD00880
UPD00890
UPD00900
UPD00910
UPD00920
UPD00930
UPD00940
UPD00950
UPD00960
UPD00970
UPD00980
UPD00990
UPD01000
UPD01010
UPD01020
UPD01030
UPD01040
UPD01050
UPD01060
UPD01070
UPD01080
UPD01090
UPD01100

```

```

C
C MULTIPLY FREQ. BY A FACTOR; EXP((1**2+J**2)*(2.0*PI*Z/(NN*DELTA))),
C FOR 1=0,2,2.....NN AND J=0,1,2.....NNN
C
      DO 121 I=1,NN
      IF(I.GT.(NN/2+1)) GO TO 11
      A=I-1
      GO TO 12
11  A=NN+1-I
12  CONTINUE
      K=(I-1)*NNN+1
      L=K+NNN-1
      DO 121 J=K,L
      IF(J.GT.((L+K)/2+1)) GO TO 13
      B=J-1-(NN*(I-1))
      GO TO 14
13  B=NN+1-J+(NN*(I-1))
14  CONTINUE
      XYA=(SQRT(A**2+B**2)*2.0*3.14159*Z)/(FLOAT(NN)*DELTA)
      CONT=EXP(XYA)
      IF(ID.EQ.0) GO TO 15
      CONTDI=(SQRT(A**2+B**2)*(2.0*3.14159)/(FLOAT(NN)*DELTA))**ID
15  CONTINUE
      X(J)=X(J)*CONT
      Y(J)=Y(J)*CONT
      IF(ID.EQ.0) GO TO 121
      X(J)=X(J)*CONTDI
      Y(J)=Y(J)*CONTDI
121 CONTINUE
      J=0
      DO 250 J3=1,NOPTS
      J=J+1
C
C REPLACE FOURIER COEFFS. BY COMPLEX CONJUGATE
C
      F=Y(J)
      Y(J)=-F
250 CONTINUE
      CALL ZERO(S,NOPTS)
      CALL ARMDFT(N,X,Y,S)
      J=0
      DO 350 J4=1,NOPTS
      J=J+1
C TAKE COMPLEX CONJUGATE
      GG=Y(J)
      Y(J)=-GG
350 CONTINUE
      J=0
      DO 400 J5=1,NOPTS
      J=J+1
      X(J)=X(J)/FLOAT(NOPTS)
      Y(J)=Y(J)/FLOAT(NOPTS)
400 CONTINUE
C
C RESET NN AND NNN. PICK UP USEFUL SIZE OF RESULTS
C
      WRITE(2,316)
      WRITE(2,317)
      WRITE(2,320)
      WRITE(2,325)
      NN=(NN+2)/2
      NNN=(NNN+2)/2

```

```

UPD01110
UPD01120
UPD01130
UPD01140
UPD01150
UPD01160
UPD01170
UPD01180
UPD01190
UPD01200
UPD01210
UPD01220
UPD01230
UPD01240
UPD01250
UPD01260
UPD01270
UPD01280
UPD01290
UPD01300
UPD01310
UPD01320
UPD01330
UPD01340
UPD01350
UPD01360
UPD01370
UPD01380
UPD01390
UPD01400
UPD01410
UPD01420
UPD01430
UPD01440
UPD01450
UPD01460
UPD01470
UPD01480
UPD01490
UPD01500
UPD01510
UPD01520
UPD01530
UPD01540
UPD01550
UPD01560
UPD01570
UPD01580
UPD01590
UPD01600
UPD01610
UPD01620
UPD01630
UPD01640
UPD01650
UPD01660
UPD01670
UPD01680
UPD01690
UPD01700
UPD01710
UPD01720

```

```

DO 7 I=1,NN
DO 8 J=1,NNN
X1(I,J)=X((2*NN-2)*(I-1)+J)
8 CONTINUE
7 CONTINUE
DO 21 I=1,NN
WRITE(2,36) (X1(I,J),J=1,NNN)
WRITE(2,45)
21 CONTINUE
PRINT *, 'NNN=', NNN, 'NN=', NN
XMIN1=XMIN
DO 1375 I=1,NNN
XMIN1=XMIN1+TERV
YMIN1=YMIN
DO 1377 J=1,NN
YMIN1=YMIN1+TERV
WRITE(3,1112) XMIN1,YMIN1,X1(I,J)
1112 FORMAT(F8.3,1X,F8.3,1X,E16.4)
1377 CONTINUE
1375 CONTINUE
WRITE(2,50)
WRITE(2,45)
WRITE(2,45)
WRITE(2,23) Z,DELT
WRITE(2,45)
WRITE(2,22) ID,NN
STOP
END
SUBROUTINE ZERO(X,NOPTS)
C
C SETS VECTOR TO ZERO
C
REAL X(15000)
DO 1 J=1,NOPTS
X(J)=0.0
1 CONTINUE
RETURN
END
SUBROUTINE AR ID FT (N,X,Y,S)
C
C ARBITRARY RADIX ONE DIMENSIONAL FOURIER TRANSFORM
C
INTEGER N
REAL X (15000), Y (15000), S(15000)
C
CALL GR ID FT (N,X,Y)
CALL GR ID FS (N,X,Y,S)
RETURN
END
C
SUBROUTINE GR ID FT (NOPTS,X,Y)
C
C ONE DIMENSIONAL FOURIER TRANSFORM
C
REAL X(15000),Y(15000)
C
INTEGER J,K,M,MR,J1,J2,J3,J4,J5,JT
REAL I1,I2,I3,I4,I5
INTEGER P,PMAX,U,V
C
C NEEDS SORT ID TO RECOVER UNSCRAMBLED FOURIER COEFICIENTS
C
C THIS SUBROUTINE REPLACES X + I Y BY ITS FOURIER TRANSFORM WHERE
C X(F)+IY(F) = SUM T=0,(NOPTS-1) OF (X(T)+IY(T))*EXP(-F*T/NOPTS).

```

```

UPD01730
UPD01740
UPD01750
UPD01760
UPD01770
UPD01780
UPD01790
UPD01800
UPD01810
UPD01820
UPD01830
UPD01840
UPD01850
UPD01860
UPD01870
UPD01880
UPD01890
UPD01900
UPD01910
UPD01920
UPD01930
UPD01940
UPD01950
UPD01960
UPD01970
UPD01980
UPD01990
UPD02000
UPD02010
UPD02020
UPD02030
UPD02040
UPD02050
UPD02060
UPD02070
UPD02080
UPD02090
UPD02100
UPD02110
UPD02120
UPD02130
UPD02140
UPD02150
UPD02160
UPD02170
UPD02180
UPD02190
UPD02200
UPD02210
UPD02220
UPD02230
UPD02240
UPD02250
UPD02260
UPD02270
UPD02280
UPD02290
UPD02300
UPD02310
UPD02320
UPD02330
UPD02340

```

C		UPD02350
C	REAL I (PMAX), R (PMAX), C(PMAX,PMAX), S (PMAX,PMAX),	UPD02360
C	1A ((PMAX-1)**2+1), B((PMAX-1)**2+1)	UPD02370
C		UPD02380
C	REAL I (13), R(13),C(13,13), S(13,13), A(145), B(145)	UPD02390
C		UPD02400
C	PMAX=13	UPD02410
C		UPD02420
	TWOPI=6.283185307	UPD02430
	M=NOPTS	UPD02440
100	CONTINUE	UPD02450
	IF (M .NE. (M/4)*4) GO TO 400	UPD02460
C		UPD02470
C	FACTORS OF FOUR	UPD02480
C		UPD02490
	MR=M	UPD02500
	M=M/4	UPD02510
	DO 300 J=1,M	UPD02520
	ARG= TWOPI*FLOAT(J-1)/FLOAT(MR)	UPD02530
	C1=COS (ARG)	UPD02540
	S1=SIN (ARG)	UPD02550
	C2=COS (2.0*ARG)	UPD02560
	S2=SIN (2.0*ARG)	UPD02570
	C3=COS (3.0*ARG)	UPD02580
	S3=SIN (3.0*ARG)	UPD02590
	DO 200 K=MR,NOPTS,MR	UPD02600
	J1=J+K-MR	UPD02610
	J2=J1+M	UPD02620
	J3=J2+M	UPD02630
	J4=J3+M	UPD02640
	R1=X (J1)+X (J3)	UPD02650
	R2=X (J1)-X (J3)	UPD02660
	I1=Y (J1)+Y (J3)	UPD02670
	I2=Y (J1)-Y (J3)	UPD02680
	R3=X (J2)+X (J4)	UPD02690
	R4=X (J2)-X (J4)	UPD02700
	I3=Y (J2)+Y (J4)	UPD02710
	I4=Y (J2)-Y (J4)	UPD02720
	X (J1)=R1+R3	UPD02730
	Y (J1)=I1+I3	UPD02740
	X (J2)=(R2+I4)*C1+(I2-R4)*S1	UPD02750
	Y (J2)=(I2-R4)*C1-(R2+I4)*S1	UPD02760
	X (J3)=(R1-R3)*C2+(I1-I3)*S2	UPD02770
	Y (J3)=(I1-I3)*C2-(R1-R3)*S2	UPD02780
	X (J4)=(R2-I4)*C3+(I2+R4)*S3	UPD02790
	Y (J4)=(I2+R4)*C3-(R2-I4)*S3	UPD02800
200	CONTINUE	UPD02810
300	CONTINUE	UPD02820
	GO TO 100	UPD02830
400	CONTINUE	UPD02840
	IF (M .NE. (M/2)*2) GO TO 700	UPD02850
C		UPD02860
C	FACTORS OF TWO	UPD02870
C		UPD02880
	MR=M	UPD02890
	M=M/2	UPD02900
	DO 600 J=1,M	UPD02910
	ARG=TWOPI*FLOAT(J-1)/FLOAT(MR)	UPD02920
	C1=COS (ARG)	UPD02930
	S1=SIN (ARG)	UPD02940
	DO 500 K=MR,NOPTS,MR	UPD02950
	J1=J+K-MR	UPD02960

	J2=J1+M	UPD02970
	R1=X(J1)+X(J2)	UPD02980
	R2=X(J1)-X(J2)	UPD02990
	I1=Y(J1)+Y(J2)	UPD03000
	I2=Y(J1)-Y(J2)	UPD03010
	X(J1)=R1	UPD03020
	Y(J1)=I1	UPD03030
	X(J2)=R2*C1+I2*S1	UPD03040
	Y(J2)=I2*C1-R2*S1	UPD03050
500	CONTINUE	UPD03060
600	CONTINUE	UPD03070
	GO TO 400	UPD03080
700	CONTINUE	UPD03090
	IF (M .NE. (M/3)*3) GO TO 1000	UPD03100
C		UPD03110
C	FACTORS OF THREE	UPD03120
C		UPD03130
	MR=M	UPD03140
	M=M/3	UPD03150
	A1=COS(TWOPI/3.0)	UPD03160
	B1=SIN(TWOPI/3.0)	UPD03170
	A2=COS(2.0*TWOPI/3.0)	UPD03180
	B2=SIN(2.0*TWOPI/3.0)	UPD03190
	DO 900 J=1,M	UPD03200
	ARG=TWOPI*FLOAT(J-1)/FLOAT(MR)	UPD03210
C		UPD03220
C	ABSORB TWIDDLE FACTOR INTO ANALYSIS COEFFICIENTS	UPD03230
C		UPD03240
	C21=COS(ARG)	UPD03250
	S21=SIN(ARG)	UPD03260
	C22=C21*A1-S21*B1	UPD03270
	S22=C21*B1+S21*A1	UPD03280
	C23=C21*A2-S21*B2	UPD03290
	S23=C21*B2+S21*A2	UPD03300
	C31=COS(2.0*ARG)	UPD03310
	S31=SIN(2.0*ARG)	UPD03320
	C32=C31*A2-S31*B2	UPD03330
	S32=C31*B2+S31*A2	UPD03340
	C33=C31*A1-S31*B1	UPD03350
	S33=C31*B1+S31*A1	UPD03360
	DO 800 K=MR,NOPTS,MR	UPD03370
	J1=J+K-MR	UPD03380
	J2=J1+M	UPD03390
	J3=J2+M	UPD03400
	R1=X(J1)	UPD03410
	I1=Y(J1)	UPD03420
	R2=X(J2)	UPD03430
	I2=Y(J2)	UPD03440
	R3=X(J3)	UPD03450
	I3=Y(J3)	UPD03460
	X(J1)=R1+R2+R3	UPD03470
	Y(J1)=I1+I2+I3	UPD03480
	X(J2)=R1*C21+I1*S21+R2*C22+I2*S22+R3*C23+I3*S23	UPD03490
	Y(J2)=I1*C21-R1*S21+I2*C22-R2*S22+I3*C23-R3*S23	UPD03500
	X(J3)=R1*C31+I1*S31+R2*C32+I2*S32+R3*C33+I3*S33	UPD03510
	Y(J3)=I1*C31-R1*S31+I2*C32-R2*S32+I3*C33-R3*S33	UPD03520
800	CONTINUE	UPD03530
900	CONTINUE	UPD03540
	GO TO 700	UPD03550
1000	CONTINUE	UPD03560
	IF (M .NE. (M/5)*5) GO TO 1300	UPD03570
C		UPD03580

C	FACTORS OF FIVE	UPD03590
C		UPD03600
	MR=M	UPD03610
	M=M/5	UPD03620
	A1=COS(TWOPI/5.0)	UPD03630
	B1=SIN(TWOPI/5.0)	UPD03640
	A2=COS(2.0*TWOPI/5.0)	UPD03650
	B2=SIN(2.0*TWOPI/5.0)	UPD03660
	A3=COS(3.0*TWOPI/5.0)	UPD03670
	B3=SIN(3.0*TWOPI/5.0)	UPD03680
	A4=COS(4.0*TWOPI/5.0)	UPD03690
	B4=SIN(4.0*TWOPI/5.0)	UPD03700
	DO 1200 J=1,M	UPD03710
	ARG=TWOPI*FLOAT(J-1)/FLOAT(MR)	UPD03720
C		UPD03730
C	ABSORB TWIDDLE FACTOR INTO ANALYAIS COEFFICIENTS	UPD03740
C		UPD03750
	C21=COS(ARG)	UPD03760
	S21=SIN(ARG)	UPD03770
	C22=C21*A1-S21*B1	UPD03780
	S22=C21*B1+S21*A1	UPD03790
	C23=C21*A2-S21*B2	UPD03800
	S23=C21*B2+S21*A2	UPD03810
	C24=C21*A3-S21*B3	UPD03820
	S24=C21*B3+S21*A3	UPD03830
	C25=C21*A4-S21*B4	UPD03840
	S25=C21*B4+S21*A4	UPD03850
	C31=COS(2.0*ARG)	UPD03860
	S31=SIN(2.0*ARG)	UPD03870
	C32=C31*A2-S31*B2	UPD03880
	S32=C31*B2+S31*A2	UPD03890
	C33=C31*A4-S31*B4	UPD03900
	S33=C31*B4+S31*A4	UPD03910
	C34=C31*A1-S31*B1	UPD03920
	S34=C31*B1+S31*A1	UPD03930
	C35=C31*A3-S31*B3	UPD03940
	S35=C31*B3+S31*A3	UPD03950
	C41=COS(3.0*ARG)	UPD03960
	S41=SIN(3.0*ARG)	UPD03970
	C42=C41*A3-S41*B3	UPD03980
	S42=C41*B3+S41*A3	UPD03990
	C43=C41*A1-S41*B1	UPD04000
	S43=C41*B1+S41*A1	UPD04010
	C44=C41*A4-S41*B4	UPD04020
	S44=C41*B4+S41*A4	UPD04030
	C45=C41*A2-S41*B2	UPD04040
	S45=C41*B2+S41*A2	UPD04050
	C51=COS(4.0*ARG)	UPD04060
	S51=SIN(4.0*ARG)	UPD04070
	C52=C51*A4-S51*B4	UPD04080
	S52=C51*B4+S51*A4	UPD04090
	C53=C51*A3-S51*B3	UPD04100
	S53=C51*B3+S51*A3	UPD04110
	C54=C51*A2-S51*B2	UPD04120
	S54=C51*B2+S51*A2	UPD04130
	C55=C51*A1-S51*B1	UPD04140
	S55=C51*B1+S51*A1	UPD04150
	DO 1100 K=MR,NOPTS,MR	UPD04160
	J1=J+K-MR	UPD04170
	J2=J1+M	UPD04180
	J3=J2+M	UPD04190
	J4=J3+M	UPD04200

```

J5=J4+M
R1=X(J1)
I1=Y(J1)
R2=X(J2)
I2=Y(J2)
R3=X(J3)
I3=Y(J3)
R4=X(J4)
I4=Y(J4)
R5=X(J5)
I5=Y(J5)
X(J1)=R1+R2+R3+R4+R5
Y(J1)=I1+I2+I3+I4+I5
X(J2)=R1*C21+I1*S21+R2*C22+I2*S22+R3*C23+I3*S23+R4*C24+I4*S24+
1R5*C25+I5*S25
Y(J2)=I1*C21-R1*S21+I2*C22-R2*S22+I3*C23-R3*S23+I4*C24-R4*S24+
1I5*C25-R5*S25
X(J3)=R1*C31+I1*S31+R2*C32+I2*S32+R3*C33+I3*S33+R4*C34+I4*S34+
1R5*C35+I5*S35
Y(J3)=I1*C31-R1*S31+I2*C32-R2*S32+I3*C33-R3*S33+I4*C34-R4*S34+
1I5*C35-R5*S35
X(J4)=R1*C41+I1*S41+R2*C42+I2*S42+R3*C43+I3*S43+R4*C44+I4*S44+
1R5*C45+I5*S45
Y(J4)=I1*C41-R1*S41+I2*C42-R2*S42+I3*C43-R3*S43+I4*C44-R4*S44+
1I5*C45-R5*S45
X(J5)=R1*C51+I1*S51+R2*C52+I2*S52+R3*C53+I3*S53+R4*C54+I4*S54+
1R5*C55+I5*S55
Y(J5)=I1*C51-R1*S51+I2*C52-R2*S52+I3*C53-R3*S53+I4*C54-R4*S54+
1I5*C55-R5*S55
1100 CONTINUE
1200 CONTINUE
GO TO 1000
1300 CONTINUE
IF (M .LE. 1) GO TO 2400
C
C GENERAL FACTORS
C
DO 1400 J=2, PMAX
P=J
IF (M .EQ. (M/P)*P) GO TO 1500
1400 CONTINUE
CALL FCT ERR
1500 CONTINUE
JT=(P-1)**2+1
C
C SET UP ARBITRARY FACTORS
C
DO 1600 J=1, JT
ARG=TWOPI*FLOAT(J-1)/FLOAT(P)
A(J)=COS(ARG)
B(J)=SIN(ARG)
1600 CONTINUE
MR=M
M=M/P
DO 2300 J=1, M
ARG=TWOPI*FLOAT(J-1)/FLOAT(MR)
C
C ABSORB TWIDDLE FACTOR INTO ANALYSIS COEFFICIENTS
C
DO 1800 U=1, P
C(U,1)=COS(FLOAT(U-1)*ARG)
S(U,1)=SIN(FLOAT(U-1)*ARG)

```

```

DO 1700 V=2,P                                UPD04830
JT=(U-1)*(V-1)+1                             UPD04840
C(U,V)=C(U,1)*A(JT)-S(U,1)*B(JT)            UPD04850
S(U,V)=C(U,1)*B(JT)+S(U,1)*A(JT)          UPD04860
1700 CONTINUE                                 UPD04870
1800 CONTINUE                                 UPD04880
DO 2200 K=MR,NOPTS,MR                       UPD04890
C                                              UPD04900
C      GENERAL ANALYSIS                      UPD04910
C                                              UPD04920
DO 1900 U=1,P                                UPD04930
JT=J+K-MR+(U-1)*M                          UPD04940
R(U)=X(JT)                                  UPD04950
I(U)=Y(JT)                                  UPD04960
1900 CONTINUE                                 UPD04970
DO 2100 U=1,P                                UPD04980
XT=0.0                                       UPD04990
YT=0.0                                       UPD05000
DO 2000 V=1,P                                UPD05010
XT=XT+R(V)*C(U,V)+I(V)*S(U,V)             UPD05020
YT=YT+I(V)*C(U,V)-R(V)*S(U,V)           UPD05030
2000 CONTINUE                                 UPD05040
JT=J+K-MR+(U-1)*M                          UPD05050
X(JT)=XT                                    UPD05060
Y(JT)=YT                                    UPD05070
2100 CONTINUE                                 UPD05080
2200 CONTINUE                                 UPD05090
2300 CONTINUE                                 UPD05100
GO TO 1300                                   UPD05110
2400 CONTINUE                                 UPD05120
RETURN                                       UPD05130
END                                           UPD05140
SUBROUTINE GR ID FS (NOPTS,X,Y,S)          UPD05150
UNSCRAMBLING PROGRAM FOR ONE DIMENSIONAL FOURIER COEFFICIENTS UPD05160
C                                              UPD05170
REAL X(15000),Y(15000),S(15000)          UPD05180
C                                              UPD05190
INTEGER JT                                   UPD05200
INTEGER DO, LIM(13), STEP(13), P, PMAX    UPD05210
INTEGER A,B,C,D,E,F,G,H,I,J,K,L,M,AL,BL,CL,DL,EL,FL,GL,HL,IL,JL, UPD05220
1KL,LL,ML,AS,BS,CS,DS,ES,FS,GS,HS,IS,JS,KS,LS,MS UPD05230
C                                              UPD05240
C      DIGIT REVERSER FOR USE WITH FOUR ID . S MUST BE THE SAME SIZE AS UPD05250
C      X AND Y                               UPD05260
C                                              UPD05270
C      EQUIVALENCES TO ALLOW INDEXING TO SET PARAMETERS AND ALLOW SCALARS UPD05280
C      FOR USE IN DO LOOPS.                 UPD05290
C                                              UPD05300
C      EQUIVALENCE (AS,STEP(1)),(BS,STEP(2)),(CS,STEP(3)),(DS,STEP(4)), UPD05310
1(ES,STEP(5)),(FS,STEP(6)),(GS,STEP(7)),(HS,STEP(8)),(IS,STEP(9)), UPD05320
2(JS,STEP(10)),(KS,STEP(11)),(LS,STEP(12)),(MS,STEP(13)) UPD05330
EQUIVALENCE (AL,LIM(1)),(BL,LIM(2)),(CL,LIM(3)),(DL,LIM(4)), UPD05340
1(EL,LIM(5)),(FL,LIM(6)),(GL,LIM(7)),(HL,LIM(8)),(IL,LIM(9)), UPD05350
2(JL,LIM(10)),(KL,LIM(11)),(LL,LIM(12)),(ML,LIM(13)) UPD05360
C                                              UPD05370
C      PMAX IS SET TO AGREE WITH FOUR ID    UPD05380
C                                              UPD05390
C      PMAX=13                              UPD05400
C                                              UPD05410
C      SET LIMITS AND STEP SIZES FROM INNER LOUPS GOING OUT UPD05420
C                                              UPD05430
DO=13                                       UPD05440

```

	M=NOPTS	UPD05450
100	CONTINUE	UPD05460
C		UPD05470
C	CHECK FOR FACTORS OF FOUR	UPD05480
C		UPD05490
	IF (M .NE. (M/4)*4) GO TO 200	UPD05500
	M=M/4	UPD05510
C		UPD05520
C	REALLY WANT 0-4*M-1 BUT WE GO FROM 1 TO 4*M. 4 STEPS OF M WITH	UPD05530
C	MAXIMUM DISPLACEMENT OF M INITIALLY	UPD05540
C		UPD05550
	LIM(DO)=4*M	UPD05560
	STEP(DO)=M	UPD05570
	DO=DO-1	UPD05580
	GO TO 100	UPD05590
200	CONTINUE	UPD05600
C		UPD05610
C	CHECK FOR REMAINING FACTORS	UPD05620
C		UPD05630
	IF (M .LE. 1) GO TO 500	UPD05640
C		UPD05650
C	FACTORS OF 2,3,5,7,11,13	UPD05660
C		UPD05670
	DO 300 JT=2,PMAX	UPD05680
	P=JT	UPD05690
	IF (M .EQ. (M/P)*P) GO TO 400	UPD05700
300	CONTINUE	UPD05710
C		UPD05720
C	ERROR EXIT IF FACTORS ABOVE PMAX ARE NEEDED	UPD05730
C		UPD05740
	CALL FCT ERR	UPD05750
400	CONTINUE	UPD05760
	M=M/P	UPD05770
C		UPD05780
C	REALLY WANT 0-P*M-1 BUT WE USE 1 TO P*M. P STEPS OF M WITH	UPD05790
C	MAXIMUM INITIAL DISPLACEMENT OF M	UPD05800
C		UPD05810
	LIM(DO)=P*M	UPD05820
	STEP(DO)=M	UPD05830
	DO=DO-1	UPD05840
	GO TO 200	UPD05850
500	CONTINUE	UPD05860
C		UPD05870
C	FINISH OUT THE DO LOOPS TO MAKE OUTER LOOPS EXECUTE ONLY ONCE	UPD05880
C		UPD05890
	DO 600 JT=1,DO	UPD05900
	LIM(JT)=1	UPD05910
	STEP(JT)=1	UPD05920
600	CONTINUE	UPD05930
C		UPD05940
C	SET JT SO THAT JT RUNS FROM 1 TO NOPTS IN STEPS OF 1 WHILE M WILL	UPD05950
C	RUN WITH REVERSE DIGITS	UPD05960
C		UPD05970
	JT=0	UPD05980
	DO 700 A=1,AL,AS	UPD05990
	DO 700 B=A,BL,BS	UPD06000
	DO 700 C=B,CL,CS	UPD06010
	DO 700 D=C,DL,DS	UPD06020
	DO 700 E=D,EL,ES	UPD06030
	DO 700 F=E,FL,FS	UPD06040
	DO 700 G=F,GL,GS	UPD06050
	DO 700 H=G,HL,HS	UPD06060

	DO 700 I=H,IL,IS	UPD06070
	DO 700 J=I,JL,JS	UPD06080
	DO 700 K=J,KL,KS	UPD06090
	DO 700 L=K,LL,LS	UPD06100
	DO 700 M=L,ML,MS	UPD06110
	JT=JT+1	UPD06120
	S(JT)=X(M)	UPD06130
700	CONTINUE	UPD06140
C		UPD06150
C	COPY BACK OUT THE SCRATCH ARRAY	UPD06160
C		UPD06170
	DO 800 JT=1,NOPTS	UPD06180
	X(JT)=S(JT)	UPD06190
800	CONTINUE	UPD06200
	JT=0	UPD06210
	DO 900 A=1,AL,AS	UPD06220
	DO 900 B=A,BL,BS	UPD06230
	DO 900 C=B,CL,CS	UPD06240
	DO 900 D=C,DL,DS	UPD06250
	DO 900 E=D,EL,ES	UPD06260
	DO 900 F=E,FL,FS	UPD06270
	DO 900 G=F,GL,GS	UPD06280
	DO 900 H=G,HL,HS	UPD06290
	DO 900 I=H,IL,IS	UPD06300
	DO 900 J=I,JL,JS	UPD06310
	DO 900 K=J,KL,KS	UPD06320
	DO 900 L=K,LL,LS	UPD06330
	DO 900 M=L,ML,MS	UPD06340
	JT=JT+1	UPD06350
	S(JT)=Y(M)	UPD06360
900	CONTINUE	UPD06370
C		UPD06380
C	COPY BACK OUT OF THE SCRATCH ARRAY	UPD06390
C		UPD06400
	DO 950 JT=1,NOPTS	UPD06410
	Y(JT)=S(JT)	UPD06420
950	CONTINUE	UPD06430
	RETURN	UPD06440
	END	UPD06450
	SUBROUTINE FCT ERR	UPD06460
C	FACTORIZING ERROR	UPD06470
C		UPD06480
C	FACTORIZING ERROR IN FOUR ID OR SORT ID.	UPD06490
C		UPD06500
C	CURRENTLY TAKEN IF A FACTOR ABOVE 13 IS REQUIRED. (THE ARRAYS	UPD06510
C	ARE NOT BIG ENOUGH TO HANDLE THINGS ABOVE 13.)	UPD06520
C		UPD06530
	WRITE (6,100)	UPD06540
	CALL EXIT	UPD06550
100	FORMAT (1X,15HFACTORIZING ERROR)	UPD06560
	RETURN	UPD06570
	END	UPD06580
	SUBROUTINE AR MD FT (N,X,Y,S)	UPD06590
C	ARBITRARY RADIX MULTI DIMENSIONAL FOURIER TRANSFORM	UPD06600
C		UPD06610
C	FIRST SUBSCRIPT VARIES FASTEST IN KEEPING WITH FORTRAN CONVENTIONS	UPD06620
C		UPD06630
	INTEGER N (10)	UPD06640
	REAL X (15000), Y(15000),S(15000)	UPD06650
C		UPD06660
	CALL GR MD FT (N,X,Y)	UPD06670
	CALL GR MD FS (N,X,S)	UPD06680

	Y(J1)=(I0-I2)*C2-(R0-R2)*S2	UPD07310
	X(J3)=(R1-I3)*C3+(I1+R3)*S3	UPD07320
	Y(J3)=(I1+R3)*C3-(R1-I3)*S3	UPD07330
400	CONTINUE	UPD07340
500	CONTINUE	UPD07350
	GO TO 300	UPD07360
600	CONTINUE	UPD07370
	IF (M/SO .NE. M/SO/2*2) GO TO 900	UPD07380
	MR=M	UPD07390
	M=M/2	UPD07400
	DO 800 J=1,M	UPD07410
	ARG=TWOPI*FLOAT((J-1)/SO)/FLOAT(MR/SO)	UPD07420
	C1=COS(ARG)	UPD07430
	S1=SIN(ARG)	UPD07440
	DO 700 K=MR,PROD,MR	UPD07450
	J0=J+K-MR	UPD07460
	J1=J0+M	UPD07470
	R0=X(J0)+X(J1)	UPD07480
	R1=X(J0)-X(J1)	UPD07490
	I0=Y(J0)+Y(J1)	UPD07500
	I1=Y(J0)-Y(J1)	UPD07510
	X(J0)=R0	UPD07520
	Y(J0)=I0	UPD07530
	X(J1)=R1*C1+I1*S1	UPD07540
	Y(J1)=I1*C1-R1*S1	UPD07550
700	CONTINUE	UPD07560
800	CONTINUE	UPD07570
	GO TO 600	UPD07580
900	CONTINUE	UPD07590
	IF (M/SO .NE. M/SO/3*3) GO TO 1200	UPD07600
	MR=M	UPD07610
	M=M/3	UPD07620
	A1=COS(TWOPI/3.0)	UPD07630
	B1=SIN(TWOPI/3.0)	UPD07640
	A2=COS(2.0*TWOPI/3.0)	UPD07650
	B2=SIN(2.0*TWOPI/3.0)	UPD07660
	DO 1100 J=1,M	UPD07670
	ARG=TWOPI*FLOAT((J-1)/SO)/FLOAT(MR/SO)	UPD07680
	C10=COS(ARG)	UPD07690
	S10=SIN(ARG)	UPD07700
	C11=C10*A1-S10*B1	UPD07710
	S11=C10*B1+S10*A1	UPD07720
	C12=C10*A2-S10*B2	UPD07730
	S12=C10*B2+S10*A2	UPD07740
	C20=COS(2.0*ARG)	UPD07750
	S20=SIN(2.0*ARG)	UPD07760
	C21=C20*A2-S20*B2	UPD07770
	S21=C20*B2+S20*A2	UPD07780
	C22=C20*A1-S20*B1	UPD07790
	S22=C20*B1+S20*A1	UPD07800
	DO 1000 K=MR,PROD,MR	UPD07810
	J0=J+K-MR	UPD07820
	J1=J0+M	UPD07830
	J2=J1+M	UPD07840
	R0=X(J0)	UPD07850
	I0=Y(J0)	UPD07860
	R1=X(J1)	UPD07870
	I1=Y(J1)	UPD07880
	R2=X(J2)	UPD07890
	I2=Y(J2)	UPD07900
	X(J0)=R0+R1+R2	UPD07910
	Y(J0)=I0+I1+I2	UPD07920

	X(J1)=R0*C10+I0*S10+R1*C11+I1*S11+R2*C12+I2*S12	UPD07930
	Y(J1)=I0*C10-R0*S10+I1*C11-R1*S11+I2*C12-R2*S12	UPD07940
	X(J2)=R0*C20+I0*S20+R1*C21+I1*S21+R2*C22+I2*S22	UPD07950
	Y(J2)=I0*C20-R0*S20+I1*C21-R1*S21+I2*C22-R2*S22	UPD07960
1000	CONTINUE	UPD07970
1100	CONTINUE	UPD07980
	GO TO 900	UPD07990
1200	CONTINUE	UPD08000
	IF (M/SO .NE. M/SO/5*5) GO TO 1500	UPD08010
	MR=M	UPD08020
	M=M/5	UPD08030
	A1=COS(TWOPI/5.0)	UPD08040
	B1=SIN(TWOPI/5.0)	UPD08050
	A2=COS(2.0*TWOPI/5.0)	UPD08060
	B2=SIN(2.0*TWOPI/5.0)	UPD08070
	A3=COS(3.0*TWOPI/5.0)	UPD08080
	B3=SIN(3.0*TWOPI/5.0)	UPD08090
	A4=COS(4.0*TWOPI/5.0)	UPD08100
	B4=SIN(4.0*TWOPI/5.0)	UPD08110
	DO 1400 J=1,M	UPD08120
	ARG=TWOPI*FLOAT((J-1)/SO)/FLOAT(MR/SO)	UPD08130
	C10=COS(ARG)	UPD08140
	S10=SIN(ARG)	UPD08150
	C11=C10*A1-S10*B1	UPD08160
	S11=C10*B1+S10*A1	UPD08170
	C12=C10*A2-S10*B2	UPD08180
	S12=C10*B2+S10*A2	UPD08190
	C13=C10*A3-S10*B3	UPD08200
	S13=C10*B3+S10*A3	UPD08210
	C14=C10*A4-S10*B4	UPD08220
	S14=C10*B4+S10*A4	UPD08230
	C20=COS(2.0*ARG)	UPD08240
	S20=SIN(2.0*ARG)	UPD08250
	C21=C20*A2-S20*B2	UPD08260
	S21=C20*B2+S20*A2	UPD08270
	C22=C20*A4-S20*B4	UPD08280
	S22=C20*B4+S20*A4	UPD08290
	C23=C20*A1-S20*B1	UPD08300
	S23=C20*B1+S20*A1	UPD08310
	C24=C20*A3-S20*B3	UPD08320
	S24=C20*B3+S20*A3	UPD08330
	C30=COS(3.0*ARG)	UPD08340
	S30=SIN(3.0*ARG)	UPD08350
	C31=C30*A3-S30*B3	UPD08360
	S31=C30*B3+S30*A3	UPD08370
	C32=C30*A1-S30*B1	UPD08380
	S32=C30*B1+S30*A1	UPD08390
	C33=C30*A4-S30*B4	UPD08400
	S33=C30*B4+S30*A4	UPD08410
	C34=C30*A2-S30*B2	UPD08420
	S34=C30*B2+S30*A2	UPD08430
	C40=COS(4.0*ARG)	UPD08440
	S40=SIN(4.0*ARG)	UPD08450
	C41=C40*A4-S40*B4	UPD08460
	S41=C40*B4+S40*A4	UPD08470
	C42=C40*A3-S40*B3	UPD08480
	S42=C40*B3+S40*A3	UPD08490
	C43=C40*A2-S40*B2	UPD08500
	S43=C40*B2+S40*A2	UPD08510
	C44=C40*A1-S40*B1	UPD08520
	S44=C40*B1+S40*A1	UPD08530
	DO 1300 K=MR,PROD,MR	UPD08540

J0=J+K-MR	UPD08550
J1=J0+M	UPD08560
J2=J1+M	UPD08570
J3=J2+M	UPD08580
J4=J3+M	UPD08590
R0=X(J0)	UPD08600
I0=Y(J0)	UPD08610
R1=X(J1)	UPD08620
I1=Y(J1)	UPD08630
R2=X(J2)	UPD08640
I2=Y(J2)	UPD08650
R3=X(J3)	UPD08660
I3=Y(J3)	UPD08670
R4=X(J4)	UPD08680
I4=Y(J4)	UPD08690
X(J0)=R0+R1+R2+R3+R4	UPD08700
Y(J0)=I0+I1+I2+I3+I4	UPD08710
X(J1)=R0*C10+I0*S10+R1*C11+I1*S11+R2*C12+I2*S12+R3*C13+I3*S13+ 1R4*C14+I4*S14	UPD08720
Y(J1)=I0*C10-R0*S10+I1*C11-R1*S11+I2*C12-R2*S12+I3*C13-R3*S13+ 1I4*C14-R4*S14	UPD08730
X(J2)=R0*C20+I0*S20+R1*C21+I1*S21+R2*C22+I2*S22+R3*C23+I3*S23+ 1R4*C24+I4*S24	UPD08740
Y(J2)=I0*C20-R0*S20+I1*C21-R1*S21+I2*C22-R2*S22+I3*C23-R3*S23+ 1I4*C24-R4*S24	UPD08750
X(J3)=R0*C30+I0*S30+R1*C31+I1*S31+R2*C32+I2*S32+R3*C33+I3*S33+ 1R4*C34+I4*S34	UPD08760
Y(J3)=I0*C30-R0*S30+I1*C31-R1*S31+I2*C32-R2*S32+I3*C33-R3*S33+ 1I4*C34-R4*S34	UPD08770
X(J4)=R0*C40+I0*S40+R1*C41+I1*S41+R2*C42+I2*S42+R3*C43+I3*S43+ 1R4*C44+I4*S44	UPD08780
Y(J4)=I0*C40-R0*S40+I1*C41-R1*S41+I2*C42-R2*S42+I3*C43-R3*S43+ 1I4*C44-R4*S44	UPD08790
1300 CONTINUE	UPD08800
1400 CONTINUE	UPD08810
GO TO 1200	UPD08820
1500 CONTINUE	UPD08830
IF (M .LE.S0) GO TO 2600	UPD08840
DO 1600 J=2, PMAX	UPD08850
P=J	UPD08860
IF (M/S0 .EQ. M/S0/P*P) GO TO 1700	UPD08870
1600 CONTINUE	UPD08880
GO TO 2800	UPD08890
1700 CONTINUE	UPD08900
MR=M	UPD08910
M=M/P	UPD08920
DO 1800 U=1, P	UPD08930
ARG=TWOPI*FLOAT(U-1)/FLOAT(P)	UPD08940
A(U)=COS(ARG)	UPD08950
B(U)=SIN(ARG)	UPD08960
1800 CONTINUE	UPD08970
DO 2500 J=1, M	UPD08980
ARG=TWOPI*FLOAT((J-1)/S0)/FLOAT(MR/S0)	UPD08990
DO 2000 U=1, P	UPD09000
C(U,1)=COS(FLOAT(U-1)*ARG)	UPD09010
S(U,1)=SIN(FLOAT(U-1)*ARG)	UPD09020
DO 1900 V=2, P	UPD09030
JJ=(U-1)*(V-1)-(U-1)*(V-1)/P*P+1	UPD09040
C(U,V)=C(U,1)*A(JJ)-S(U,1)*B(JJ)	UPD09050
S(U,V)=C(U,1)*B(JJ)+S(U,1)*A(JJ)	UPD09060
1900 CONTINUE	UPD09070
2000 CONTINUE	UPD09080
	UPD09090
	UPD09100
	UPD09110
	UPD09120
	UPD09130
	UPD09140
	UPD09150
	UPD09160

```

DO 2400 K=MR,PROD,MR
DO 2100 U=1,P
JJ=J+K-MR+(U-1)*M
R(U)=X(JJ)
I(U)=Y(JJ)
2100 CONTINUE
DO 2300 U=1,P
XT=0.0
YT=0.0
DO 2200 V=1,P
XT=XT+R(V)*C(U,V)+I(V)*S(U,V)
YT=YT+I(V)*C(U,V)-R(V)*S(U,V)
2200 CONTINUE
JJ=J+K-MR+(U-1)*M
X(JJ)=XT
Y(JJ)=YT
2300 CONTINUE
2400 CONTINUE
2500 CONTINUE
GO TO 1500
2600 CONTINUE
IF (DIMEN .GT. 0) GO TO 200
2700 CONTINUE
RETURN
2800 CONTINUE
DIMEN=DIMEN+1
WRITE (6,2900) DIMEN,N(DIMEN)
GO TO 2700
2900 FORMAT (1X,28HFACTORING ERROR IN DIMENSION,I2,10H. N(DIM)=,I5)
END
SUBROUTINE GR MD FS (PTS,X,T)
C GENERAL RADIX MULTI DIMENSIONAL FOURIER SORT
C
INTEGER PTS(10)
REAL X(15000),T(15000)
C
INTEGER DIMEN,DO,II,JJ,P,PMAX,SO,S(19),U(19)
INTEGER A,B,C,D,E,F,G,H,I,J,K,L,M,N,O,Q,R,V,W,AL,BL,CL,DL,EL,FL,
1GL,HL,IL,JL,KL,LL,ML,NL,OL,QL,RL,VL,WL,AS,BS,CS,DS,ES,FS,GS,HS,IS
2,JS,KS,LS,MS,NS,OS,QS,RS,VS,WS
EQUIVALENCE (AS,S(1)),(BS,S(2)),(CS,S(3)),(DS,S(4)),(ES,S(5)),
1(FS,S(6)),(GS,S(7)),(HS,S(8)),(IS,S(9)),(JS,S(10)),(KS,S(11)),
2(LS,S(12)),(MS,S(13)),(NS,S(14)),(OS,S(15)),(QS,S(16)),
3(RS,S(17)),(VS,S(18)),(WS,S(19)),(AL,U(1)),(BL,U(2)),(CL,U(3)),
4(DL,U(4)),(EL,U(5)),(FL,U(6)),(GL,U(7)),(HL,U(8)),(IL,U(9)),
5(JL,U(10)),(KL,U(11)),(LL,U(12)),(ML,U(13)),(NL,U(14)),(OL,U(15))
6,(QL,U(16)),(RL,U(17)),(VL,U(18)),(WL,U(19))
C
PMAX=19
C
DO=19
DIMEN=1
SO=1
100 CONTINUE
M=PTS(DIMEN)
200 CONTINUE
IF (M .LE. 1) GO TO 500
DO 300 J=2,PMAX
P=J
IF (M .EQ. M/P*P) GO TO 400
300 CONTINUE
GO TO 1100
UPD09170
UPD09180
UPD09190
UPD09200
UPD09210
UPD09220
UPD09230
UPD09240
UPD09250
UPD09260
UPD09270
UPD09280
UPD09290
UPD09300
UPD09310
UPD09320
UPD09330
UPD09340
UPD09350
UPD09360
UPD09370
UPD09380
UPD09390
UPD09400
UPD09410
UPD09420
UPD09430
UPD09440
UPD09450
UPD09460
UPD09470
UPD09480
UPD09490
UPD09500
UPD09510
UPD09520
UPD09530
UPD09540
UPD09550
UPD09560
UPD09570
UPD09580
UPD09590
UPD09600
UPD09610
UPD09620
UPD09630
UPD09640
UPD09650
UPD09660
UPD09670
UPD09680
UPD09690
UPD09700
UPD09710
UPD09720
UPD09730
UPD09740
UPD09750
UPD09760
UPD09770
UPD09780

```

400	CONTINUE	UPD09790
	U(DO)=M*S0	UPD09800
	S(DO)=M/P*S0	UPD09810
	M=M/P	UPD09820
	DO=DO-1	UPD09830
	GO TO 200	UPD09840
500	CONTINUE	UPD09850
	SO=SO*PTS(DIMEN)	UPD09860
	DIMEN=DIMEN+1	UPD09870
	IF (PTS(DIMEN) .GT. 0) GO TO 100	UPD09880
	IF (DO .LE. 0) GO TO 700	UPD09890
	DO 600 J=1,DO	UPD09900
	U(J)=1	UPD09910
	S(J)=1	UPD09920
600	CONTINUE	UPD09930
700	CONTINUE	UPD09940
	JJ=0	UPD09950
	DO 800 A=1,AL,AS	UPD09960
	DO 800 B=1,BL,BS	UPD09970
	DO 800 C=1,CL,CS	UPD09980
	DO 800 D=1,DL,DS	UPD09990
	DO 800 E=1,EL,ES	UPD10000
	DO 800 F=1,FL,FS	UPD10010
	DO 800 G=1,GL,GS	UPD10020
	DO 800 H=1,HL,HS	UPD10030
	DO 800 I=1,IL,IS	UPD10040
	DO 800 J=1,JL,JS	UPD10050
	DO 800 K=1,KL,KS	UPD10060
	DO 800 L=1,LL,LS	UPD10070
	DO 800 M=1,ML,MS	UPD10080
	DO 800 N=1,NL,NS	UPD10090
	DO 800 O=1,OL,OS	UPD10100
	DO 800 Q=1,QL,QS	UPD10110
	DO 800 R=1,RL,RS	UPD10120
	DO 800 V=1,VL,VS	UPD10130
	DO 800 W=1,WL,WS	UPD10140
	II=A+B+C+D+E+F+G+H+I+J+K+L+M+N+O+Q+R+V+W-18	UPD10150
	JJ=JJ+1	UPD10160
	T(JJ)=X(II)	UPD10170
800	CONTINUE	UPD10180
	DO 900 J=1,S0	UPD10190
	X(J)=T(J)	UPD10200
900	CONTINUE	UPD10210
1000	CONTINUE	UPD10220
	RETURN	UPD10230
1100	CONTINUE	UPD10240
	WRITE (6,1200) DIMEN,PTS(DIMEN)	UPD10250
	GO TO 1000	UPD10260
1200	FORMAT (1X,28HFACTORED IN DIMENSION,I2,10H. N(DIM)=,I5)	UPD10270
	END	UPD10280

UDD FORTRAN

Written By: Ruddman and Blackley

```

C THIS PROGRAM FOLLOWS HENDERSONS TECHNIQUE FOR UPWARD AND DOWNWARD UDD00010
C CONTINUATION AND FIRST AND SECOND DERIVATIVES. WRITTEN FOR FORTRAN UDD00020
C 77. OUTPUT MAPS ARE THE SIZE OF INPUT MAPS. UP TO AND MAXIMUM ARRAY UDD00030
C OF 25 X 25. UDD00040
C UDD00050
C UDD00060
C DIMENSION STATEMENTS FOR DATA UP TO 25 X 25 UDD00070
C UDD00080
C DIMENSION ISET(20),P(75,75), C(11,19), R(26,26,11),HEAD(70) UDD00090
C COMMON P,C,R UDD00100
C READ IN HEADING AND ISELECT(CONTAINS CODES FOR LIST OF MAPS DESIRED UDD00110
C CODES ARE IDENTIFIED LATER IN THIS PROGRAM. UDD00120
C UDD00130
C READ(1,1) (HEAD(I),I=1,70) UDD00140
1 FORMAT (70A1) UDD00150
C READ(1,*) (ISET(L),L=1,19) UDD00160
C UDD00170
C READ IN MAXIMUM VALUE OF I. I BEGINS AT 26 AND MUST BE 50 OR LESS. SI UDD00180
C FOR JMAX. READ IN ON SAME CARD THE VALUE (BASE) TO BE SUBTRACTED FORM UDD00190
C VALUES P(I,J). NEXT READ A SCALE VALUE TO MODIFY DATA TO FIT THE LIM UDD00200
C SIZE MAP FORMAT OF F4.0. P(I,J) DATA IS MULTIPLIED BY THIS SCALE FAC UDD00210
C UDD00220
C READ(1,*) IMAX, JMAX, BASE, YMIN, XMIN, TERV UDD00230
C PRINT *, IMAX, JMAX, BASE UDD00240
C READ(1,*) SCALE UDD00250
C UDD00260
C READ ON P(I,J) DATA. SUBTRACT BASE. MULTIPLY BY SCALE. PRINT HEADIN UDD00270
C AND PLOT ON MAP TYPE OUTPUT. MAP IS PRINTED FROM P(26,26) TO P(IMA UDD00280
C IF DATA IS LESS THAN 25 X 25 A BLANK IS PRINTED IN THE SPACES TO FI UDD00290
C THE MAP. UDD00300
C UDD00310
C READ(1,1111) ((P(I,J), I=26,IMAX), J=26,JMAX) UDD00320
C111 FORMAT(12X,F8.2) UDD00330
1111 FORMAT(F8.6) UDD00340
C UDD00350
C UDD00360
C DO 6 J=26,JMAX UDD00370
C DO 5 I=26,IMAX UDD00380
5 P(I,J)=(P(I,J)-BASE)*SCALE UDD00390
6 CONTINUE UDD00400
C UDD00410
C WRITE(2,7) UDD00420
7 FORMAT(1H1) UDD00430
C UDD00440
C WRITE(2,101) (HEAD(I),I=1,70) UDD00450
101 FORMAT(20X,70A1,/) UDD00460
C UDD00470
C WRITE(2,8) BASE, SCALE UDD00480
8 FORMAT(20X,'INPUT DATA LESS BASE OF ',F6.2,3X,'MULTIPLIED BY SCA UDD00490
+LE OF',F5.2,/) UDD00500
C UDD00510
C DO 9 J=26,JMAX UDD00520
C WRITE(2,222) UDD00530
222 FORMAT(4X,24(1H*,4X),1H*) UDD00540
C WRITE(2,10) (P(I,J),I=26,IMAX) UDD00550
10 FORMAT(2X,25(F4.0,1X),/) UDD00560
C UDD00570

```

```

        IF (IMAX.LT.50) THEN                                UDD00580
            WRITE(2,601)                                    UDD00590
601         FORMAT(1H1)                                     UDD00600
            END IF                                         UDD00610
9          CONTINUE                                        UDD00620
C                                                  UDD00630
            IF (JMAX.LT.50) THEN                            UDD00640
                LMAX=50-JMAX                                UDD00650
                DO 603 LL=1,LMAX                            UDD00660
603         WRITE(2,604)                                    UDD00670
604         FORMAT(4X,24(1H*,4X),1H*,//)                  UDD00680
            END IF                                         UDD00690
C                                                  UDD00700
C          NEXT SECTION PREPARES REGIONS BEYOND EDGE OF MAP TO BE USED IN AN UDD00710
C          APPROACH IS TO FILL THE SURROUNDING SPACE BY EXTENDING EACH EDGE UDD00720
C          NORMAL TO THE MAP FOR 25 UNITS.                 UDD00730
C                                                  UDD00740
            IMAX1=IMAX + 1                                  UDD00750
            IMAX25= IMAX +25                                UDD00760
            JMAX1= JMAX + 1                                  UDD00770
            JMAX25= JMAX + 25                                UDD00780
C                                                  UDD00790
            DO 14 J=26,JMAX                                  UDD00800
            DO 15 I=1,25                                     UDD00810
15         P(I,J)=P(26,J)                                   UDD00820
            DO 16 I=IMAX1,IMAX25                           UDD00830
16         P(I,J)=P(IMAX,J)                                UDD00840
14         CONTINUE                                        UDD00850
C                                                  UDD00860
            DO 17 I=26,IMAX                                  UDD00870
            DO 18 J=1,25                                     UDD00880
18         P(I,J)=P(I,26)                                   UDD00890
            DO 19 J=JMAX1,JMAX25                            UDD00900
19         P(I,J)=P(I,JMAX)                                UDD00910
17         CONTINUE                                        UDD00920
C                                                  UDD00930
C                                                  UDD00940
            DO 20 I=1,25                                     UDD00950
            DO 21 J=1,25                                     UDD00960
21         P(I,J)=P(26,26)                                  UDD00970
20         CONTINUE                                        UDD00980
C                                                  UDD00990
C                                                  UDD01000
            DO 22 I=IMAX1, IMAX25                            UDD01010
            DO 23 J=1,25                                     UDD01020
23         P(I,J)=P(IMAX,26)                                UDD01030
22         CONTINUE                                        UDD01040
C                                                  UDD01050
C                                                  UDD01060
            DO 24 I=1,25                                     UDD01070
            DO 25 J=JMAX1,JMAX25                            UDD01080
25         P(I,J)=P(26,JMAX)                                UDD01090
24         CONTINUE                                        UDD01100
C                                                  UDD01110
C                                                  UDD01120
            DO 26 I=IMAX1,IMAX25                            UDD01130
            DO 27 J=JMAX1,JMAX25                            UDD01140
27         P(I,J)=P(IMAX,JMAX)                                UDD01150
26         CONTINUE                                        UDD01160
C                                                  UDD01170
C          CALCULATION OF AVERAGE VALUE OF DATA ON RINGS CENTERED AT EACH MAP POUDD01180
C          CALL THESE R(I,J,K), WHERE K=1 TO 11.           UDD01190

```

```

C          M=0                                UDD01200
          DO 28 I=26,IMAX                      UDD01210
            M=M+1                                UDD01220
            N=0                                  UDD01230
          DO 29 J=26,JMAX                      UDD01240
            N=N+1                                UDD01250
          UDD01260
C          R(M,N,1)=P(I,J)                    UDD01270
          UDD01280
C          R(M,N,2)=(P(I,J+1)+P(I,J-1)+P(I+1,J)+P(I-1,J))/4.0 UDD01290
          UDD01300
C          R(M,N,3)=(P(I+1,J+1)+P(I+1,J-1)+P(I-1,J+1)+P(I-1,J-1))/4.0 UDD01310
          UDD01320
C          R(M,N,4)=(P(I+2,J+1)+P(I+2,J-1)+P(I-2,J+1)+P(I-2,J-1)+
          *P(I+1,J+2)+P(I+1,J-2)+P(I-1,J+2)+P(I-1,J-2))/8.0 UDD01330
          UDD01340
          IF(I.EQ.26.AND.J.EQ.26) THEN          UDD01350
            PRINT *, P(I+2,J+1),P(I+2,J-1),P(I-2,J+1),P(I-2,J-1),P(I+1,J+2) UDD01360
            *,P(I+1,J+2),P(I-1,J+2),P(I-1,J-2),R(M,N,4) UDD01370
          END IF                                UDD01380
          UDD01390
C          R(M,N,5)=(P(I+2,J+2)+P(I+2,J-2)+P(I-2,J+2)+P(I-2,J-2))/4.0 UDD01400
          UDD01410
C          R(M,N,6)=(P(I+2,J+3)+P(I+2,J-3)+P(I-2,J+3)+P(I-2,J-3)+
          *P(I+3,J+2)+P(I+3,J-2)+P(I-3,J+2)+P(I-3,J-2))/8. UDD01420
          UDD01430
C          R(M,N,7)=(P(I+5,J)+P(I-5,J)+P(I,J+5)+P(I,J-5)+P(I+3,J+4)
          *+ P(I+3,J-4)+P(I+4,J+3)+P(I+4,J-3)+P(I-4,J+3)+P(I-4,J-3)+
          *P(I-3,J+4)+P(I-3,J-4))/12. UDD01440
          UDD01450
C          R(M,N,8)=(P(I+7,J+1)+P(I+1,J+7)+P(I+7,J-1)+P(I+1,J-7)+
          *P(I-7,J+1)+P(I-1,J+7)+P(I-7,J-1)+P(I-1,J-7)+P(I+5,J+5)+
          *P(I+5,J-5)+P(I-5,J+5)+P(I-5,J-5))/12. UDD01460
          UDD01470
C          R(M,N,9)=(P(I+10,J+6)+P(I+10,J-6)+P(I+6,J+10)+P(I+6,J-10)
          *+P(I-10,J+6)+P(I-10,J-6)+P(I-6,J+10)+P(I-6,J-10))/8. UDD01480
          UDD01490
C          R(M,N,10)=(P(I+7,J+15)+P(I+15,J+7)+P(I-7,J+15)+P(I-15,J+7)
          *+P(I+7,J-15)+P(I+15,J-7)+P(I-7,J-15)+P(I-15,J-7))/8. UDD01500
          UDD01510
C          R(M,N,11)=(P(I,J+25)+P(I,J-25)+P(I-20,J+15)+P(I-15,J+20)
          *+P(I-20,J-15)+P(I-15,J-20)+P(I+20,J+15)+P(I+15,J+20)+
          *P(I+20,J-15)+P(I+15,J-20)+P(I+25,J)+P(I-25,J))/12. UDD01520
          UDD01530
C          CONTINUE                            UDD01540
          UDD01550
29         CONTINUE                            UDD01560
28         CONTINUE                            UDD01570
          UDD01580
C          UDD01590
C          FOR EACH MAP THERE IS A SET OF COEFFICIENTS C(K,L), WHERE K UDD01600
C          RING NUMBER AND L IS THE CODED INTGER FOR THE DESIRED MAP. CODES ARE UDD01610
C          'ONE' IF THE MAP IS DESIRED, OR 'ZERO' IF IT IS NOT. CODES ARE EN- UDD01620
C          TERED ON THE ISELECT INPUT FROM COLUMNS 1 TO 19. THE FOLLOWING LIST UDD01630
C          GIVES THE CODES. THUS, A 'ONE' IN COLUMN 1 REQUESTS A MAP CONTINUED UDD01640
C          UPWARD ONE GRID UNIT. A 'ZERO' IN COULMNS W WILL SUPPRESS THE MAP UDD01650
C          THAT IS CONTINUED UPWARD 2 GRID UNITS, ETC. UDD01660
C          UDD01670
C          UDD01680
C          UDD01690
C          UDD01700
C          UDD01710
C          UDD01720
C          UDD01730
C          UDD01740
C          UDD01750
C          COEFFICENTS FOR UPWARD CONTINUATION 1. CODE L=1. UDD01760
C          UDD01770
C          C(1,1)=.11193 UDD01780
C          C(2,1)=.32193 UDD01790
C          C(3,1)=.06062 UDD01800
C          C(4,1)=.15206 UDD01810

```

	C(5,1)=.05335	UDD01820
	C(6,1)=.06586	UDD01830
	C(7,1)=.06650	UDD01840
	C(8,1)=.05635	UDD01850
	C(9,1)=.03855	UDD01860
	C(10,1)=.02273	UDD01870
	C(11,1)=.03015	UDD01880
C		UDD01890
C		UDD01900
C	COEFFICIENTS FOR UPWARD CONTINUATION 2, CODE L=2	UDD01910
C		UDD01920
	C(1,2)=.04034	UDD01930
	C(2,2)=.12988	UDD01940
	C(3,2)=.07588	UDD01950
	C(4,2)=.14559	UDD01960
	C(5,2)=.07651	UDD01970
	C(6,2)=.09902	UDD01980
	C(7,2)=.11100	UDD01990
	C(8,2)=.13051	UDD02000
	C(9,2)=.07379	UDD02010
	C(10,2)=.04464	UDD02020
	C(11,2)=.05998	UDD02030
C		UDD02040
C	COEFFICIENTS FOR UPWARD CONTINUATION 3. CODE L=3	UDD02050
C		UDD02060
	C(1,3)=.01961	UDD02070
	C(2,3)=.06592	UDD02080
	C(3,3)=.05260	UDD02090
	C(4,3)=.10563	UDD02100
	C(5,3)=.07146	UDD02110
	C(6,3)=.10226	UDD02120
	C(7,3)=.12921	UDD02130
	C(8,3)=.13635	UDD02140
	C(9,3)=.10322	UDD02150
	C(10,3)=.06500	UDD02160
	C(11,3)=.08917	UDD02170
C		UDD02180
C	COEFFICIENTS FOR UPWARD CONTINUATION 4. CODE L=4	UDD02190
C		UDD02200
	C(1,4)=.01141	UDD02210
	C(2,4)=.03908	UDD02220
	C(3,4)=.03566	UDD02230
	C(4,4)=.07450	UDD02240
	C(5,4)=.05841	UDD02250
	C(6,4)=.09173	UDD02260
	C(7,4)=.12915	UDD02270
	C(8,4)=.15474	UDD02280
	C(9,4)=.12565	UDD02290
	C(10,4)=.08323	UDD02300
	C(11,4)=.11744	UDD02310
C		UDD02320
C	COEFFICIENTS FOR UPWARD CONTINUATION 5. CODE L=5	UDD02330
C		UDD02340
	C(1,5)=.00742	UDD02350
	C(2,5)=.02566	UDD02360
	C(3,5)=.02509	UDD02370
	C(4,5)=.05377	UDD02380
	C(5,5)=.04611	UDD02390
	C(6,5)=.07784	UDD02400
	C(7,5)=.11986	UDD02410
	C(8,5)=.16159	UDD02420
	C(9,5)=.14106	UDD02430

	C(10,5)=.09897	UDD02440
	C(11,5)=.14458	UDD02450
C		UDD02460
C	COEFFICIENTS FOR DOWNWARD CONTINUATION 1. CODE L=6	UDD02470
C		UDD02480
	C(1,6)=4.8948	UDD02490
	C(2,6)=-3.0113	UDD02500
	C(3,6)=.0081	UDD02510
	C(4,6)=-.5604	UDD02520
	C(5,6)=-.0376	UDD02530
	C(6,6)=-.0689	UDD02540
	C(7,6)=-.0605	UDD02550
	C(8,6)=-.0534	UDD02560
	C(9,6)=-.0380	UDD02570
	C(10,6)=-.0227	UDD02580
	C(11,6)=-.0302	UDD02590
C		UDD02600
C	COEFFICIENTS FOR DOWNWARD CONTINUATION 2. CODE L=7	UDD02610
C		UDD02620
	C(1,7)=16.1087	UDD02630
	C(2,7)=-13.2209	UDD02640
	C(3,7)=.4027	UDD02650
	C(4,7)=-1.9459	UDD02660
	C(5,7)=.0644	UDD02670
	C(6,7)=-.0596	UDD02680
	C(7,7)=-.0522	UDD02690
	C(8,7)=-.0828	UDD02700
	C(9,7)=-.0703	UDD02710
	C(10,7)=-.0443	UDD02720
	C(11,7)=-.0600	UDD02730
C		UDD02740
C	COEFFICIENTS FOR DOWNWARD CONTINUATION 3. CODE L=8	UDD02750
C		UDD02760
	C(1,8)=41.7731	UDD02770
	C(2,8)=-38.2716	UDD02780
	C(3,8)=1.7883	UDD02790
	C(4,8)=-4.7820	UDD02800
	C(5,8)=.5367	UDD02810
	C(6,8)=.1798	UDD02820
	C(7,8)=.1342	UDD02830
	C(8,8)=-.0560	UDD02840
	C(9,8)=-.0900	UDD02850
	C(10,8)=-.0639	UDD02860
	C(11,8)=-.0891	UDD02870
C		UDD02880
C	COEFFICIENTS FOR DOWNWARD CONTINUATION 4. CODE L=9	UDD02890
C		UDD02900
	C(1,9)=92.5362	UDD02910
	C(2,9)=-89.7403	UDD02920
	C(3,9)=5.1388	UDD02930
	C(4,9)=-9.9452	UDD02940
	C(5,9)=1.7478	UDD02950
	C(6,9)=.8908	UDD02960
	C(7,9)=.6656	UDD02970
	C(8,9)=.0718	UDD02980
	C(9,9)=-.0890	UDD02990
	C(10,9)=-.0802	UDD03000
	C(11,9)=-.1173	UDD03010
C		UDD03020
C	COEFFICIENTS FOR DOWNWARD CONTINUATION 5. CODE L=10	UDD03030
C		UDD03040
	C(1,10)=183.2600	UDD03050

C(2,10)=-183.9380	UDD03060
C(3,10)=11.8804	UDD03070
C(4,10)=-18.6049	UDD03080
C(5,10)=4.2324	UDD03090
C(6,10)=2.4237	UDD03100
C(7,10)=1.7777	UDD03110
C(8,10)=.3606	UDD03120
C(9,10)=-.0571	UDD03130
C(10,10)=-.0921	UDD03140
C(11,10)=-.1444	UDD03150
C	UDD03160
C COEFFICIENTS FOR FIRST DERIVATIVE ON SURFACE. CODE L=11	UDD03170
C	UDD03180
C(1,11)=1.87282	UDD03190
C(2,11)=-1.13625	UDD03200
C(3,11)=-.05949	UDD03210
C(4,11)=-.30210	UDD03220
C(5,11)=-.05857	UDD03230
C(6,11)=-.07597	UDD03240
C(7,11)=-.07072	UDD03250
C(8,11)=-.05758	UDD03260
C(9,11)=-.03905	UDD03270
C(10,11)=-.02286	UDD03280
C(11,11)=-.05020	UDD03290
C	UDD03300
C COEFFICIENTS FOR FIRST DERIVATIVE DOWN 1. CODE L=12	UDD03310
C	UDD03320
C(1,12)=6.62394	UDD03330
C(2,12)=-5.62446	UDD03340
C(3,12)=.12727	UDD03350
C(4,12)=-.88750	UDD03360
C(5,12)=.00361	UDD03370
C(6,12)=-.04856	UDD03380
C(7,12)=-.04007	UDD03390
C(8,12)=-.04575	UDD03400
C(9,12)=-.03615	UDD03410
C(10,12)=-.02233	UDD03420
C(11,12)=-.05000	UDD03430
C	UDD03440
C COEFFICIENTS FOR FIRST DERIVATIVE DOWN 2. CODE L=13	UDD03450
C	UDD03460
C(1,13)=16.98074	UDD03470
C(2,13)=-16.05517	UDD03480
C(3,13)=.76135	UDD03490
C(4,13)=-1.98701	UDD03500
C(5,13)=.23820	UDD03510
C(6,13)=.09219	UDD03520
C(7,13)=.07475	UDD03530
C(8,13)=-.00768	UDD03540
C(9,13)=-.02726	UDD03550
C(10,13)=-.02077	UDD03560
C(11,13)=-.04934	UDD03570
C	UDD03580
C COEFFICIENT FOR FIRST DERIVATIVE DOWN 3. CODE L=14	UDD03590
C	UDD03600
C(1,14)=36.11116	UDD03610
C(2,14)=-35.96237	UDD03620
C(3,14)=2.17080	UDD03630
C(4,14)=-3.83054	UDD03640
C(5,14)=.76745	UDD03650
C(6,14)=.42646	UDD03660
C(7,14)=.32573	UDD03670

	C(8,14)=.06859	UDD03680
	C(9,14)=-.01084	UDD03690
	C(10,14)=-.01812	UDD03700
	C(11,14)=-.04832	UDD03710
C		UDD03720
C	COEFFICIENTS FOR FIRST DERIVATIVE DOWN 4. CODE L=15	UDD03730
C		UDD03740
	C(1,15)=67.88049	UDD03750
	C(2,15)=-69.68033	UDD03760
	C(3,15)=4.76651	UDD03770
	C(4,15)=-6.69004	UDD03780
	C(5,15)=1.74330	UDD03790
	C(6,15)=1.05352	UDD03800
	C(7,15)=.77613	UDD03810
	C(8,15)=.19699	UDD03820
	C(9,15)=.01469	UDD03830
	C(10,15)=-.01433	UDD03840
	C(11,15)=-.04693	UDD03850
C		UDD03860
C	COEFFICIENT FOR 2ND DERIVATIVE ON THE SURFACE. CODE L=16.	UDD03870
C		UDD03880
	C(1,16)=2.82994	UDD03890
	C(2,16)=-2.49489	UDD03900
	C(3,16)=.05173	UDD03910
	C(4,16)=-.39446	UDD03920
	C(5,16)=.00932	UDD03930
	C(6,16)=-.00732	UDD03940
	C(7,16)=.00304	UDD03950
	C(8,16)=.00219	UDD03960
	C(9,16)=.00040	UDD03970
	C(10,16)=.00004	UDD03980
	C(11,16)=.00	UDD03990
C		UDD04000
C	COEFFICIENTS FOR 2ND DERIVATIVE DOWN 1. CODE L=17	UDD04010
C		UDD04020
	C(1,17)=7.08408	UDD04030
	C(2,17)=-6.93715	UDD04040
	C(3,17)=.36265	UDD04050
	C(4,17)=-.80764	UDD04060
	C(5,17)=.13050	UDD04070
	C(6,17)=.07231	UDD04080
	C(7,17)=.06502	UDD04090
	C(8,17)=.02312	UDD04100
	C(9,17)=.00565	UDD04110
	C(10,17)=.00103	UDD04120
	C(11,17)=.00043	UDD04130
C		UDD04140
C	COEFFICIENTS FOR 2ND DERIVATIVE DOWN 2. CODE L=18.	UDD04150
C		UDD04160
	C(1,18)=14.15751	UDD04170
	C(2,18)=-14.51327	UDD04180
	C(3,18)=.96018	UDD04190
	C(4,18)=-1.42970	UDD04200
	C(5,18)=.35907	UDD04210
	C(6,18)=-.22256	UDD04220
	C(7,18)=.17330	UDD04230
	C(8,18)=.05501	UDD04240
	C(9,18)=.01239	UDD04250
	C(10,18)=.0021	UDD04260
	C(11,18)=.00085	UDD04270
C		UDD04280
C	COEFFICIENTS FOR 2ND DERIVATIVE DOWN 3. CODE L=19	UDD04290

C		UDD04300
	C(1,19)=24.74755	UDD04310
	C(2,19)=-26.02351	UDD04320
	C(3,19)=1.92719	UDD04330
	C(4,19)=-2.30269	UDD04340
	C(5,19)=.72474	UDD04350
	C(6,19)=.46253	UDD04360
	C(7,19)=.3392	UDD04370
	C(8,19)=.09985	UDD04380
	C(9,19)=.02070	UDD04390
	C(10,19)=.00322	UDD04400
	C(11,19)=.00122	UDD04410
C		UDD04420
C	THIS SECTION MAKE THE FINAL CALCULATIONS FOR THOSE MAPS SELECTED BY	UDD04430
C	USER IN HIS ISELECT CODE.	UDD04440
C		UDD04450
	DO 30 L=1,19	UDD04460
	LEVEL=L	UDD04470
	IF (ISET(L)) 30,30,555	UDD04480
C		UDD04490
555	WRITE(2,1113)	UDD04500
1113	FORMAT(////////////////////////////////////)	UDD04510
C		UDD04520
	WRITE(2,7)	UDD04530
	WRITE(2,101) (HEAD(I),I=1,70)	UDD04540
C		UDD04550
	IF (L.EQ.1) THEN	UDD04560
	WRITE(2,171)	UDD04570
	ELSE IF (L.EQ.2) THEN	UDD04580
	WRITE(2,172)	UDD04590
	ELSE IF (L.EQ.3) THEN	UDD04600
	WRITE(2,173)	UDD04610
	ELSE IF (L.EQ.4) THEN	UDD04620
	WRITE(2,174)	UDD04630
	ELSE IF (L.EQ.5) THEN	UDD04640
	WRITE(2,175)	UDD04650
	ELSE IF (L.EQ.6) THEN	UDD04660
	WRITE(2,176)	UDD04670
	ELSE IF (L.EQ.7) THEN	UDD04680
	WRITE(2,177)	UDD04690
	ELSE IF (L.EQ.8) THEN	UDD04700
	WRITE(2,178)	UDD04710
	ELSE IF (L.EQ.9) THEN	UDD04720
	WRITE(2,179)	UDD04730
	ELSE IF (L.EQ.10) THEN	UDD04740
	WRITE(2,180)	UDD04750
	ELSE IF (L.EQ.11) THEN	UDD04760
	WRITE(2,181)	UDD04770
	ELSE IF (L.EQ.12) THEN	UDD04780
	WRITE(2,182)	UDD04790
	ELSE IF (L.EQ.13) THEN	UDD04800
	WRITE(2,183)	UDD04810
	ELSE IF (L.EQ.14) THEN	UDD04820
	WRITE(2,184)	UDD04830
	ELSE IF (L.EQ.15) THEN	UDD04840
	WRITE(2,185)	UDD04850
	ELSE IF (L.EQ.16) THEN	UDD04860
	WRITE(2,186)	UDD04870
	ELSE IF (L.EQ.17) THEN	UDD04880
	WRITE(2,187)	UDD04890
	ELSE IF (L.EQ.18) THEN	UDD04900
	WRITE(2,188)	UDD04910

```

        ELSE
            WRITE(2,189)
            END IF
        DO 33 I=26,IMAX
        DO 34 J=26,JMAX
            P(I,J)=0.0
        DO 35 K=1,11
C
            Q1=C(K,L)*R(I-25,J-25,K)
35      P(I,J)=P(I,J)+Q1
34      CONTINUE
33      CONTINUE
C
C NEXT SECTION PRINTS ALL MAPS IN SAME FORMAT AS INPUT MAP.
C
        DO 36 J=26,JMAX
            WRITE(2,223)
223     FORMAT(4X,24(1H*,4X),1H*)
            WRITE(2,37) (P(I,J),I=26,IMAX)
37      FORMAT(2X,25(F4.0,1X),/)
            IF (IMAX.LT.50) THEN
                WRITE(2,701)
701     FORMAT(1H1)
            END IF
36      CONTINUE
C
        XMIN1=XMIN
        DO 122 J=26,JMAX
            XMIN1=XMIN1+TERV
            YMIN1=YMIN
        DO 123 I=26,IMAX
            YMIN1=YMIN1+TERV
1112    FORMAT(3,1112) XMIN1,YMIN1,P(I,J)
123     CONTINUE
122     CONTINUE
            IF (JMAX.LT.50) THEN
                LMAX=50-JMAX
                DO 703 LL=1,LMAX
703     WRITE(2,704)
704     FORMAT(4X,24(1H*,4X),1H*,//)
            END IF
705     CONTINUE
30      CONTINUE
        STOP
C
        WRITE(2,91)
C1     FORMAT(1X,'ERROR, TOO LARGE L VALUE')
171    FORMAT(20X,'MAP CONTINUED UPWARD 1 GRID UNIT',//)
172    FORMAT(20X,'MAP CONTINUED UPWARD 2 GRID UNIT',//)
173    FORMAT(20X,'MAP CONTINUED UPWARD 3 GRID UNIT',//)
174    FORMAT(20X,'MAP CONTINUED UPWARD 4 GRID UNIT',//)
175    FORMAT(20X,'MAP CONTINUED UPWARD 5 GRID UNIT',//)
176    FORMAT(20X,'MAP CONTINUED DOWNWARD 1 GRID UNIT',//)
177    FORMAT(20X,'MAP CONTINUED DOWNWARD 2 GRID UNIT',//)
178    FORMAT(20X,'MAP CONTINUED DOWNWARD 3 GRID UNIT',//)
179    FORMAT(20X,'MAP CONTINUED DOWNWARD 4 GRID UNIT',//)
180    FORMAT(20X,'MAP CONTINUED DOWNWARD 5 GRID UNIT',//)
181    FORMAT(20X,'MAP OF FIRST DERIVATIVE ON SURFACE',//)
182    FORMAT(20X,'MAP OF FIRST DERIVATIVE DOWN 1 GRID UNIT',//)
183    FORMAT(20X,'MAP OF FIRST DERIVATIVE DOWN 2 GRID UNIT',//)
184    FORMAT(20X,'MAP OF FIRST DERIVATIVE DOWN 3 GRID UNIT',//)
185    FORMAT(20X,'MAP OF FIRST DERIVATIVE DOWN 4 GRID UNIT',//)

```

```

UDD04920
UDD04930
UDD04940
UDD04950
UDD04960
UDD04970
UDD04980
UDD04990
UDD05000
UDD05010
UDD05020
UDD05030
UDD05040
UDD05050
UDD05060
UDD05070
UDD05080
UDD05090
UDD05100
UDD05110
UDD05120
UDD05130
UDD05140
UDD05150
UDD05160
UDD05170
UDD05180
UDD05190
UDD05200
UDD05210
UDD05220
UDD05230
UDD05240
UDD05250
UDD05260
UDD05270
UDD05280
UDD05290
UDD05300
UDD05310
UDD05320
UDD05330
UDD05340
UDD05350
UDD05360
UDD05370
UDD05380
UDD05390
UDD05400
UDD05410
UDD05420
UDD05430
UDD05440
UDD05450
UDD05460
UDD05470
UDD05480
UDD05490
UDD05500
UDD05510
UDD05520
UDD05530

```

186	FORMAT(20X,'MAP OF SECOND DERIVATIVE ON SURFACE',//)	UDD05540
187	FORMAT(20X,'MAP OF SECOND DERIVATIVE DOWN 1 GRID UNIT',//)	UDD05550
188	FORMAT(20X,'MAP OF SECOND DERIVATIVE DOWN 2 GRID UNIT',//)	UDD05560
189	FORMAT(20X,'MAP OF SECOND DERIVATIVE DOWN 3 GRID UNIT',//)	UDD05570
	END	UDD05580

APPENDIX I-D

ANALYSIS OF GRAVMOD FORTRAN

GRAVMOD FORTRAN is designed to give the modeler a two dimensional approximation of the subsurface geology, for a selected traverse. The model is comprised of polygons that approximate the subsurface geology. Each polygon is assigned a density, based on the known geology. The contrast densities used in the program are the difference between the polygonal density and the value 2.67 g/cm^3 (average crustal density). In addition, the number of polygonal sides, polygonal coordinates, traverse length, station spacing, number of stations, and observed Bouguer anomalies are the other input variables.

The program uses the input variables to generate a series of theoretical Bouguer curves, along the traverse, for each polygon. Theoretical anomalies are summed, after the last polygonal curve is calculate, at each station. A theoretical Bouguer curve for the model is the result of this summation. To test the validity of a model the theoretical and Bouguer curves are compared. If the sum of the residuals values between curves is a low value the model is accepted;

otherwise, the input is modified and the process is repeated. In this study, a model was accepted if a majority of the residuals values were less than 0.5 milligals.

GRAVMOD FORTRAN is based on an algorithm first introduced by Talwani and others (1959). This algorithm is based on the equation 2:

$$A(0,0) = 2G\Delta\rho \sum_{j=1}^n \left[\frac{x_j z_{j+1} - x_{j+1} z_j}{(x_{j+1} - x_j)^2 + (z_{j+1} - z_j)^2} \right] \\ \left[\frac{z_{j+1} - z_j}{2} \ln \left(\frac{x_{j+1}^2 + z_{j+1}^2}{x_j^2 + z_j^2} \right) + \right. \\ \left. (x_{j+1} - x_j) \left(\arctan \left(\frac{x_{j+1}}{z_{j+1}} \right) - \arctan \left(\frac{x_j}{z_j} \right) \right) \right]$$

where

$A(0,0)$: Gravity anomaly at point 0,0

G : Newton's Gravitational constant

delta P: Density contrast between polygonal unit and 2.67 g/cm³.

n : Number of polygons

X_j, Z_j : X and Z coordinates of the polygon

This equation provides interesting insight to the limitations of the algorithm. This method assumes an infinite extension of the geologic formation along strike. Because of this assumption, variations of lithology along strikes are not modelled. This is the primary reason, that residual values

between theoretical and observed Bouguer curves often are not equal to zero. A second limitation of this method is that an infinite number of models exists that satisfy the criteria of acceptance. This is because the polygonal density and polygonal shape are unknowns, in the geologic sense. Remember from linear algebra if an equation has two unknowns then the number of solutions is infinite. This is why it is imperative to have geologic constraints, such as lithologic densities, and structures for the traverse. These constraints make the number of possible solutions finite because they limit the possible number of unknowns. Lastly, Talwani's method does not accurately predict the boundary values of the model.

GRAVMOD FORTRAN

```

C      ROUTINE GRAVMOD (MODIFIED FROM PARASNIS,1973,PG.380)          GRA00010
C      MODIFIED FOR IBM NOWROOZI 1985                               GRA00020
C      PROGRAM TO CALCULATE THE GRAVITY ANOMOLY ALONG A GROUND      GRA00030
C      PROFILE AT RIGHT ANGLES TO THE STRAKE OF A TWO-DIMENSIONAL  GRA00040
C      FEATURE OF ARBITRARY, UNIFORM CROSS-SECTION.                GRA00050
C                                                                    GRA00060
C      ANY NUMBER OF K(<36) MODELS CAN BE HANDLED. EACH MODEL MUST GRA00070
C      HAVE THE FOLLOWING PARAMETER SET:                             GRA00080
C          NCOR: NUMBER OF POLYGON CORNERS                           GRA00090
C          NCR: NUMBER OF POLYGON CORNERS + 1                       GRA00100
C          XS,XF:(XS<XF) CORRINATES OF END POINTS OF PROFILE (NEAR- GRA00110
C              EST MDX MUST BE POSITIVE.)                            GRA00120
C          D:CALCULATION INTERVAL (METERS)                           GRA00130
C          X(),Z():X-Z CORRINATES OF EACH CORNER OF THE POLYGON, MOV- GRA00140
C              ING CW. EACH CORRINATE IS ON A SEPERATE LINE.       GRA00150
C          N:NUMBER OF DATA POINTS                                  GRA00160
C      OUTPUT IS A TABLE OF X(METERS) VS GRAVITY ANOMOLY (MGALS)  GRA00170
CCCCCCCCCCCCCCCCCCCCCCCCCCCCCCCCCCCCCCCCCCCCCCCCCCCCCCCCCCCCGRA00180
C                                                                    GRA00190
C          CHARACTER * 1 C(30,128),LAY,HAY,BAY                      GRA00200
C          DIMENSION X(33),Z(33),A(500),G(35,500),S(500),TITL(80),R(500) GRA00210
C          +,S1(500),DDD(500,3)                                     GRA00220
C                                                                    GRA00230
C          READ(1,*) XS,D,XF,N                                       GRA00240
C          XS=NINT(XS)/3.281                                         GRA00250
C          D=NINT(D)/3.281                                           GRA00260
C          XF=NINT(XF)/3.281                                         GRA00270
C                                                                    GRA00280
C          DATA C/3840 * ' '/LAY/'1'/HAY/'2'/BAY/'3'/             GRA00290
C          DATA (C(15,I),I=1,128)/128 * '-'/                       GRA00300
C          DATA (C(I,1),I=1,30)/30 * '|'/                           GRA00310
C                                                                    GRA00320
C                                                                    GRA00330
C          READ IN TITLE AND PARAMETERS                               GRA00340
C                                                                    GRA00350
C          READ(1,1) (TITL(I),I=1,80)                                GRA00360
1          FORMAT(80A1)                                              GRA00370
C          K=NUMBER OF MODELS                                        GRA00380
C          READ(1,*) K                                               GRA00390
C          READ LIMIT VALUES                                       GRA00400
C          READ(1,*) XMIN,XMAX                                       GRA00410
C          XS=STARTING POINT; D=INTERVALS; XF=END POINT; N=(XF-XS)/D +1 GRA00420
3          WRITE(2,3) (TITL(I),I=1,80)                               GRA00430
C          FORMAT(80A1)                                              GRA00440
C          WRITE(2,2) K,N,XS,D,XF                                     GRA00450
2          FORMAT('///',5X,'K=',I5,5X,'N=',I5,3X,'XS=',F5.2,3X,'D=',F5.2 GRA00460
C          +,5X,'XF=',F9.2)                                         GRA00470
C                                                                    GRA00480
C          CALCULATE ANOMALY FOR EACH MODEL                           GRA00490
C                                                                    GRA00500
C          PRINT *,K,XS,XF,D,N                                       GRA00510
C          DO 50 M=1,K                                               GRA00520
C          RHO=0.0                                                    GRA00530
C          P=XS                                                       GRA00540
C          READ(1,*) NCOR,RHO                                         GRA00550
C          PRINT *, NCOR,RHO                                         GRA00560
C          WRITE(2,4) NCOR,RHO,M                                       GRA00570
4          FORMAT('///', 'NCOR=',I5,10X,'RHO=',F5.2,10X,'MODEL=',I5) GRA00580
C          READ(1,*) (X(I),Z(I),I=1,NCOR)                             GRA00590

```

```

DO 121 I=1,NCOR
X(I)=NINT(X(I))/3.281
Z(I)=NINT(Z(I))/3.281
121 CONTINUE
WRITE(2,6)
6 FORMAT('///',' XCOR ZCOR ')
WRITE(2,7) (X(I),Z(I),I=1,NCOR)
7 FORMAT(5X,F10.2,15X,F10.2)
WRITE(2,2000) M
IF (P.GT.XF) GO TO 50
DO 40 I=1,N
S(I)=0.0
CALL PRISMG(P,0.0,X,Z,NCOR,ANOM)
ANOM=ANOM*1000.0*RHO
WRITE(2,2001) P,ANOM
A(I)=P
G(M,I)=ANOM
P=P+D
40 CONTINUE
50 CONTINUE
C
C STACK ANOMALIES INTO ONE PROFILE MODEL
C
WRITE(2,8) K
8 FORMAT('1','SUMMATION OF ALL K = ',I5,5X,'MODELS',30X,'OBSERVED GGRA00840
+RAVITY VALUES')
C
CHUD=-200.
AMIN=0.0
AMAX=0.0
BMIN=0.0
BMAX=0.0
DO 60 I=1,N
S(I)=0.0
CHUD=CHUD+200.
DO 70 J=1,K
S(I)=S(I)+G(J,I)
70 CONTINUE
IF (CHUD.LT.XMIN.OR.CHUD.GT.XMAX) THEN
R(I)=0.0
WRITE(2,2001) A(I), CHUD, S(I), R(I)
WRITE(3,2003) CHUD,S(I),R(I)
ELSE
READ(1,*) R(I)
WRITE(2,2001) A(I), CHUD, S(I), R(I)
WRITE(3,2003) CHUD,S(I),R(I)
2003 FORMAT(1X,E8.3,2X,F9.3,2X,F9.3)
END IF
BMIN=MIN(BMIN,A(I))
BMAX=MAX(BMAX,A(I))
AMIN=MIN(AMIN,S(I),R(I))
AMAX=MAX(AMAX,S(I),R(I))
60 CONTINUE
C
PRINT *, 'AMIN=', AMIN, 'AMAX=', AMAX, 'BMIN=', BMIN, 'BMAX=', BMAX
DO 123 I=1,N
CALL PLOT1(A(I),S(I),C,30,128,LAY,AMIN,AMAX,BMIN,BMAX)
CALL PLOT1(A(I),R(I),C,30,128,HAY,AMIN,AMAX,BMIN,BMAX)
C CALL PLOT1(A(I),S1(I),C,30,128,BAY,AMIN,AMAX,BMIN,BMAX)
123 CONTINUE
C
CALL OOUT(C,30,128,D,AMIN,AMAX)

```



```

14      GO TO 2000                                GRAO1840
5       IF (S2-C2*TP) 16,17,17                  GRAO1850
17      ANOM=ANOM+A*SP*CP*(THETA2-1.570796327+TP*ALOG(S2-C2*TP)) GRAO1860
16      GO TO 2000                                GRAO1870
2000    CONTINUE                                  GRAO1880
        ANOM=FACTOR*ANOM                          GRAO1890
        RETURN                                     GRAO1900
        END                                        GRAO1910
C                                             GRAO1920
C                                             GRAO1930
C                                             GRAO1940
C                                             GRAO1950
        SUBROUTINE PLOT1(X1,Y1,GP,NA,NF,HELP,AMIN,AMAX,BMIN,BMAX) GRAO1960
        CHARACTER * 1 GP(NA,NF), HELP           GRAO1970
        REAL X2, Y2                               GRAO1980
        Y2=NINT((Y1-AMIN)/(AMAX-AMIN)*NA)+1     GRAO1990
        X2=NINT((X1-BMIN)/(BMAX-BMIN)*NF)+1     GRAO2000
C       PRINT *, Y2,X2                           GRAO2010
        IF (Y2.GE.1.AND.Y2.LE.NA.AND.X2.GE.1.AND.X2.LE.NF) THEN GRAO2020
        GP(Y2,X2)=HELP                           GRAO2030
        END IF                                    GRAO2040
        RETURN                                     GRAO2050
        END                                        GRAO2060
C                                             GRAO2070
        REAL FUNCTION FUNMIN(X,NC,NR,NL,NM)       GRAO2080
        REAL X(NC,NR)                             GRAO2090
        FUNMIN=X(1,NL)                            GRAO2100
        DO 100 I=NL,NM                            GRAO2110
        DO 100 J=1,NC                              GRAO2120
        IF (FUNMIN.GT.X(J,I)) FUNMIN=X(J,I)       GRAO2130
100     CONTINUE                                  GRAO2140
        RETURN                                     GRAO2150
        END                                        GRAO2160
C                                             GRAO2170
C                                             GRAO2180
        REAL FUNCTION FUNMAX(X,NC,NR,NL,NM)       GRAO2190
        REAL X(NC,NR)                             GRAO2200
        FUNMAX=X(1,NL)                            GRAO2210
        DO 100 I=NL,NM                            GRAO2220
        DO 100 J=1,NC                              GRAO2230
        IF (FUNMAX.LT.X(J,I)) FUNMAX=X(J,I)       GRAO2240
100     CONTINUE                                  GRAO2250
        RETURN                                     GRAO2260
        END                                        GRAO2270
C                                             GRAO2280
        SUBROUTINE OOUT(X,NA,NF,D,AMIN3,AMAX3)    GRAO2290
        CHARACTER * 1 X(NA,NF)                   GRAO2300
        DIMENSION T(21)                          GRAO2310
        INTEGER Y1                                GRAO2320
C                                             GRAO2330
        WRITE(2,500)                              GRAO2340
        PRINT *, 'AMAX=',AMAX3,'AMIN=',AMIN3    GRAO2350
        DO 100 I=NA,6,-6                          GRAO2360
        IF (I.EQ.NA) THEN                          GRAO2370
        Y1=NINT(AMAX3)                             GRAO2380
        ELSE                                        GRAO2390
        Y1=Y1-NINT(((AMAX3-AMIN3)/FLOAT(NA))*6)   GRAO2400
        END IF                                     GRAO2410
C                                             GRAO2420
        WRITE(2,1000) Y1, (X(I,J),J=1,NF)        GRAO2430
C                                             GRAO2440
        DO 100 J=I-1,I-5,-1                       GRAO2450

```

```
      WRITE(2,2000) (X(J,K),K=1,NF)
100  CONTINUE
C
C      RETURN
C
500  FORMAT(////////,50X,'THEORITICAL AND OBSERVED BOUGER ANOMALIES',//)
1000 FORMAT(I4,128A1)
2000 FORMAT(4X,128A1)
      END
```

GRA02460
GRA02470
GRA02480
GRA02490
GRA02500
GRA02510
GRA02520
GRA02530
GRA02540
GRA02550

APPENDIX I-E

ANALYSIS OF QUAD BAS

QUAD.BAS was developed by Decker and James (1988) to statistically analyze rectified stream data. The algorithm of this program is based the quadrat presence/absence method proposed by Abdel-Rahman and Hay (1978). Prior to the quadrat presence/absence method the two most common techniques for sampling geological fractures was the quadrat length and quadrat frequency methods.

The quadrat length method sums the lengths of all fractures in a specified orientation class interval. A rose diagram of the summed lengths could then be plotted. This method does not distinguish between one long fracture and several shorter independent fractures in the same orientation class. Statistical analysis of the fracture data using this method is complex and yield random results.

The quadrat frequency method counts the total number of fractures in a specified orientation class, regardless of length. As a result, different trends are distinguished, and because the data are true frequencies of individuals statistical tests based on frequencies are possible. Abdel-Rahman and Hay (1979) point out that this method does not give a true representation of the population because the individual fractures in a quadrat may represent a cluster of fractures related to a small scale geologic event.

The quadrat presence/absence method determines whether a certain orientation class is present or absent using a sample size of 50 or more random quadrat sample units. Using this methodology, a single fracture may be counted more than once if it falls in more than one sampling quadrat. This means there is a higher probability that a long fracture will be counted more than once resulting in the close approximation to the pattern of fracture lengths. Using this method data can be statistical analyzed quickly while minimizing measurement errors.

The algorithm used in QUAD.BAS is based on the Poisson equation below:

$$p(n) = \frac{e^{-x} x^n}{n!}$$

where

n : number of points falling in any one class category

e : base of the natural logarithm

x : mean of the number of observations in each class

(Total number of observations, N, divided by number of classes)

The program QUAD BAS is located on the diskette along with several input files name *.STR (* means all files ending with the prefix STR).

QUAD BAS

```

DECLARE SUB writm1 (class1, class2, pp!, mm)
DECLARE SUB writm (class, pp!, mm)
DECLARE SUB tails (meen!, level!, tn!, pn!)
DECLARE SUB prob (x!, n!, p!)
DECLARE SUB quadrat (qx!, qy!, qr!, q!())
DECLARE SUB group (meen!, pn!, tn!, tot!())

' ----- QUADRAT.BAS -----
' ----- Circular statistics using Poisson distributions -----
' program to create data set of quadrats from any given 'lineament' file
' data must be in x1,y1 - x2,y2 format
,
RESET: SCREEN 2: CLOSE : KEY OFF
CONST pi# = 3.1415927#, pi2# = pi * 2, rad# = pi / 180
      DIM q(361), tot(361)

'get name of file to work on
begin0: CLS : PRINT : PRINT
INPUT "[DD:\path] filename . ext = "; ifil$
'ON ERROR GOTO handle1
begin: OPEN ifil$ FOR INPUT AS #1
'ON ERROR GOTO handler
      GOTO skip1

' error handler for file name
handle1: BEEP: LOCATE 10, 5
        IF ERR = 53 THEN PRINT "That file was not found" ELSE PRINT "error #"; ERR
        RESUME begin0

'skip error handler above
skip1: CLS :
      LOCATE 3, 10: PRINT " Determining graphic limits of "; ifil$
      LOCATE 6, 37: PRINT "n= 1";
' begin with a lower and upper set from the data
      ct% = 1
      INPUT #1, x1, Y1, x2, y2
      llx = x1: urx = x2
      IF x2 < x1 THEN llx = x2: urx = x1
      lly = Y1: ury = y2
      IF y2 < Y1 THEN lly = y2: ury = Y1
getlim: IF EOF(1) THEN CLOSE #1: GOTO step2
      ct% = ct% + 1
      LOCATE 6, 40: PRINT ct%
      INPUT #1, x1, Y1, x2, y2
' lower x
      IF llx > x1 THEN llx = x1
      IF llx > x2 THEN llx = x2
' lower y
      IF lly > Y1 THEN lly = Y1
      IF lly > y2 THEN lly = y2
' upper x
      IF urx < x1 THEN urx = x1
      IF urx < x2 THEN urx = x2
' upper y
      IF ury < Y1 THEN ury = Y1
      IF ury < y2 THEN ury = y2

```

```

GOTO getlim

step2:

  vy% = 190
  dx = ABS(llx - urx) ' total change in X
  dy = ABS(ury - lly) ' total change in Y
  cdd = dy / dx
  vx% = 310 - CINT(181 / cdd)
  IF vx% < 0 THEN vx% = 9: vy% = 190 - CINT(181 * cdd)

' setup screen for map
  SCREEN 1, 0: CLS
  VIEW (vx%, 9)-(310, vy%), , 2
  WINDOW (llx, lly)-(urx, ury)

  LOCATE 1, 1: PRINT SPC(39);
  LOCATE 1, 1: PRINT "Is data in 1> 360 or 2>180 format"
getfmt:  a$ = INPUT$(1)
  dfmt% = VAL(a$)
  IF dfmt% <> 1 AND dfmt% <> 2 THEN BEEP: GOTO getfmt
  arend% = 360 / dfmt% - 1

' check for type of analysis
  LOCATE 1, 1: PRINT SPC(39);
  LOCATE 1, 1: PRINT "1> whole or 2> quadrat analysis"
getan:  a$ = INPUT$(1)
  ana% = VAL(a$)
  IF ana% <> 1 AND ana% <> 2 THEN BEEP: GOTO getan
  IF ana% = 1 THEN
    nq = 1
    IF dx > dy THEN qr = dx ELSE qr = dy
    qr = qr / 2
    qx = .5 * dx + llx
    qy = .5 * dy + lly
    paflg% = 1
    GOTO comence
  END IF

  LOCATE 1, 1: PRINT SPC(39);
  LOCATE 1, 1: INPUT "# of quadrats= ", nq
  LOCATE 1, 1: PRINT SPC(39);
  LOCATE 25, 1: PRINT "dx="; dx; " dy="; dy;
  LOCATE 1, 1: INPUT "radius of quardat= ", qr
  IF qr > dx / 10 THEN qr = dx / 10
  LOCATE 1, 1: PRINT SPC(39);
  LOCATE 25, 1: PRINT SPC(39);

' determine qx and qy for quadrat center
comence: RANDOMIZE TIMER
  FOR iq = 1 TO nq
ON ana% GOTO skpq, quad

quad: LOCATE 25, 1: PRINT "quadrat #"; iq;
redo: qx = RND(1) * dx + llx
  qy = RND(1) * dy + lly

' display quadrat
  LOCATE 1, 1: PRINT "qx="; qx; " qy="; qy

' CLS 1 ' clear graphics screen only

```

```

LINE (qx - qr, qy - qr)-(qx + qr, qy + qr), 1, B
skpq:
CALL quadrat(qx, qy, qr, q())
' change q() to presence/absence and check for empty set if paflg%=0
IF paflg% = 1 THEN GOTO skppa
  chk = 0
  FOR i = 0 TO arend%
    IF q(i) > 0 THEN q(i) = 1: chk = 1
  NEXT i
IF chk = 0 THEN
  LINE (qx - qr, qy - qr)-(qx + qr, qy + qr), 0, B
  GOTO redo
END IF

' keep track of all data [in the case of once through no problem
skppa: FOR i = 0 TO arend%
  tot(i) = tot(i) + q(i)
NEXT i
NEXT iq

SCREEN 0

' now the probability shit
' get n
ntot = 0
FOR i = 0 TO arend%
  ntot = ntot + tot(i)
NEXT i

SCREEN 2: CLS
LOCATE 10, 20: PRINT "Which Probability Level Do You Desire ?"
LOCATE 11, 30: INPUT " ex. 99 or 95 :", level
  level = 1 - level / 100
  meen = (ntot / arend%)
LOCATE 15, 20: PRINT "Mean value is.....", meen

CALL tails(meen, level, tn, pn)

CLS
LOCATE 5, 10: PRINT "Peak = "; pn
LOCATE 7, 10: PRINT "Trough ="; tn
a$ = INPUT$(1)

' display data set
CLS : LOCATE 10, 10: PRINT "Do you want a hardcopy of the data set ? [Y/N]"
a$ = UCASE$(INPUT$(1))
IF a$ <> "Y" THEN GOTO noprt
getpv: LOCATE 15, 10: PRINT "1> all data or 2> just peaks and troughs"
pval = VAL(UCASE$(INPUT$(1)))
IF pval <> 1 AND pval <> 2 THEN BEEP: GOTO getpv
CLS : LOCATE 10, 35: PRINT "working"
' print header info
LPRINT "
Azimuthal data from "; ifil$
IF ana% = 1 THEN LPRINT "
Whole data frequency analysis"
IF aUME begin0

SUB group (meen, pn, tn, tot())
SHARED arend%, ntot

```

'this program looks for significant peaks and groups them into larger classes
'with max. class determined by user

LOCATE 15, 10: INPUT "please give maximum class grouping desired: ", max
' outer loop determines significant peaks around which to group

```
FOR i = 0 TO arend%
  IF tot(i) < pn GOTO 1
  ii = 0: ll = 1: mm = 1: lll = 0: iii = 0
  g1 = tot(i)
  meen = ntot / (360 / 1)
  CALL prob(meen, g1, pp)
  CALL writm(i, pp, mm)
```

'this loop finds the groupings about the significant peaks

```
FOR j = i TO (i + max)
  ii = ii + 1
  IF (i - ii) >= 0 THEN kk = i - ii
  IF (i - ii) < 0 THEN kk = (360 + i) - ii

  mm = mm + 1
```

'to correct for counting above 359 or below zero

```
IF (j + ll) > 359 THEN ll = -360
```

'test to see which class has higher frequency on either side of peak
'to save time, two if statements are used to check for troughs before
'grouping is done

```
IF lll = -999 GOTO stepp2
IF tot(j + ll) <= tn THEN lll = -999
IF tot(j + ll) > tot(kk) THEN
  g1 = g1 + tot(j + ll)
  meen = ntot / (360 / mm)
'calcualte probability of occurrence for this grouping
'  PRINT "g1="; g1; "j="; j; "meen="; meen; "tot="; tot(j + ll)
'  a$ = INPUT$(1)
  CALL prob(meen, g1, pp)
'write to printer the results of test
  CALL writm(j + ll, pp, mm)
  ii = ii - 1
  GOTO 2
END IF
```

' check for troughs

```
stepp2: IF iii = -999 GOTO step3
IF tot(kk) <= tn THEN iii = -999
IF tot(j + ll) < tot(kk) THEN
  g1 = g1 + tot(kk)
  meen = ntot / (360 / mm)
'calcualte probablitiy of occurrence for this grouping
  CALL prob(meen, g1, pp)
' write results to printer
  CALL writm(kk, pp, mm)
  ll = ll - 1
  GOTO 2
END IF
```

' check to see if two classes either side of grouping are equal

```

stna% = 2 THEN LPRINT "          using "; nq; " quadrats with a "; qr; " radius."
  LPRINT CINT((1 - level) * 100); "% critical values          min peak="; pn; "
  max trough="; tn
  LPRINT

  FOR i = 0 TO arend%
  ON pval GOTO pall, ptp

ptp: IF tot(i) >= pn OR tot(i) <= tn THEN GOTO pall
  GOTO skipprt

pall: LPRINT USING "      ###"; i;
  LPRINT USING "      #####"; tot(i);

' mark peaks and troughs
  IF tot(i) >= pn THEN
    LPRINT "      +"
  ELSEIF tot(i) <= tn THEN
    LPRINT "      -"
  ELSE LPRINT "      "
  END IF
skipprt: NEXT i
' now determine grouping of the various peaks
noprt: CALL group(meen, pn, tn, tot())

' make a file of angular data for plotting in the rose program
  OPEN "\000\poisson.roz" FOR OUTPUT AS #2
  FOR i = 0 TO arend%
  FOR j = 1 TO tot(i)
  PRINT #2, i
  NEXT j
  NEXT i

SCREEN 2

  END

handler: CLS : LOCATE 5, 1: PRINT "Error handler"
  LOCATE 6, 1: PRINT "error= #"; ERR
  a$ = INPUT$(1)
  RESDECLARE SUB makeang (ang!, dlen!)
DECLARE SUB smooth (sdat!())
DECLARE SUB autocor ()
DECLARE SUB crosscor ()
' ----- ROSE corr.BAS -----
' program to plot a rose diagram to the screen
' also does some simple statistics
' ----- written by Bill Decker 6/21/87 ---- modified 6/29/88

COMMON SHARED nf
  RESET
  CONST pi# = 3.141592654#, pi2# = 2 * pi, hpi# = pi / 2, rad# = pi / 180
  DIM dat(361, 2), pdat(361, 2, 2), bdat(361), stot(2), tot(2)
  SCREEN 2: KEY OFF: CLS

' constants and counters
begin: tot(1) = 0: tot(2) = 0: stot(1) = 0: stot(2) = 0: cbar = 0: sbar = 0:
nf = 1

```

```

FOR i = 0 TO 360
  dat(i, 1) = 0
  dat(i, 2) = 0
  pdat(i, 1, 1) = 0: pdat(i, 2, 1) = 2
  pdat(i, 1, 2) = 0: pdat(i, 2, 2) = 2
  bdat(i) = 0
NEXT i

' get data format
20 PRINT : PRINT
  PRINT "Is the data in <1> 360 or <2> 180 degree format?"
  a$ = INPUT$(1)

dfmt = VAL(a$)
  IF dfmt < 1 OR dfmt > 2 THEN BEEP: GOTO 20

' get increment
30 PRINT : PRINT
  PRINT "  Increment for rose diag. construction  "
  INPUT "    equal subdivision of 360 degrees    = ", inc
  inc = ABS(inc)
  IF inc = 0 THEN GOTO 30
  IF 360 MOD inc <> 0 THEN BEEP: GOTO 30 ' not an even subdivision of 360

'double increment if 180 degree format
'*****
  inc = inc * dfmt

inf: CLS : LOCATE 3, 15: PRINT "INPUT DD [path] NAME . EXT for input file "
      LOCATE 5, 20: INPUT "Filename: ", flin$(nf)

      LOCATE 10, 5: PRINT "Is data <A> angular or <L> linear (x1-y1 x2-y2) ?"
getform: a$ = UCASE$(INPUT$(1))
          IF a$ = "A" THEN datflg = 2: GOTO 70
          IF a$ = "L" THEN
            datflg = 1

' get length weighting
  PRINT : PRINT
  PRINT "Use length weighted formula? [Y/N]"
  lw$ = UCASE$(INPUT$(1))

  IF lw$ <> "Y" THEN minl = 0: maxl = 1000: GOTO 70 'skip min/max if no length
weighting
' set minimum length
  PRINT : PRINT
  INPUT "Input minimum length ", minl

```

APPENDIX I-F

REMAINING PROGRAMS

The remaining programs mentioned in this paper are listed below:

TWOLINE SAS: This program is used to plot two simultaneous curves on the same graph.

```

OPTIONS MPRINT ;
%MACRO GPH(DATTA);
  /* INTIALIZE AXIS LABELS */
  %LET XTIT=DISTANCE (KM);
  %LET YTIT=MILLIGALS;
  %LET TIT2=THEORETICAL AND BOUGUER;
  %LET TIT3=          ANOMALIES          ;
  %LET DESC=THEORETICAL/BOUGUER VS DIST;
  %LET XSCALE=15;

  /* INTIALIZE PAGE TITLE */

  %IF &DATTA=IN.D622 %THEN %DO;
    %LET TIT1=STATE ROAD 622;
    %LET NAM=SR622;
    %LET INC=0.5;
  %END;
  %IF &DATTA=IN.D60 %THEN %DO;
    %LET TIT1= U.S. 60 ;
    %LET NAM=US60;
    %LET INC=0.5;
  %END;
  %IF &DATTA=IN.D634 %THEN %DO;
    %LET TIT1=STATE ROAD 634;
    %LET NAM=SR634;
    %LET INC=1.0;
  %END;
  %IF &DATTA=IN.D636 %THEN %DO;
    %LET TIT1=STATE ROAD 636;
    %LET NAM=SR636;
    %LET INC=1.0;
  %END;
  %IF &DATTA=IN.D637 %THEN %DO;
    %LET TIT1=STATE ROAD 637;
    %LET NAM=SR637;
    %LET INC=1.0;
  %END;
  %IF &DATTA=IN.D460 %THEN %DO;
    %LET TIT1= U.S. 460 ;
  %END;

```

```

%LET NAM=US460;
%LET INC=1.0;
%END;

DATA MOD;
  SET &DATTA;
  DIST=(DIST/3.2808)/1000;
RUN;
/*Find the maximum x value */

PROC MEANS DATA= MOD NOPRINT;
  VAR DIST;
  OUTPUT OUT=MOD1 MAX=MAXX ;
RUN;

DATA MOD2;
  set mod1;
  MAXX= ROUND(MAXX,.5)+.5;
  CALL SYMPUT('MAX',MAXX);
  %LET XMAX=&MAX;

run;
/* use sas annotate graphic macros*/
/* %label and %line are listed in the Model SAS program
DATA ANNO;
%DCLANNO;
LENGTH TEXT $40;
%LABEL(50,75,"&TIT2",BLACK,0,0,4.0,SIMPLEX,5);
%LABEL(50,72,"&TIT3",BLACK,0,0,4.0,SIMPLEX,5);
%LABEL(20,25,'+',BLUE,0,0,2.0,SIMPLEX,5);
%LABEL(22,25,'BOUGUER ANOMALY',BLACK,0,0,2.0,SIMPLEX,6);
%LABEL(60,25,'*',RED,0,0,2.0,SIMPLEX,5);
%LABEL(62,25,'THEORETICAL ANOMALY',BLACK,0,0,2.0,SIMPLEX,6);
%LINE(42,21,43,21,BLACK,1,3);
%LABEL(50,21,'REGIONAL TREND',BLACK,0,0,2.0,SIMPLEX,5);
RUN;
/* GET READY FOR PLOTTING */
SYMBOL1 V=PLUS C=BLUE I=JOIN;
SYMBOL2 V=STAR C=RED I=JOIN;
SYMBOL3 V=NONE C=BLACK W=3 I=RL;

PROC GPLOT DATA=MOD;*OUT=IN.gpHH ANNOTATE=ANNO;
  AXIS1 LABEL=(H=2.5 C=BLACK F=SIMPLEX "&YTIT")
    VALUE=(H=2.5 F=SIMPLEX C=BLACK) color=black
    ORDER=0 TO &XMAX BY &INC LENGTH=10 CM;
  AXIS2 LABEL=(H=2.5 F=SIMPLEX C=BLACK J=L A=90 "&YTIT")
    VALUE=(H=2.5 C=BLACK F=SIMPLEX)
    ORDER=10 TO 20 BY 2 COLOR=BLACK
    LENGTH=10 CM;
  PLOT1 BANOM*DIST=1 TANOM*DIST=2 / NOLEGEND
        HAXIS=AXIS1 OVERLAY
        VAXIS=AXIS2
        NAME="&NAM"
        DES="&DESC";
  PLOT2 BANOM*DIST=3/VAXIS=AXIS2;
RUN;
%MEND GPH;

GOPTIONS DEV=TEK4010 GEPILOG='18'X GPROLOG='1B0C' GPROTOCOL=GSAS7171
  NOTEXT82 HPOS=100 VPOS=100
  COLORS=(BLACK RED BLUE GREEN YELLOW PURPLE BROWN ORANGE);
%GPH(IN.D622);
%GPH(IN.D60);

```



```
%GPH(IN.D634);
%GPH(IN.D636);
%GPH(IN.D637);
%GPH(IN.D460);
```

CONTOUR SAS: This program contours three dimensional data in a X, Y, Z format.

```
GOPTIONS NOTEXT82 DEVICE=ZETA836C
HSIZE=9.0
VSIZE=15.0
ROTATE;
CMS FI GOOD DISK GMAP DATA B;
DATA AREA;
    INFILE GOOD;
    INPUT X Y Z;
RUN;
PROC G3GRID DATA=AREA OUT=GPH;
    GRID Y*X=Z / PARTIAL
        NEAR=25
        AXIS1=37.26 TO 37.600 BY .01
        AXIS2=-78.49 TO -78.26 BY .010;
RUN;
TITLE1 J=C H=3 F=NONE C=BLACK
'CONTOUR GRAVITY MAP OF FARMVILLE BASIN';
FOOTNOTE2 J=C H=1 F=NONE C=BLACK 'CONTOUR LINE ';
PROC GCONTOUR DATA=GPH;
    PLOT Y*X=Z/LEVELS=10 TO 20 BY .5;
RUN;
```

MODEL SAS: This program is used to generate the gravity models shown in this study. Note all graphic macros listed below were written by SAS Institute, Cary North Carolina.

```
OPTIONS MPRINT DQUOTE;
```

```
%MACRO SEQUEN(SEQ);
IF UPCASE("&SEQ")='AFTER' OR UPCASE("&SEQ")='A' THEN WHEN="A";
ELSE WHEN = "B";
```

```
%MEND SEQUEN;
%MACRO SYSTEM(XS,YS,HS);
XSYS = "&XS"; YSYS = "&YS"; HSYS = "&HS";
%MEND SYSTEM;
```

```
%MACRO DCLANNO;
length function color style $ 8.;
length xsys ysys hsys $ 1.;
length when position $ 1.;
retain xsys ysys hsys;
```

```
x= .; y= .;
style=" "; position = "5"; color = " "; function= " ";
```

```

%system(4,4,4);
%sequen(BEFORE);
%MEND DCLANNO;

%MACRO POLY(X1,Y1,COLR,PATTERN,LINTYP);
X=&X1;
Y=&Y1;
LINE= &LINTYP;
STYLE = &PATTERN;
COLOR = &COLR;
FUNCTION ="POLY      "; OUTPUT;
%MEND POLY;
%MACRO POLYCON(X1,Y1,COLIN);
X=&X1;
Y=&Y1;
COLOR=&COLIN;
FUNCTION ='POLYCONT'; OUTPUT;
%MEND POLYCON;
%MACRO FRAME(COLIN,LINTYP,WIDTH,PATTERN);
X=.;
Y=.;
IF "&COLIN"=: '*' THEN; ELSE COLOR="&COLIN";
STYLE="&PATTERN";
LINE=&LINTYP;
SIZE=&WIDTH;
FUNCTION ='FRAME    '; OUTPUT;
%MEND FRAME;
%MACRO PUSH;
X=.;
Y=.;
FUNCTION='PUSH     '; OUTPUT;
%MEND PUSH;

%MACRO SWAP;
X=.;
Y=.;
FUNCTION='SWAP     '; OUTPUT;
%MEND SWAP;

%MACRO CNTL2TX;
X=.;
Y=.;
FUNCTION='CNTL2TXT'; OUTPUT;
%MEND CNTL2TX;

%MACRO TXT2CNT;
X=.;
Y=.;
FUNCTION="TXT2CNTL"; OUTPUT;
%MEND TXT2CNT;

%MACRO POP;
X=.;
Y=.;
FUNCTION="POP      "; OUTPUT;
%MEND POP;

%MACRO DRAW2TX(COLIN,LINTYP,WIDTH);
X=.;
Y=.;
SIZE=&WIDTH;
LINE=&LINTYP;

```

```

    IF "&COLIN"=: '*' THEN; ELSE COLOR="&COLIN";
FUNCTION="DRAW2TXT"; OUTPUT;
%MEND DRAW2TX;

%MACRO LINE(X1,Y1,X2,Y2,COLIN,LINTYP,WIDTH);
%MOVE(&X1,&Y1);
%DRAW(&X2,&Y2,&COLIN,&LINTYP,&WIDTH);
%MEND LINE;

%MACRO MOVE (X1,Y1);
X=&X1;
Y=&Y1;
FUNCTION= "MOVE  "; OUTPUT;
%MEND MOVE;
%MACRO DRAW(X1, Y1, COLIN, LINTYP, WIDTH);
X=&X1;
Y=&Y1;
LINE = &LINTYP;
SIZE = &WIDTH;
    IF "&COLIN" =: '*' THEN ; ELSE COLOR = "&COLIN";
FUNCTION = "DRAW  "; OUTPUT;
%MEND DRAW;
%MACRO LABEL(X1, Y1, TXT, COLTXT, ANG, ROT, HGT, FONT, POS);
X=&X1;
Y=&Y1;
ANGLE= &ANG;
ROTATE= &ROT;
SIZE= &HGT;
STYLE= "&FONT";
TEXT= &TXT;
    IF "&POS" =: '*' THEN; ELSE POSITION = "&POS";
    IF "&COLTXT" =: '*' THEN ; ELSE COLOR = "&COLTXT";
FUNCTION = "LABEL  "; OUTPUT;
%MEND LABEL;
%MACRO RECT(X1,Y1,X2,Y2,COLIN,LINTYP, WIDTH );
%MOVE (&X1, &Y1);
%DRAW (&X2, &Y1, &COLIN, &LINTYP, &WIDTH);
%DRAW (&X2, &Y2, &COLIN, &LINTYP, &WIDTH);
%DRAW (&X1, &Y2, &COLIN, &LINTYP, &WIDTH);
%DRAW (&X1, &Y1, &COLIN, &LINTYP, &WIDTH);
%MEND RECT;
%MACRO BAR (X1, Y1, X2, Y2, COLOR, BARTYP, PATTERN );
%MOVE (&X1, &Y1);
X= &X2;
Y= &Y2;
LINE = &BARTYP;
STYLE = "&PATTERN"
    IF "&COLOR" =: '*' THEN ; ELSE COLOR = "&COLOR";
FUNCTION = "BAR  "; OUTPUT;
%MEND BAR;
%MACRO MODEL(DATTA);
    %LOCAL MAX YSCALE MINXY;
    /* INTIALIZE AXIS LABELS */
    %LET XTIT=DISTANCE (KM);
    %LET YTIT=DEPTH (KM);
    %LET TIT2=GRAVITY MODEL;
    %LET DESC=GRAVITY MODEL;
    %LET XSCALE=15;

/* INTIALIZE PAGE TITLE */

```

```

%IF &DATTA=IN.MOD622 %THEN %DO;
  %LET TIT1=STATE ROAD 622;
  %LET NAM=SR622;
  %LET INC=0.5;
%END;
%IF &DATTA=IN.MOD60 %THEN %DO;
  %LET TIT1= U.S. 60 ;
  %LET NAM=US60;
  %LET INC=0.5;
%END;
%IF &DATTA=IN.MOD634 %THEN %DO;
  %LET TIT1=STATE ROAD 634;
  %LET NAM=SR634;
  %LET INC=1.0;
%END;
%IF &DATTA=IN.MOD636 %THEN %DO;
  %LET TIT1=STATE ROAD 636;
  %LET NAM=SR636;
  %LET INC=1.0;
%END;
%IF &DATTA=IN.MOD637 %THEN %DO;
  %LET TIT1=STATE ROAD 637;
  %LET NAM=SR637;
  %LET INC=1.0;
%END;
%IF &DATTA=IN.MOD460 %THEN %DO;
  %LET TIT1= U.S. 460 ;
  %LET NAM=US460;
  %LET INC=1.0;
%END;
DATA CONVERT;
  SET &DATTA;
  XX=XX/3280.8;
  YY=YY/3280.8;
RUN;
PROC MEANS DATA= CONVERT NOPRINT;
  VAR XX;
  OUTPUT OUT=MOD1 MAX=MAXX ;
RUN;

PROC MEANS DATA= CONVERT NOPRINT;
  VAR YY;
  OUTPUT OUT=MOD2 MIN=MAXY ;
RUN;

DATA MOD3;
  set MOD1;
  MAXX= ROUND(MAXX,.5)+.5;
  CALL SYMPUT('MAX',MAXX);
  if maxx > 5 then call symput('inc','1');
  else call symput('inc','.5');
  set MOD2;
  MAXY= ROUND(ABS(MAXY),.5)+.5;
  YSCALE=(MAXY*&XSCALE)/MAXX;
  MINXY=-1*MAXY;
  CALL SYMPUT('MINXY',MINXY);
  CALL SYMPUT('YSCALE',YSCALE);
run;
/* GET READY FOR PLOTTING */
SYMBOL1 V=NONE;

DATA DAT1;

```

```

XX=0;
YY=0;
RUN;

DATA ANNO(DROP =ID XX YY RHO RHO1 RH1 RH2 RH3 RH4 PATTERN);
LENGTH CLR $8.;
%DCLANNO;
%SYSTEM(2,2,4);
%SEQUEN(AFTER);
SET CONVERT;
CALL SYMPUT('RHO',RHO);
CALL SYMPUT('RHO1',RHO1);
CALL SYMPUT('ID',ID);
RH1=-0.12;RH2=0.18;RH3=0.21;RH4=0.11;
CALL SYMPUT('RH1',RH1);
CALL SYMPUT('RH2',RH2);
CALL SYMPUT('RH3',RH3);
CALL SYMPUT('RH4',RH4);
ID1=4;
CALL SYMPUT('ID1',ID1);

IF SYMGET('RHO') =SYMGET('RH1') THEN DO;
  PATTERN='M3N035'; CLR="GREEN";
END;
IF SYMGET('RHO') =SYMGET('RH2') THEN DO;
  PATTERN='M4N320'; CLR="PURPLE";
END;
IF SYMGET('RHO') =SYMGET('RH3') THEN DO;
  PATTERN='S'; CLR="RED";
END;
IF SYMGET('RHO') =SYMGET('RH4') THEN DO;
  PATTERN='M4X320'; CLR="ORANGE";
END;
IF SYMGET('RHO') NE SYMGET('RHO1') THEN DO;
  %POLY(XX,YY,CLR,PATTERN,1);
  OUTPUT;
END;
ELSE IF SYMGET('RHO') = SYMGET('RHO1') THEN DO;
  %POLYCON(XX,YY,BLACK);
  OUTPUT;
END;

RUN;
TITLE1;
PROC Gplot DATA=DAT1 ANNOTATE=ANNO;*OUT=IN.GPHH;
AXIS1 LABEL=(H=2.5 C=BLACK F=SIMPLEX "&XTIT")
  VALUE=(H=2.5 F=SIMPLEX C=BLACK)
  ORDER=0 TO &MAX BY &INC LENGTH=10 CM COLOR=BLACK;
AXIS2 LABEL=(H=2.5 C=BLACK F=SIMPLEX J=L A=90 "&YTIT") COLOR=BLACK
  VALUE=(H=2.5 C=BLACK F=SIMPLEX)
  ORDER=&MINXY TO 0 BY .5
  LENGTH=10 CM;
PLOT1 XX*YY / NOLEGEND
  HAXIS=AXIS1 OVERLAY VMINOR=5
  VAXIS=AXIS2 HMINOR=10
  NAME="&NAM"
  DES="&DESC";
PLOT2 XX*YY/VAXIS=AXIS2 VMINOR=5;
RUN;
%MEND MODEL;
GOPTIONS DEV=TEK4010 GEPILOG='18'X GPROLOG='1BOC' GPROTOCOL=GSAS7171
  NOTEXT82 HPOS=100 VPOS=100 NODISPLAY;

```

```
%MODEL ( IN.MOD622 );  
%MODEL ( IN.MOD60 );  
%MODEL ( IN.MOD634 );  
%MODEL ( IN.MOD636 );  
%MODEL ( IN.MOD637 );  
%MODEL ( IN.MOD460 );
```

APPENDIX II

LISTING OF GRAVITY DATA

PROFILE

- A. U.S. HIGHWAY 460E
- B. STATE ROAD 637
- C. STATE ROAD 636
- D. STATE ROAD 634
- E. U.S. HIGHWAY 60
- F. STATE ROAD 622

U.S. HIGHWAY 460E GRAVITY READINGS

PRINCIPAL FACTS AT GRAVITY STATIONS

STA NAME AND NUM	LATITUDE NORTH	LONGITUDE EAST	ELEVATION FEET	SUPP ELEV METERS	OBSERVED G MEAL	FREE AIR MEAL	DRUMMER MEAL	THEOD G MEAL
2 BASE 1031	37 17.80	-78 27.89	399.700	0.000	979932.676	28.173	14.840	979942.280
25 10000	37 18.70	-78 27.61	454.240	0.000	979933.187	31.927	16.434	979944.000
26 10100	37 18.70	-78 27.56	453.140	-230.820	979933.167	31.746	16.331	979944.000
27 10200	37 18.68	-78 27.63	452.630	979933.250	31.846	16.409	979944.000
28 10300	37 18.67	-78 27.44	453.010	3.125	979933.312	31.836	16.417	979943.937
29 10400	37 18.65	-78 27.45	453.660	4.258	979933.937	31.695	16.258	979943.937
30 10500	37 18.63	-78 27.41	454.450	5.320	979933.000	31.665	16.354	979943.937
31 10600	37 18.62	-78 27.38	454.190	4.016	979933.002	31.669	16.444	979943.678
32 10700	37 18.60	-78 27.31	457.000	0.000	979933.612	31.664	16.326	979943.678
33 10800	37 18.58	-78 27.24	457.760	979933.600	31.667	16.000	979943.612
34 10900	37 18.57	-78 27.23	458.490	0.000	979933.582	31.628	16.212	979943.612
35 11000	37 18.57	-78 27.23	458.490	0.000	979933.500	31.798	16.160	979943.612
36 11100	37 18.55	-78 27.20	459.830	979933.500	31.918	16.250	979943.612
37 11200	37 18.53	-78 27.16	460.410	0.000	979933.325	31.767	16.029	979943.750
38 11300	37 18.52	-78 27.13	461.410	0.000	979933.325	31.862	16.114	979943.667
39 11400	37 18.50	-78 27.11	461.710	1.023	979933.125	31.823	16.073	979943.667
40 11500	37 18.50	-78 27.05	461.270	0.000	979933.167	31.872	16.120	979943.667
41 11600	37 18.47	-78 27.01	460.390	-1040.079	979931.937	31.874	16.875	979943.667
42 11700	37 18.47	-78 26.98	458.510	0.000	979931.750	31.239	16.149	979943.626
43 11800	37 18.43	-78 26.98	458.590	0.000	979932.062	31.289	16.029	979943.562
44 11900	37 18.42	-78 26.96	458.190	979932.167	31.289	16.764	979943.600
45 12000	37 18.38	-78 26.93	456.830	0.000	979932.312	30.987	16.747	979943.600
46 12100	37 18.37	-78 26.93	456.830	0.005	979932.600	31.060	16.893	979943.437
47 12200	37 18.30	-78 26.84	441.450	979932.250	30.836	16.062	979943.378
48 12300	37 18.27	-78 26.83	436.690	979932.250	30.874	16.149	979943.378
49 12400	37 18.27	-78 26.80	431.660	-80.830	979933.562	30.674	16.144	979943.312
50 12500	37 18.20	-78 26.80	426.250	979933.575	30.580	16.234	979943.250
51 12600	37 18.20	-78 26.80	426.250	0.000	979933.575	30.580	16.230	979943.167
52 12700	37 18.17	-78 26.76	414.810	0.000	979934.562	30.364	16.132	979943.167
53 12800	37 18.13	-78 26.74	408.450	979934.612	30.064	16.110	979943.125
54 12900	37 18.12	-78 26.73	402.510	-2800.044	979935.125	29.447	16.110	979943.125
55 13000	37 18.05	-78 26.70	396.460	0.000	979935.562	29.612	16.200	979943.062
56 13100	37 18.03	-78 26.68	390.530	979935.937	29.639	16.320	979943.062
57 13200	37 18.00	-78 26.66	384.320	979936.062	29.209	16.100	979943.000
58 13300	37 17.97	-78 26.64	378.670	979936.375	29.042	16.157	979943.937
59 13400	37 17.95	-78 26.63	372.610	-1800.092	979936.375	28.716	16.010	979943.937
60 13500	37 17.92	-78 26.61	365.630	0.000	979937.167	28.300	16.054	979943.678
61 13600	37 17.86	-78 26.60	360.900	0.000	979937.167	28.160	16.094	979943.612
62 13700	37 17.83	-78 26.58	354.420	-749.312	979937.562	28.160	16.057	979943.612
63 13800	37 17.83	-78 26.56	348.950	0.000	979938.000	28.055	16.183	979943.750
64 13900	37 17.80	-78 26.54	344.410	979938.375	28.049	16.242	979943.667
65 14000	37 17.75	-78 26.51	341.850	979938.625	28.143	16.466	979943.667
66 14100	37 17.72	-78 26.50	341.320	2.004	979938.687	28.740	16.571	979943.662
67 14200	37 17.72	-78 26.48	335.610	0.000	979939.000	28.740	16.643	979943.600
68 14300	37 17.67	-78 26.46	329.900	979939.612	29.321	17.012	979943.437
69 14400	37 17.62	-78 26.44	324.360	0.000	979939.800	28.750	17.167	979943.437
70 14500	37 17.60	-78 26.41	318.710	-2404.044	979939.250	29.264	17.430	979943.375
71 14600	37 17.57	-78 26.39	313.220	0.000	979939.937	30.667	17.566	979943.312
72 14700	37 17.50	-78 26.38	309.670	-2049.504	979939.625	31.065	17.760	979943.250
73 14800	37 17.47	-78 26.34	294.040	0.000	979939.312	31.649	17.973	979943.167
74 14900	37 17.45	-78 26.33	404.440	0.000	979939.875	31.731	17.926	979943.167
75 15000	37 17.42	-78 26.32	409.870	0.000	979939.687	32.063	18.064	979943.125
76 15100	37 17.38	-78 26.31	414.040	-3104.064	979939.312	32.263	18.113	979943.125
77 15200	37 17.35	-78 26.28	419.970	0.000	979939.687	32.072	17.762	979943.062
78 15300	37 17.32	-78 26.26	423.160	979939.062	31.819	17.368	979943.000
79 15400	37 17.30	-78 26.25	428.700	979939.675	31.922	17.402	979943.000
80 15500	37 17.27	-78 26.21	427.860	979939.562	31.898	17.304	979943.937
81 15600	37 17.25	-78 26.20	429.300	0.000	979939.312	31.800	17.166	979943.678
82 15700	37 17.22	-78 26.18	420.060	979939.125	31.749	17.061	979943.678
83 15800	37 17.20	-78 26.16	425.920	979939.167	31.780	17.117	979943.612
84 15900	37 17.18	-78 26.13	429.870	1.044	979939.000	31.664	16.922	979943.612
85 16000	37 17.16	-78 26.09	427.880	979939.062	31.527	16.938	979943.750
86 16100	37 17.13	-78 26.04	425.710	0.000	979939.250	31.820	17.010	979943.750
87 16200	37 17.10	-78 26.05	423.250	979939.167	31.313	16.877	979943.667
88 16300	37 17.08	-78 26.01	420.750	979939.250	31.178	16.826	979943.667
89 16400	37 17.07	-78 26.00	416.070	979939.167	30.877	16.616	979943.626
90 16500	37 17.05	-78 26.00	415.260	979939.250	30.609	16.522	979943.626
91 16600	37 17.02	-78 25.91	412.760	979939.250	30.534	16.456	979943.562
92 16700	37 17.00	-78 25.89	409.820	1.044	979939.437	30.423	16.468	979943.662
93 16800	37 16.98	-78 25.88	404.890	0.000	979939.437	30.210	16.341	979943.600
94 16900	37 16.97	-78 25.84	404.360	0.000	979939.312	29.825	16.044	979943.600
95 17000	37 16.95	-78 25.81	401.730	979939.562	29.876	16.175	979943.600
96 17100	37 16.92	-78 25.78	396.760	1.044	979939.625	29.674	16.073	979943.437
97 17200	37 16.92	-78 25.74	394.360	0.000	979939.612	29.694	16.176	979943.437
98 17300	37 16.90	-78 25.74	393.720	0.000	979939.675	29.823	16.094	979943.375
99 17400	37 16.87	-78 25.68	391.100	-2687.189	979939.000	29.441	16.102	979943.375
100 17500	37 16.85	-78 25.64	388.560	979939.250	29.448	16.106	979943.312
101 17600	37 16.83	-78 25.61	385.070	1.000	979939.167	29.220	16.061	979943.250
102 17700	37 16.82	-78 25.56	383.520	0.000	979939.375	29.216	16.128	979943.250
103 17800	37 16.75	-78 25.54	380.660	979939.437	29.061	16.077	979943.167
104 17900	37 16.73	-78 25.51	376.260	979939.600	28.900	16.999	979943.167
105 18000	37 16.70	-78 25.48	375.910	0.000	979939.600	28.789	16.937	979943.125
106 18100	37 16.68	-78 25.46	373.170	979939.562	28.678	16.850	979943.062
107 18200	37 16.65	-78 25.43	370.500	979939.750	28.566	16.829	979943.062
108 18300	37 16.62	-78 25.39	367.880	979939.612	28.442	16.696	979943.000
109 18400	37 16.58	-78 25.38	365.360	979939.125	28.541	16.079	979943.937
110 18500	37 16.57	-78 25.36	362.810	979939.167	28.399	16.024	979943.937
111 18600	37 16.53	-78 25.33	360.400	979939.312	28.327	16.046	979943.678
112 18700	37 16.52	-78 25.31	357.740	979939.562	28.258	16.164	979943.612

STATE ROAD 637 - GRAVITY READINGS

PRINCIPAL FACTS AT GRAVITY STATIONS

STA NAME AND NUM	LATITUDE NORTH °	LONGITUDE EAST °	ELEVATION FEET	SUPP ELEV METERS	OBSERVED G MGAL	FACE AIR MGAL	BOUSSERA MGAL	THEOD G MGAL	
3 BASE	1031	37 17.60	-78 22.49	398.700	0.000	079932.678	26.172	14.640	079942.280
1	1000	37 20.08	-78 26.64	446.910	-748.312	079926.667	23.336	17.411	079947.280
2	2000	37 20.02	-78 26.61	446.060	0.000	079926.667	23.216	17.410	079947.187
3	3000	37 20.64	-78 26.60	443.800	0.000	079926.667	23.087	17.272	079947.167
4	4000	37 20.44	-78 26.60	443.000	0.000	079926.667	23.176	17.430	079947.126
5	5000	37 20.42	-78 26.64	449.820	2.004	079926.612	22.640	17.267	079947.061
6	6000	37 20.78	-78 26.63	446.870	0.000	079927.042	22.644	17.328	079947.000
7	7000	37 20.73	-78 26.61	449.460	0.000	079927.376	22.710	17.368	079946.927
8	8000	37 20.72	-78 26.60	443.240	0.000	079927.676	22.614	17.490	079946.829
9	9000	37 20.70	-78 26.46	426.210	-2404.085	079926.000	22.021	17.168	079946.876
10	10000	37 20.66	-78 26.46	424.870	0.000	079926.667	21.508	17.207	079946.812
11	11000	37 20.63	-78 26.63	413.660	-2040.104	079926.260	21.261	17.238	079946.813
12	12000	37 20.60	-78 26.41	401.660	0.000	079926.927	20.814	17.238	079946.760
13	13000	37 20.67	-78 26.39	388.700	0.000	079940.780	20.679	17.322	079946.667
14	14000	37 20.62	-78 26.26	392.720	0.000	079940.437	20.677	17.182	079946.612
15	15000	37 20.67	-78 26.26	401.230	0.000	079926.676	20.761	17.063	079946.676
16	16000	37 20.66	-78 26.22	402.280	-3104.084	079926.612	20.646	17.120	079946.612
17	17000	37 20.68	-78 26.29	403.900	0.000	079926.000	20.642	18.000	079946.612
18	18000	37 20.66	-78 26.26	408.610	0.000	079926.260	20.709	18.237	079946.612
19	19000	37 20.66	-78 26.22	421.210	0.000	079927.476	20.204	18.276	079946.612
20	20000	37 20.44	-78 26.60	411.460	0.000	079926.427	20.200	18.472	079946.612
21	21000	37 20.67	-78 26.16	402.000	0.000	079926.642	20.673	18.632	079946.676
22	22000	37 20.68	-78 26.12	398.160	0.000	079926.647	20.204	18.762	079946.612
23	23000	37 20.63	-78 26.09	391.020	0.000	079926.042	20.027	18.690	079946.612
24	24000	37 20.40	-78 26.06	389.370	1.044	079926.042	20.020	18.640	079946.760
25	25000	37 20.64	-78 26.06	384.260	0.000	079926.642	20.020	18.472	079946.612
26	26000	37 20.67	-78 26.06	402.870	0.000	079927.042	20.167	18.231	079946.667
27	27000	37 20.44	-78 26.60	402.870	0.000	079927.042	20.167	18.117	079946.667
28	28000	37 20.63	-78 27.06	407.100	0.000	079927.260	24.911	18.022	079946.667
29	29000	37 20.60	-78 27.06	399.860	0.000	079927.600	24.488	18.068	079946.626
30	30000	37 20.60	-78 27.49	394.640	0.000	079927.376	24.242	18.440	079946.626
31	31000	37 20.60	-78 27.46	392.460	0.000	079927.760	24.021	18.428	079946.626
32	32000	37 20.44	-78 27.63	398.020	0.000	079927.667	24.222	18.760	079946.662
33	33000	37 20.44	-78 27.60	395.160	0.000	079927.260	24.160	18.568	079946.662
34	34000	37 20.44	-78 27.74	392.070	0.000	079927.600	27.471	18.464	079946.662
35	35000	37 20.44	-78 27.71	390.760	0.000	079927.427	27.091	18.283	079946.662
36	36000	37 20.44	-78 27.46	386.430	0.000	079926.612	27.060	18.091	079946.662
37	37000	37 20.47	-78 27.43	384.260	1.044	079926.760	27.424	18.021	079946.662
38	38000	37 20.47	-78 27.66	387.070	0.000	079941.000	28.212	18.068	079946.662
39	39000	37 20.47	-78 27.61	322.000	0.000	079941.260	28.044	18.472	079946.662
40	40000	37 20.44	-78 27.60	322.160	-2887.000	079941.260	28.062	18.067	079946.662
41	41000	37 20.46	-78 27.46	329.020	0.000	079940.626	26.061	18.629	079946.642
42	42000	37 20.43	-78 27.43	327.760	1.044	079940.082	26.210	18.701	079946.600
43	43000	37 20.43	-78 27.29	347.210	0.000	079926.376	26.488	18.682	079946.600
44	44000	37 20.42	-78 27.28	283.230	0.000	079926.927	26.260	18.067	079946.600
45	45000	37 20.42	-78 27.24	287.160	0.000	079926.626	26.789	18.076	079946.600
46	46000	37 20.40	-78 27.24	269.930	0.000	079927.676	26.124	18.562	079946.600
47	47000	37 20.40	-78 27.22	268.220	0.000	079926.042	26.622	18.466	079946.600
48	48000	37 20.40	-78 27.29	262.040	0.000	079926.376	26.971	18.423	079946.600
49	49000	37 20.42	-78 27.26	271.120	0.000	079926.042	26.471	18.613	079946.600
50	50000	37 20.43	-78 27.22	276.120	0.000	079927.626	26.400	18.662	079946.600
51	51000	37 20.48	-78 27.20	281.000	0.000	079927.260	26.676	18.066	079946.642
52	52000	37 20.47	-78 27.16	281.960	0.000	079926.427	26.720	18.201	079946.662
53	53000	37 20.44	-78 27.12	401.260	0.000	079926.676	27.016	18.226	079946.662
54	54000	37 20.44	-78 27.09	410.140	0.000	079926.167	27.192	18.204	079946.662
55	55000	37 20.60	-78 27.06	411.760	0.000	079926.167	27.200	18.266	079946.626
56	56000	37 20.40	-78 27.03	412.270	0.000	079926.126	27.220	18.190	079946.626
57	57000	37 20.46	-78 26.94	411.410	0.000	079926.126	27.026	18.226	079946.642
58	58000	37 20.47	-78 26.94	404.220	0.000	079926.642	26.468	18.164	079946.600
59	59000	37 20.43	-78 26.96	401.260	0.000	079926.626	26.026	18.270	079946.600
60	60000	37 20.40	-78 26.96	400.680	0.000	079926.626	26.013	18.232	079946.600
61	61000	37 20.38	-78 26.06	398.160	0.000	079926.927	26.613	18.332	079946.437
62	62000	37 20.27	-78 26.06	388.110	0.000	079926.427	26.622	18.208	079946.437
63	63000	37 20.37	-78 26.01	374.260	0.000	079927.000	26.181	18.289	079946.437
64	64000	37 20.36	-78 26.08	371.620	0.000	079927.600	26.084	18.412	079946.376
65	65000	37 20.36	-78 26.06	364.850	1.044	079927.612	26.043	18.421	079946.376
66	66000	37 20.33	-78 26.43	358.250	0.000	079926.542	26.547	18.470	079946.376
67	67000	37 20.33	-78 26.41	348.750	0.000	079926.126	26.264	18.462	079946.376
68	68000	37 20.33	-78 26.76	342.710	0.000	079926.250	26.062	18.204	079946.376
69	69000	37 20.33	-78 26.74	344.640	0.161	079926.927	24.945	18.122	079946.376
70	70000	37 20.32	-78 26.73	344.190	1.044	079926.676	24.472	18.248	079946.376
71	71000	37 20.32	-78 26.70	328.220	0.000	079926.927	24.144	18.293	079946.376
72	72000	37 20.32	-78 26.68	318.320	0.000	079940.542	23.929	18.284	079946.312
73	73000	37 20.30	-78 26.66	312.000	0.000	079940.876	23.905	18.326	079946.312
74	74000	37 20.30	-78 26.43	310.160	0.000	079941.042	23.659	18.327	079946.312
75	75000	37 20.24	-78 26.66	304.790	0.000	079941.126	23.977	18.392	079946.250
76	76000	37 20.27	-78 26.60	310.210	0.000	079940.376	24.313	18.281	079946.250
77	77000	37 20.27	-78 26.46	328.490	0.000	079926.750	26.268	18.736	079946.250
78	78000	37 20.27	-78 26.43	327.460	0.000	079926.626	26.000	18.465	079946.250
79	79000	37 20.27	-78 26.39	388.430	0.000	079926.626	26.000	18.957	079946.250
80	80000	37 20.27	-78 26.36	375.650	0.000	079927.647	26.764	18.977	079946.250
81	81000	37 20.27	-78 26.33	376.620	0.000	079927.600	26.467	18.977	079946.250
82	82000	37 20.26	-78 26.29	376.490	0.000	079927.642	26.714	18.907	079946.167
83	83000	37 20.16	-78 26.24	370.670	0.000	079927.642	26.292	18.461	079946.126
84	84000	37 20.16	-78 26.23	371.630	0.000	079927.250	26.109	18.427	079946.126
85	85000	37 20.17	-78 26.20	376.900	1.044	079926.667	26.006	18.162	079946.126
86	86000	37 20.16	-78 26.14	375.760	0.000	079926.667	26.004	18.097	079946.126
87	87000	37 20.20	-78 26.11	372.820	0.000	079926.667	26.423	18.672	079946.167
88	88000	37 20.20	-78 26.08	368.260	0.000	079927.000	26.161	18.479	079946.167
89	89000	37 20.18	-78 26.01	366.160	0.000	079926.750	26.046	18.586	079946.126
90	90000	37 20.18	-78 26.00	368.270	0.000	079926.427	26.010	18.246	079946.126
91	91000	37 20.18	-78 25.98	344.460	0.000	079926.750	26.449	18.416	079946.126

STATE ROAD 637 - GRAVITY READINGS

PRINCIPAL FACTS AT GRAVITY STATIONS

STA NAME AND NUM	LATITUDE NORTH +	LONGITUDE EAST +	ELEVATION FEET	SUPP ELEV METERS	OBSERVED G MGAL	FREE AIR MGAL	BOUSSUA MGAL	THEOD G MGAL	
84	86000	27 20.20	-78 25.91	325.120	-745.312	079939.760	24.462	12.220	079946.167
84	86000	27 20.20	-78 25.86	325.210	0.000	079936.812	24.246	12.146	079946.167
87	87000	27 20.20	-78 25.83	325.000	0.000	079937.126	24.226	12.217	079946.167
84	86000	27 20.20	-78 25.60	322.650	0.000	079937.126	24.160	12.128	079946.167
84	86000	27 20.20	-78 25.74	349.430	3.004	079937.260	23.928	12.006	079946.167
100	10000	27 20.20	-78 25.70	348.110	0.000	079937.312	23.716	11.911	079946.167
101	10100	27 20.20	-78 25.64	349.300	0.000	079937.626	23.420	11.858	079946.167
102	10200	27 20.20	-78 25.61	327.700	0.000	079937.627	23.327	12.008	079946.167
102	10200	27 20.20	-78 25.56	329.940	-2404.064	079936.126	23.062	11.796	079946.167
104	10400	27 20.20	-78 25.63	323.230	0.000	079936.667	22.831	11.904	079946.167
106	10600	27 20.20	-78 25.44	317.320	-2046.664	079939.062	22.726	11.912	079946.167
106	10600	27 20.20	-78 25.45	312.900	0.000	079939.662	22.660	12.174	079946.167
107	10700	27 20.20	-78 25.39	312.900	0.000	079936.812	23.177	12.471	079946.167
108	10800	27 20.20	-78 25.34	315.600	0.000	079939.676	23.289	12.628	079946.167
109	10900	27 20.20	-78 25.32	319.460	0.000	079939.927	23.766	12.685	079946.167
110	11000	27 20.18	-78 25.25	322.000	0.000	079939.626	23.764	12.603	079946.167
111	11100	27 20.17	-78 25.23	321.160	0.000	079939.167	24.174	12.662	079946.167
112	11200	27 20.17	-78 25.20	348.350	0.000	079936.427	24.061	12.160	079946.167
113	11300	27 20.18	-78 25.14	351.770	0.000	079937.780	24.701	12.703	079946.167
114	11400	27 20.18	-78 25.11	354.010	0.000	079937.427	24.602	12.820	079946.167
115	11500	27 20.20	-78 25.06	359.320	0.000	079937.260	24.782	12.861	079946.167
116	11600	27 20.20	-78 25.01	351.700	0.000	079936.667	24.646	12.844	079946.167
117	11700	27 20.22	-78 24.98	358.940	1.048	079936.812	24.416	12.152	079946.167
118	11800	27 20.22	-78 24.98	358.940	0.000	079937.062	24.220	12.179	079946.167
119	11900	27 20.23	-78 24.92	355.810	0.000	079937.260	24.464	12.362	079946.167
120	12000	27 20.25	-78 24.89	355.600	0.000	079937.312	24.896	12.423	079946.167
121	12100	27 20.25	-78 24.85	359.370	0.000	079937.376	24.680	12.642	079946.167
122	12200	27 20.27	-78 24.84	368.220	0.000	079937.126	25.212	12.757	079946.167
123	12300	27 20.26	-78 24.81	345.910	0.000	079936.667	24.660	12.444	079946.167
124	12400	27 20.25	-78 24.76	357.950	0.000	079936.427	24.744	12.212	079946.167
125	12500	27 20.25	-78 24.73	367.070	0.000	079936.260	24.848	12.020	079946.167
126	12600	27 20.23	-78 24.70	364.460	1.044	079936.260	24.206	11.878	079946.167
127	12700	27 20.23	-78 24.66	365.000	0.000	079936.167	24.210	11.796	079946.167
128	12800	27 20.23	-78 24.61	365.370	0.000	079936.312	24.466	11.893	079946.167
129	12900	27 20.23	-78 24.58	367.240	0.000	079936.000	24.312	11.786	079946.167
130	13000	27 20.23	-78 24.52	371.760	1.048	079935.876	24.621	11.961	079946.167
131	13100	27 20.25	-78 24.48	372.600	0.000	079935.667	24.462	11.747	079946.167
132	13200	27 20.25	-78 24.45	379.950	0.000	079935.800	24.116	11.462	079946.167
133	13300	27 20.27	-78 24.41	371.410	-2287.166	079935.600	24.164	11.484	079946.167
134	13400	27 20.27	-78 24.38	372.900	0.000	079935.626	24.423	11.704	079946.167
135	13500	27 20.27	-78 24.34	375.510	1.048	079935.427	24.497	11.680	079946.167
136	13600	27 20.28	-78 24.29	374.640	0.000	079935.427	24.896	11.746	079946.167
137	13700	27 20.28	-78 24.25	379.660	0.000	079935.167	24.464	11.666	079946.167
138	13800	27 20.28	-78 24.21	389.190	0.000	079935.000	24.477	11.610	079946.167
139	13900	27 20.26	-78 24.16	385.900	0.000	079934.876	24.407	11.460	079946.167
140	14000	27 20.24	-78 24.12	364.000	0.000	079934.750	24.647	11.467	079946.167
141	14100	27 20.24	-78 24.08	384.360	0.000	079934.612	25.012	11.766	079946.167
142	14200	27 20.30	-78 24.03	394.470	0.000	079934.500	25.262	11.600	079946.167
143	14300	27 20.32	-78 24.00	402.020	0.000	079934.260	25.706	11.664	079946.167
144	14400	27 20.32	-78 23.98	407.860	0.000	079933.927	25.666	12.000	079946.167
145	14500	27 20.32	-78 23.91	407.610	0.000	079933.667	25.467	12.762	079946.167
146	14600	27 20.25	-78 23.86	405.960	0.000	079933.927	25.700	11.692	079946.167
147	14700	27 20.27	-78 23.82	407.810	0.000	079934.062	25.090	12.091	079946.167
148	14800	27 20.36	-78 23.80	410.260	0.000	079934.062	24.192	12.198	079946.167
149	14900	27 20.40	-78 23.74	413.420	0.000	079933.612	24.263	12.163	079946.167
150	15000	27 20.42	-78 23.71	414.420	0.000	079933.500	24.173	11.870	079946.167
151	15100	27 20.42	-78 23.68	420.400	0.000	079933.312	24.222	11.992	079946.167
152	15200	27 20.42	-78 23.64	422.660	0.000	079932.927	24.264	11.916	079946.167
153	15300	27 20.46	-78 23.61	422.160	0.000	079932.612	24.968	11.854	079946.167
154	15400	27 20.45	-78 23.56	424.490	0.000	079932.167	24.642	12.066	079946.167
155	15500	27 20.45	-78 23.52	427.420	0.000	079932.260	24.822	12.240	079946.167
156	15600	27 20.45	-78 23.48	440.520	0.000	079932.567	27.562	12.547	079946.167
157	15700	27 20.45	-78 23.44	449.110	0.000	079932.000	27.714	12.290	079946.167
158	15800	27 20.45	-78 23.41	455.000	1.048	079931.626	27.466	12.247	079946.167

STATE ROAD 636 - GRAVITY READINGS

PRINCIPAL FACTS AT GRAVITY STATIONS

STA NAME AND NUM	LATITUDE NORTH	LONGITUDE EAST	ELEVATION FEET	SUPP ELEV METERS	OBSERVED G MGAL	FREE AIR MGAL	BUQUER MGAL	THEOR G MGAL
1 8000	1031	37 17.80	-78 23.89	289.700	0.000	979922.876	28.173	16.660 979942.280
2 100	100	37 23.42	-78 29.04	846.200	-745.312	979922.662	34.066	16.664 979950.612
3 200	200	37 22.40	-78 29.03	667.920	0.000	979922.900	36.121	16.760 979950.812
4 300	300	37 23.24	-78 28.98	668.470	0.000	979922.312	35.076	16.647 979950.312
5 400	400	37 23.27	-78 28.96	644.910	0.000	979922.628	34.690	16.620 979950.760
6 500	500	37 23.27	-78 28.91	652.240	0.000	979922.428	34.748	16.144 979950.760
7 600	600	37 23.25	-78 28.84	642.070	0.000	979924.212	34.748	16.190 979950.760
8 700	700	37 23.23	-78 28.84	645.630	0.000	979922.912	34.497	16.201 979950.667
9 800	800	37 23.30	-78 28.76	648.600	-2404.066	979922.612	34.813	16.324 979950.667
10 1000	1000	37 23.30	-78 28.71	654.170	0.000	979922.687	34.148	16.120 979950.667
11 1100	1100	37 23.30	-78 28.68	657.630	-2049.508	979922.375	34.050	16.330 979950.667
12 1200	1200	37 23.30	-78 28.63	648.920	0.000	979924.260	34.683	16.611 979950.667
13 1300	1300	37 23.30	-78 28.58	637.760	0.000	979926.128	34.748	16.612 979950.667
14 1400	1400	37 23.30	-78 28.53	624.070	0.000	979926.427	34.748	16.641 979950.667
15 1500	1500	37 23.30	-78 28.48	622.060	0.000	979926.427	34.819	16.641 979950.667
16 16000	16000	37 23.28	-78 28.45	629.200	0.000	979928.760	34.683	16.613 979950.628
17 17000	17000	37 23.28	-78 28.39	626.140	0.000	979926.000	34.821	16.613 979950.628
18 18000	18000	37 23.27	-78 28.38	625.440	0.000	979926.312	35.004	17.116 979950.628
19 19000	19000	37 23.27	-78 28.35	623.240	0.000	979926.427	35.067	17.219 979950.628
20 20000	20000	37 23.25	-78 28.31	622.740	0.000	979926.312	34.984	17.124 979950.628
21 21000	21000	37 23.25	-78 28.29	625.120	0.000	979926.062	34.812	17.003 979950.600
22 22000	22000	37 23.18	-78 28.26	627.400	0.000	979926.760	34.678	16.884 979950.600
23 23000	23000	37 23.18	-78 28.23	616.340	1.068	979926.862	34.613	17.000 979950.600
24 24000	24000	37 23.18	-78 28.18	607.090	0.000	979926.760	34.454	17.426 979950.600
25 25000	25000	37 23.17	-78 28.14	625.440	0.000	979926.000	34.182	17.273 979950.600
26 26000	26000	37 23.15	-78 28.11	648.920	0.000	979926.062	33.993	17.160 979950.600
27 27000	27000	37 23.17	-78 28.08	490.320	0.000	979926.260	33.678	17.229 979950.437
28 28000	28000	37 23.18	-78 28.06	442.220	0.000	979928.760	33.721	17.270 979950.437
29 29000	29000	37 23.18	-78 28.00	475.420	0.000	979926.962	33.227	17.000 979950.437
30 30000	30000	37 23.15	-78 27.96	475.060	0.000	979926.927	32.872	16.461 979950.437
31 31000	31000	37 23.15	-78 27.91	472.920	0.000	979926.000	32.771	16.734 979950.437
32 32000	32000	37 23.18	-78 27.88	470.180	1.068	979926.128	32.466	16.689 979950.437
33 33000	33000	37 23.18	-78 27.83	467.620	0.000	979926.000	32.469	16.794 979950.600
34 34000	34000	37 23.17	-78 27.78	465.300	0.000	979926.274	32.662	16.666 979950.600
35 35000	35000	37 23.17	-78 27.74	463.160	0.000	979926.662	32.603	16.796 979950.600
36 36000	36000	37 23.16	-78 27.70	460.480	1.068	979926.667	32.424	16.787 979950.600
37 37000	37000	37 23.20	-78 27.64	458.840	0.000	979929.612	32.286	16.768 979950.600
38 38000	38000	37 23.20	-78 27.61	456.460	0.000	979929.937	32.126	16.488 979950.642
39 39000	39000	37 23.22	-78 27.68	455.160	-2687.199	979929.937	32.126	16.689 979950.642
40 40000	40000	37 23.22	-78 27.64	453.440	0.000	979940.000	32.172	16.703 979950.642
41 41000	41000	37 23.22	-78 27.61	451.320	1.068	979940.128	31.927	16.678 979950.642
42 42000	42000	37 23.22	-78 27.58	451.360	0.000	979940.062	32.007	16.677 979950.642
43 43000	43000	37 23.22	-78 27.48	452.300	0.000	979940.000	31.929	16.603 979950.642
44 44000	44000	37 23.22	-78 27.41	449.630	0.000	979940.187	31.762	16.619 979950.642
45 45000	45000	37 23.22	-78 27.38	448.980	0.000	979940.260	31.776	16.607 979950.642
46 46000	46000	37 23.22	-78 27.33	447.660	0.000	979940.260	31.800	16.611 979950.642
47 47000	47000	37 23.22	-78 27.28	446.600	0.000	979940.000	31.892	16.428 979950.642
48 48000	48000	37 23.22	-78 27.25	445.300	0.000	979940.812	31.820	16.329 979950.600
49 49000	49000	37 23.20	-78 27.20	445.170	0.000	979939.625	31.784	16.357 979950.600
50 50000	50000	37 23.20	-78 27.14	452.740	0.000	979939.760	31.522	16.264 979950.600
51 51000	51000	37 23.18	-78 27.13	446.760	0.000	979940.000	31.194	16.346 979950.600
52 52000	52000	37 23.17	-78 27.09	435.670	0.000	979940.647	30.842	16.172 979950.600
53 53000	53000	37 23.15	-78 27.06	431.300	0.000	979940.760	31.121	16.186 979950.437
54 54000	54000	37 23.15	-78 27.01	427.900	0.000	979940.375	31.604	16.256 979950.437
55 55000	55000	37 23.13	-78 26.98	447.020	0.000	979939.937	31.657	16.686 979950.437
56 56000	56000	37 23.12	-78 26.93	448.220	0.000	979939.937	31.078	16.011 979950.437
57 57000	57000	37 23.12	-78 26.83	444.140	0.000	979939.937	30.737	16.616 979950.376
58 58000	58000	37 23.10	-78 26.86	437.470	0.000	979940.000	29.941	16.726 979950.376
59 59000	59000	37 23.10	-78 26.81	416.620	0.000	979941.125	29.104	16.566 979950.376
60 60000	60000	37 23.10	-78 26.76	386.660	0.000	979942.187	28.718	16.660 979950.376
61 61000	61000	37 23.10	-78 26.73	388.700	0.000	979942.562	28.286	16.223 979950.376
62 62000	62000	37 23.12	-78 26.70	360.340	0.000	979942.612	27.882	15.123 979950.437
63 63000	63000	37 23.12	-78 26.66	372.620	1.068	979942.128	27.432	15.001 979950.437
64 64000	64000	37 23.12	-78 26.63	364.470	0.000	979943.562	27.218	14.746 979950.376
65 65000	65000	37 23.10	-78 26.60	365.100	0.000	979943.260	27.025	14.682 979950.376
66 66000	66000	37 23.10	-78 26.54	344.630	0.000	979943.125	27.012	14.463 979950.376
67 67000	67000	37 23.10	-78 26.51	348.240	0.181	979942.760	27.301	14.617 979950.376
68 68000	68000	37 23.10	-78 26.46	377.740	1.068	979942.128	27.344	14.166 979950.376
69 69000	69000	37 23.08	-78 26.43	386.310	0.000	979941.375	27.181	14.016 979950.376
70 70000	70000	37 23.08	-78 26.39	385.940	0.000	979941.260	27.129	14.088 979950.312
71 71000	71000	37 23.07	-78 26.34	382.320	0.000	979941.600	27.036	14.084 979950.312
72 72000	72000	37 23.07	-78 26.28	380.210	0.000	979941.625	26.782	14.010 979950.312
73 73000	73000	37 23.05	-78 26.21	372.070	0.000	979941.412	26.498	13.605 979950.312
74 74000	74000	37 23.03	-78 26.16	372.120	0.000	979941.760	26.449	13.757 979950.312
75 75000	75000	37 23.03	-78 26.14	374.670	0.000	979941.375	26.306	13.627 979950.312
76 76000	76000	37 23.02	-78 26.11	376.600	0.000	979940.937	26.265	13.297 979950.260
77 77000	77000	37 23.02	-78 26.08	381.760	0.000	979939.760	26.376	12.254 979950.260
78 78000	78000	37 23.02	-78 26.08	389.960	0.000	979940.312	26.266	13.201 979950.260
79 79000	79000	37 23.00	-78 26.01	392.660	0.000	979940.000	26.612	13.240 979950.260
80 80000	80000	37 23.00	-78 25.96	389.840	0.000	979939.187	26.542	12.648 979950.147
81 81000	81000	37 22.98	-78 25.96	405.740	0.000	979938.937	26.694	12.066 979950.147
82 82000	82000	37 22.95	-78 25.89	411.320	0.000	979938.427	26.954	12.926 979950.147
83 83000	83000	37 22.92	-78 25.84	412.960	1.068	979938.187	26.922	12.637 979950.126
84 84000	84000	37 22.90	-78 25.81	409.900	0.000	979938.375	26.717	12.634 979950.126
85 85000	85000	37 22.87	-78 25.78	403.220	0.000	979938.312	26.281	12.492 979950.062
86 86000	86000	37 22.83	-78 25.74	397.200	0.000	979938.675	26.228	12.474 979950.000
87 87000	87000	37 22.82	-78 25.70	386.400	0.000	979938.437	26.123	12.647 979950.000
88 88000	88000	37 22.80	-78 25.68	384.930	0.000	979939.427	25.724	12.691 979949.937
89 89000	89000	37 22.78	-78 25.66	378.620	0.000	979940.062	25.448	12.633 979949.937
90 90000	90000	37 22.77	-78 25.64	370.810	0.000	979940.962	25.000	12.603 979949.678
91 91000	91000	37 22.73	-78 25.61	372.510	0.000	979939.675	25.063	12.237 979949.678
92 92000	92000	37 22.69	-78 25.60	369.960	0.000	979939.312	24.930	12.492 979949.678
93 93000	93000	37 22.68	-78 25.56	391.940	0.000	979938.687	25.771	12.404 979949.750
94 94000	94000	37 22.65	-78 25.54	386.120	0.000	979938.187	25.690	12.311 979949.750
95 95000	95000	37 22.63	-78 25.51	386.760	0.000	979938.062	25.626	12.226 979949.667
96 96000	96000	37 22.62	-78 25.46	387.600	0.000	979938.125	25.626	12.278 979949.667
97 97000	97000	37 22.62	-78 25.46	389.110	0.000	979937.760	25.786	12.146 979949.628

STATE ROAD 636 - GRAVITY READINGS

PRINCIPAL FACTS AT GRAVITY STATIONS

STA NAME AND NUM	LATITUDE NORTH °	LONGITUDE EAST °	ELEVATION FEET	SUPP ELEV METERS	OBSERVED G MGAL	FREE AIR MGAL	BOUGUER MGAL	THEOR G MGAL	
100	10000	27 22.87	-74 28.41	402.200	0.000	070027.042	26.780	12.060	070040.624
101	10100	27 22.88	-74 28.38	407.260	0.000	070027.167	26.823	12.042	070040.662
102	10200	27 22.88	-74 28.36	407.040	0.000	070027.167	26.884	11.978	070040.642
103	10300	27 22.83	-74 28.33	407.050	0.000	070027.042	26.776	11.882	070040.657
104	10400	27 22.82	-74 28.29	408.620	0.000	070026.937	26.842	11.905	070040.662
105	10500	27 22.82	-74 28.28	411.900	0.000	070026.826	26.847	11.764	070040.662
106	10600	27 22.80	-74 28.25	416.470	0.000	070026.126	26.442	11.624	070040.600
107	10700	27 22.80	-74 28.20	416.000	0.000	070026.070	26.493	11.436	070040.600
108	10800	27 22.60	-74 28.16	416.900	0.000	070026.126	26.726	11.837	070040.600
109	10900	27 22.44	-74 28.09	414.670	0.000	070026.126	26.622	11.642	070040.600
110	11000	27 22.44	-74 28.08	412.220	1.048	070026.187	26.672	11.476	070040.600
111	11100	27 22.47	-74 28.98	414.810	0.000	070026.126	26.670	11.523	070040.427
112	11200	27 22.46	-74 28.96	416.900	0.000	070026.937	26.424	11.441	070040.427
113	11300	27 22.45	-74 28.91	416.900	0.000	070026.624	26.560	11.291	070040.427
114	11400	27 22.42	-74 28.88	420.450	0.000	070026.427	26.842	11.202	070040.427
115	11500	27 22.42	-74 28.84	421.640	0.000	070026.187	26.465	11.078	070040.427
116	11600	27 22.42	-74 28.81	422.620	0.000	070026.000	26.406	10.980	070040.378
117	11700	27 22.42	-74 28.78	426.450	0.000	070024.687	26.222	10.811	070040.378
118	11800	27 22.40	-74 28.74	426.880	0.000	070024.600	26.250	10.701	070040.378
119	11900	27 22.40	-74 28.68	426.900	0.000	070024.250	26.242	10.722	070040.378
120	12000	27 22.40	-74 28.64	421.160	0.000	070024.187	26.424	10.717	070040.378
121	12100	27 22.40	-74 28.60	422.700	0.000	070022.937	26.207	10.601	070040.378
122	12200	27 22.38	-74 28.56	426.700	0.000	070022.760	26.274	10.814	070040.378
123	12300	27 22.38	-74 28.51	426.000	0.000	070022.862	26.446	10.906	070040.378
124	12400	27 22.38	-74 28.46	442.410	0.000	070022.312	26.600	10.811	070040.378
125	12500	27 22.37	-74 28.38	449.840	0.000	070022.062	26.661	10.476	070040.312
126	12600	27 22.36	-74 28.34	449.260	0.000	070022.126	26.767	10.262	070040.312
127	12700	27 22.36	-74 28.31	446.220	0.000	070022.042	26.466	10.467	070040.312
128	12800	27 22.35	-74 28.28	446.970	0.000	070022.250	26.426	10.680	070040.350
129	12900	27 22.32	-74 28.26	436.760	0.000	070022.626	26.446	10.662	070040.280
130	13000	27 22.30	-74 28.21	430.810	0.000	070022.812	26.297	10.601	070040.260
131	13100	27 22.28	-74 28.18	426.900	1.048	070024.126	26.448	10.761	070040.167
132	13200	27 22.28	-74 28.11	426.020	0.000	070024.312	26.202	10.722	070040.126
133	13300	27 22.28	-74 28.11	426.020	0.000	070024.187	26.184	10.448	070040.126
134	13400	27 22.23	-74 28.08	426.670	0.000	070024.126	26.002	10.404	070040.126
135	13500	27 22.23	-74 28.01	426.220	0.000	070024.126	26.066	10.422	070040.126
136	13600	27 22.23	-74 28.01	426.220	0.000	070024.427	26.066	10.624	070040.126
137	13700	27 22.23	-74 28.96	416.200	0.000	070024.642	26.926	10.607	070040.126
138	13800	27 22.23	-74 28.93	416.900	0.000	070024.076	26.884	10.697	070040.126
139	13900	27 22.23	-74 28.88	412.990	0.000	070026.126	26.628	10.742	070040.126
140	14000	27 22.22	-74 28.84	410.370	0.000	070026.250	26.668	10.701	070040.126
141	14100	27 22.23	-74 28.81	408.640	0.000	070026.427	26.786	10.811	070040.126
142	14200	27 22.23	-74 28.76	407.020	0.000	070026.427	26.417	10.726	070040.126
143	14300	27 22.23	-74 28.75	406.450	0.000	070026.427	26.474	10.622	070040.126
144	14400	27 22.23	-74 28.68	406.620	0.000	070026.862	26.678	10.810	070040.126
145	14500	27 22.23	-74 28.64	406.440	0.000	070026.427	26.718	10.767	070040.126
146	14600	27 22.22	-74 28.60	411.120	0.000	070026.250	26.648	10.822	070040.126
147	14700	27 22.20	-74 28.56	412.640	0.000	070026.126	26.948	10.842	070040.062
148	14800	27 22.18	-74 28.51	416.120	0.000	070026.000	26.067	10.664	070040.062
149	14900	27 22.17	-74 28.48	416.210	0.000	070026.626	26.816	10.662	070040.000

STATE ROAD 634 - GRAVITY READINGS

PRINCIPAL FACTS AT GRAVITY STATIONS

STA NAME AND NUM	LATITUDE NORTH *	LONGITUDE EAST *	ELEVATION FEET	SUPP ELEV METERS	OBSERVED S MEAL	FREE AIR MEAL	BOUQUER MEAL	THEOD S MEAL
2 BASE	1021	37 17.60	-78 23.49	399.700	0.000	979942.476	28.123	14.640 979942.260
1	1000	37 24.42	-78 23.61	473.230	-749.312	979944.125	33.025	17.785 979954.447
3	3000	37 28.42	-78 23.60	469.970	0.000	979944.167	32.670	17.640 979954.467
3	3000	37 28.42	-78 23.64	466.560	0.000	979944.167	32.412	17.600 979954.467
4	4000	37 28.40	-78 23.63	466.170	0.000	979947.937	32.009	17.145 979954.426
5	5000	37 28.77	-78 23.43	463.940	0.000	979947.462	32.406	18.750 979954.326
6	6000	37 28.78	-78 23.44	463.440	0.000	979947.467	32.466	18.661 979954.562
7	7000	37 28.70	-78 23.39	462.710	0.000	979944.167	32.266	18.466 979954.600
8	8000	37 28.67	-78 23.34	447.990	-2404.044	979944.625	32.302	17.023 979954.437
9	10000	37 28.62	-78 23.34	444.980	0.000	979944.676	32.318	17.141 979954.437
10	11000	37 28.60	-78 23.34	446.060	-2049.504	979944.760	32.262	17.093 979954.376
11	12000	37 28.67	-78 23.34	446.630	0.000	979944.600	32.279	17.091 979954.312
12	13000	37 28.62	-78 23.34	449.670	0.000	979944.312	32.225	16.992 979954.260
13	14000	37 28.60	-78 23.32	442.640	0.000	979944.126	32.184	17.045 979954.167
14	15000	37 28.48	-78 23.23	437.600	0.000	979944.126	32.219	17.223 979954.167
15	16000	37 28.45	-78 23.21	436.300	-2104.044	979944.260	32.176	17.291 979954.126
16	17000	37 28.42	-78 23.20	436.700	0.000	979944.312	32.177	17.316 979954.126
17	18000	37 28.36	-78 23.20	437.460	0.000	979944.167	32.600	17.339 979954.062
18	19000	37 28.35	-78 23.20	442.260	0.000	979944.625	32.225	17.140 979954.000
19	20000	37 28.32	-78 23.26	440.990	0.000	979944.760	32.247	17.226 979957.476
20	21000	37 28.28	-78 23.26	438.095	0.000	979944.760	31.904	17.035 979957.476
21	22000	37 28.27	-78 23.23	437.600	0.000	979944.760	31.893	17.042 979957.412
22	23000	37 28.22	-78 23.21	434.630	0.000	979944.760	31.664	17.062 979957.412
23	24000	37 28.22	-78 23.16	434.330	1.044	979944.612	31.607	16.910 979957.412
24	25000	37 28.20	-78 23.14	436.530	0.000	979944.600	31.404	16.688 979957.412
25	26000	37 28.20	-78 23.11	434.110	0.000	979944.427	31.028	16.502 979957.760
26	27000	37 28.18	-78 23.06	425.640	0.000	979944.760	30.426	16.252 979957.760
27	28000	37 28.16	-78 23.02	421.440	0.000	979944.676	30.426	16.177 979957.760
28	29000	37 28.17	-78 23.00	418.110	0.000	979944.260	30.845	16.266 979957.760
29	30000	37 28.17	-78 23.00	415.000	0.000	979944.260	30.430	16.216 979957.667
30	31000	37 28.16	-78 23.01	413.740	1.044	979944.260	30.264	16.230 979957.667
31	32000	37 28.12	-78 23.00	413.640	0.000	979944.125	30.258	16.249 979957.626
32	33000	37 28.06	-78 23.00	410.730	0.000	979944.312	30.440	16.299 979957.662
33	34000	37 28.03	-78 23.01	412.490	0.000	979944.167	30.527	16.440 979957.437
34	35000	37 28.02	-78 23.05	416.010	1.044	979944.000	30.274	16.405 979957.376
35	36000	37 27.97	-78 23.06	411.230	0.000	979944.427	30.242	16.196 979957.312
36	37000	37 27.97	-78 23.00	407.000	-2527.192	979944.427	30.276	16.237 979957.667
37	38000	37 27.92	-78 23.01	407.000	0.000	979944.600	30.262	16.230 979957.376
38	39000	37 27.92	-78 23.03	408.470	1.044	979944.260	30.163	16.196 979957.312
39	40000	37 27.87	-78 23.03	410.930	0.000	979944.937	29.811	16.027 979957.260
40	41000	37 27.86	-78 23.01	407.070	0.000	979944.612	29.722	16.758 979957.167
41	42000	37 27.82	-78 23.00	397.290	0.000	979944.125	29.120	16.644 979957.126
42	43000	37 27.78	-78 23.08	382.220	0.000	979944.125	28.916	16.466 979957.126
43	44000	37 27.78	-78 23.05	385.430	0.000	979944.125	28.671	16.347 979957.062
44	45000	37 27.72	-78 23.05	393.760	0.000	979944.000	28.671	16.098 979957.000
45	46000	37 27.70	-78 23.01	397.700	0.000	979944.662	28.321	14.723 979956.876
46	47000	37 27.68	-78 22.99	399.520	0.000	979944.125	28.264	14.466 979956.812
47	48000	37 27.65	-78 22.88	398.190	0.000	979944.167	28.965	14.456 979956.612
48	49000	37 27.60	-78 22.81	396.770	0.000	979947.937	27.970	14.517 979956.750
49	50000	37 27.67	-78 22.60	397.010	0.000	979947.612	27.592	14.366 979956.667
50	51000	37 27.62	-78 22.74	396.170	0.000	979947.600	27.410	14.267 979956.667
51	52000	37 27.62	-78 22.70	396.460	-749.312	979947.662	27.266	14.219 979956.667
52	53000	37 27.50	-78 22.70	394.260	0.000	979947.662	26.664	13.890 979956.626
53	54000	37 27.48	-78 22.62	391.760	0.000	979947.760	26.664	13.959 979956.626
54	55000	37 27.47	-78 22.49	387.730	0.000	979947.612	26.179	13.744 979956.800
55	56000	37 27.45	-78 22.64	385.630	2.064	979947.612	26.912	13.454 979956.000
56	57000	37 27.43	-78 22.64	382.670	0.000	979947.937	26.576	13.607 979956.427
57	58000	37 27.43	-78 22.63	379.660	0.000	979947.937	26.330	13.392 979956.376
58	59000	37 27.40	-78 22.61	376.330	0.000	979947.937	26.728	13.284 979956.376
59	60000	37 27.37	-78 22.60	372.550	-2404.044	979944.167	26.074	12.922 979956.312
60	61000	37 27.33	-78 22.48	366.890	0.000	979944.125	25.984	12.864 979956.312
61	62000	37 27.32	-78 22.46	366.440	-2049.504	979944.260	25.974	12.864 979956.312
62	63000	37 27.28	-78 22.45	363.740	0.000	979944.427	25.320	12.647 979956.260
63	64000	37 27.27	-78 22.41	360.760	0.000	979944.376	25.179	12.296 979956.167
64	65000	37 27.27	-78 22.38	367.230	0.000	979944.376	24.695	12.240 979956.126
65	66000	37 27.25	-78 22.38	367.230	0.000	979944.376	24.466	12.144 979956.062
66	67000	37 27.22	-78 22.34	364.060	-2104.044	979944.376	24.339	12.126 979956.062
67	68000	37 27.20	-78 22.31	362.410	0.000	979944.427	24.203	12.140 979956.000
68	69000	37 27.18	-78 22.29	362.330	0.000	979944.260	24.201	12.246 979956.937
69	70000	37 27.18	-78 22.28	363.870	0.000	979944.000	24.022	12.126 979956.937
70	71000	37 27.17	-78 22.26	357.460	0.000	979947.600	23.860	12.063 979956.876
71	72000	37 27.13	-78 22.23	350.350	0.000	979947.600	23.781	11.977 979956.876
72	73000	37 27.12	-78 22.20	363.150	0.000	979947.627	23.685	11.961 979956.812
73	74000	37 27.08	-78 22.18	364.610	0.000	979946.625	23.675	12.126 979956.750
74	75000	37 27.05	-78 22.15	364.000	1.044	979946.662	23.634	12.118 979956.750
75	76000	37 27.03	-78 22.13	361.270	0.000	979946.662	23.642	12.079 979956.626
76	77000	37 27.00	-78 22.11	357.800	0.000	979944.760	23.637	12.218 979956.626
77	78000	37 26.97	-78 22.09	353.470	0.000	979944.937	23.461	11.861 979956.562
78	79000	37 26.95	-78 22.06	350.760	0.000	979947.125	23.479	12.407 979956.437
79	80000	37 26.93	-78 22.05	348.820	0.000	979947.125	23.240	12.391 979956.376
80	81000	37 26.90	-78 22.01	347.950	0.000	979947.062	23.076	12.447 979956.312
81	82000	37 26.88	-78 21.99	346.610	0.000	979947.062	22.876	12.447 979956.312
82	83000	37 26.85	-78 21.98	348.640	1.044	979947.260	22.834	12.118 979956.750
83	84000	37 26.82	-78 21.95	344.420	0.000	979947.260	22.642	12.126 979956.750
84	85000	37 26.80	-78 21.93	343.600	0.000	979947.260	22.736	12.079 979956.626
85	86000	37 26.77	-78 21.91	343.150	0.000	979947.260	22.461	11.861 979956.562
86	87000	37 26.73	-78 21.89	341.600	1.044	979947.260	22.479	12.407 979956.437
87	88000	37 26.70	-78 21.88	341.210	0.000	979947.062	22.479	12.391 979956.376
88	89000	37 26.65	-78 21.85	339.600	0.000	979947.062	22.320	12.447 979956.312
89	90000	37 26.62	-78 21.84	338.830	-2527.192	979947.662	22.320	12.391 979956.437
90	91000	37 26.60	-78 21.84	338.660	0.000	979947.676	22.340	12.391 979956.376
91	92000	37 26.67	-78 21.85	324.630	0.000	979946.376	22.076	12.447 979956.312
92	93000	37 26.65	-78 21.83	318.060	0.000	979946.667	22.076	12.447 979956.312
93	94000	37 26.62	-78 21.82	311.630	0.000	979944.125	22.076	12.447 979956.312

STATE ROAD 634 - GRAVITY READINGS

PRINCIPAL FACTS AT GRAVITY STATIONS

STA NAME AND NUM	LATITUDE NORTH °	LONGITUDE EAST °	ELEVATION FEET	SUPP ELEV METERS	OBSERVED & FREE AIR MGAL	BOUSSER MGAL	THEOD G MGAL
95	37 26.48	-78 21.60	204.750	0.000	979949.600	22.904	12.810
96	37 26.47	-78 21.76	207.260	0.000	979949.937	22.628	12.489
97	37 26.46	-78 21.73	200.970	0.000	979950.562	22.689	12.765
98	37 26.42	-78 21.70	208.210	0.000	979950.687	22.896	12.766
99	37 26.40	-78 21.66	207.270	0.000	979950.600	22.244	12.845
100	37 26.38	-78 21.64	208.000	0.000	979950.687	22.628	12.804
101	37 26.37	-78 21.61	209.210	0.000	979950.662	22.641	12.772
102	37 26.33	-78 21.68	209.380	0.000	979950.378	23.112	12.827
103	37 26.32	-78 21.64	209.950	0.000	979949.600	22.491	12.864
104	37 26.30	-78 21.61	221.570	0.000	979948.600	23.684	12.731
105	37 26.28	-78 21.61	225.200	0.000	979947.672	24.165	12.817
106	37 26.28	-78 21.48	246.800	0.000	979947.187	24.631	12.903
107	37 26.25	-78 21.40	261.590	0.000	979946.062	25.129	12.786
108	37 26.23	-78 21.34	276.480	0.000	979945.187	25.688	12.847
109	37 26.23	-78 21.31	284.900	0.000	979944.562	26.022	12.894
110	37 26.20	-78 21.28	288.760	0.000	979944.437	26.130	12.870
111	37 26.18	-78 21.26	287.370	0.000	979944.128	26.704	12.852
112	37 26.17	-78 21.23	285.990	0.000	979944.128	26.677	12.812
113	37 26.13	-78 21.20	284.990	1.049	979944.000	26.426	12.311
114	37 26.12	-78 21.18	288.480	0.000	979943.937	26.604	12.274
115	37 26.08	-78 21.16	291.440	0.000	979943.437	26.842	12.162
116	37 26.05	-78 21.14	297.290	0.000	979943.250	26.939	12.265
117	37 26.02	-78 21.13	403.850	0.191	979942.937	26.122	12.819
118	37 26.00	-78 21.13	410.490	0.000	979942.378	26.427	12.426
119	37 25.97	-78 21.11	416.510	0.000	979941.812	26.487	12.281
120	37 25.93	-78 21.09	421.140	0.000	979941.687	26.781	12.417
121	37 25.90	-78 21.09	423.640	0.000	979941.562	26.927	12.464
122	37 25.87	-78 21.09	427.190	0.000	979941.187	27.000	12.430
123	37 25.83	-78 21.06	429.180	0.000	979941.312	27.310	12.672
124	37 25.82	-78 21.06	431.550	0.000	979941.000	27.269	12.560
125	37 25.78	-78 21.06	433.800	0.000	979941.000	27.494	12.702
126	37 25.75	-78 21.09	434.970	0.000	979940.687	27.347	12.812
127	37 25.72	-78 21.11	437.160	0.000	979940.687	27.601	12.691
128	37 25.70	-78 21.13	439.890	0.000	979940.312	27.630	12.623
129	37 25.67	-78 21.13	442.200	0.000	979940.000	27.809	12.427
130	37 25.63	-78 21.12	443.370	0.000	979939.628	27.285	12.121
131	37 25.67	-78 21.09	444.710	0.000	979939.878	27.774	12.606
132	37 25.65	-78 21.06	446.790	1.068	979938.678	27.884	12.442
133	37 25.63	-78 21.03	448.740	0.000	979938.687	27.814	12.676
134	37 25.62	-78 21.00	447.690	0.000	979939.378	27.644	12.268
135	37 25.60	-78 20.96	448.690	0.000	979939.312	27.624	12.232
136	37 25.60	-78 20.93	452.020	0.000	979939.187	27.812	12.264
137	37 25.60	-78 20.89	456.600	0.000	979938.600	27.887	11.984
138	37 25.47	-78 20.86	459.430	0.000	979938.600	27.873	12.203
139	37 25.35	-78 20.86	464.840	0.000	979938.812	27.988	12.445

U.S. HIGHWAY 60 - GRAVITY READINGS

PRINCIPAL FACTS AT GRAVITY STATIONS

STA NAME AND NUM	LATITUDE NORTH °	LONGITUDE EAST °	ELEVATION FEET	SUPP ELEV METERS	OBSERVED G MGAL	FARE AIR MGAL	BOUSSER MEAL	THEOD G MEAL
2 BASE 1031	37 17.50	-78 23.59	399.700	0.000	979932.875	26.173	14.540	979942.250
4 21100	37 24.97	-78 19.01	290.310	-749.312	979954.312	22.720	12.319	979954.375
5 20900	37 24.94	-78 19.05	291.550	0.000	979954.687	23.144	13.230	979954.937
4 20700	37 24.94	-78 19.09	291.700	0.000	979954.687	23.179	13.230	979954.937
3 20500	37 24.00	-78 19.13	289.540	0.000	979954.675	23.177	13.302	979954.937
2 20300	37 29.02	-78 19.16	284.240	0.004	979955.147	23.023	13.304	979954.937
1 20100	37 29.03	-78 19.21	278.720	0.000	979955.600	22.744	13.238	979959.000
1 11900	37 29.05	-78 19.30	275.100	0.000	979954.062	21.255	11.752	979959.000
2 10700	37 29.07	-78 19.34	278.100	0.000	979954.437	22.644	12.146	979959.042
3 19500	37 29.04	-78 19.34	279.720	-2404.046	979955.250	22.470	12.930	979959.042
4 19300	37 29.10	-78 19.43	280.050	0.000	979955.062	22.231	12.700	979959.062
5 19200	37 29.10	-78 19.48	280.800	-2049.808	979955.000	22.231	12.704	979959.062
6 18900	37 29.12	-78 19.51	278.410	0.000	979954.812	21.873	12.277	979959.125
7 18700	37 29.12	-78 19.55	281.950	0.000	979954.612	22.309	12.692	979959.125
8 18500	37 29.13	-78 19.50	282.410	0.000	979954.625	22.041	12.442	979959.125
9 18300	37 29.15	-78 19.54	284.440	0.000	979954.612	22.264	12.641	979959.187
10 18100	37 29.15	-78 19.68	285.720	-2104.044	979954.682	22.200	12.846	979959.187
11 17900	37 29.17	-78 19.73	287.210	0.000	979954.625	22.432	12.636	979959.187
12 17700	37 29.18	-78 19.76	288.320	0.000	979954.375	22.209	12.442	979959.187
13 17500	37 29.20	-78 19.81	289.890	0.000	979954.250	22.244	12.341	979959.250
14 17300	37 29.20	-78 19.84	289.890	0.000	979954.000	22.342	12.364	979959.250
15 17100	37 29.22	-78 19.89	288.600	0.000	979953.937	22.756	12.671	979959.250
16 16900	37 29.23	-78 19.93	304.620	0.000	979953.862	22.930	12.830	979959.312
17 16700	37 29.23	-78 19.98	306.840	1.048	979953.250	23.027	12.494	979959.312
18 16500	37 29.25	-78 20.01	312.010	0.000	979953.000	23.042	12.400	979959.312
19 16300	37 29.27	-78 20.06	312.090	0.000	979952.875	23.120	12.442	979959.312
20 16100	37 29.27	-78 20.09	312.070	0.000	979952.750	22.889	12.244	979959.312
21 15900	37 29.28	-78 20.13	309.450	0.000	979952.625	22.806	11.962	979959.375
22 15700	37 29.30	-78 20.18	305.740	0.000	979952.147	22.574	12.146	979959.375
23 15500	37 29.30	-78 20.21	301.840	0.000	979952.437	22.449	12.156	979959.375
24 15300	37 29.32	-78 20.26	295.920	0.000	979952.625	22.082	11.990	979959.375
25 15100	37 29.33	-78 20.30	285.720	0.000	979954.125	21.664	11.888	979959.437
26 14900	37 29.33	-78 20.34	279.110	1.048	979954.612	21.619	12.099	979959.437
27 14700	37 29.35	-78 20.40	275.940	0.000	979955.250	21.724	12.212	979959.437
28 14500	37 29.37	-78 20.43	275.940	0.000	979955.375	21.650	12.439	979959.500
29 14300	37 29.37	-78 20.46	275.240	0.000	979955.662	22.052	12.631	979959.600
30 14100	37 29.38	-78 20.51	283.230	1.048	979955.687	22.826	12.178	979959.600
31 13900	37 29.38	-78 20.54	294.060	0.000	979956.250	23.421	13.291	979959.600
32 13700	37 29.40	-78 20.60	305.710	0.000	979954.647	23.009	13.443	979959.600
33 13500	37 29.42	-78 20.64	315.150	-2567.153	979954.147	24.277	13.528	979959.662
34 13300	37 29.43	-78 20.68	322.500	0.000	979953.687	24.478	13.479	979959.662
35 13100	37 29.43	-78 20.73	328.610	1.048	979953.312	24.674	13.466	979959.662
36 12900	37 29.45	-78 20.76	331.690	0.000	979953.042	24.688	13.242	979959.625
37 12700	37 29.47	-78 20.80	331.710	0.000	979952.750	24.266	13.050	979959.625
38 12500	37 29.47	-78 20.85	331.710	0.000	979952.875	24.677	13.153	979959.625
39 12300	37 29.48	-78 20.89	328.620	0.000	979953.062	24.962	13.544	979959.625
40 12100	37 29.50	-78 20.93	342.840	0.000	979953.000	25.685	13.692	979959.687
42 11700	37 29.52	-78 21.01	346.410	0.000	979952.312	25.376	13.493	979959.687
43 11500	37 29.53	-78 21.06	347.310	0.000	979952.275	25.325	13.480	979959.687
44 11300	37 29.53	-78 21.09	344.520	0.000	979952.662	25.249	13.498	979959.687
45 11100	37 29.55	-78 21.14	343.400	0.000	979952.675	25.485	13.744	979959.750
46 10900	37 29.57	-78 21.18	342.090	0.000	979953.125	25.655	13.487	979959.750
47 10700	37 29.58	-78 21.23	340.620	0.000	979953.375	25.649	14.031	979959.812
48 10500	37 29.58	-78 21.26	339.300	0.000	979953.647	25.624	14.262	979959.812

STATE ROAD 622 - GRAVITY READINGS

PRINCIPAL FACTS AT GRAVITY STATIONS

STA NAME AND NUM	LATITUDE NORTH °	LONGITUDE EAST °	ELEVATION FEET	SUPP ELEV METERS	OBSERVED G MGAL	FREE AIR MGAL	BOUGUER MGAL	THEOR G MGAL	
3 BASE	1021	37 17.50	-78 23.49	399.700	0.000	979932.875	24.133	14.540	979942.250
1	1000	37 32.44	-78 17.43	345.030	-748.312	979964.525	31.323	19.555	979965.750
2	3000	37 32.45	-78 17.43	345.040	0.000	979965.062	31.000	19.584	979965.627
3	3000	37 32.42	-78 17.44	329.900	*****	979965.437	30.403	19.552	979965.525
4	4000	37 32.47	-78 17.44	321.490	*****	979965.500	30.205	19.226	979965.562
5	5000	37 32.53	-78 17.44	315.430	2.004	979965.750	29.944	18.168	979965.500
6	6000	37 32.52	-78 17.43	308.450	0.000	979966.312	28.441	19.307	979965.500
7	7000	37 32.60	-78 17.40	301.250	*****	979966.525	29.497	19.222	979965.500
8	8000	37 32.47	-78 17.54	294.890	0.000	979966.750	29.073	19.014	979966.427
9	9000	37 32.45	-78 17.53	287.370	-2404.655	979966.937	28.554	18.751	979966.378
10	10000	37 32.43	-78 17.51	280.910	0.000	979967.250	28.143	18.433	979966.375
11	11000	37 32.40	-78 17.48	274.220	-3045.584	979967.167	27.629	18.408	979965.312
12	12000	37 32.37	-78 17.45	275.880	0.000	979967.437	28.044	18.677	979965.312
13	13000	37 32.35	-78 17.45	275.160	0.000	979967.437	28.041	18.656	979965.250
14	14000	37 32.32	-78 17.43	271.640	*****	979967.552	27.862	18.618	979965.167
15	15000	37 32.28	-78 17.40	266.290	-3104.084	979967.662	27.462	18.380	979965.167
16	16000	37 32.27	-78 17.38	257.060	0.000	979968.125	27.157	18.300	979965.125
17	17000	37 32.25	-78 17.34	250.590	*****	979968.125	26.879	18.029	979965.125
18	18000	37 32.23	-78 17.31	247.240	*****	979967.562	25.543	17.184	979965.042
19	19000	37 32.22	-78 17.28	244.750	0.000	979967.875	25.617	17.350	979965.042
20	20000	37 32.20	-78 17.20	242.370	0.000	979967.000	24.904	18.508	979965.000
21	21000	37 32.18	-78 17.25	240.600	*****	979968.612	25.219	18.706	979965.042
22	22000	37 32.16	-78 17.16	235.970	1.048	979968.250	25.474	18.580	979965.000
23	23000	37 32.17	-78 17.09	241.470	*****	979968.612	25.619	18.474	979964.937
24	24000	37 32.15	-78 17.05	240.060	0.000	979968.375	25.774	18.285	979964.937
25	25000	37 32.15	-78 17.01	235.880	*****	979964.812	25.951	18.268	979964.937
26	26000	37 32.15	-78 16.96	245.140	*****	979964.125	26.373	18.255	979964.937
27	27000	37 32.18	-78 16.93	295.390	*****	979963.562	26.240	18.943	979964.937
28	28000	37 32.13	-78 16.84	301.910	*****	979962.812	26.469	18.099	979964.937
29	29000	37 32.12	-78 16.85	316.370	*****	979962.062	27.399	18.424	979964.875
30	30000	37 32.10	-78 16.80	321.740	1.048	979962.000	27.145	18.155	979964.875
31	31000	37 32.10	-78 16.80	321.740	0.000	979961.812	27.023	18.104	979964.875
32	32000	37 32.07	-78 16.73	320.020	0.000	979961.750	27.067	18.055	979964.812
33	33000	37 32.05	-78 16.70	325.340	*****	979961.167	27.229	18.005	979964.812
34	34000	37 32.02	-78 16.65	329.090	1.048	979961.062	27.307	18.016	979964.750
35	35000	37 32.02	-78 16.64	324.130	0.000	979960.375	27.579	18.162	979964.750
36	36000	37 32.02	-78 16.64	324.130	0.000	979960.662	27.475	18.260	979964.627
37	37000	37 32.00	-78 16.60	340.550	*****	979960.125	27.292	18.555	979964.625
38	38000	37 32.00	-78 16.53	344.140	0.000	979959.562	27.261	18.453	979964.625
39	39000	37 32.02	-78 16.48	344.510	0.000	979959.312	27.213	18.270	979964.525
40	40000	37 32.02	-78 16.48	350.170	*****	979958.875	27.150	18.585	979964.562
41	41000	37 32.00	-78 16.40	350.310	*****	979958.000	27.357	18.954	979964.562
42	42000	37 32.00	-78 16.40	352.530	0.000	979957.667	27.320	18.854	979964.562
43	43000	37 32.07	-78 16.34	352.530	*****	979957.500	27.155	18.732	979964.562
44	44000	37 32.07	-78 16.31	355.510	*****	979957.437	27.025	18.665	979964.562
45	45000	37 32.07	-78 16.26	344.320	*****	979957.500	26.938	18.463	979964.437
46	46000	37 32.05	-78 16.23	341.810	*****	979957.000	26.815	18.344	979964.437
47	47000	37 32.05	-78 16.21	345.770	*****	979956.812	26.675	18.213	979964.375
48	48000	37 32.00	-78 16.20	345.650	*****	979956.125	26.450	18.915	979964.312
49	49000	37 32.00	-78 16.16	345.390	*****	979956.667	26.723	18.100	979964.312
50	50000	37 32.00	-78 16.16	345.390	*****	979956.125	26.450	18.915	979964.312
51	51000	37 32.02	-78 16.16	358.570	*****	979956.125	26.723	18.100	979964.312
52	52000	37 32.00	-78 16.14	370.410	*****	979956.167	26.723	18.100	979964.312

APPENDIX III

LISTING OF GEOLOGIC DATA

Below are a listing of structural readings taken during the course of this investigation. The legend that follows is a reference to where the readings were taken.

LEGEND

Location

629: B, C, D, E: The location of these readings are from State Road 629 in the Gold Hill quadrangle, at Winston Lake. The readings are from SE to NW away from Winston Lake along the blue line valley leading toward State Road 629.

R.R.: N, S, 2N, 3N, 3S: The location of these readings are from the Railroad Cut approximately 1/2 mile west of the Farmville Train Station. The train station is located off business 460 in Farmville, Virginia (Farmville Triangle).

R.C: 1, 2, 3, 5: The location of these readings are from Rock Creek, off of U.S. Highway 60. Readings 1, 2, and 3 are from the creek south of U.S. 60, while the fifth location was along the creek north of U.S. 60. Rock Creek is located in the northern portion of the Hillcrest Quadrangle, at the U.S.

Highway 60 Bridge.

US60 : The location of these readings are from a blue line creek that parallels U.S. Highway 60 at the Buckingham and Cumberland County crossing. The creek is located north of U.S. Highway 60 in the Hillcrest quadrangle.

634 : The location of these readings are from a blue line creek south of State Road 634 in the western portion of the Hillcrest quadrangle. The stream starts at the base of Bridge 289 along State Road 634 approximately 2 kilometers west of Browns Store on State Road 45.

636 : 1, 100, 17DC, PC: The location of these readings are from creeks that run along State Road 636. Locations 1, 100, and 17DC are from Dry Creek starting at Raines Tavern and ending where Dry Creek crosses State Road 600. All readings are located in the north east portion of the Farmville quadrangle. The readings at the PC location are from Perkins Creek. The readings start at Bridge 366 along State Road 636 in the Willis Mountain quadrangle and continue west until Perkins Creek forks.

460: E and W: The location of these readings are from creeks that parallel U.S. Highway 460, in the southern portion of the

Farmville quadrangle. The E location readings start at a blue line stream that starts at the intersection of U.S. Highway 460 and U.S. Route 15. The stream lies south of U.S. 460E, and terminates at Buffalo Creek. The W location readings start at a blue line stream that begins at the intersection of U.S. 460 and State Road 45. The stream lies north of U.S. 460 and terminates at Little Buffalo Creek.

Plant : The location of these readings is at the City Of Farmville Treatment Plant, off of U.S. Highway 460 business in the Farmville quadrangle.

638 : The location of these readings is from the Ganaway Creek north of the Appomattox River in the south western portion of the Farmville quadrangle. The readings start where Ganaway Creek crosses State Road 683 and continue southward until the Buckingham and Cumberland county line.

KFC : The location of these readings is from an outcrop located at the Kentucky Fried Chicken off of U.S. Highway 460 business in the City of Farmville.

CAMP : 1, 2, 3: The location of these readings are from a creek located north of the Bear Creek campground in the Gold Hill quadrangle. The readings start at the terminus of the creek, at the dam, and continue until the creek forks.

Marr : 2 : These locations all come from strikes and dips on the geologic map of the Willis Mountain quadrangle (Marr, 1980).